SYNERGISTIC TREATMENT OF LUNG CANCER WITH GENETICALLY MODIFIED CELL THERAPY AND CHEMOTHERAPY

Krishna Kalyan Kolluri

University College London

UCL Respiratory

Lungs for Living Research Centre

A thesis submitted for the degree of Doctor of Philosophy

2015

Declaration

I, Krishna Kalyan Kolluri, confirm that the work presented in this thesis is my own. Where information has been derived from other sources I confirm that this has been indicated and acknowledged.

Abstract

Lung cancer and malignant pleural mesothelioma (MPM) carry a high mortality. Conventional therapies are ineffective in their treatment and there is a need to develop novel therapies. Tumour necrosis factor-related apoptosis-inducing ligand (TRAIL) is a pro-apoptotic agent that triggers the extrinsic death pathway selectively in cancer cells. Mesenchymal stem cells (MSCs) are a type of bone marrow-derived stem cell that have been widely shown to home to and to infiltrate areas of the tumour microenvironment. This homing capacity can be exploited to deliver pro-apoptotic agents, including TRAIL, straight into the tumour micro-environment.

Earlier studies show cancers can be treated with TRAIL-expressing MSCs (MSC-flT cells). However, some cell lines are resistant to MSC-flT cells. This study aimed to increase the efficiency of tumour cell killing using MSCs that are engineered to express TRAIL. This study investigates if cancer cell-killing by MSC-flT cells could be enhanced for the treatment of TRAIL-resistant cancers. The aims of this study were to increase the tumour cell-killing efficiency of MSCs engineered to express TRAIL by identifying whether the full-length or soluble form of TRAIL expressed by MSCs is superior in tumour cell killing, whether cancer cell-killing by MSC-flT cells can be increased by combining them with novel chemotherapeutic agents and to identify a biomarker to predict sensitivity to TRAIL.

Cancer cell-killing by MSCs expressing full-length TRAIL was superior to that of MSCs expressing the shortened soluble form of TRAIL. MSC-flT cells showed a synergistic cancer killing affect when combined with novel chemotherapeutic agents.

In collaboration with McDermott's laboratory in the Wellcome Trust Sanger Institute, it was found that *BAP1*-mutated MPM cells are sensitive to TRAIL. This was validated by knock-in and knockdown experiments. It was shown that *BAP1*-mutated tumours are sensitive to TRAIL *in vivo*. Further work was done to delineate the mechanism of BAP1-induced TRAIL resistance. The deubiquitinating function of BAP1 and its nuclear localization were shown to be required for TRAIL resistance. This indicates that loss of function of BAP1 is a biomarker for TRAIL sensitivity.

Acknowledgements

I am very grateful and obliged to three people who are responsible not only for me doing a PhD but also for making me the person I am.

Firstly, I would like to thank my supervisor **Prof Sam Janes** for his constant belief in me and for instilling self-confidence in me when I needed it the most. If I hadn't met Sam, I might never have done a PhD. His eternal optimism and kindness is something that I aspire to.

I would like to thank **Narendra Chowdary Kolla**. Without his help I might never have even dreamt of stepping into UCL. His tremendous hard-working nature is always an inspiration.

I would like to thank my grandfather **Garikipati Venkata Narayana Rao** for nurturing curiosity in me since childhood and for encouraging me to follow my own path even though sometimes it was rather unconventional. This work is dedicated to my grandparents **Garikipati Venkata Narayana Rao and Nagamani**.

I am grateful to UCL Grand Challenges and UCL Overseas Research Studentship (ORS) for funding me.

I would like to thank my secondary supervisor Prof Emma Morris for her helpful feedback. I am very grateful to Beth for teaching me cell biology techniques and for her encouragement throughout, to Qiang for teaching me molecular biology techniques and for being such a kind-hearted person, and to Adam for teaching me animal techniques. I am very thankful to Kate - one of the kindest people I ever met. Without her help I wouldn't have been able to complete my thesis. I also thank Neelu for her hard work and support in the past year.

There are amazing people that I have come across in the past four years and without their help - both technical and moral - this work could have been very difficult. I will try to thank them in chronological order of when I first met them. Special thanks to Colin (for late night TC during my initial days in the lab and for being the lab's scapegoat), Jim, Vitor (for help with gene expression analysis and being a close friend), Sofia (for teaching me about viruses), Noura (for teaching me RNAi and for being supportive through thick and thin), Rob (my point of contact for discussing ideas), Sab (for the amazing times we spent in the animal house and for teaching me to play squash), Tanvi (a nice friend but we argue more often than not), Laura (such a lovely person who gets so excited about science), Nick, Cat, Paul and Ricky (for being an amazing friend and for enlightening me about public health in India).

I would like to thank Rachel, Robin, Manu, Dave and Lizzy in CITR.

I am fortunate to have built good collaborations and to have learned from experts during this work. I am very grateful to Prof Ultan McDermott and Dr Constantine Alifrangis at the Welcome Trust Sanger Institute, Cambridge, for their collaboration on the BAP1-TRAIL project. Thanks to Dr Derek Davies (CRUK-LRI) and Dr Ayad Edoudi (UCL-ICH) for teaching me FACS and to Dr Daniel Zicha (CRUK-LRI) for teaching me confocal microscopy. Thanks to the Walzack lab for providing IZTRAIL.

I would like to thank Dr Ross Breckenridge (UCL) and Dr Jaqueline Corness (University of Hertfordshire) for their help in securing my admission to UCL.

I appreciate the help and support of my friends Praneet, Narendra Kondaveeti, Srinadh, Siva, Nagababu, Balu, Sundar, Sirisha, Vijay, Prasad, Harsha, Madhu and Ashok.

I am very thankful to my family for their unending support and love. Special thanks go to my parents Seshagiri Rao and Tulasi, and to my aunts and uncles - Rama Devi, Nageswara Rao & Sudharani, Pornachandra Rao & Madhavi. I am very lucky to have my sisters and brothers Pratyusha, Pragnya, Kranthi Krishna and my brother-in-law Rama Krishna.

List of contents

List of figures

CHAPTER I

Introduction

1 INTRODUCTION

1.1 Lung cancer

Lung cancer is a highly invasive, rapidly metastasising cancer and is one of the leading causes of cancer mortality worldwide. It accounts for 13% of total diagnosed cases of cancer and 18% of cancer-related deaths worldwide [1]. In the United Kingdom in 2008, 38,741 cases of cancers in the lungs, bronchi and trachea were diagnosed in males and 24,781 in females [2]. Lung cancer can arise at different sites in the bronchial tree and is very heterogeneous. About 70% of lung cancer cases are detected at an advanced stage and this late diagnosis is partly responsible for the high mortality of lung cancer [3].

1.1.1 Classification of lung cancer

The WHO classification of lung cancer was revised in 2004 on the basis of histological and cytological examinations. However, recent advances in understanding tumorigenesis of lung cancer have led to further subclassification of the histological types of lung cancer into groups based on the mutations that the cancer cells may harbour [3, 4]. This method of classification not only facilitates the determination of the treatment regimen for the patient but also aids in getting an indication of prognosis.

Lung cancer is broadly classified into two types:

1. Small cell lung carcinoma (SCLC)
2. Non-small cell lung carcinoma (NSCLC)

1.1.1.1 Small cell lung carcinoma (SCLC)

SCLC accounts for about 14% of all lung cancer cases [3]. It can be further classified into pure SCLC or into a combination of SCLC and NSCLC. There is no difference in the clinical outcome and the approach to therapy between pure SCLC and combined SCLC. SCLC shows a strong correlation with cigarette smoking and is extremely rare in persons who have never smoked; only 2% of SCLC patients are non-smokers [5].

Treatment of small cell lung carcinoma (SCLC)

30% of SCLC patients are diagnosed with limited stage disease (LS-SCLC) [6]. These patients are often treated radically by either surgical resection or a combination of platinum-based chemotherapy and radiotherapy [7]. Prophylactic cranial irradiation can be prescribed to avert brain metastasis. SCLC spreads very early and is almost always inoperable at presentation. 70% of SCLC patients are diagnosed with extensive stage disease (ES-SCLC) at the time of diagnosis [6]. These tumours do respond to chemotherapy and radiotherapy, but the prognosis is generally poor due to the aggressive nature of the tumour by the time of diagnosis. Current treatment includes a combination of platinum-based chemotherapy and radiotherapy with prophylactic cranial irradiation [7]. This strategy shows a strong initial response but recurrence is commonly observed. Individuals with recurrent SCLC may undergo further second-line chemotherapy. However, palliative care is often the mainstay of the treatment.

1.1.1.2 Non-small cell lung carcinoma (NSCLC)

NSCLC accounts for about 85% of all lung cancers and can be further classified into large cell carcinoma (LCC), squamous cell carcinoma and adenocarcinoma.

Large cell carcinoma (LCC)

LCC accounts for 3% of all lung cancers. It can be further classified into large cell neuroendocrine carcinoma, basaloid carcinoma and large cell carcinoma with rhabdoid phenotype.

Squamous cell carcinoma (SCC)

SCC accounts for 25-30% of lung cancers [8]. While one third of SCC are peripheral tumours, the rest are tumours in the central lung. SCC can be further classified into papillary, clear cell, small cell and basaloid subtypes [3]. 60-80% of SCC arises in the proximal tracheobronchial tree, through a sequence of progressive cellular dyskaryosis, involving squamous metaplasia, dysplasia and carcinoma-in-situ (squamous carcinoma-in-situ). A minority of cases occur peripherally and may be associated with bronchiectasis cavities or scars. Although metastasis is frequent, it normally occurs late.

Adenocarcinoma (ACC)

Lung adenocarcinoma accounts for 40% of all lung cancers [8] and is the most common type of lung cancer. It arises from the mucus cells of the bronchial epithelium and thus can cause excessive mucus secretion. ACC is subclassified into atypical adenomatous hyperplasia, adenocarcinoma-in-situ, minimally invasive adenocarcinoma, invasive adenocarcinoma and variant invasive mucinous adenocarcinoma [3]. ACC commonly metastasises to the mediastinal lymph nodes and the pleura, and spreads to the brain and bones.

1.1.2 Staging and treatment of NSCLC

The international TNM-based staging system is used to describe the anatomical extent of the disease [9]. This system helps in determining the treatment plan, the disease prognosis and in evaluating the outcome of the treatment. The NSCLC stages range from stage I to stage IV. A low stage indicates low levels of cancer spread. In the TNM-based system, T describes the size and the extent of the primary tumour. The N category describes the extent of tumour that has spread to the regional lymph nodes, while M describes the presence of distant metastases [9].

Treatment of stage I and II NSCLC

The best strategy for the treatment of stage I and II NSCLC is surgery and resection of the tumour [10]. The 5-year survival after surgery has been shown to be 60-80% for stage I disease and 30-50% for stage II disease [11]. An adjuvant platinum-based chemotherapy is beneficial after surgical resection of the tumour for stage II disease but not for stage I disease [8, 12, 13].

Treatment of stage III NSCLC

Stage III NSCLC is a heterogeneous disease and ranges from resectable tumours with metastases in the lymph nodes to unresectable tumours with multiple nodal metastases. Surgical removal of the tumour is recommended wherever possible but it is determined by the location and the size of the tumour along with the location of the metastases. Adjuvant chemotherapy or radiotherapy significantly increases patient survival following surgery [14, 15]. For patients with unresectable tumours, sequential or concurrent platinum-based chemotherapy and radiotherapy is recommended[8].

Treatment of stage IV NSCLC

The standard treatment options for stage IV NSCLC depend on various factors, such as histology, the physical status of the patient and, more recently, the mutational features of the tumour. The treatments options include chemotherapy, radiotherapy and targeted therapy with the focus of the therapy being to extend patient survival and to alleviate patient suffering. Chemotherapy is recommended for patients who are physically fit and able to tolerate the treatment. First-line chemotherapy treatment includes a platinum-based drug with a combination of other cytotoxic drugs such as taxanes (for example, paclitaxel, docetaxal or vinorelbine), anti-metabolites (for example, gemcitabine or pemetrexed) or vinca alkaloids (for example,vinblastine) [16]. The 1-year overall survival of patients with stage IV NSCLC increases from 10-20% to 30-50% in patients having chemotherapy [17].

1.1.3 Mutational status and targeted therapies of NSCLC

Conventional cytotoxic chemotherapeutic agents and radiotherapy are not very effective at treating NSCLC, especially in the advanced stages of the disease. Recent advances in DNA sequencing technology and other innovations have led to a better understanding of the pathobiology of lung tumours. This has led to the development of targeted therapies based on the mutational status of the tumours.

Proto-oncogenes such as EGFR, KRAS, BRAF, HER2, MEK and PI3K are frequently activated in NSCLC and these can be targeted with specific protein inhibitors. Tumour suppressors such as PTEN, TP53, RB1, CDKN2A (also known as P16) are frequently inactivated in NSCLC [8]. About 230 adenocarcinoma tumour samples have been subjected to molecular profiling as part of the Cancer Genome Atlas Research

Network. This study showed that these samples had a significant number of genomic alterations, such as point mutations, rearrangements and copy number variations, in 18 genes [18].

EGFR tyrosine kinase inhibition

Gain-of-function mutations in EGFR lead to the constant activation of this receptor and consequently in signalling for cell growth and division through its tyrosine kinase domains. Tyrosine kinase inhibitors (TKIs) such as erlotinib and gefitinib inhibit EGFR signalling. These drugs are therefore recommended for patients that have lung cancers with EGFR gain-of-function mutations. Large randomised clinical trials demonstrated that erlotinib or gefitinib are better than platinum-based drugs as a first-line therapy [19-22]. Although there was no increase in overall survival of patients given erlotinib or gefitinib compared with platinum-based chemotherapy, the progression-free survival of patients increased from 5.2 to 9.7 months [23].

ALK/MET inhibition

ALK and *EML4* genes are located on the p-arm of chromosome 2. About 4.9% of NSCLC patients have a fusion of these genes, leading to constitutive activation of ALK kinase, which in turn leads to increased cell growth and proliferation [24]. EGFR and EML4-ALK mutations are mutually exclusive and EML4-ALK mutations are found in tumours that are resistant to EGFR inhibition [25]. The ALK kinase inhibitor crizotinib has been shown to improve the survival of patients with advanced stage NSCLC who have an ALK-EML4 fusion mutation [26, 27].

1.2 Malignant pleural mesothelioma (MPM)

Malignant pleural mesothelioma is a rare but highly aggressive tumour originating from the mesothelial cell lining of the pleura, which is the outer lining of the lungs. Although MPM is a thoracic cancer it is not classified as a lung cancer. However, a significant amount of work was done on MPM in the course of this study.

The background incidence of MPM is very low. However, industrialisation has led to an increase in exposure to MPM risk factors and this has resulted in an increase in the incidence of MPM. The overall median survival of patients with MPM is 9-12 months, regardless of the stage of the disease [28]. There were 8458 cases of MPM reported in England between 2002 and 2006, which resulted in 5656 deaths. The United States has more cases of MPM than anywhere else in the world. The incidence of MPM is increasing in other countries such as Russia, China and India [29].

1.2.1 Causes of MPM

Although factors such as exposure to Simian virus 40 (SV40) and radiation have been shown to trigger MPM, 80% of MPM cases are attributed to exposure to asbestos [30]. As a result of its fire-resistant properties, industrialisation led to the mining and the application of asbestos for a variety of purposes. Asbestos was widely applied in constructions, heating arrangements, electrical works and plumbing. The people who were exposed to asbestos as a result of their work have been subjected to an occupational hazard of developing MPM.

The disease is characterised by a long latency period of 20-50 years after the exposure to asbestos (Figure 1-1). As a result of the associated risks of asbestos exposure, several countries, including the UK and the USA, have banned the mining and the use

of asbestos. However, the long latency period means that cases of MPM continue to increase and that numbers of MPM cases are projected to peak in England in the 2020s [31].

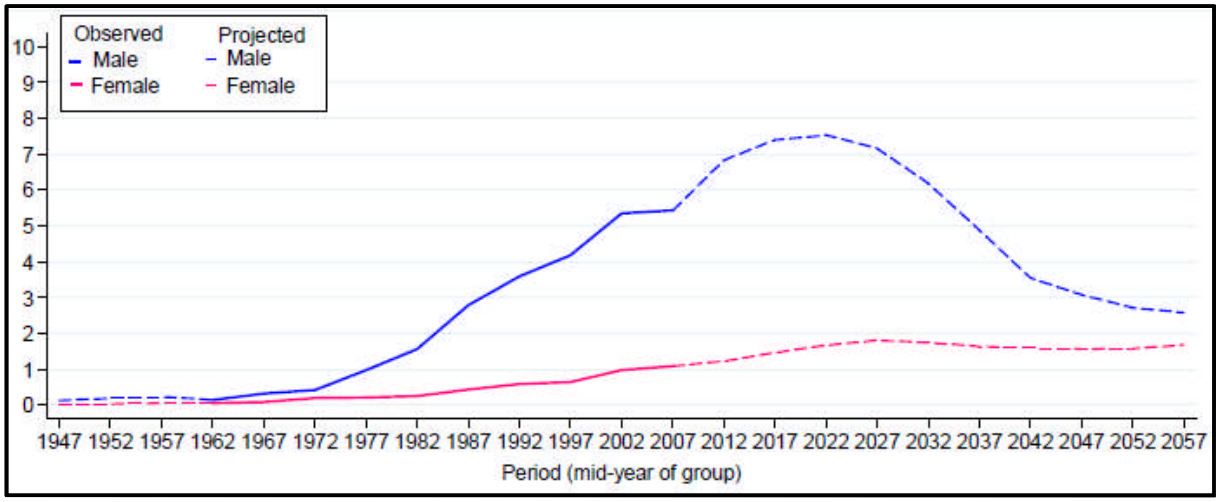

Figure 1-1 Predictions of incidence of MPM in south-east England.

Observed (thick lines) and predicted (dashed lines) age-standardised rates (per 100,000 European standard population) of mesothelioma, south-east England, 1947-2057, by sex and period. Source: [31]

1.2.2 Mechanism of asbestos-induced carcinogenesis

The mechanism of asbestos-induced carcinogenesis is so far not fully understood. It is believed that there are several pathogenic factors or events leading to the development of MPM in the latency period.

The asbestos fibres are very thin and long; they are approximately 8 µm in length and 0.25 µm in width. The fine structure of the fibres enables them to penetrate through the lung and to reach the pleural lining. In the pleural lining, they are incorporated into the normal (non-malignant) pleural cells. Exposure of human mesotheliomal cells to asbestos fibres *in vitro* results in cytotoxicity. This cytotoxicity is dose dependent and

thus there might be several factors *in vivo* that induce these cells to become malignant during the latency period.

In 2006, Yang et al [32] demonstrated the vital role played by macrophages in the development of MPM. They proposed that when the asbestos fibres accumulate in pleural cells it results in macrophage accumulation. The macrophages secrete tumour necrosis factor-α (TNFα) and induce mesothelial cells to express TNF receptor and to produce TNFα. Therefore, the TNF pathway is triggered by both paracrine (macrophages) and autocrine (mesothelial cell) signalling. TNFα activates nuclear factor-κB (NF-κB), which induces several pro-survival functions. Mesotheliomal cells with DNA damage are therefore encouraged to divide rather than to die.

1.2.3 Diagnosis and staging of MPM

The clinical symptoms of MPM are visible 2-3 months after the development of the disease and include dyspnoea and chest pain. Chest X-ray may reveal a unilateral pleural effusion or thickening but a CT scan of the chest and a biopsy sample for histological tests are recommended to confirm the diagnosis [33]. There are three distinct subtypes of MPM: epithelioid (50-60% of MPM cases), sarcomatoid (10% of MPM cases) and biphasic (30-40% of MPM cases) [34]. The epithelial-type MPM can be further classified into subtypes such as tubular, papillary, giant/large cell, small cell, myxoid and others that reflect morphological similarities to carcinomas of other origins [35]. The sarcomatoid-type MPM is characterised pathologically by spindle-shaped cells similar to those seen in fibrosarcomas and by poor prognosis compared with other types of MPM. The biphasic-type MPM has features of both the sarcomatoid and epithelial-types of MPM [35].

A TNM-type system for staging MPM was proposed by the International Mesothelioma Interest Group (IMIG) and is the most widely accepted system for staging MPM [36]. As per this classification, stage I MPM includes lymph node-negative patients with a tumour restrained to the parietal pleura (stage Ia) or with minimal visceral pleural involvement (stage Ib). Stage II MPM includes lymph node-negative patients with confluent superficial tumour on all pleural surfaces or with involvement of the diaphragmatic muscle or lung parenchyma. Stage III MPM includes patients with tumour metastasis to the hilar (N1) or ipsilateral mediastinal (N2) lymph nodes or those with extension of tumour into the soft tissues of the chest wall, the endothoracic fascia, the mediastinal fat or the pericardium (T3 tumour). Most of the patients are diagnosed as stage III [37]. Stage IV MPM includes patients who have a locally advanced tumour extensively invading the spine, the ribs or the chest wall, transdiaphragmatic spread or contralateral pleural spread. Patients with stage IV disease may also have contralateral or supraclavicular lymph node involvement (N3) or distant metastases.

1.2.4 Treatment of MPM

There have been innumerable attempts to treat MPM by surgery, radiation and chemotherapy but no intervention has had a significant effect on the disease.

1.2.4.1 Surgery

Although complete surgical resection of the tumour is theoretically the most effective treatment, it is rarely achieved due to the usual spread of MPM throughout the hemithorax. Removal of the bulk of the tumour will be done during the surgery but generally microscopic pieces of tumour are left behind [37].

Three types of surgical procedures are employed in the surgical management of MPM. They are thoracoscopy with pleurodesis, pleurectomy/decortication (P/D) and extrapleural pneumonectomy (EPP) [38]. No comparative studies have been done to determine the most effective procedure. Although stage I and II patients have potentially resectable tumours, surgery has been shown to be ineffective and may even worsen the outcome [39].

1.2.4.2 Radiotherapy

MPM grows as a diffuse sheet around the lungs. This limits the use of radiation as high doses of radiation cannot be used on a large area, especially in the thoracic region in which vital organs are enclosed. Therefore, radiotherapy has many complications and is only employed as a palliative measure for pain relief. Thus, radiotherapy may be used in disease palliation but has no real impact on survival [38].

1.2.4.3 Chemotherapy

Many chemotherapeutic agents have been tested in clinical trials for MPM as systemic therapies and chemotherapy is the only treatment option in the majority of patients; however, chemotherapy has been largely ineffective in treating MPM. The current first-line chemotherapy is a combination of a platinum-based drug (cisplatin) with pemetrexed. This therapy has been shown to increase mean patient survival to 12 months compared with patients treated with cisplatin alone who had a mean survival of 9 months [40, 41]. However, the median survival remains at nearly 12 months. This justifies the need for a new and innovative therapy.

1.2.5 Genomic alterations in MPM

Advances in technologies for high-throughput sequencing of DNA have enabled the comprehensive characterisation of mutations in MPM at an unprecedented resolution. This has also been facilitated by a drastic fall in the cost of sequencing. Guo et al [42] performed exome sequencing on samples from 22 MPM tissues and matched normal samples and found frequent inactivation of BAP1, NF2, CUL1 and CDKN2A as a result of somatic mutations and/or copy number alterations.

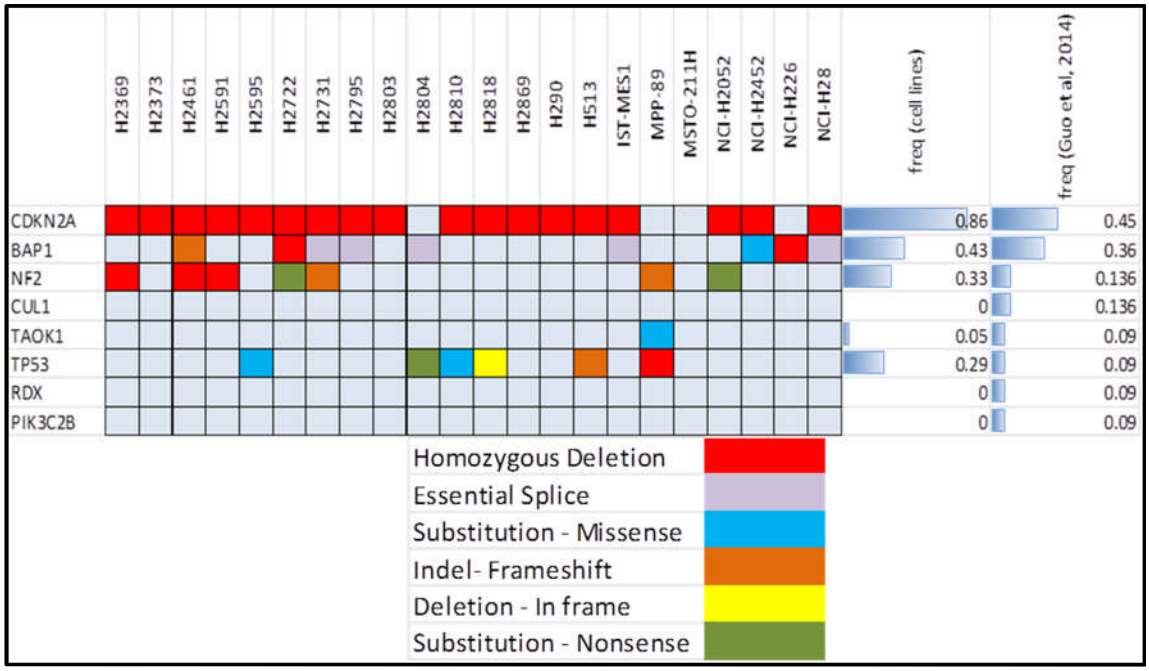

Figure 1-2 Mutations and loss-of-function events in MPM cell lines

Mutational characterization of 21 MPM cell lines (H226 was not part of this panel but it has homologous deletion of the BAP1 *gene). The most recurrent mutations are observed in* CDKN2A*,* BAP1 *and* NF2*.*

This figure was provided by Dr McDermott's Lab (WTSI) as part of collaboration.

Ultan McDermott's laboratory at Wellcome Trust Sanger Institute (WTSI) analysed the recurrent mutations in 21 MPM cell lines and found frequent mutations in CDKN2A, BAP1, NF2 and TP53. A detailed description of BAP1 is given in section 1.3 as chapters IV and V describe the use of loss-of-function mutations of BAP1 as a biomarker for TRAIL-mediated apoptosis.

1.3 BRCA1-associated protein 1 (BAP1)

BRCA1-associated protein 1 (BAP1) was discovered by Jensen et al in 1998 [43]. It was found to interact with the known tumour suppressor BRCA1. The *BAP1* gene is located on the short arm of chromosome 3 at position 21.1 (3p21.1) and codes for a 729 amino acid protein. BAP1 is found to be frequently deleted in lung carcinoma cell lines, thus leading to the conclusion that it might be a tumour suppressor. It was also proposed by Jensen et al that BAP1 might be a deubiquitinating (DUB) enzyme as the N terminus of BAP1 is homologous to the UCH domain, which is a characteristic feature of UCH deubiquitinating enzymes [44].

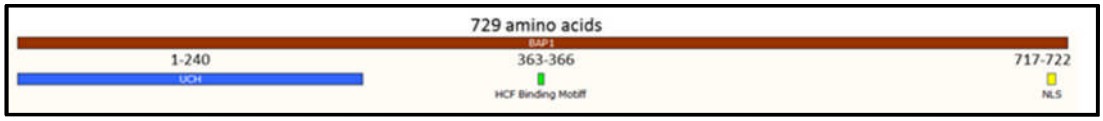

Figure 1-3 BAP1 protein

BAP1 is a 729 amino acid protein with a UCH domain at the N terminus and a nuclear localisation signal in the C terminus.

1.3.1 Deubiquitinating enzymes (DUBs)

Ubiquitin (Ub) is a 76 amino acid polypeptide that is covalently bonded to other proteins by sequential action of Ub activation (E1), Ub conjugating (E2) and Ub ligase (E3) enzymes, forming an isopeptide bond between the C terminus of Ub and the lysine residues of the substrates [45].

Ubiquitination was initially only thought to mark a protein for degradation but since then several types of ubiquitination have been identified that have important roles in several other cellular processes. Ubiquitination is a reversible process and deubiquitination of proteins is done by specialised proteins called DUBs. DUBs are

proteases that specifically cleave the isopeptide bond between the Ɛ-amino group of lysine side chains in target proteins and the C-terminal group of ubiquitin, or the peptide bond between the α-amino group of the target protein and the C-terminal group of ubiquitin [46]. The process of ubiquitination and deubiquitination acts as an 'on-off' switch and has an important role in cell signalling. Ubiquitinating and deubiquitinating enzymes control several biological processes such as DNA repair, transcription regulation, cell differentiation and oncogenesis [47].

DUBs belong to a superfamily of proteases and at least 98 DUBs have been identified and classified into six families [47]:

1. Ubiquitin-specific proteases (USPs)
2. Ubiquitin carboxy-terminal hydrolases (UCHs)
3. Ovarian-tumour proteases (OTUs)
4. Machado–Joseph disease protein domain proteases
5. JAMM/MPN domain-associated metallopeptidases (JAMMs)
6. Monocyte chemotactic protein-induced protein (MCPIP) family

Apart from JAMMs, all other families are cysteine peptidases and the presence of cysteine at the active site is required for their activity.

UCH enzymes can only target small peptides from the C terminus of ubiquitin as they have a confined loop that precludes the processing of polyubiquitin chains and large folded proteins [47]. There are four UCHs in humans: UCHL1, UCHL3, UCHL5/UCH37 and BAP1. BAP1 is the biggest member of the UCH family of DUBs, comprising 729 amino acids, and is characterised by a UCH domain, which is a conserved catalytic domain with about 230 amino acids.

1.3.2 The role of BAP1 in several cellular processes

BAP1 plays a key role in several important biological processes, including development, DNA repair, transcription regulation, chromatin remodelling and oncogenesis [48]. BAP1 is involved in these processes as a result of its interactions with various other proteins. These interactions are facilitated by the long polypeptide chain that follows the UCH domain. BAP1 possesses a nuclear localisation signal (NLS) at the C terminus that enables BAP1 to be sequestered in the nucleus [49]. BAP1 has an HCF-binding motif (HBM) through which it binds to host cell factor 1 (HCF1) [50]. Lysine at amino acid 691 helps in the interaction of BAP1 with BRCA1 [43]. BAP1 is also found to be phosphorylated at different amino acids enabling it to interact with FOXK1 [51], and its phosphorylation at serine 592 helps in DNA repair [52]. The amino acids required for the interaction of BAP1 with various proteins are shown in Figure 1-4.

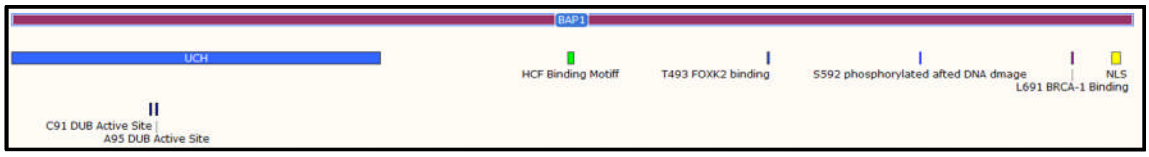

Figure 1-4 Interactions of BAP1 with other proteins

C91 and A95 are required for the DUB activity of BAP1. HBM is required for interacting with HCF1. Threonine 493 must be phosphorylated to enable the BAP1-FOXK2 interaction. Serine 592 is phosphorylated during DNA damage. Lysine 692 is required for BAP1 to interact with BRCA1. NLS helps BAP1 to be sequestered in the nucleus.

1.3.2.1 BAP1 in development

BAP1 forms a complex with Polycomb group (PcG) proteins and plays a role in development [53]. The PcG proteins are transcriptional repressors that control several processes, such as stem cell pluripotency and the maintenance of cell fate decisions.

The complex of PcG proteins with BAP1 is termed the Polycomb repressive deubiquitinase (PR-DUB) complex [53]. PR-DUB plays an important role in controlling the monoubiquitination status of histone H2A. Both the catalytic function of BAP1 and the presence of the ASX subunit of PcG proteins are required for this function. PcG proteins also play a role in DNA damage repair [54] and it is possible that the PR-DUB complex might be involved in this process.

BAP1$^{-/-}$ mice show developmental retardation at embryonic day 8.5 (E8.5) and are not detected beyond E9.5, indicating that BAP1 plays an important role in embryo development [55]. Furthermore, depletion of BAP1 in uveal melanoma cells results in loss of differentiation and gain of stem cell-like properties, including expression of stem cell markers such as NANOG [56].

1.3.2.2 BAP1 in DNA repair

BRCA1 is a known tumour suppressor and is most commonly mutated in breast cancers. It forms a complex with BARD1 and plays a key role in DNA repair. A fraction of BAP1 is associated with BRCA1 but BAP1 has not been shown to deubiquitinate BRCA1 [57]. However, it was proposed that the complex of BAP1 and BRCA1 can deubiquitinate other proteins and can be involved in the DNA repair.

BAP1 primarily interacts with BARD1. BRCA1 is involved in enhancing the interaction between BAP1 and BARD1, however BAP1 is capable of interacting with BARD1 independently of BRCA1 [50]. The interaction of BARD1 and BAP1 results in the dissociation of the BARD1-BRCA1 complex. This affect is not the result of the deubiquitination function of BAP1. Cells that are depleted of BAP1 are sensitive to ionising radiation [50]; as BARD1 is known to play an important role in DNA repair,

BAP1 might be involved in DNA repair through its interaction with BARD1. In addition, BAP1 is phosphorylated in response to DNA damage on consensus sites that are recognised by the DNA repair proteins ATM and ATR [50]. In addition, after UV irradiation, BAP1 is phosphorylated on serine 592 of its polypeptide chain [58]. This phosphorylation occurs during S-phase of the cell cycle, following UV irradiation, and dephosphorylation occurs upon completion of DNA replication. Phosphorylated BAP1 is predominantly dissociated from chromatin [58]. The phosphorylation of BAP1 also occurs in response to replication stress. This could be a way of regulating transcription and replication after DNA damage or stress.

BAP1 is recruited to sites of DNA damage at DNA double strand breaks (DSBs) [59]. The deubiquitination function of BAP1 is necessary for this recruitment. BAP1 mediates the recruitment of the PR-DUB complex to the site of DNA damage and BAP1 in turn is recruited by PARP1. Although BAP1 is phosphorylated at serine 592 by ATM, this phosphorylation is not required for BAP1 to be recruited to the site of DNA damage. As BAP1 is found to be dissociated from chromatin after phosphorylation [50] but is found to be associated with DNA at DSBs [58], BAP1 might be dissociating from chromatin at the site of transcription but might be associating with sites of DNA damage.

After DNA damage, DNA repair occurs through two mechanisms: non-homologous end joining (NHEJ) or homologous repair (HR). The proteins that are involved in NHEJ merely join the ends of broken DNA strands. This is an error-prone mechanism as there is no template to make sure that the repair has been accurately done. Conversely, the HR mechanism uses a template and joins the ends accurately and is thus less error prone.

BAP1 promotes the recruitment of HR proteins after DNA damage and thus mediates DSB repair via the HR pathway [52]. BAP1 is phosphorylated at serine 592 after DSBs occur and is recruited to the site of the DSB. BAP1 at DSBs promotes DNA repair by HR by recruiting DNA repair proteins such as BRCA1 and RAD51 [52]. The catalytic activity and phosphorylation of BAP1 are required to promote DNA repair. Germline BAP1 mutants are more likely to use the error-prone NEHJ mechanism for DNA repair and thus are more sensitive to ionising radiation. BAP1-deficient cells are also sensitive to agents that induce DSBs.

1.3.2.3 BAP1 in transcription regulation

BAP1, as part of PR-DUB, removes monoubiquitin from histone H2A and plays a role in the repression of HOX genes [53]. BAP1 lacks a DNA-binding domain and hence cannot directly interact with DNA. However, it interacts with several transcription factors and transcription regulators, thus regulating transcription.

One protein with which BAP1 interacts to regulate transcription is HCF1. HCF1 is a nuclear protein that is important in a variety of cellular processes. HCF1 is translated as one large precursor protein that is proteolytically cleaved into two subunits, HCF1-N and HCF1-C. However, these cleaved subunits remain stably associated [60]. HCF1 interacts with several DNA-binding proteins through multiple interaction domains. BAP1 interacts with HCF1 through the β-propeller domain of HCF1-N [60]. The deubiquitination function of BAP1 is not necessary for this interaction, rather BAP1 binds to HCF1 through its HBM. HBM is a four amino acid motif comprising NHNY located between 363-366 on the BAP1 polypeptide chain; mutating these amino acids to alanine inhibits the interaction between BAP1 and HCF1 [60]. HCF1 is only present in

the nucleus and most of BAP1 is also found in the nucleus. Most of the nuclear BAP1 fraction can be immunoprecipitated along with HCF1 by using an excess of HCF1 antibody, indicating that most, if not all, BAP1 is associated with HCF1 in the nucleus [61]. BAP1 continuously removes K48 ubiquitin linkages from HCF1; indeed, mutating the amino acids at the active site of BAP1 increases K48 ubiquitin linkages on HCF1 [60]. Thus, BAP1 controls the levels of HCF1 in the cell.

BAP1 also interacts with the transcription regulator yin yang 1 (YY1). YY1 is a zinc finger protein that is capable of both transcription activation and repression. The transcription regulation of YY1 is dependent on the coactivators or corepressors it interacts with. BAP1 can simultaneously interact with HCF1 and YY1 but the interaction of BAP1 with YY1 is HCF1-dependent [61]. Indeed, the BAP1 mutant lacking the HBM domain shows weak interaction with YY1. BAP1 forms a complex with HCF1 and YY1 and regulates gene expression, mostly by activating transcription. The DUB activity of BAP1 is necessary for transcription activation by this complex [61]. *COX7C* is one of several genes that are regulated by the BAP1-HCF1-YY1 complex. The BAP1-HCF1-YY1 complex regulates the transcription of several genes that are involved in various cellular processes, such as cell cycle, DNA replication and repair, apoptosis and metabolism [61].

The BAP1-containing PR-DUB also binds to FOXK2 [62]. Forkhead transcription factors have an important role in transcription regulation. They directly bind to DNA with the help of their forkhead winged helix-turn-helix DNA-binding domain. FOXK1 and FOXK2 are important members of the forkhead transcription factor family. BAP1 is phosphorylated at threonine 493 and this enables its interaction with FOXK2, which

recruits BAP1 to chromatin [51]. BAP1 in turn recruits HCF1, forming a ternary complex that represses FOXK2 target genes. Depletion of BAP1 increases the expression of FOXK2 target genes such as *MCM3*, *CDC14* and *CDKN1B* [62]. The DUB activity of BAP1 is required for the repression of these genes; however, HBM-mutated BAP1 represses FOXK2 target genes, indicating that the interaction of BAP1 with HCF1 is not required for this repression of gene expression. Furthermore, mutation of threonine 493 to alanine (T493A) abolishes FOXK2 target gene regulation [51]. BAP1 loss results in the PRC-1-mediated upregulation of FOXK2 target genes, and it is possible that it represses gene expression through the formation of the PR-DUB complex.

O-linked N-acetylglucosamine (OGT) is a glycosyltransferase that catalyses the addition of a single N-acetylglucosamine by O-glycosidic linkage to serine or threonine residues, which indirectly affects transcription. OGT has been shown to be decreased in BAP1-knockout splenocytes and these cells show reduced O-GlcNAcylation [55]. OGT is deubiquitinated by the BAP1/ASLX1 complex and BAP1 might form a core complex with HCF1 and OGT to recruit additional histone-modifying enzymes to regulate gene expression [63]. BAP1 also plays a key role in the regulation of metabolism by interacting with OGT and HCF1. PGC-1α is a key regulator of gluconeogenesis and the activity of PGC-1α is controlled by post-translational modifications. HCF1 recruits OGT to O-glcNAcylate PGC-1α. O-GlcNAcylation of PGC-1α enables BAP1 to deubiquitinate PGC-1α and to protect it from degradation, thereby promoting gluconeogenesis [64].

Another protein with which BAP1 interacts is INO80. INO80 is a chromatin-remodelling complex that can alter chromatin structure by nucleosome sliding, histone eviction and histone exchange. INO80 is involved in various chromosomal processes, including DNA

repair, telomere regulation, centromere stabilization and the transcription of genes. BAP1 stabilizes INO80 by deubiquitination and this contributes to DNA replication [65].

1.3.2.4 BAP1 in cell cycle regulation

BAP1 is important in the progress of the cell cycle. One study [50] showed that BAP1 inhibition caused S-phase retardation while another study [49] showed that it caused accelerated S-phase entry. These studies demonstrate that BAP1 is involved in S to G1 phase transition. HCF1-N plays an important role in G1 phase cell cycle progression. Given that BAP1 and HCF1 interact, the BAP1-HCF1 complex might be involved in the regulation of G1 to S phase transitions [66]. However, there are cell lines in which BAP1 is deleted or in which BAP1 has a loss-of-function mutation that continue to grow, indicating that BAP1 is not absolutely required for cell cycle regulation; rather, BAP1 might be involved in preventing uncontrollable cell growth, thus acting as a tumour suppressor.

1.3.3 BAP1 as a tumour suppressor

The tumour suppressor activity of BAP1 was confirmed by Venti et al[49]. They used H226 cells that have a homozygous BAP1 deletion to show that the expression of wild-type BAP1 in these cells reduced tumour growth *in vivo*. They demonstrated that the deubiquitinase activity of BAP1 is necessary for its tumour suppressor function. Indeed, mutating cysteine 91 or alanine 95 in the BAP1 polypeptide chain, which are both located at the active site of the DUB activity, abolishes the tumour suppressor function of BAP1. In addition, the nuclear localisation of BAP1 is necessary for its tumour suppressor function [49]. The C terminus of BAP1 proteins contains a NLS — six amino acids (RRKRSR) located between amino acids 317 and 322 — and this help BAP1

to migrate into the nucleus from the cytoplasm. Mutating these amino acids abolishes the tumour suppressor function of BAP1 [49].

1.3.3.1 BAP1 loss-of-function mutations in cancer

Germline mutations of the *BAP1* gene were identified in 2 out of 26 sporadic mesothelioma samples investigated by Testa et al [67]. In this study, the patients with germline mutations in BAP1 had already been diagnosed with uveal melanoma. Germline BAP1 mutations might result in a hereditary cancer syndrome that predisposes patients to mesothelioma, uveal melanoma and other cancers [67]. Furthermore, exposure to asbestos in people with germline BAP1 mutations might trigger the development of mesothelioma: indeed, in this study, in one family, five out of five people with MPM with a germline BAP1 mutation lived in a home with detectable levels of asbestos [67]. Xu et al [68] showed that heterozygous BAP1-mutant mice (*BAP1*$^{+/-}$ mice) succumb to mesothelioma earlier than their wild-type littermates upon asbestos exposure. This demonstrates that germline haploinsufficiency for BAP1 causes increased susceptibility to asbestos-induced malignant mesothelioma.

Integrated genomic analysis of 53 MPM tumours samples uncovered somatic inactivating BAP1 mutations in 12 out of 53 (23%) samples [69]. In addition to uveal melanoma and mesothelioma, BAP1 mutations are also detected in 15% of renal cell carcinomas [70] and also in other cancers [48]. Furthermore, people with germline BAP1 mutations are predisposed to renal cell carcinoma [71]. There is also evidence that germline BAP1 mutation leads to the development of basal cell carcinoma (BCC) [72, 73] and oesophageal squamous cell carcinoma (ESCC) [74]. Furthermore, germline

mutation of BAP1 leads to a cancer predisposal syndrome in which the probands are susceptible to a variety of cancers. Chung et al [75] provided further evidence of tumour susceptibility syndrome in individuals who have a germline BAP1 mutation: individuals in a family with a germline BAP1 mutation manifested two or more different types of cancer. Interestingly, the location of the BAP1 mutation does not determine the type of cancer that an individual develops [75].

High expression of BAP1 is a good prognostic biomarker in advanced NSCLC: patients with high BAP1 expression have a longer median survival relative to patients with lower BAP1 expression [76]. Interestingly, BAP1 mutation might lead to synthetic lethality as BAP1 mutants are more sensitive to HDAC inhibitors because loss of BAP1 leads to lower HDAC2 expression [77]. However, not all BAP1-mutat cell lines are sensitive to HDAC inhibitors, possibly because they might be adapted to low HDAC2 expression.

1.4 Novel therapies for thoracic tumours

Several novel approaches to treat thoracic tumours that incorporate new chemotherapeutic, biological and targeted therapies are under development. Some of the relatively new therapies such as EGFR inhibition and ALK kinase inhibition have already been approved for clinical use.

Angiogenesis plays an important role in fostering tumour growth and is regulated by pro-angiogenic factors such as vascular endothelial growth factor (VEGF), fibroblast growth factor (FGF), platelet-derived growth factor (PDGF) and angiopoietins. Bevaxizumab, which is a monoclonal antibody that binds to VEGF, significantly improved response rates, progression-free survival and overall survival when used in

combination with platinum-based drugs in patients with NSCLC [78]. Bevacizumab in combination with other agents also showed beneficial effects when used in patients with ES-SCLC [79]. Other anti-angiogenic agents such as sorfenib and sunitinib are under clinical investigation.

Immunotherapy is another novel cancer therapy that offers an exciting and promising outlook for the treatment of lung cancer. Clinical trials are under way to investigate antigen-dependent and antigen-independent immunotherapies. One of the most promising antigen-dependent immunotherapy approaches to treat lung cancer is vaccination using melanoma-associated antigen A3 (MAGE A3). MAGE A3 is a tumour-specific antigen that is expressed in 35% of NSCLC, frequently in SCC [80]. In a randomised Phase II trial, MAGE A3 vaccination seemed to affect disease-free survival in patients with resected stage Ib or II tumours [81]. However, a large randomised, blinded, placebo-controlled Phase III trial investigating the efficacy of the MAGE A3 vaccine in patients with MAGE A3-positive tumours (MAGRIT trial) was terminated following assessment because of a lack of efficacy [82].

Tumour-infiltrating lymphocytes are major effector cells in the dynamic host immune response to tumour-associated antigens that are expressed by the cancer cells. However, cancer cells employ various methods to evade immune detection. One of the mechanisms by which tumours inhibit lymphocytes involves a receptor-ligand interaction in which lymphocyte cytolytic activity is controlled by inhibitory signalling from the tumour, by immune checkpoint inhibitory receptors. T cell inhibitory receptors limit T-cell functions by negatively regulating signals in immune cells (for

example, T cells and natural killer cells), including negatively regulating activating signals mediated by the T cell receptor (TCR)[83].

Modulation of these immune checkpoints is an antigen-independent immunotherapy approach that is being investigated to treat lung cancer; one such approach is the inhibition of cytotoxic T-lymphocyte-associated antigen 4 (CTLA-4). CTLA-4, expressed on the surface of T cells, functions to downregulate the immune response. Therefore, inhibition of CTLA-4 using CTLA-4-specific antibodies inhibits the early suppression of initial tumour-infiltrating T cells and prolongs the immune response. Interestingly, CTLA-4-specific antibodies have shown clinical efficacy in randomised Phase II trials for NSCLC [81]. Ipilimumab, a CTLA-4-specific antibody, in combination with paclitaxel and carboplatin was shown to improve progression-free survival in patients with NSCLC [84], and therefore this antibody warrants additional investigation in a Phase III clinical trial. Furthermore, in a Phase II study, ipilimumab in combination with paclitaxel and carboplatin in extensive-disease-small-cell lung cancer (ED-SCLC) showed increased progression-free survival and overall survival in patients with ED-SCLC [85].

The immune checkpoint receptor programmed death 1 receptor (PD-1) is another promising target in the area of antigen-independent immunotherapies. Inhibition of PD-1, which represents one of the key checkpoints involved in immunosuppression, using either specific PD-1 or PD-1 ligand (PD-L1) antibodies, has been shown to be safe [86, 87] with impressive response rates in patients; it is now being investigated extensively.

Pro-apoptotic agents can be used to trigger apoptosis in cancer cells and these represent another novel cancer therapy. Death receptors (DRs) are classified under the

tumour necrosis factor (TNF) superfamily and are expressed on the cell membrane. Death receptor ligands (DRLs) bind to the death receptors and, in some cases, are capable of triggering apoptosis of the cell. The important DRLs are TNFα, FASL (also known as CD95) and TNF-related apoptosis-inducing ligand (TRAIL). TNFα was initially thought to trigger apoptosis but systemic treatment with TNFα has been shown to induce a lethal inflammatory shock syndrome, therefore it would be unsuitable to use as a therapy for cancer [88]. Subsequent identification of the FAS receptor and its respective ligand FASL led to the hope that it could be used in cancer therapy to induce tumour-specific apoptosis, but treatment of animals with FASL induced massive hepatocyte apoptosis, making this unsuitable as a cancer therapy.

TRAIL was identified independently by Wiley et al [89] and Ashkenazi et al [90] in 1995 and 1996, respectively. TRAIL was shown to induce apoptosis in many cancer cells and also showed no signs of toxicity to normal cells either *in vitro* and *in vivo*. This led to clinical trials studying the use of either recombinant TRAIL or agonistic antibodies against the TRAIL receptors DR4 and DR5 for therapeutic purposes. However, mapatumumab and apomab, which are antibodies against TRAIL receptors, did not show a therapeutic effect either as a monotherapy or in combination with chemotherapies in treatment of NSCLC [91, 92]. Dulanermin, a recombinant TRAIL protein, was well tolerated with no toxicity or adverse effects in patients with NSCLC in a Phase I study [93]. However, the combination of dulanermin with traditional chemotherapy did not seem to significantly increase antitumoral activity in a Phase II study [91].

1.5 Tumour necrosis factor-related apoptosis inducing ligand (TRAIL)

TRAIL is the most studied and best characterised pro-apoptotic agent. TRAIL, also known as APO2 ligand, is a type II transmembrane protein with 281 amino acids and is a member of TNF death ligand superfamily. TRAIL triggers the extrinsic death pathway (Figure 1-6). The physiological function of TRAIL is not fully understood, but it is believed to play a role in the control of autoreactive immune cells and immune surveillance, especially against transformed cells [94].

There are five types of TRAIL receptors that have been identified to date and they include TRAIL-R1 (also known as DR4), TRAIL-R2 (also known as DR5), TRAIL-R3, TRAIL-R4 and osteoprotegerin. Osteoprotegerin is a soluble protein that has the capability of binding to TRAIL with low affinity [95]. This protein is not expressed on the cell surface. Only TRAIL-R1 and TRAIL-R2 are able to induce a signal into the cell after TRAIL binds to their extracellular domains. The receptors TRAIL-R3 and TRAIL-R4 do possess extracellular domains capable of binding to the ligand but lack an intracellular cytoplasmic domain, thus they fail to mediate death signals to the intracellular apoptotic machinery. Hence, TRAIL-R3 and TRAIL-R4 act as decoy receptors that antagonise TRAIL-induced apoptosis.

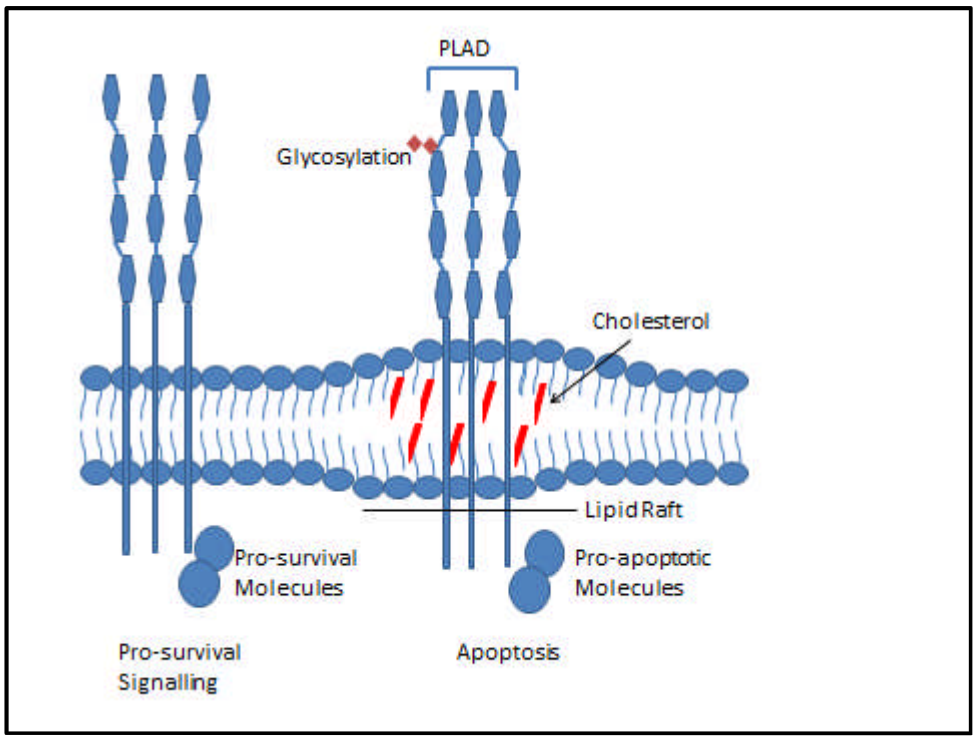

Figure 1-5 TRAIL signalling varies based on death receptor location and glycosylation

TRAIL induces apoptosis pathways when the death receptors are glycosylated or forms a pre-ligand binding assembly domain (PLAD) when located on lipid rafts.

1.5.1 TRAIL as an anti-cancer therapy

The novelty of TRAIL is that it only induces apoptosis in transformed cells and has virtually no effect on normal cells. This makes TRAIL a unique therapeutic with very few of the off-target adverse effects that are characteristic of chemotherapeutic agents and radiation. The mechanism for this selective targeting of tumour cells is not well characterised. The decoy receptor theory states that normal cells express decoy receptors while transformed cells express DR4 and DR5, thus making them vulnerable to TRAIL [96]. However, this theory is not widely accepted and it is believed that the selective cytotoxicity of TRAIL occurs intracellularly. One intriguing study shows that, in tumours, TRAIL receptors induce apoptosis when expressed within lipid rafts of the cell membrane (Figure 1-5). These rafts concentrate pro-apoptotic downstream signalling molecules internally. However, in normal cells the receptors are largely expressed in

the non-raft areas and TRAIL binding can actually lead to pro-survival pathway activation [97]. Other studies have suggested that TRAIL receptor glycosylation status [98] and the pre-ligand-binding assembly domain (PLAD) of TRAIL receptors have roles in TRAIL sensitivity [99]. It is likely that the TRAIL sensitivity is multifactorial and cannot be ascribed to any single mechanism.

1.5.2 TRAIL apoptotic pathway

Cells can undergo apoptosis either through activation of the extrinsic or the intrinsic apoptotic pathway. Death receptor ligands trigger the extrinsic apoptotic pathway. When TRAIL binds to a death receptor, the death receptors trimerise and trigger the extrinsic apoptotic pathway (Figure 1-6). This leads to recruitment of FAS-activated death domain (FADD) to the intracellular death domain of the trimerised receptors. FADD in turn recruits several other proteins, including caspase-8, cellular FLICE-like inhibitory protein (cFLIP) and others to form a death-inducing signalling complex (DISC). Caspase-8 is cleaved into its active form in the DISC and this then activates effector caspase-3, which carries out the apoptosis of the cell. There is another apoptosis pathway, the intrinsic apoptotic pathway, which is triggered by chemotherapeutic agents or radiation. Chemotherapy or radiation lead to DNA damage in cells and this damage is recognised by proteins such as P53. P53, through BAX/BAK, makes the mitochondrial membrane permeable, enabling it to release cytochrome c(cyt-c), which activates caspase-9 through apoptotic protease-activating factor 1 (APAF-1). Caspase-9 in turn activates the effector caspases to carry out the function of apoptosis. There is a cross talk between the extrinsic and the intrinsic apoptotic pathways that is mediated by BID. When caspase-8 is activated it cleaves BID to truncated BID (t-BID), which induces BAX/BAK to permeabilise mitochondria.

It would be ideal to trigger the simultaneous activation of both pathways to induce their synergistic effects. There is known synergy between traditional chemotherapeutic agents and TRAIL: this synergy results in increased apoptosis as a result of amplification of apoptotic signals through cross talk between the two apoptotic pathways [100].

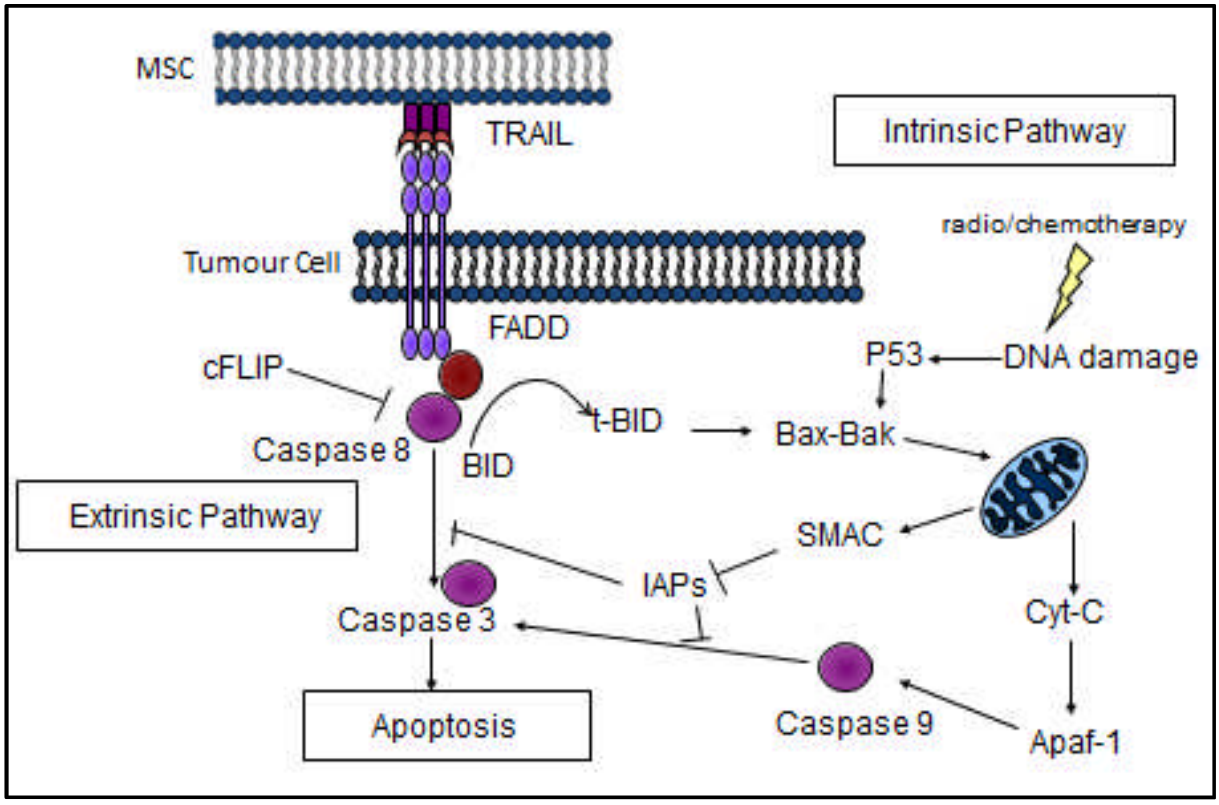

Figure 1-6 TRAIL signalling induces extrinsic apoptotic pathway

TRAIL triggers the extrinsic apoptotic pathway while conventional chemotherapeutics and radiotherapy trigger the intrinsic apoptotic pathway that is mediated by mitochondria. There is cross talk between the two pathways, which is mediated by cleavage of BID into t-BID by caspase-8. cFLIP and IAPs are potent inhibitors of apoptotic pathways and their inhibition could induce synergistic effects by simultaneously triggering both pathways.

TRAIL: tumour necrosis factor apoptosis-inducing ligand, FADD: FAS activated death domain, cFLIP: cellular FLICE inhibitory protein, BID: BH3 interacting-domain death agonist, IAPs: inhibitors of apoptosis proteins, BAK: BCL-2 homologous antagonist, Cyt-C: cytochrome c, APAF-1: apoptotic protease-activating factor 1.

Several chemotherapeutic agents such as cisplatin [101], SAHA (vorinostat) [102], pemetrexed [103], sunitinib [104], etoposide [105], doxorubicin [105], bortezomib[106] and others have been shown to act synergistically with rTRAIL. This synergy can be exploited to treat TRAIL resistant cancers.

Identifying and targeting proteins responsible for TRAIL resistance may increase the anti-tumour potency of TRAIL. Proteins such as cFLIP [107, 108], members of the IAP family that comprises cIAP1/2 [109], XIAP[110-112] and the BCL-2 family of anti-apoptotic proteins have been shown to have an important role in TRAIL resistance.

1.5.2.1 Cellular FLICE-like inhibitory protein(cFLIP)

cFLIP is a catalytically inactive caspase-8/10 homologue. It has an important role in resistance to TRAIL-mediated apoptosis [113] as well as being important in resistance to a wide range of chemotherapeutic drugs in several human malignancies [114]. There are three main forms of cFLIP: cFLIP-L, cFLIP-S and cFLIP-R. cFLIP-S, a 24 KDa protein, and cFLIP-L, a 55 KDa protein, are widely expressed in tumour cells [115]. All three cFLIP variants contain two DEDs at their N termini (Figure 1-7). In addition to two DEDs, cFLIP-L contains a large (p20) and a small (p12) caspase-like domain without catalytic activity. cFLIP-S and cFLIP-R consist of two DEDs and a small C terminus. cFLIP-L, cFLIP-S, cFLIP-R and two cleavage products of cFLIP (p43-FLIP and p22-FLIP) act as anti-apoptotic proteins. p43-FLIP and p22-FLIP are generated from cFLIP-L by procaspase-8 cleavage at D376 [116]. As it is a caspase homologue, cFLIP binds to FADD with the help of the DED domain, but as it lacks the active caspase domain it functions as a competitive inhibitor of FADD, thereby preventing the binding of

caspases and the subsequent activation of apoptotic signals initiated by death ligands such as TRAIL [117].

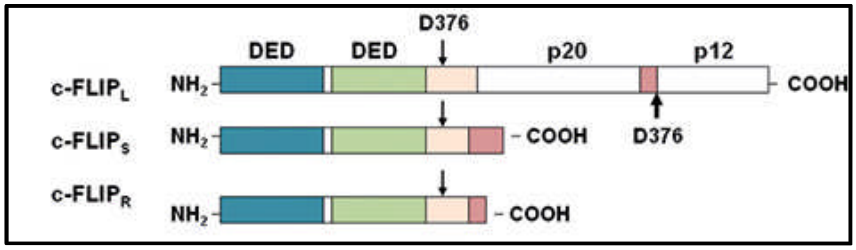

Figure 1-7 Different variants of cFLIP

cFLIP exists in 3 variants: cFLIP-L, cFLIP-S and cFLIP-R. All of them have 2 death effector domains (DEDs), which aid in attaching to FADD. Caspase-8 cleaves cFLIP-L into p20 and p12 fragments, which possess pro-survival functions. *Source: [116]*

In addition to imparting the tumour cell with apoptotic resistance, cFLIP may also be involved in metastasis[118]. This makes it an ideal target for tumour therapy. Several chemotherapeutic agents such as cisplatin [119], SAHA [120] and doxorubicin[121] have been shown to inhibit cFLIP at the transcriptional level.

1.5.2.2 Inhibitors of apoptosis proteins (IAPs)

The IAP family of proteins is characterised by the presence of a baculovirus IAP repeat (BIR) domain. IAPs contain 1–3 BIR domains (Figure 1-8) of 70–80 amino acids, which encode a C2HC-type zinc-finger motif [122]. There are several IAP family members, including XIAP, cIAP1, cIAP2, survivin, NIAP and others. This study is confined to XIAP, cIAP1 and cIAP2. IAPs are potent inhibitors of both extrinsic and intrinsic apoptotic pathways and are constitutively expressed in most cells. To circumvent IAPs, mitochondria release a protein called second mitochondria-derived activator of caspases (SMAC), which binds to IAPs and inhibits their function [123].

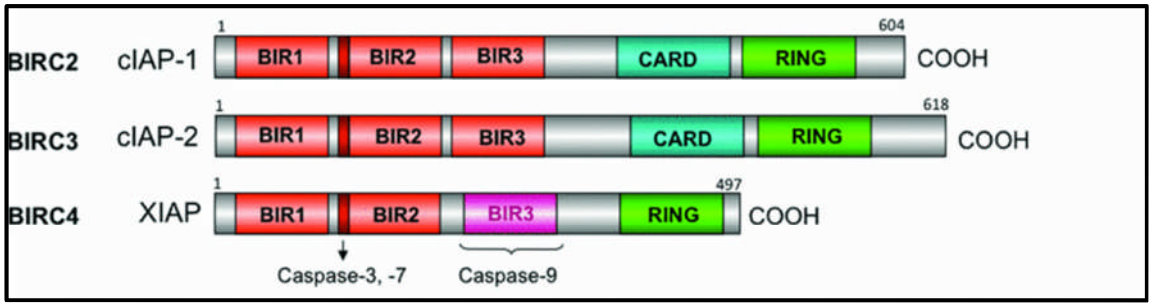

Figure 1-8 Inhibitors of apoptosis proteins (IAPs)

All IAPs possess characteristic BIR domains. cIAP1, cIAP2 and XIAP also consist of a RING (really interesting new gene), which is an E3 ubiquitin ligase. cIAP1 and cIAP2 also contain a CARD (caspase recruitment domain) at the C-terminal region and the function of this is unknown. The caspase binding of each BIR domain is indicated. Source: [124]

XIAP: XIAP has 3 BIR domains and a really interesting new gene (RING) domain [125]. Its ability to inhibit caspase-3 has been attributed to the BIR domain and the RING domain is important in its role as an E3 ubiquitin [124]. XIAP was shown to be a potent inhibitor of caspase-3, thus inhibiting both extrinsic and intrinsic apoptotic pathways [125, 126].

cIAP1/2: cIAP1 and cIAP2 possess 3 BIR domains, a RING domain and also a CARD domain, thefunction of which has not yet been identified [124]. Initially, it was believed that cIAP1 and cIAP2 were involved in binding and inhibiting caspases [127, 128]. However, the role of IAPs has been continuously evaluated and it was found that cIAP1/2 cannot directly inhibit caspases under physiological conditions and only XIAP can inhibit caspases by direct binding. However, cIAP1/2 can bind to SMAC and can prevent its function of inhibiting XIAP, thus paving the way for XIAP to inhibit caspases [128]. In addition to downstream caspase inhibition, cIAP1/2 were found to play important roles early in the TNF signalling pathway. cIAP1/2 have been shown to determine downstream signalling after TNF receptor activation. Their presence would

facilitate the activation of pro-survival pathways such as NF-kB, while their absence could trigger the apoptotic pathway [129].

1.5.2.3 BCL-2 family of anti-apoptotic proteins

Mitochondria regulate apoptosis through a process called mitochondrial outer membrane permeabilization (MOMP). It is a very important and hence is highly regulated through interactions between pro- and anti-apoptotic proteins in the B cell lymphoma 2 (BCL-2) family. The BCL-2 family proteins share one or more of the BCL-2 homology (BH) domains named BH1, BH2, BH3 and BH4. This protein family acts as regulators of apoptosis, particularly of the intrinsic apoptotic pathway, and can be divided into three groups based on the role they play in regulating apoptosis (Figure 1-9) [130]. Proteins such as BIM/BAD and NOXA have only one BH3 domain and act as sensors of cellular stress and activate the executor of MOMP. BID contains BH3 and BH4 and is activated as a result of cleavage by caspase-8. Cleaved BID, also known as truncated BID (t-BID) activates the executor of MOMP. BAX and BAK contain 4 BH domains, BH 1-4, and are pro-apoptotic as they induce MOMP. The anti-apoptotic members of BCL-2 family are BCL-2, BCL-X_L and MCL-1 [130]. There are several other members of the BCL-2 family that have a relatively smaller role in regulating apoptosis.

After the activation by BIM/BAD, NOXA or t-BID, the BCL-2 family members BAX and BAK undergo structural changes and homo-oligomerization, enabling them to target mitochondria [131]. The mechanism by which activated BAK and BAX permeabilize mitochondria is not well understood. Two models have been proposed to explain the mechanism of MOMP induction: in one model, BAX and BAK can form proteinacious pores in the mitochondria outer membrane, while in the other model, BAX and BAK

form lipidic pores on the outer membrane of mitochondria [131]. This leads to the release of cytochrome c into the cytoplasm, where it binds to APAF-1. This in turn leads to activation of APAF-1 and to the formation of heptamers, which recruit and activate caspase-9. Activated caspase-9 cleaves and activates effector caspase-7, which leads to apoptosis.

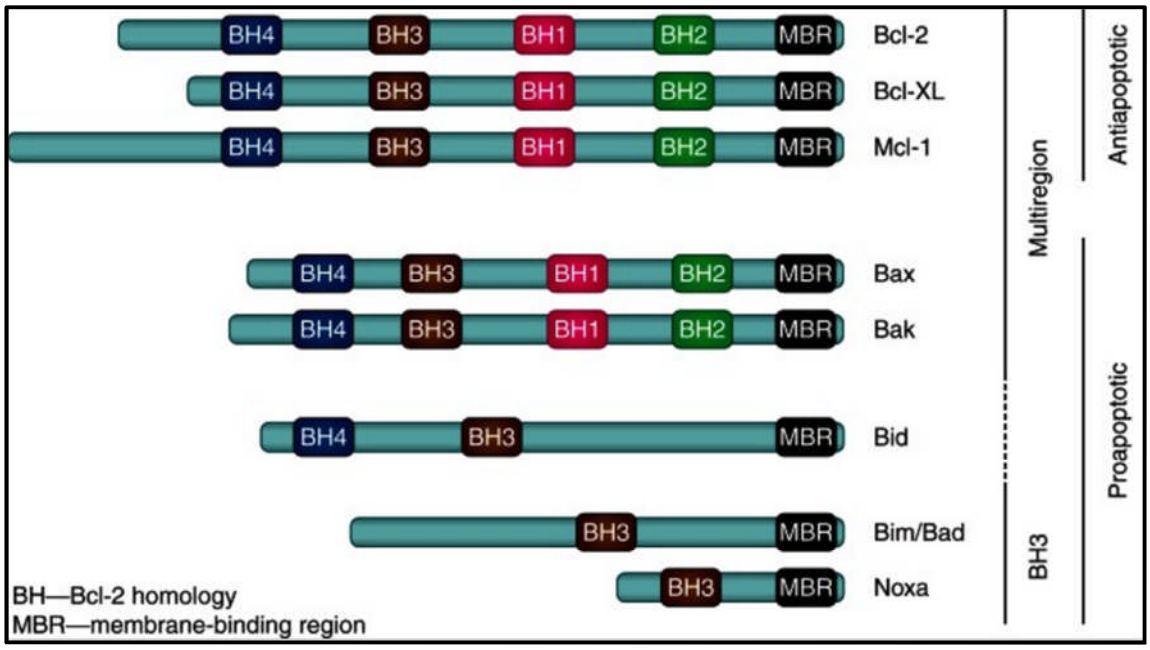

Figure 1-9 Key BCL-2 family proteins

The BCL-2 family members possess at least one BH domain. Most members also contain membrane binding region (MBR) on their C-terminal. Source: [130]

The anti-apoptotic BCL-2 family members inhibit apoptosis by preventing MOMP. MOMP might be induced by pro-apoptotic BCL-2 family members only after cells have resisted the action of anti-apoptotic BCL-2 family members. Inhibition of the anti-apoptotic BCL-2 family members using small molecules facilitates the pro-apoptotic BCL-2 family members to surpass the anti-apoptotic threshold, thereby leading to MOMP.

1.5.2.4 Chemotherapeutic agents used in this study

Suberoyl anilide hydroxamic acid (SAHA): This drug is also called Vorinostat and is a histone deacetylase inhibitor. It is found to inhibit the transcription of several anti-apoptotic proteins including cFLIP which prevents the activation of extrinsic apoptotic pathway[132, 133]. A significant importance is given to this drug as it is reported to inhibit cFLIP and underwent a Phase III clinical trial for treatment of MPM as a second line therapy. The results of this trial were not yet available in public domain.

LCL161: This drug is classified as a SMAC mimetic as it degrades the cIAP1/2 proteins and inhibits the function of XIAP protein. This drug is being developed by Novartis and is currently being investigated in combination with paclitaxel in a Phase II clinical trial of solid tumours.

Obatoclax mesylate (Obatoclax): Obatoclax is a small molecule indole bipyrrole compound that antagonises anti-apoptotic BCL-2 family members: BCL-2, BCL-X_L, BCL-w and MCL-1[134]. It neutralises these anti-apoptotic BCL-2 proteins and thereby facilitates MOMP and facilitates apoptosis.

SNS-032: SNS-032 is a CDK9 inhibitor and CDK9 inhibition results in the downregulation of cellular cFlip and MCL-1 at both the mRNA and protein levels. Treatment with a combination of SNS-032 and TRAIL resulted in a synergistic increase in cell death *in vitro* and in orthotopic lung cancer xenografts *in vivo* [135]. SNS-032 has also been reported to affect the transcription of XIAP [136]. Thus, this drug is promising as it simultaneously targets cFLIP, the BCL-2 family anti-apoptotic protein MCL-1 and also the IAP family protein XIAP.

1.6 Mesenchymal stem cells (MSCs)

MSCs are a type of bone marrow-derived stem cell (BMSC) that adhere to plastic and can differentiate into osteoblasts, chondrocytes and adipocytes. MSCs were initially identified in the bone marrow but have since been found in many other organs of the body, including muscle, amniotic fluid and adipose tissue [137-140]. They do not possess any unique markers so their identification relies on expression of CD73, CD90 and CD105, as well as a lack of expression of CD34, CD45 and other haematopoietic stem cell markers [141].

MSCs lack expression of MHC class II and its co-stimulatory molecules CD80, CD86 and CD40 [142]. MSCs show low immunogenicity and this may mean that allogeneic MSCs are incapable of eliciting an immune response when used in immunocompetent patients. This would avoid the need for human leucocyte antigen (HLA) matching and would allow the generation of an 'off-the-shelf' therapy [143]. This paves the way for using MSCs as cell-based therapeutic vectors for the treatment of cancers. Indeed, clinical trials using MSCs for treatment of a wide variety of diseases including graft versus host disease (GVHD) and Crohn's disease have shown that the delivery of allogeneic MSCs is safe. In addition, MSCs are easily extracted from the bone marrow and can be readily expanded, showing up to 50 population doublings in 10 weeks [144]. Indeed, these properties may enable the creation of MSC cell banks.

1.6.1 MSC homing to tumours and the mediators involved

It has been widely demonstrated that MSCs home to and infiltrate into areas of new stroma formation possibly forming crucial stromal support [145]. This has been shown in several models, including lung metastasis [146, 147], Kaposi's sarcoma [148] and

glioma [149]. However, there is little evidence to suggest that these cells integrate into tissues and what their role might be within the tumour environment is unknown.

The precise mechanism by which MSCs home to tumours is not been fully mapped, but it was widely accepted that the chemokines released by tumours are involved in recruiting MSCs. This hypothesis is supported by the presence of a wide variety of chemokine receptors on the MSC cell surface and by experiments carried out *in vitro* and in mouse models that show a change in MSC homing capabilities as a result of the over- or underexpression of these receptors [150-154]. There are several different ligands and receptors postulated to play a role in MSC migration. However, there is general agreement that the studies that have so far been carried out have not been able to pinpoint the exact chemokine and its respective receptor that governs MSC tumour tropism, and there may indeed be a combination of receptors and chemokines responsible.

CXCL12 and its receptor CXCR4 have generated particular interest in the context of MSC homing. Mice in which either CXCR4 or CXCL12 have been knocked out die *in utero* and the role of this chemokine axis in the migration of haematopoietic cell migration has been well characterised [155, 156]. Several tumours are known to release CXCL12 [157, 158], which suggests that this chemokine axis may also be important in the migration of MSCs to tumours. Interestingly, studies have shown that overexpression of CXCR4 on MSCs leads to increased MSC migration to sites of infarcted myocardium [159]. However, knockdown of CXCR4 did not mitigate this MSC homing capability [160]. It is therefore possible that the CXCL12 ligand and its receptor CXCR4 might be capable of inducing some MSC migration but that these are not the

only receptors responsible for MSC homing. This is further substantiated by the fact that some MSCs do not express this receptor at all but still migrate [154].

Work on MSC homing is complicated and varying results may be explained by a number of factors. MSCs are extracted from various tissues and their lack of unique identification markers means that different populations are probably being used by different groups, making cross referencing results difficult. Furthermore, variations in *in vitro* culture conditions and the passage numbers of cells that are used alter the expression of cell surface receptors [152, 161]. This is important as MSC migration is highly likely to be dependent on the expression of a number of chemokine receptors on their cell surface [162, 163]. This means that there is a lack of consistency in the MSCs being used in different laboratories and this probably explains the variability in results that have been seen.

1.6.2 MSCs as delivery vectors for pro-apoptotic agents

The homing capability of MSCs can be exploited to deliver pro-apoptotic agents straight into the tumour microenvironment. Several studies have used this technique with varying success; these studies are summarised in Table 1-1

The majority of studies have used MSCs engineered to express and deliver a variety of cytokines. The immune modulatory cytokine IL-2, when overexpressed by MSCs, has been shown to improve immune surveillance against tumours and to reduce metastasis from a subcutaneous model [164]. Similarly CX_3CL1, a chemokine that activates both T cells and natural killer cells, when delivered by MSCs leads to a substantial decrease in the number of lung tumours that are induced by intravenous delivery of melanoma cells [165]. Interferon-β, which induces differentiation and S-

phase accumulation leading to apoptosis, when expressed by genetically engineered MSCs suppresses pancreatic tumours, prostate cancer, breast cancer and melanoma in animal models [166-169]. Finally, a similar beneficial effect occurs with the delivery of IL-12-expressing MSCs in renal cell carcinoma [170].

An exciting group of viruses that selectively target and inhibit tumour cells without affecting normal cells are termed oncolytic viruses [171]. These viruses are genetically engineered to selectively infect and destroy tumour cells. However, their delivery to the tumour site remains a major challenge [172]. Using MSC tumour tropism raises a new possible mode of virus delivery. MSCs would act as carrier vectors for the oncolytic virus and this delivery mechanism comes with the added advantage of keeping the recipient immune response to the virus to a minimum. This technique has been successfully used in several tumour models, including breast and lung metastasis [173] [174] and ovarian cancer [175]. Indeed a recent study has demonstrated the feasibility of treating ovarian cancer using MSC-oncolytic virus, paving way for a Phase I clinical trial [176].

MSCs have also been engineered to express an enzyme that converts a prodrug into a cytotoxic agent at the site of tumours. This has been successfully used in a glioma model [177] in which MSCs were engineered to express the herpes simplex virus-thymidine kinase (HSV-tk), which converts the prodrug ganciclovir at the site of tumours. However, this approach may be limited by the toxicity to the carrier MSCs. A similar approach has been used to convert 5-fluorocytosine (5-FC) to 5-fluorouracil by MSCs expressing cytosine deaminase both in melanoma [178] and colon cancer models [179]. MSCs have also been genetically modified to express the rabbit carboxylesterase

enzyme (rCE), which can efficiently convert the prodrug CPT-11 into the active drug SN-38, which acts as a potent topoisomerase I inhibitor [180]. In a different approach, nano-sized exosomes, which are mass produced by MSCs [181], have been extracted and used to deliver a variety of therapeutics including siRNA [182].

There is increasing interest in the use of nanoparticles in a variety of biomedical applications. However, the ability to deliver them efficiently to a disease that is systemically distributed remains a key challenge. Again, MSC tumour tropism has been used as a method of tumour targeting. In one study, a silica nanorattle-doxorubicin drug delivery system was efficiently anchored to MSCs via specific antibody targeting of CD90 on the MSC cell surface and was successfully delivered to a glioma model [183]. Interest has also arisen in using nanoparticles as a method of tracking MSC homing to tumours. Indeed, iron oxide nanoparticles phagocytized by MSCs have been used to identify MSC homing to pulmonary lung metastases using magnetic resonance imaging (MRI) [147].

Table 1-1 Pro-apoptotic agents delivered by MSCs

Agent	Rationale	Model	References
IL-2	Immune-modulatory	Subcutaneous model	[164]
CX_3CL	Activates T cells and NK cells	Melanoma lung metastasis	[165]
Interferon-β	Induces differentiation and S-phase arrest	Pancreatic cancer, prostate cancer, breast cancer and Melanoma	[166-169]
IL-12	Activates T cells and NK cells	Renal cell carcinoma	[170]
Oncolytic virus	Destroys tumours by viral infection	Breast cancer, lung cancer, ovarian cancer and lung metastasis	[171-176]
HSV-tk	Converts ganciclovir to active cytotoxic drugs	Glioma	[177]
Cytosine deaminase	Converts 5-fluorocytosine to 5-flurouracil	Melanoma and colon cancer	[178, 179]
rCE	Converts the prodrug CPT-11 to SN-38, a potent topoisomerase I Inhibitor	Glioma	[180]
Nanoparticle	Silica nanorattle-doxorubicin	Glioma	[183]
TRAIL	Tumour-specific death ligand	Glioma, MPM, lung metastasis and pancreatic cancer	[146, 184-186]

1.6.3 Immunosuppressive effects of MSCs

The ability of MSCs to home effectively to tumours makes them an attractive therapeutic option. However, MSCs are not merely vehicles that transport the therapies but are cells that have physiological properties.

It is widely accepted that in large numbers MSCs possess immunosuppressive effects *in vitro*. They are capable of arresting immune cells in G0/G1 phases, thus preventing the S-phase entry and the subsequent cell division. This has been demonstrated in T cells [187], B cells [188] and dendritic cells [189]. This leads to reduced cytotoxic capability of T cells and antibody production of B cells. MSCs also exert an immunosuppressive effect through the activation of regulatory T cells. These properties of MSCs have been clinically exploited for the treatment of GVHD after bone marrow transplantation [190].

These anti-inflammatory effects have been investigated in a number of clinical trials in inflammatory conditions such as inflammatory bowel disease and COPD, and in other diseases such as cardiac disease. Several studies show enhanced cardiac function [191-194] and reduced infarct size [193] following injection of MSCs after myocardial infarction and chronic ischemic heart failure. The exact mechanisms of this effect remain to be characterised but have been attributed to the anti-inflammatory properties of MSCs. These anti-inflammatory properties have also been demonstrated in murine models of pulmonary fibrosis and acute lung injury and are thought to be the result of the paracrine effect of secreted factors on immune cells [195]. The Battacharya laboratory has also shown that MSCs can protect against acute lung injury (ALI) by donating their mitochondria to alveolar epithelial cells [196].

However, the immunosuppressive capability of MSCs could be a double-edged sword. Their immunosuppressive nature could potentially interfere with any physiological anti-cancer immune cell function in the tumour environment.

1.6.4 Direct effects of MSCs on tumour biology

Reports on the effects of untransduced MSC on tumour growth are mixed. The majority of work suggests that MSCs not only home to tumours but also have intrinsic anti-tumour properties. MSCs alone are therapeutically beneficial in a murine glioma model [197], in our studies of pulmonary metastases and in a breast cancer metastasis model: either intravenous or intratumour delivery of MSCs significantly reduced tumour growth and metastasis [106]. The mechanism of this anti-tumour effect is not fully understood, although MSCs have been shown to downregulate many pro-survival genes, such as AKT in a Kaposi's sarcoma mouse model [148] and NF-κB in hepatoma and breast cancer cells [198].

However, in a specific context MSCs appear to be tumour promoting This was demonstrated by when tumours developed in mice after subcutaneous co-administration of MSCs with allogeneic melanoma cells but not after administration of allogeneic melanoma cells on their own [199]. This effect was attributed to MSCs suppressing the host immune reaction to the allogeneic melanoma cells.

As discussed earlier, MSCs produce a wide array of chemokine, cytokines and growth factors. They may also produce and secrete growth factor signalling molecules that promotes survival in tumour cells, resulting in enhanced tumour burden and metastasis. It has been demonstrated that MSCs enhance the *in vivo* growth of

Burkett's lymphoma cells through a VEGF-dependent mechanism [200]. Furthermore, the growth of breast cancer cells was augmented by IL-6 secreted by MSCs via STAT3 activation [201, 202]. It has also been shown that MSCs can downregulate cyclin D2 and arrest chronic myeloid leukaemia cells in GO/G1 phase, preserving their proliferative capacity and reducing apoptosis *in vivo* [189]. Furthermore, under the nutrient-depleted conditions of the tumour microenvironment, MSCs use autophagy for survival and secrete anti-apoptotic factors that facilitate solid tumour survival and growth in breast cancer cells [203].

Another important and serious concern is the question of whether MSCs might themselves undergo malignant transformation. Karyotype abnormalities have been noticed after *in vitro* passage of murine MSCs [204-206] and transformations of bone marrow-derived cells have been implicated in a murine gastric carcinoma model [207]. However, human MSCs have stable karyotypes in culture and exhibit senescence, with shortening telomeres over a 44-week culture period [208]. There have been about 300 clinical trials in ClinicalTrials.gov injecting MSCs for cell therapy in a range of diseases and there have been no reported incidents of malignant transformation of MSCs.

1.6.5 From bench to bedside

Developing a cellular therapy using MSCs as delivery vectors is the ultimate goal of this area of research and MSCs have exhibited the potential for clinical translation. MSCs can be easily isolated, cultured in flasks and genetically modified. Their allogeneic application confers on them an added advantage of being a possible 'off-the-shelf' therapeutic. Their ability to target metastases and to provide a high local concentration of their cargo makes them unique and promising as cancer therapeutics.

Many Phase I and Phase II clinical trials using MSCs for a variety of diseases have been recorded in the largest clinical trial database, ClinicalTrials.gov. The diseases MSCs are being used to treat include GVHD, ischemic cardiac disease, Crohn's disease, COPD and many others [209]. However, there are no reported trials using MSCs as delivery agents for tumour therapy to date. Given the potential therapeutic benefit of using MSCs to deliver anti-tumour agents, this technique warrants further investigation and optimisation.

1.6.6 MSCs as delivery vectors for TRAIL

The selective tumour-specific cytotoxicity of TRAIL has led to it being hailed as a 'silver bullet' for the treatment of cancer. However, its limited bioavailability and its poor pharmacokinetic profile have made its use a serious challenge. The half-life of TRAIL is very short at only around 30 minutes [210]. To circumvent this problem, mesenchymal stem cells can be engineered to constitutively express TRAIL (MSC-TRAIL). This has been shown to be effective in several models, including glioma [184] pancreatic cancer [110] and a lung metastasis model [179]. MSC-TRAIL cells home into the tumours and, through their expression of TRAIL, lead to selective apoptosis of tumour cells with no detectable cytotoxicity to the surrounding tissue [146, 186].

1.7 Hypothesis and aims

The cancer cell-killing capacity of MSC-TRAIL can be enhanced by using the most effective form of TRAIL in combination with chemotherapeutic agents and by identifying a biomarker to predict TRAIL sensitivity.

- Aim 1: To identify whether the full-length or the soluble form of TRAIL is better at killing tumour cells when expressed by MSCs.
- Aim 2: To increase the cancer cell-killing capacity of MSC-TRAIL cells by combining them with novel chemotherapeutic agents that inhibit the anti-apoptotic proteins involved in the TRAIL pathway.
- Aim 3: To identify a biomarker to predict sensitivity to TRAIL to enable patient-specific treatment.

CHAPTER II

Materials and Methods

2 MATERIALS AND METHODS

2.1 General chemicals, solvents and plastic ware

All chemicals used were of analytical grade or above and obtained from Sigma Aldrich (Poole, UK) unless otherwise stated. Water used for preparation of buffers was distilled and deionised (ddH_2O) using a Millipore water purification system (Millipore R010 followed by Millipore Q plus; Millipore Ltd., MA, US). Polypropylene centrifuge tubes and pipettes were obtained from Becton Dickenson (Oxford, UK).

2.2 Cell Culture

2.2.1 Cell lines

All sterile culture media, sterile tissue culture grade trypsin/EDTA, tissue culture antibiotics and fetal bovine serum (FBS) were purchased from Invitrogen (Paisley, UK) unless otherwise stated. Sterile tissue culture flasks and plates were purchased from Nunc (Roskilde, Denmark) unless otherwise stated.

The cell culture media used are Dulbeccos' modified Eagle's medium (DMEM), Dulbeccos' modified Eagle's medium nutrient mixture F-12 (DMEM/F-12) and Roswell Park Memorial Institute 1640 (RPMI) supplemented with 4mM L-Glutamine, 50U/ml penicillin and 50µg/ml streptomycin and 10% (v/v) FBS. Cancer cell lines were used, including 5 lung cancer lines, A549, NCI-H460, NCI-H727, NCI-H23 and PC9, 11 pleural mesothelioma lines, JU77, NCI-H2052, H2795, H2804, H2731, H226, H2810, H2818, H226, H2452 and H2869, 3 colon cancer lines, Colo205, HT29 and RKO, 2 renal cancer lines, RCC10 and HA7-RCC, 1 human oral squamous cell carcinoma line, H357, and 1 human breast adenocarcinoma line, MDAMB-231. HeLa, 293T, A549, H357 and

MDAMB-231 were obtained from Cancer Research UK. JU77 cells were a kind gift from Professor Bruce Robinson (Lung Institute of Western Australia, University of Western Australia). H226 cells were a kind gift from Professor Peter Szlosarek (Barts cancer institute, London). Other cell lines were kind gifts from the Wellcome Trust Sanger Institute, Cambridge, UK. H226, NCI-H23, HT29 and Colo205 cells were cultured in RPMI-1640 medium with 10% fetal bovine serum (FBS); H2818 and RKO cells were cultured in DMEM/F-12 with 10% FBS; H357 cells were cultured in DMEM/F-12 (3:1) supplemented with 0.5 μg/ml hydrocortisone and 10-10 M cholera toxin (Sigma-Aldrich, UK), 10 ng/ml epithelial growth factor (EGF) (Cambridge Biosciences, UK) and 5 μg/ml human insulin (MP Biomedicals, Europe); and all other cell lines were grown in the DMEM containing 10% FBS.

Media was changed every 3 days. Cells were grown until approximately 80% confluent and mobilised by washing with sterile phosphate-buffered saline (PBS) followed by 0.05% trypsin in EDTA. After detachment cells were pelleted by centrifugation at 300g for 5 minutes and plated into 75 or 175 cm^2 tissue culture flasks at ratios of 1:3 to 1:10 every 5-10 days depending on rate of proliferation. For long term storage of cells, harvest and centrifugation was performed as described and the cell pellet was resuspended in 1ml of freezing medium; 50% (v/v) medium, 40% (v/v) FBS and 10% (v/v) dimethyl sulfoxide (DMSO). The cell suspension was transferred to a cryovial, placed in an isopropanol freezing container and left at -80^oC for 24 hours to allow slow freezing. Cells were then transferred to liquid nitrogen for long term storage. For subsequent use, cryovials were removed from the liquid nitrogen and thawed rapidly in a water bath at 37^oC. The cell suspension was added to standard cell culture media

and plated in flasks overnight to allow cells to adhere. Once cells were adherent medium was exchanged for fresh medium.

2.2.2 Mesenchymal stem cell culture

Well-characterized human adult MSCs (passage 1) were purchased from the Texas A&M Health Science Center. They were cultured in α-minimum essential medium (αMEM) supplemented with 4mM L-Glutamine, 50U/ml penicillin and 50µg/ml streptomycin and 16% (v/v) FBS.

Human adult MSCs were plated at 150-200 cells/cm^2 every 10-14 days depending on the rate of proliferation. Media was changed every 3 days. Cells were grown until approximately 80% confluent and mobilised by washing with sterile phosphate-buffered saline (PBS) followed by 0.05% trypsin in EDTA. After detachment cells were pelleted by centrifugation at 300g for 5 minutes, counted and 35,000-60,000 cells plated into 175 cm^2 tissue culture flasks. For long term storage of cells, harvest and centrifugation was performed as described and the cell pellet was resuspended in 1ml of freezing medium; 65% (v/v) medium, 40% (v/v) FBS and 10% (v/v) dimethyl sulfoxide (DMSO). The cell suspension was transferred to a cryovial, placed in an isopropanol freezing container and left at -80^oC for 24 hours to allow slow freezing. Cells were then transferred to liquid nitrogen for long term storage. For subsequent use, cryovials were removed from the liquid nitrogen and thawed rapidly in a water bath at 37^oC. The cell suspension was added to standard cell culture media and plated in flasks overnight to allow cells to adhere. Once cells were adherent medium was exchanged for fresh medium.

2.3 Stock solutions and additives

All drugs and solutions used in tissue culture were sterile filtered through a 0.22µm filter unless otherwise stated. All solvents were tissue-culture grade. The drugs and solutions were stored as per manufacturer's instructions. The list of additives and drugs used in this study were listed in Table 2-1. Isoleucine zipper TRAIL used in Chapters 5 and 6 was made in the Walczak lab, UCL as per established procedure [211].

Table 2-1 Stock solution of additives and drugs used

Drug/Additive	Solvent	Stock Concentration	Supplier
Polybrene	Water	4 mg/ml	Sigma Aldrich
Ampicillin	Water	100 µg/ml	Sigma Aldrich
Puromycin	Media	100 µg/ml	Invitrogen
D-Luciferin	PBS	10 mg/ml	Regis Technologies Inc. USA
Human recombinant TRAIL	PBS	10 µg/ml	Peprotech
LCL161	DMSO	1 mg/ml	Active Biochem
Obatoclax mesylate	Water	1 mM	Cayman Chemicals
SAHA	DMSO	5 mM	Cayman Chemicals
SNS-032	DMSO	1 mM	Selleckchem

2.4 Lentiviral vectors and transduction

The plasmids were used to generate lentiviral vectors to express GFP, TRAIL, BAP1 and luciferase. The packaging plasmids pCMV-dR8.74 and pMD2.G and ZS-green luciferase plasmid (pHIV-Luc-ZsGreen Plasmid #39196) (Figure 2-1) were obtained from Addgene. The mstrawberry-luciferase plasmid was a kind gift from Dr Scott Lyons (Cancer research UK). All the shRNA expressing plasmids were obtained from Dharmacon through the UCL RNAi library. The lentiviral transfer plasmid approved for clinical use (pCCL-c-Fes-Gfp) was a kind gift from Prof Thrasher, University College London.

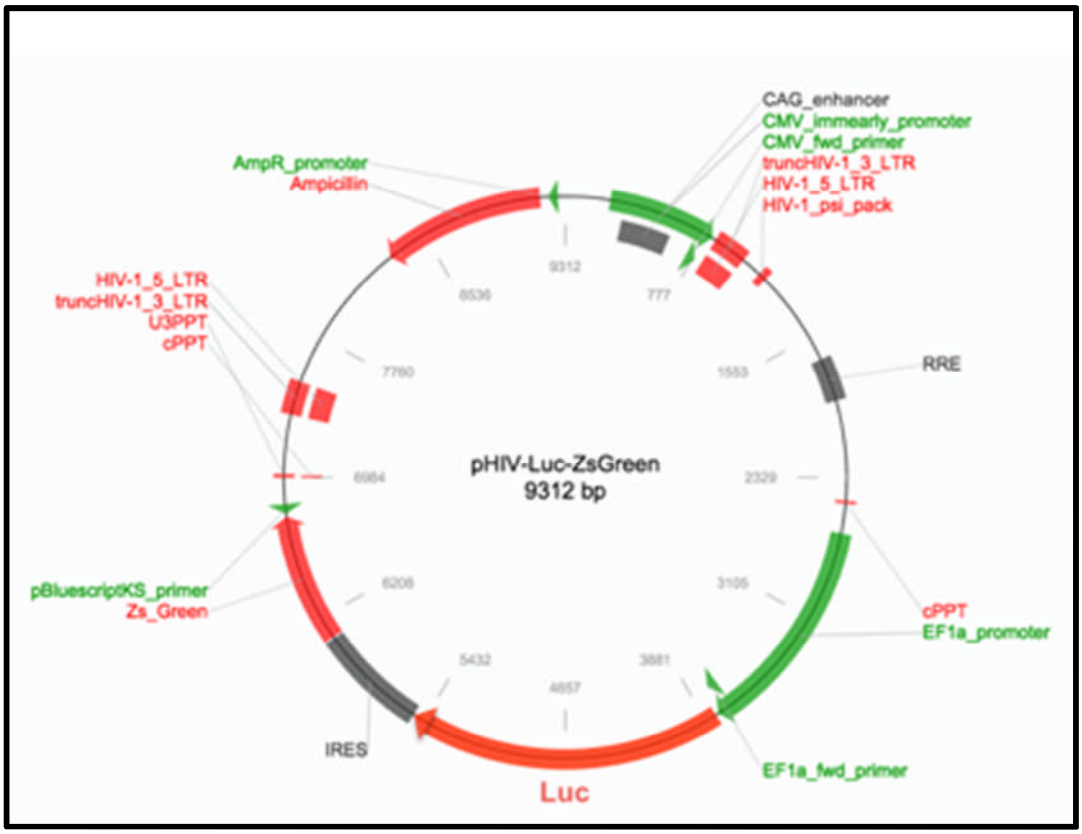

Figure 2-1 pHIV-Luc-ZsGreen vector map

The pHIV-Luc-ZsGreen expresses luciferase through EF1-a promoter. The lentiviral vector contain ampicillin antibiotic resistance gene to facilitate selection of plasmid expressing bacteria. It contains ZsGreen fluorescent protein as an indicator of transduction.

2.4.1 Cloning of TRAIL expressing lentiviral vectors

The construction of the lentiviral vectors for the expression of flT and sT was based on the lentiviral plasmid pCCL-c-Fes-Gfp [212]. The promoter of the backbone plasmid was replaced by the cytomegalovirus (CMV) promoter/enhancer [213] at XhoI and BamHI restriction sites. The CMV promoter/enhancer was amplified by PCR using the pCMV--dR8.74 plasmid as a template. To create the flT vector, the flT-encoding cDNA was amplified by PCR using our previously constructed inducible flT plasmid [214] as a template and inserted into the backbone in place of the GFP sequence using BamHI and SalI sites; the resulting new plasmid being designated pCCL-CMV-flT (Figure 2-2). To create the sT vector, an open reading frame (ORF) encoding an N-terminal truncated extracellular portion of human TRAIL (amino acids 95–281) was amplified by PCR, which was then used as template for sequential PCRs to fuse the isoleucine zipper (MKQIEDKIEEILSKIYHIENEIARIKKLIGERE) [215] in-frame and the murine immunoglobulin K-chain (IgK; 5´-ATGGAGACAGACACACTCCTGCTATGGGTACTGCTGCTCTGGGTTCCAGGTTCCACTGGTGAC-3´) leader sequence [216] to its N-terminal. The obtained sT sequence was inserted into the pCCL-CMV-flT in place of flT via BamHI and SalI sites, creating the sT vector designated pCCL-CMV-sT.

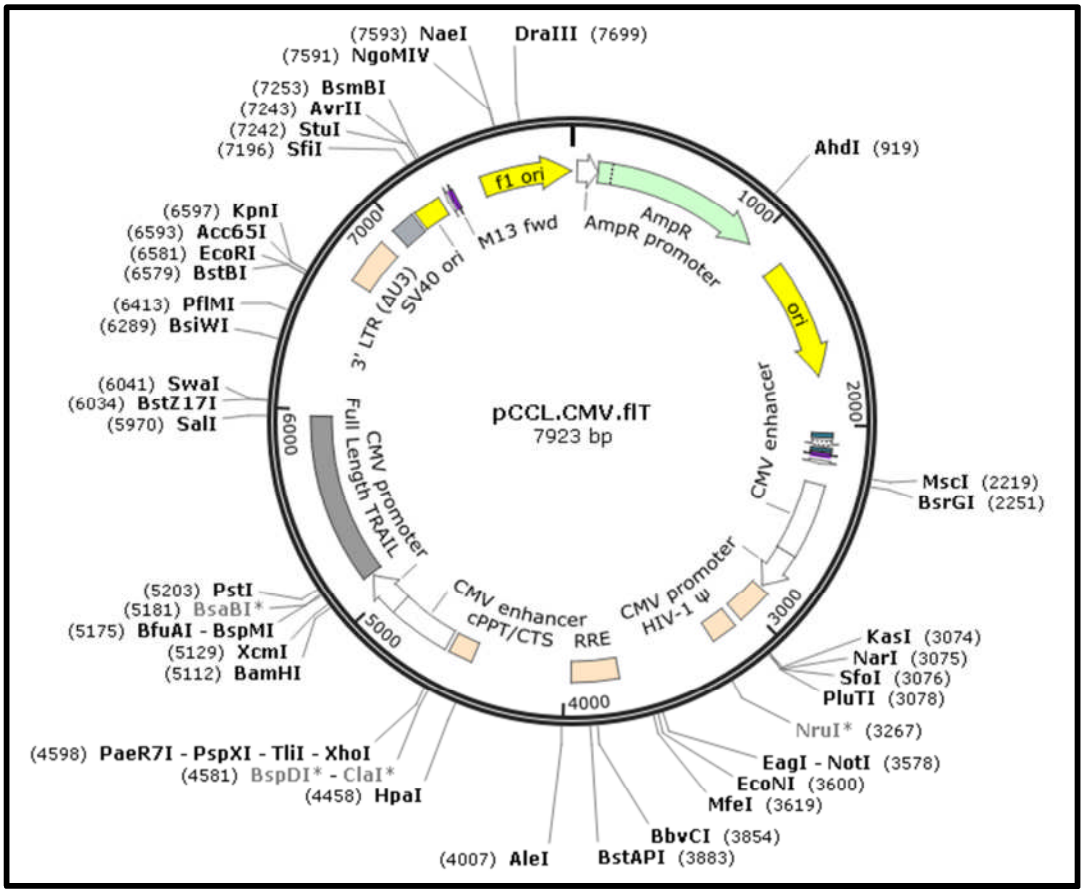

Figure 2-2 pCCL.CMV.FLT vector map

The pCCL.CMV.FLT expresses full length TRAIL through CMV promoter. The lentiviral vector contain ampicillin antibiotic resistance gene to facilitate selection of plasmid expressing bacteria. The full length TRAIL coding region was substituted with IZTRAIL or BAP1 coding sequence as required.

2.4.2 Cloning of BAP1 expressing lentiviral vectors

To create a BAP1 vector, BAP1 coding cDNA was amplified by PCR using a pCMV6-AC BAP1 plasmid (Origene-SC117256) as a template and was inserted into the pCCL-CMV-flT in place of flT via BamHI and SalI sites, creating the BAP1 vector designated pCCL-CMV-BAP1. The C91A, HBM, NLS, L691P and T493A mutations on the BAP1 cDNA were done using Q5 site directed mutagenesis kit (New England Biolabs-E0554) as per manufactures instructions on the pCCL-CMV-BAP1 vector. The primers used are listed in Table 2-2

Table 2-2 Primers used in BAP1 cloning

Primers	Sequence (5'-3')
BAP1 forward	CGTGGATCCGCCACCATGAATAAGGGCTGGCTGGA
BAP1 reverse	GTCGGTCGAC TCACTGGCGCTTGGCCTTGTA
BAP1 C91A mutation forward	ATACCCAACTCTGCTGCAACTCATGCCTTGCTG
BAP1 C91A mutation reverse	CAGCTGGTGGGCAAAGAACATGTTATTCACAATATCATC
BAP1 HBM deletion forward	CGCTGCTGCCAAGTCCCCCATGCAGGAGGA
BAP1 HBM deletion reverse	GCAGCGTCTAGAAAGGCCGGCAGCCGCT
NLS deletion forward	GTCGGTCGACTCAGTCAGGCTTCCGCTGCTTGTGG
NLS deletion reverse	GTCGTTCGAATCAGTCAGGCTTCCGCTGCTTGTGG
BAP1 L691P mutation forward	TGCCTTCCTGAGCCAGCATGGAG
BAP1 L691P mutation reverse	TGCTGGCCAACCCAGTGGAGCAG
BAP1 T493A mutation forward	GCAGACACGGCCTCTGAGATCGGCAGTGCT
BAP1 T493A mutation reverse	ACTCTCATTGCTGGGGGTGGGTGA

2.4.3 Propagation of lentiviral vector plasmids using *Escherichia Coli*

The large scale production of lentiviral vectors requires significant quantities of plasmid DNA. Each plasmid contains a replication sequence and an ampicillin resistance gene to allow replication of the plasmids in *Escherichia Coli (E. coli)*.

2.4.3.1 Bacterial transformation of E. Coli with plasmid DNA

Plasmids were expanded using OneShot TOP10 chemically competent *E. coli* (Invitrogen, Paisley, UK). 1µl plasmid was added to a OneShot and left on ice for 30 minutes before being heat shocked at 42^{o}C for 30 seconds and returned to ice for a

further 2 minutes. 250µl of SOC medium was added to the bacteria and incubated at 37^{o}C for 1 hour on a shaking incubator at 220rpm.

2.4.3.2 Production of single plasmid-transformed bacterial colonies and generation of starter cultures

LB (Luria Bertani) agar plates were made by dissolving 35g LB agar in 1L of dd$H_2$0, autoclaving at 121^{o}C for 15 minutes and cooling to approximately 50^{o}C prior to the addition of 50µg/ml carbenicillin. The LB agar was then poured into 90mm sterile petri dishes (Fisher) and cooled at 4^{o}C until the agar was set. Prior to use LB agar plates were pre-warmed at 37^{o}C.

Different volumes of transformed bacteria (from 10-100µl) were spread onto the agar plates and incubated overnight at 37^{o}C. The following day single bacterial colonies were selected using a sterile loop and used to inoculate 5ml LB broth (Fisher Scientific, Loughborough, UK) containing 50µg/ml carbenicillin in a 15ml falcon tube. LB broth was prepared by dissolving LB broth powder in dd$H_2$0 at 20g/L, autoclaving at 121^{o}C for 15 minutes and allowed to cool to approximately 50^{o}C prior to adding 50µg/ml carbenicillin. Falcon tubes containing the single bacterial colonies were incubated overnight in an orbital incubator at 37^{o}C and 220rpm.

2.4.3.3 Miniprep – Extraction of plasmid from starter cultures

To confirm that the bacteria had been successfully transformed with the plasmid DNA, extraction was performed using the FastPlasmid Mini Kit (Eppendorf, Cambridge, UK). Individual bacterial colonies were tested as follows. 3ml of the starter culture was centrifuged at 2000rpm for 15 minutes after which the bacterial pellet was re-

suspended in 400µl lysis buffer and left for 3 minutes at room temperature. The mixture was transferred to the spin column provided and centrifuged at 13,000rpm for 1 minute, then washed with 400µl of wash buffer and re-centrifuged at the same settings. Finally 50µl of elution buffer was added to the column, incubated at room temperature for 1 minute and centrifuged at 13,000rpm for 1 minute.

2.4.3.4 Restriction digests

All restriction digests were performed using enzymes and buffers from New England Biolabs (Hitchin, UK) as per manufacturer's instructions. DNA was purified using the QIAquick PCR Purification Kit (Clontech, 740609.10) according to the manufacturer's protocol. The purified product was run on a 1% (w/v) agarose gel using a HyperLadder I molecular weight marker (Bioline). An ultraviolet light was used to demonstrate the DNA fragments.

2.4.3.5 Maxiprep - Large scale production and extraction of plasmid DNA

To multiply the plasmid the remaining 2ml of the starter culture was added to 200ml of LB broth containing 50µg/ml carbenicillin and incubated overnight in an orbital incubator at 220rpm and 37^{o}C. DNA was purified using the Purelink HiPure Plasmid DNA Maxiprep Kit (Invitrogen, Paisley, UK) as follows. The bacteria were harvested by centrifugation of the LB broth at 4000g for 10 minutes, the pellet was resuspended in 10ml of resuspension buffer (50mM Tris-HCl pH8, 10mM EDTA) with 20mg/ml RNase A, mixed with 10ml lysis buffer (0.2M NaOH, 1% (w/v) SDS) and left to incubate for 5 minutes to release the plasmid from the bacteria. 10ml precipitation buffer (3.1M potassium acetate pH5.5) was added to precipitate the cell debris and DNA out of solution and centrifuged at 12,000g for 10 minutes at room temperature.

Equilibration filter columns are anion exchange columns which bind negatively charged phosphate molecules on the DNA backbone. These were prepared by adding 30ml equilibration buffer and allowing the buffer to drop through under gravity. Once the columns were prepared the supernatant containing the plasmid DNA was loaded into an equilibration column. The column was washed using 60ml wash buffer (0.1M sodium acetate pH5, 825mM NaCl) to remove RNA, proteins, carbohydrates and other impurities, and finally the plasmid DNA was eluted from the column with 15ml elution buffer (100mM Tris-HCl pH 8.5, 1.25M NaCl). DNA was precipitated by adding 10.5ml isopropanol and centrifuging for 30 minutes at 4500rpm at 4^{o}C. The plasmid DNA was then washed by re-suspending in 70% ethanol and was centrifuged for 15 minutes at 4500rpm at 4^{o}C. The DNA pellet was allowed to air dry before being resuspended in 500µl TE buffer (10mM Tris-HCl pH8, 0.1mM EDTA).

2.4.3.6 DNA Quantification

The DNA was quantified and purity checked using a NanoDrop 8000 spectrophotometer. Nucleic acids absorb ultraviolet light in different patterns and the amount of light absorbed at different wavelengths is an indication of their purity. The ratio of absorbance at 260nm and 280nm (A260/A280 ratio) gives a measure of purity and a ratio of >1.8 is expected for pure DNA.

2.4.4 Lentivirus production

Lentivirus is produced by transfecting 293T cells with transfer and packaging plasmids using JetPEI. On day one, the 293T cells were seeded into 18 x T175 flasks to reach 80-90% confluence the following day for transfection (usually split confluent cells 1:2 or 1:3). On the following day, 20µg transfer plasmid, 7µg pMD.G2 and 13 µg pCMV-

dR8.74 were added to 1ml of 150mM sodium chloride solution and vortexed for 10 seconds and passed through 0.2 µl filter. 80µl JetPEI was added to 1ml 150mM NaCl and vortexed for 10 seconds. NaCl/PEI solution was added to the NaCl/DNA solution, vortexed for 10 seconds and incubated at room temperature for 15-30 minutes. The obtained NaCl/DNA/PEI solution (2ml) was added to 13ml DMEM and added into T175 flask containing 293T cells. The medium was replaced with 20ml DMEM after 4 hours. The medium in the T175 flask was removed into a sterile container after 24 hours and the T175 flasks were replaced with fresh media which was also extracted after 24 hours. Lentivirus in supernatants were concentrated by ultracentrifugation at 17,000 RPM (SW28 rotor, Optima LE80K Ultracentrifuge, Beckman) for 2 hours at 4^{o}C. The virus was resuspended in DMEM, aliquoted and stored at -80^{o}C until further use.

2.4.5 Titration of lentivirus

The amount of collected virus generated by the above method was quantified by titrating different dilutions of the virus with 293T cells. In a 12-well plate, fifty thousand cells were seeded onto each well and the following day, at 30-40% cell confluency, the medium was exchanged for medium containing virus dilutions of 1/100, 1/1000, 1/10000, and 1/100000 and 4µg/ml of polybrene, which is a cationic polymer enabling efficient cellular uptake of the virus. After 48 hours, the cells were trypsinized and looked for the protein of interest. For flow cytometry detection of TRAIL expression, cells were stained with a 1:10 dilution of phycoerythrin (PE)-conjugated mouse mAb against human TRAIL (Ab47230, Abcam, UK). For flow cytometry detection of BAP1 expression, cells were stained with a 2:100 dilution of mouse mAb against BAP1 (Santa Cruz-SC28383) and then stained with AF488 conjugated anti-mice antibody (Invitrogen) at 1:200 dilution. For those viral vectors

that carry a florescent protein (GFP, mstraberry or ZS-green), staining was not required. The percentage of positive cells at each viral dilution was assessed by flow cytometry. The FACS LSRII was used for the purpose. The viral titre was calculated in virus particles/ml as below:

$$\text{Viral titre} = \frac{\text{\% of positive cells x number of cells plated}}{\text{Volume of virus added (in ml)}}$$

2.4.6 Transduction

Cells were transduced with viral particles at the required multiplicity of infection (MOI). Cells were seeded onto wells or flasks as required. An exact number of cells was also seeded onto an additional well or flask which was used to count the cells after trypsinsization on the following day. The medium was exchanged for medium containing virus at the required MOI based on the number of cells and 4μg/ml of polybrene, which is a cationic polymer enabling efficient cellular uptake of the virus. The media was exchanged with fresh culture media after 4 hours. The effectiveness of the transduction was measured after staining the protein of interest in the transduced cells and assessing by flow cytometry.

2.5 RNA Interference (RNAi)

siRNA and shRNA were used to knock down protein expression in tumour cell lines. The siRNA used were cIAP1 (Catalogue number 4390824 Silencer select validated siRNA ID:S1449 Lot no:ASO0R8MO), cIAP2(Catalogue number 4392420 Silencer select siRNA ID:S1452 Lot no:ASO0T4PG) obtained from Ambion (Life Technologies). The

Silencer Select Negative Control No. 1 siRNA was a non-targeting negative control siRNA and used as negative control. All siRNA were reconstituted in TE buffer and diluted in RNase free water to make a stock of 1µM concentration. Interferin (Polyplus Transfection). was used as the transfection reagent.

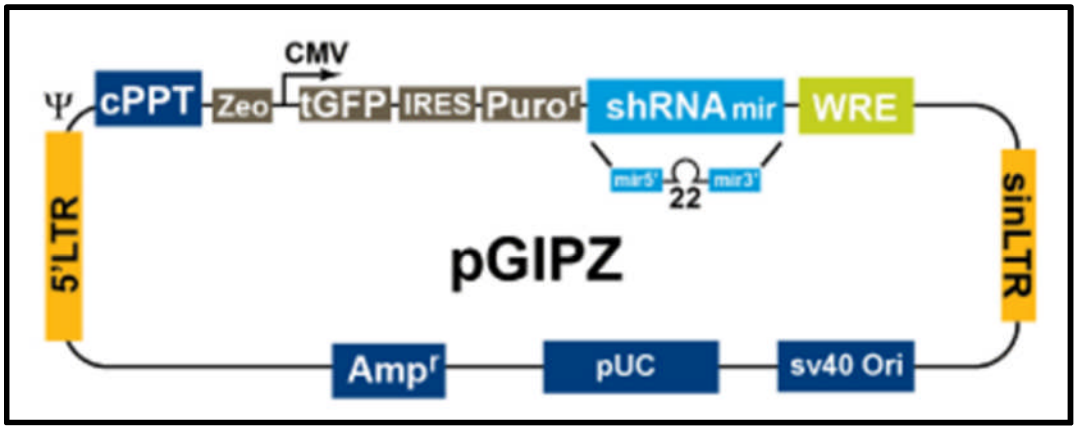

Figure 2-3 GIPZ shRNA vector map

The GIPZ shRNA expresses 22 nucleotide shRNA mir through a CMV promoter. The lentiviral vector contain ampicillin antibiotic resistance gene to facilitate selection of plasmid expressing bacteria. It contains GFP and puromycin antibiotic resistance gene to aid in selection of transduced cells.

The shRNA hairpins contained within the GIPZ vector were based on the endogenous mir-30 (Figure 2-3). By mimicking an endogenous RNA, the GIPZ hairpin is efficiently processed in the cells allowing for a more effective knockdown of the gene of interest. Bacteria expressing lentiviral vector plasmids with GIPZ hairpins were obtained from Dharmacon through UCL RNAi library. They were expanded in LB broth, plasmids extracted and virus made by the procedures described above. The tumour cell lines were transduced with lentivirus, and treated with puromycin to select the pure population expressing shRNA. The knockdown was confirmed by western

blotting. The clones used in this study are cIAP1 (GIPZ Lentiviral shRNA-V3LHS_399304), cIAP2 (GIPZ Lentiviral shRNA-V2LHS_94565) and BAP1 (GIPZ Lentiviral shRNA-V2LHS_4147).

2.6 Western blots

2.6.1 Sample collection and preparation

Cells were grown in T75 flasks or a 6 well plate. Supernatants were collected and centrifuged (300g, 5mins) to remove cells and cell debris and then stored prior to western blotting at -80^{o}C. Cell lysates were obtained by lysing the cells in RIPA buffer (1% (v/v) Igepal Ca-630, 0.5% (w/v) Sodium deoxycholate, 0.1% (w/v) sodium dodecyl sulphate (SDS)) supplemented with complete protease inhibitor cocktail (Complete-mini; Roche Diagnostics Ltd.) and left to stand for 1 hour in -80^{o}C. The cell layer was subsequently scraped with a cell scraper and the lysate centrifuged (16200g, 10 minutes, 4^{o}C) to remove insoluble cell debris. Samples were stored at -80^{o} C.

2.6.2 BCA protein assay

To ensure equivalent amounts of protein were loaded for different samples the protein concentration of cell lysates, supernatants and serum were assessed using the bicinchoninic acid (BCA) protein assay (Thermo Fisher Scientific, IL, US). The BCA assay relies on two reactions; firstly the peptide bonds in the protein reduces Cu^{2+} to Cu^{+}, a reaction that is dependent on the amount of protein present and secondly the bicinchoninic acid chelated with the Cu^{+} ions to produce a purple coloured solution. This colour strongly absorbs light in a linear fashion at 562nm. Standards were made by dissolving BSA in PBS at concentrations from 20µg/ml to 2000µg/ml.

20µl of each sample along with 20µl standard were added to a 96-well plate then 180µl of BCA working solution was added to each well and agitated on a plate shaker for 30 seconds. The plate was then incubated at 37°C for 30 minutes before reading the absorbance at 550nm. The absorbance of the samples was compared to those of known protein concentrations to determine the protein concentration.

2.6.3 Western blotting procedures

Samples were diluted in dH2O to equivalent protein concentrations and mixed with 5x Laemmli Buffer (3.125mM Tris-base pH 6.8, 10% (w/v) SDS, 20% (v/v) glycerol, 50mM Dithiothreitol (DTT), in dH2O with bromophenol blue). The samples were then incubated on a heat block for 10 min at 70°C and placed on ice prior to loading on the western blot gel. A 10% SDS-polyacrylamide resolving gel (10% (v/v) acryamide mix (0.27% bis-acrylamide)), 0.04% (v/v) tetramethylethylenediamine (TEMED), 0.1% (w/v) ammonium persulphate (APS), 0.1% (w/v) SDS, 0.3M Tris-base (pH8.8), in dH2O) with a 2.5% stacking gel (2.5% acrylamide mix, 0.05% TEMED, 0.05% APS, 0.05% SDS, 0.06M Tris (pH6.8), in dH2O) was prepared and 25µl samples added to the wells. 5µl of PageRuler pre-stained protein ladder (Thermo scientific) was also loaded. The gel was run at 150V in Tris/Glycine/SDS running buffer (0.25M Tris-base, 1.92M Glycine, 1% SDS, in dH2O).

Following separation, the gel was removed from the cassette and proteins were transferred onto a nitrocellulose membrane using an iBlot transfer system (Invitrogen) on program 3 for 7 minutes. The quality of protein transfer was assessed by briefly staining the membrane with 0.1% (w/v) PonceauS solution and then the blot was placed in Tris-buffered saline (TBS)(20mM Tris-base, 150mM NaCl, pH7.4) containing 0.1% (v/v) Tween20 (TBST). Blots were incubated with blocking buffer containing 5%

(w/v) non-fat dry milk in TBST for 1 hour. Blots were then incubated with primary antibodies in 5% (w/v) BSA in TBST overnight at 4°C. All blots were then washed 3 x 5 minutes in TBST and incubated for 1 hour at room temperature with HRP-conjugated secondary antibody. The antibodies used in this study are listed in Table 2-3. After further washing 3 x 5 minutes in TBST, 1 ml of Luminata western HRP chemiluminescence reagent (Millipore) was applied to the membrane and incubated for 3 minutes. Excess reagent was drained off and immune-reactive bands were visualized with the help of an ImageQuant LAS 4000 (GE Healthcare).

Table 2-3 Antibodies and their dilutions

Antibody	**Manufacturer**	**Catalogue number**	**Source**	**Dilution**
cIAP1	Cell signalling technology	7065	Rabbit	1:1000
cIAP2	Cell signalling technology	3130	Rabbit	1:1000
BAP1	Santa Cruz biotechnology	SC28383	Mouse	5:1000
a-Tubulin	Cell signalling technology	9099	Rabbit	1:2000
Livin	Cell signalling technology	5471	Rabbit	1:1000
Survivin	Cell signalling technology	2803	Rabbit	1:1000
TRAIL	Cell signalling technology	3219	Rabbit	1:1000
Anti-mice HRP	Cell signalling technology	7076	Horse	1:2000
Anti-rabbit HRP	Cell signalling technology	7074	Goat	1:2000

2.7 Enzyme-linked immunosorbent assay (ELISA)

All absorbance was measured using a Titertec Multiscan MCC/340 plate reader (Labsystems, Turku, Finland) and an automated plate washer was used for all assays.

Assays performed on cell cultures samples were performed in triplicate. ELISAs were performed using the human TRAIL/TNFSF10 Quantikine ELISA kit (R&D Systems, Abingdon, UK).

2.7.1 Sample collection and preparation

Cell supernatants were prepared by removing debris by centrifugation at 300g for 5 minutes. Cell lysates were prepared by washing the cells three times in cold PBS, adding the cell lysis buffer provided at 1 x 10^6 and incubating at 37^{o}C for 30 minutes with gentle shaking. Cells were then centrifuged at 500g for 15 minutes and the supernatant was retained and stored at -20^{o}C until required. Samples were placed on ice for 30 minutes and then centrifuged at 1000g for 15 minutes. The amount of protein was quantified using BCA assay as per the procedure described above.

2.7.2 TRAIL ELISA procedure

The human TRAIL ELISA kit (R&D, Abingdon, UK) was used according to the manufacturer's instructions. 100µl of assay diluent RD1S was added to each well of a 96-well plate. 50µl of samples containing equal amounts of protein were then added and incubated for 2 hours at room temperature on a horizontal orbital plate shaker at 500rpm. The plate was washed four times with wash buffer before adding 200µl TRAIL conjugate to each well and incubating for a further 2 hours on the orbital plate shaker. The plate was washed a further four times, 200µl of a colour substrate solution was added to each well and incubated for 30 minutes at room temperature in the dark. Finally 50µl stop solution was added to each well and the absorbance was measured at 450nm using the plate reader. Readings were compared to known concentrations of human recombinant TRAIL (R&D Systems) which were used to plot a standard curve to

determine the concentrations of TRAIL protein in each sample. Readings were also taken at 540nm and were subtracted from those taken at 450nm to correct for optical imperfections in the plate.

2.8 Protein array

The Human Apoptosis Array kit (R&D systems-ARY009) was used to rapidly detect the relative expression of 35 apoptosis-related proteins in a single sample. The blotting was done as per manufacturer's instructions. Briefly, the protein extract was quantified using a BCA assay. The proteins were incubated on the supplied membrane. HRP-conjugated antibodies were added and chemiluminescent substrate was used to detect the protein spots with the help of ImageQuant LAS 4000.

2.9 Immunofluorescence

Localisation of TRAIL in cells was examined by immunofluorescence staining. For intracellular staining, cells were grown on chamber slides for 2 days, fixed with 4% paraformaldehyde (PFA), permeabilized in 0.1% saponin-containing buffer, blocked in PBS buffer containing 10% FBS and 0.1% saponin, then stained with the PE-conjugated mouse anti-human TRAIL mAb B-S23 (Abcam UK, cat. no. ab47230). The counterstain Alexa-488 conjugated phalloidin (Life Technologies, UK) was also added for labelling filamentous actin (F-actin). For the cell surface TRAIL labelling, cells were stained with PE-conjugated anti-TRAIL Ab after fixation and blocking but before permeabilization and F-actin counterstaining. Stained cells were mounted with the ProLong Gold Antifade Reagent with DAPI (Invitrogen, UK), viewed and imaged by confocal microscopy (Leica TCS SP2 microscope).

2.10 Cell viability assay

Cell viability assay are done to measure the differences in cell proliferation under different conditions or different treatments. XTT assay was done to quantify the cell viability while crystal violet staining was done to visualize the difference in cell viability.

2.10.1 XTT assay

XTT is a tetrazolium derivative (Applichem-A8088) that measures cell viability based on the activity of mitochondrial enzymes in live cells that reduce XTT and are inactivated shortly after cell death. The amount of water-soluble product generated from XTT is proportional to the number of living cells in the sample and can be quantified by measuring absorbance at wavelength of 475 nm.

Cells were plated into 96-well tissue culture plates with a density of 10,000 cells per well since they will reach optimal population densities within 48 to 72 hours. Chemotherapeutic agents were added after 24 hours. The final volume of tissue culture medium in each well was made up to 100µL. The reagent was activated by adding activation reagent. 25µL of activated reagent was added to each well and incubated for 4 hours. The absorbance of the samples was measured with a spectrophotometer at a wavelength of 475 nm.

2.10.2 CellTitre-Glo assay

The CellTiter-Glo 2.0 Assay (Promega-G9241) provides a homogeneous method to determine the number of viable cells in culture by quantitating the amount of ATP present, which indicates the presence of metabolically active cells. Cells were plated into 96-well tissue culture plates with a density of 10,000 cells per well.

Chemotherapeutic agents were added after 24 hours. The assay was done as per manufacturer's instructions 24 hours after drug treatment.

2.10.3 Crystal violet staining

Cells were plated into 6-well tissue culture plates with a density of 50,000 cells per well since they will reach optimal population densities within 48 to 72 hours. Chemotherapeutic agents were added after 24 hours. Crystal violet staining was done 24 hours after treatment. The Media in the wells was removed and then washed with PBS. The cells were fixed for 5 minutes with 4% PFA and stained for 30 minutes with 0.05% crystal violet solution. The wells were washed to remove nonspecific staining and photographed.

2.11 Apoptosis assessment

Annexin V-based flow cytometry was used to identify apoptosis and death of the cells. Media, including floating cells, was collected from each well. Adherent cells were washed with PBS and mobilised with 0.05% trypsin in EDTA. All cells were collected into centrifuge tubes containing the previously removed media and pelleted by centrifugation (300g, 5 minutes). Cells were washed in medium, centrifuged (300g, 5 minutes) and then re-suspended in Annexin V binding buffer with Annexin V-647 antibody (Invitrogen) in a 1:100 ratio for 40 minutes on ice or 10 minutes at room temperature. 2µg/ml DAPI or PI was then added to each sample before flow cytometry analysis. Annexin V is a 35–36 kDa calcium-dependent phospholipid binding protein that has a high affinity for phosphatidlserine.

Phosphatidlserine is located on the cytoplasmic side of the cell membrane, inaccessible to cell surface binding proteins, in normal viable cells. In apoptotic cells, it is

translocated to the outer plasma membrane, thus exposing it to the external cellular environment and allowing binding of Annexin V. The Annexin V is also able to pass through the membrane of dead cells that have lost their membrane integrity and bind to phosphatidlserine in the interior of the cell. These dead cells however will also stain with the nuclear stains DAPI or PI. Consequently, Annexin V-/DAPI- cells were judged to be viable, AnnexinV+/DAPI- cells were considered to be undergoing apoptosis (early apoptotic phase), and Annexin V+/DAPI+ cells were considered late apoptotic or necrotic, and recorded as dead.

2.12 Active caspase-8 staining

Cancer cells were DiO labelled as per the manufacturer's instruction, before being treated for 24 hours with MSCs expressing TRAIL or GFP to induce apoptosis. The treated cells were harvested, stained with the active caspase-8 inhibitor IETD-FMK-conjugated to sulfo-rhodamine (BioVision, K198-25) as per the manufacturer's instructions and analysed by flow cytometry.

2.13 MSC phenotyping and differentiation assay

MSC phenotyping was carried out by using the human MSC Phenotyping Kit (Miltenyi Biotec, Cat. No. 130-095-198) according to the manufacturer's instructions and cells were analysed by flow cytometry. Differentiation of passage 7 MSCs with or without transductjion was performed using the StemPro Chondrogenesis, Osteogenesis or Adipogenesis Differentiation Kits (GIBCO Invitrogen Cell Culture). Adipocytes were stained with HCS LipidTOX TM Green and DAPI, osteocytes with Alizarin Red S and the chondrogenic pellet with Alcian blue, all according to the manufacturer's instructions.

2.14 Supernatant TRAIL preparation

2 million transduced MSCs were cultured in one T175 flask for 3 days with 20 ml of media. Proteins were concentrated 50-fold using the centrifugal concentration column (Millipore UFC901008, MWCO 10kDa). TRAIL levels in concentrated media were determined using the TRAIL quantification ELISA kit (R&D Systems).

2.15 Co-culture experiments

Human MSCs transduced with the TRAIL were plated at 1:4 ratios with cancer cells which are stained by DiI. 8,000 DiI stained MPM cells were plated together in 100µl of the medium in each well of a 96-well plate. The following day, 2000 MSC expressing TRAIL were added. Chemotherapeutic agents or recombinant TRAIL were added at the same time, if required. AnnexinV/DAPI aoptosis assay was performed 24 hours after treatment.

2.16 Bioluminescent imaging

Bioluminescence is the production and emission of light by living organisms and naturally occurs in fireflies, anglerfish and some species of squid. Luciferase belongs to a family of oxidative enzymes which in the presence of the substrate D-luciferin catalyse its conversion to oxyluciferin and light.

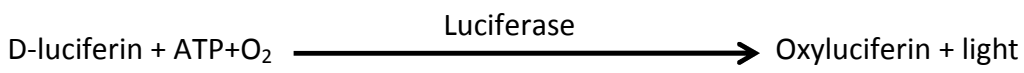

Cells can be transduced with a lentiviral vector containing firefly luciferase and can be used to detect cells both *in vitro* and *in vivo*. In this thesis bioluminescent imaging was used both to identify tumours and as a longitudinal marker of tumour burden.

All imaging was performed using an IVIS® Lumina II imaging system (Caliper Life Sciences). This system uses a sensitive charge-coupled device camera which is cooled to -90^{0}C. This camera converts the photons of light emitted from subjects within a dark sealed imaging chamber into electronic charge and can detect the rate of emission of photons of light over the course of an exposure. All images were obtained using an automatic exposure time, a medium binning resolution with an F-stop setting of 1. Grey-scale images were acquired prior to bioluminescence images to ensure correct positioning of subjects.

Data was analysed using Living Image 4.1 software (Xenogen, Caliper Life Sciences, Runcorn, UK); areas of bioluminescence were selected using the region of interest (ROI) tool and bioluminescent counts were determined as appropriate. ROI's were kept constant between subjects throughout individual experiments. The tumour volume for each group was expressed as the total photon count within the dedicated region of interest.

2.16.1 *In vitro* bioluminescent imaging

In order to confirm successful luciferase transduction of tumour, cells were plated in a 12-well plate. Cells were allowed to adhere overnight and the following day medium was exchanged for medium containing D-luciferin at a concentration of 150 µg/ml immediately prior to imaging. Cells were placed in the imaging chamber and images were acquired using automatic exposure settings, medium sensitivity binning and F-stop 1.

2.16.2 *In vivo* bioluminescent imaging

D-luciferin is a small molecule that freely diffuses across cell membranes. When injected intraperitoneally D-luciferin is not excreted but is slowly absorbed into the circulation, perfuses the tissues and is ultimately excreted by the kidneys. This means the luciferin concentration within the body is related to the pharmacokinetics of substrate inflow vs substrate outflow. As the substrate is being injected the inflow is greater that the outflow resulting in a slowly increasing bioluminescent signal. Once the substrate reaches equilibrium in the body (inflow and outflow are equal) there is a plateau in the bioluminescent signal and the counts can be used as a reliable measure of cell number. Finally the excretion of substrate is greater that the inflow resulting in a gradual reduction of bioluminescent signal. In order for bioluminescent counts to be reliable and comparable, images must be taken during the plateau phase, which is cell line dependent.

Animals injected with tumour cells expressing luciferase were imaged at predetermined time points. Prior to imaging animals were given an intrapleural injection of 200 µl D-Luciferin (10mg/ml) and stilled using isofluorane anaesthesia throughout image acquisition and placed on a heated stage to ensure they maintained an appropriate body temperature throughout anaesthesia. D-luciferin was administered 15 minutes prior to imaging.

2.16.3 Animals

Human tumour xenograft models are a well-established mode of determining the efficacy of anti-cancer therapies. In order to successfully establish human tumours in a murine model the animals must be immunosuppressed to prevent rejection of cancer

cells. NOD/SCID mice (NOD.CB17-Prkdc^{scid}) have the severe combined immunodeficiency mutation on a non-obese non-diabetic background resulting in a lack of functioning B and T-lymphocytes, lymphopenia and hypogammaglobulinaemia.

Eight to ten week old NOD/SCID mice (Charles Rivers) were kept in individually ventilated cages at the Central Biological Services Unit at University College London. Animals were kept on a 12 hours light/dark cycle at 20-25^{o}C and were provided with autoclaved food and water *ad libitum.* When mice were to be administered doxycycline, it was given in their autoclaved drinking water at a concentration of 2g/L with 3% (w/v) sucrose and administered via black water bottles to protect from light. All animal studies were approved by the University College London Biological Services Ethical Review Committee and licensed under the UK Home Office regulations and the Evidence for the Operation of Animals (Scientific Procedures) Act 1986 (Home Office, London, UK).

2.16.4 In vivo tumour xenograft models

Luciferase transduced cells were used to generate all tumour xenografts. All cells were detached from flasks using trypsin/EDTA, neutralised with serum containing medium and the cell suspension was counted. Cells were centrifuged at 300g for 5 minutes and the cell pellet was re-suspended to the required cell concentration in 100µl sterile PBS. Cells were kept on ice prior to injection. All animals were weighed prior to tumour cell inoculation and twice weekly thereafter. Animals were sacrificed when they reached >20% weight loss or if they showed other signs of distress such as piloerection, hunching or being cold to touch.

2.17 Statistics

Statistical analysis was performed using GraphPad Prism (GraphPad Software, CA, USA) and Microsoft Excel. Student's t-test was used to analyse differences between two groups whilst the analysis of variance (ANOVA) test with a Tukey post-hoc analysis was used to analyse differences between three groups. For multiple groups measured over multiple time points repeated measures ANOVA was used. Results were considered statistically significant for $p \leq 0.05$. All in vitro tests were performed in triplicate and all data are represented as mean values ± standard error of mean unless otherwise stated.

CHAPTER III

Results I: MSC delivery of full-length TRAIL was superior to soluble type for cancer therapy

3 RESULTS I: MSC DELIVERY OF FULL-LENGTH TRAIL WAS SUPERIOR TO SOLUBLE TRAIL FOR CANCER THERAPY

MSC-delivered targeted TRAIL overcomes the limited half-life of systemically delivered recombinant TRAIL. In murine models, the Janes lab have shown that systemic injection of MSCs expressing full-length human TRAIL leads to a reduction in subcutaneous tumour growth and reduced, or indeed eliminated, lung metastases [214] and attenuates malignant pleural mesothelioma development [186]. Others have shown that MSCs engineered to express soluble TRAIL are able to kill cancer cells both *in vitro* and *in vivo* [217, 218]. I hypothesised that MSCs expressing soluble TRAIL may have an advantage *in vivo* in secreting TRAIL throughout the tumour rather than relying on the cell-cell contact that is required by the membrane-bound full-length TRAIL expressed on the MSC surface. I wished to define the relative sensitivity of cancer cells to the different TRAIL forms expressed from a clinically approved lentiviral backbone. To elucidate whether soluble TRAIL or full-length TRAIL is optimal, I created MSCs expressing full-length or soluble TRAIL and compared their activity in inducing cancer cell apoptosis.

3.1 Construction of the lentiviral vectors and TRAIL expression following transduction

3.1.1 Construction of TRAIL-expressing lentiviral vectors

The lentiviral plasmid pCCL-c-Fes-GFP [212] was used to construct three lentiviral vectors, pCCL-CMV-flT (full-length human TRAIL), pCCL-CMV-sT (truncated soluble TRAIL) and pCCL-CMV-GFP (Figure 3-1A). The c-Fes promoter in the backbone vector was replaced by a CMV promoter/enhancer to give constitutive and high expression of proteins of interest. This was done by PCR amplification of the CMV promoter sequence using forward and reverse primers having overhangs of Xho1 and BamH1 restriction sites and using pLenti-TRAIL-IRES-GFP plasmid as template (Figure 3-1B). The c-Fes promoter on pCCL-c-Fes-GFP was deleted by double digesting with Xho1 and BamH1 enzymes. The CMV promoter was ligated in place of the c-Fes promoter thereby producing the pCCL-CMV-GFP plasmid (Figure 3-1C).

For the full-length TRAIL (flT) construct, the GFP sequence was replaced with human TRAIL (amino acids 1-281). The soluble TRAIL (sT) vector was made by fusing in-frame DNA sequences (from 5' to 3'), including a leader sequence from the murine immunoglobulin Κ-chain (IgΚ leader) to assist secretion, an isoleucine zipper (IZ) to enhance trimerisation and amino acids 95-281 of human TRAIL (Figure 3-1D). TRAIL lentiviruses were prepared by transfecting 293T cells with TRAIL constructs and packing plasmids.

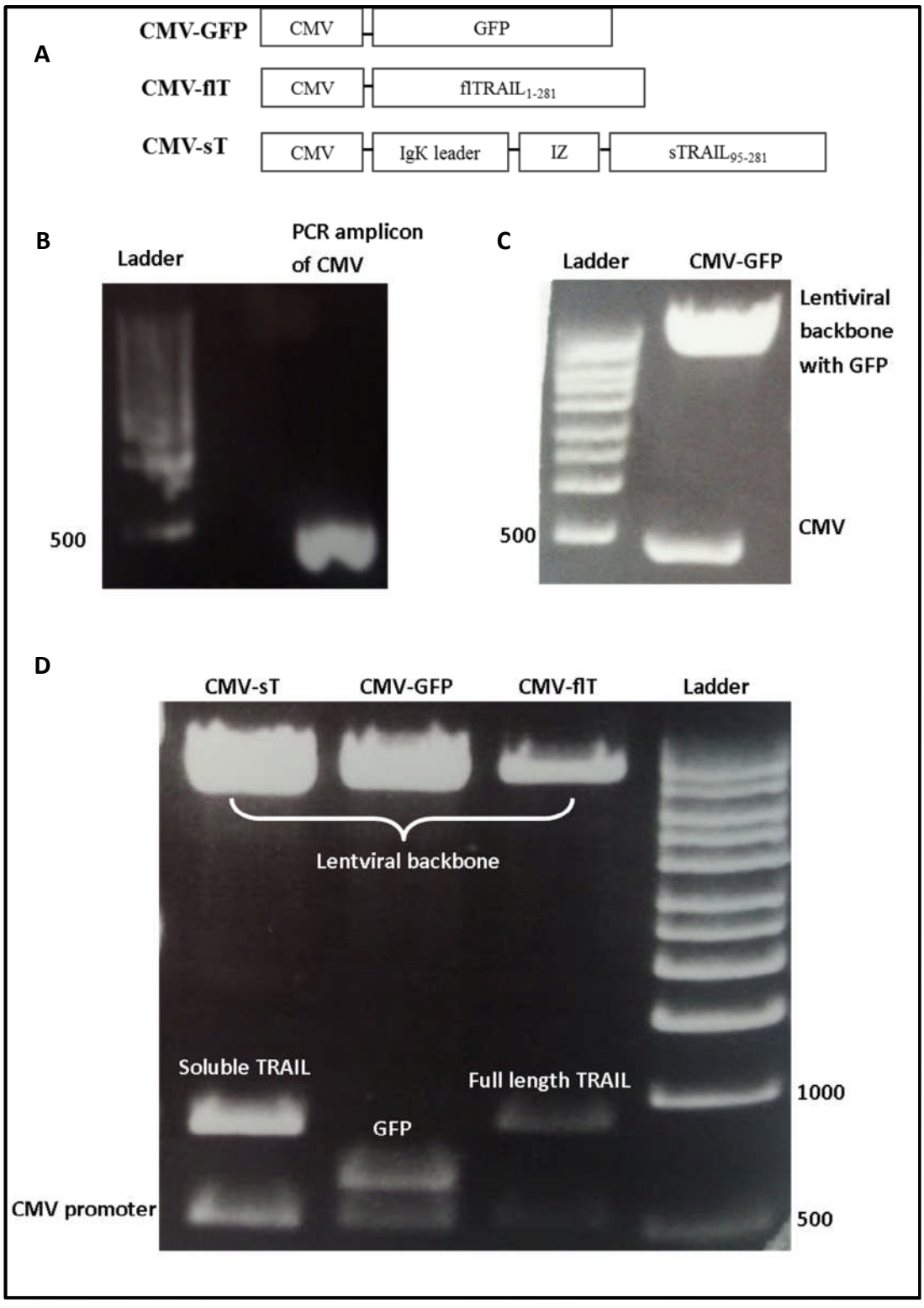

Figure 3-1 Construction of TRAIL expressing lentiviral vectors with CMV promoter

A, Schematic description of TRAIL expression constructs. B, Agarose gel showing PCR product of CMV promoter sequence amplified from pLenti-TRAIL-IRES-GFP. C, Restriction double digested pCCL.CMV-GFP run on an agarose gel. D, Restriction double digest of plasmid DNA from transformed E.coli confirming integration of soluble TRAIL and full length TRAIL into the lentiviral transfer plasmid

This work was done along with Dr Zhenqiang Yuan.

3.1.2 TRAIL expression following the transduction of MSCs

Well-characterized human adult bone marrow MSCs were purchased from the Texas A&M Health Science Center and were shown to be able to differentiate into chondrogenic, osteogenic and adipogenic lineages. In order to determine levels of TRAIL expression following transduction, TRAIL-transduced MSCs (MOI 2) were examined by flow cytometry with a PE-conjugated anti-human TRAIL antibody, which demonstrated that more than 98% of flT-transduced MSCs (MSC-flT) were positive for TRAIL expression. By contrast, only around 1% of control GFP virus-infected cells were positive for TRAIL. This shows that TRAIL expression was not the result of endogenous TRAIL induction following lentivirus infection (Figure 3-2A).

In addition, more than 97% of soluble TRAIL-transduced MSCs (MSC-sT) were positive for TRAIL expression (Figure 3-2A). Of note, full-length TRAIL expression was stable through passages 4 to 8 but expression of soluble TRAIL decreased by just under 20% during this time (Figure 3-2B). All further MSCTRAIL comparison experiments were carried out in passage 4 or 5 cells.

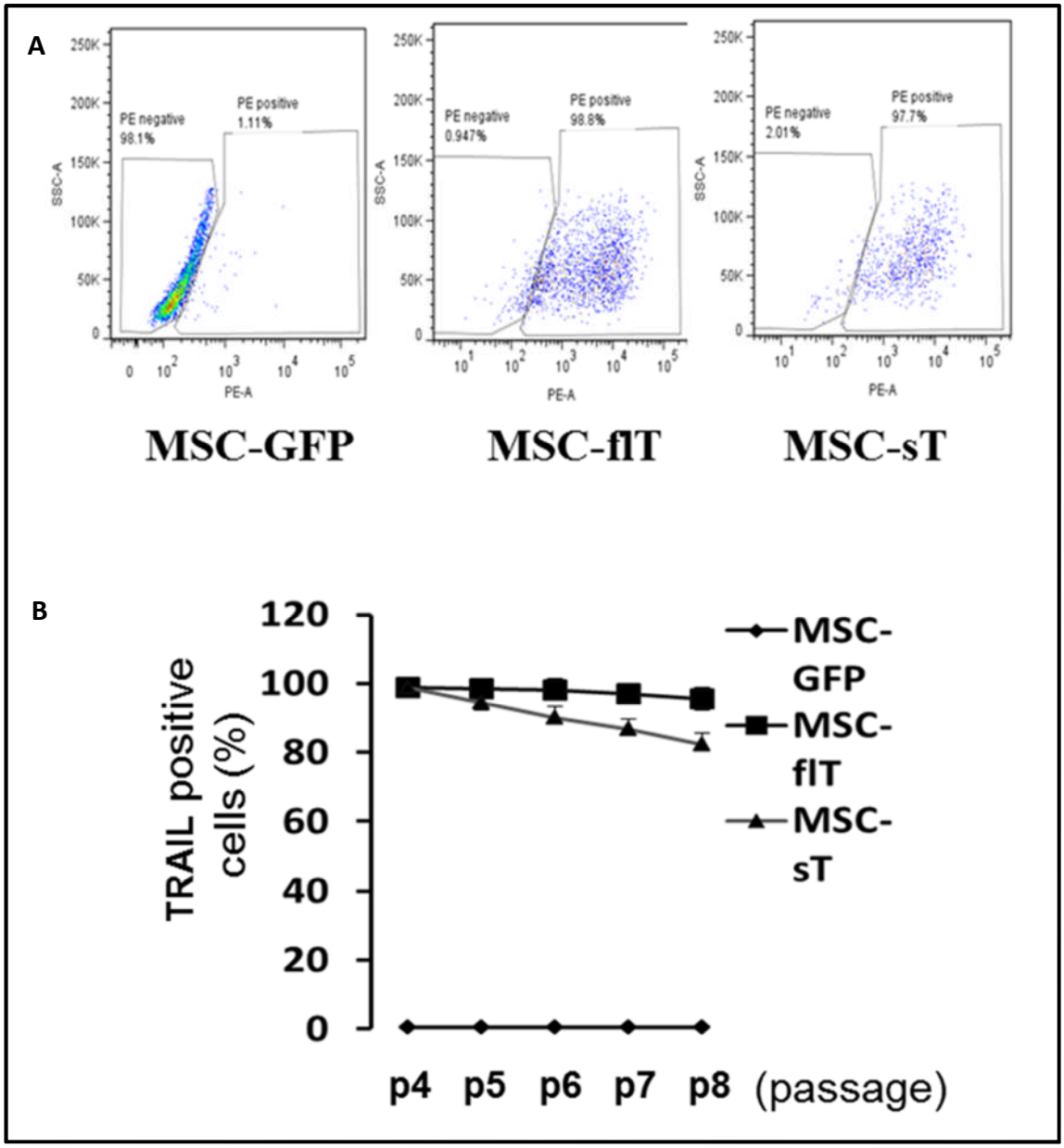

Figure 3-2 Cell surface TRAIL expression by transduced MSCs

A, FACS analysis of lentivirus-transduced MSCs to show TRAIL expression (shown by the percentage of cells that are PE positive). B, Long-term FACS analysis of TRAIL expression in MSCs that were transduced at passage 3 (p3), expanded and then passaged every 7 days until p8.

This work was done along with Dr Zhenqiang Yuan.

3.1.2.1 Confirmation of TRAIL protein Expression

To further assess MSCTRAIL expression, immunoblot analysis of cellular lysates was carried out. Both MSC-flT and MSC-sT cells expressed abundant cellular TRAIL proteins at similar levels, whereas GFP-transduced MSCs showed no detectable TRAIL expression (Figure 3-3AThe MSC-flT lysate showed a TRAIL band of ~32 kDa and the MSC-sT lysate showed a band of ~27 kDa, which was larger than its predicted size of 24 kDa, possibly as a result of the glycosylation of the ligand [219]. In addition to cellular TRAIL expression, I was also interested to investigate levels of secreted TRAIL from transduced MSCs. Secreted TRAIL protein was detected in supernatants of both MSC-sT and MSC-flT cells but not in that of GFP-transduced cells (Figure 3-3A). The MSC-sT cells secreted abundant soluble TRAIL of ~27 kDa and ~24 kDa sizes. Three soluble TRAIL molecular forms were detected in the supernatant of MSC-flT cells, that of ~35 kDa and ~32 kDa, corresponding to the glycosylated and the non-glycosylated full-length TRAIL, and that of ~24 kDa, corresponding to a cleaved form [220] (Figure 3-3A).

soluble TRAIL in MSC culture medium over 7 days. Results showed that MSC-sT cells secrete high levels of soluble TRAIL at a rate of 3.63 ± 0.71 ng/hr for every 1 million cells (Figure 0-3B). Interestingly, MSC-flT cells secrete soluble TRAIL at a lower rate of 1.3 ± 0.52 ng/hr for every 1 million cells. MSC-GFP cells did not secrete measurable TRAIL (Figure 3-3A and B).

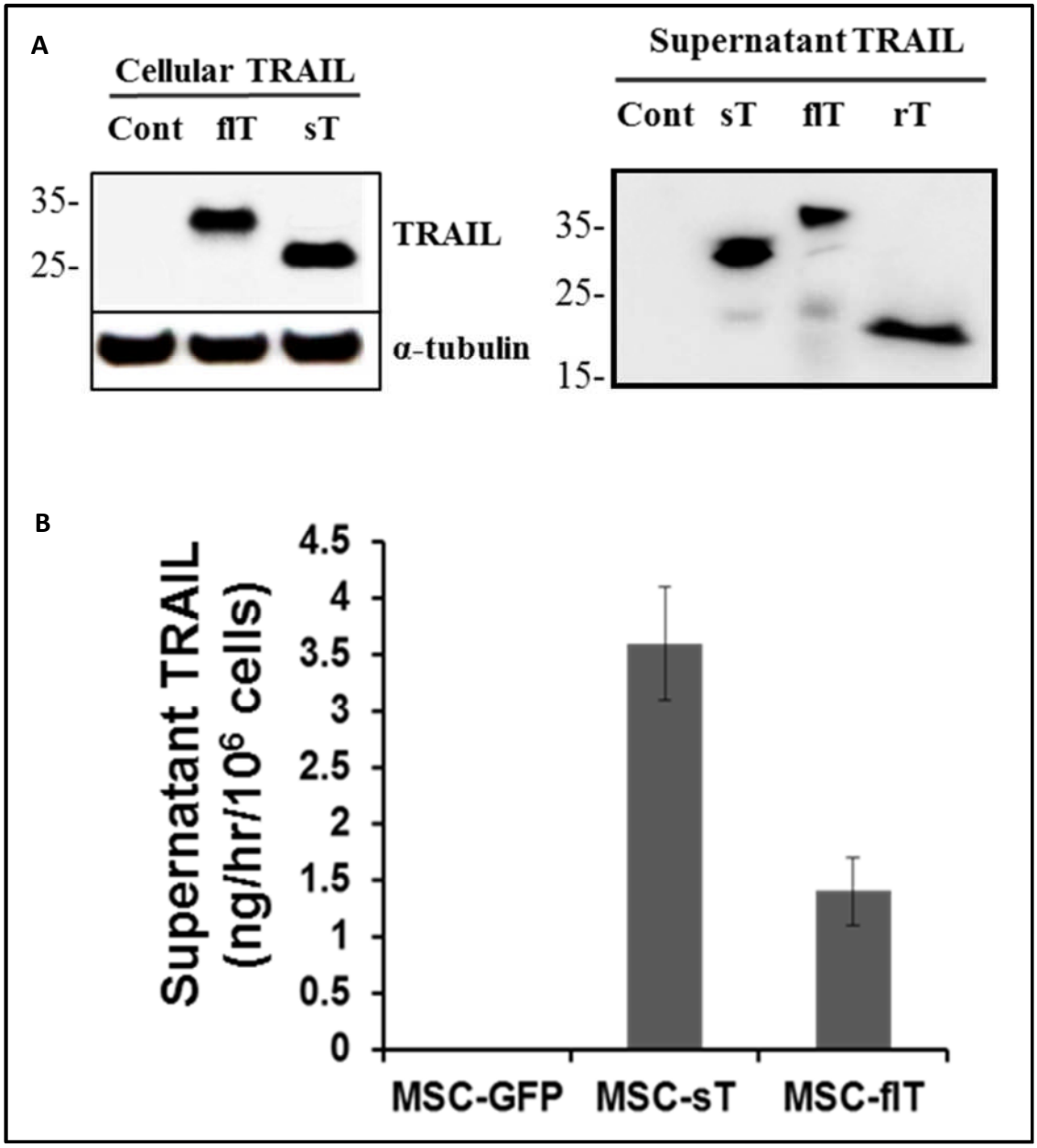

Figure 3-3: Cellular and secreted TRAIL expression by MSCs after transduction

A, Detection of cellular or secreted TRAIL expression by immunoblotting. Control (Cont.) represents MSC-GFP cell lysates or conditioned medium, flT and sT represent cell lysates or concentrated culture medium from MSC-flT and MSC-sT cells, respectively, and rT represents 1 ng of purified recombinant human TRAIL (amino acids 114-281) produced from bacterial cells (PeproTech, USA). α-tubulin is shown as a loading control. B, Quantification of levels of TRAIL in cell culture media. Levels of TRAIL were measured by ELISA from MSCs transduced at p3 and expanded for 1 passage. Data presented as TRAIL released by 1 million cells per hour (ng/hr/1×10^6 cells). Data represent mean ± S.E.M. (n = 5).

3.1.2.2 Cellular distribution of TRAIL

To examine the cellular distribution of TRAIL in transduced MSCs, immunocytochemistry using a PE-conjugated anti-TRAIL antibody was used to visualise TRAIL localisation in MSCs. As shown in (Figure 3-4), positive staining of TRAIL was observed in both MSC-flT and MSC-sT cells but not in parental untransduced cells. Fluorescence microscopy revealed that TRAIL distribution was exclusively cytoplasmic in MSC-sT cells while MSC-flT cells showed both cell surface and intracellular TRAIL expression. Interestingly, TRAIL labelling in MSC-flT cells appeared to be enriched at the leading edge of lamellipodia and at the tips of filopodia (Figure 3-4, inset).

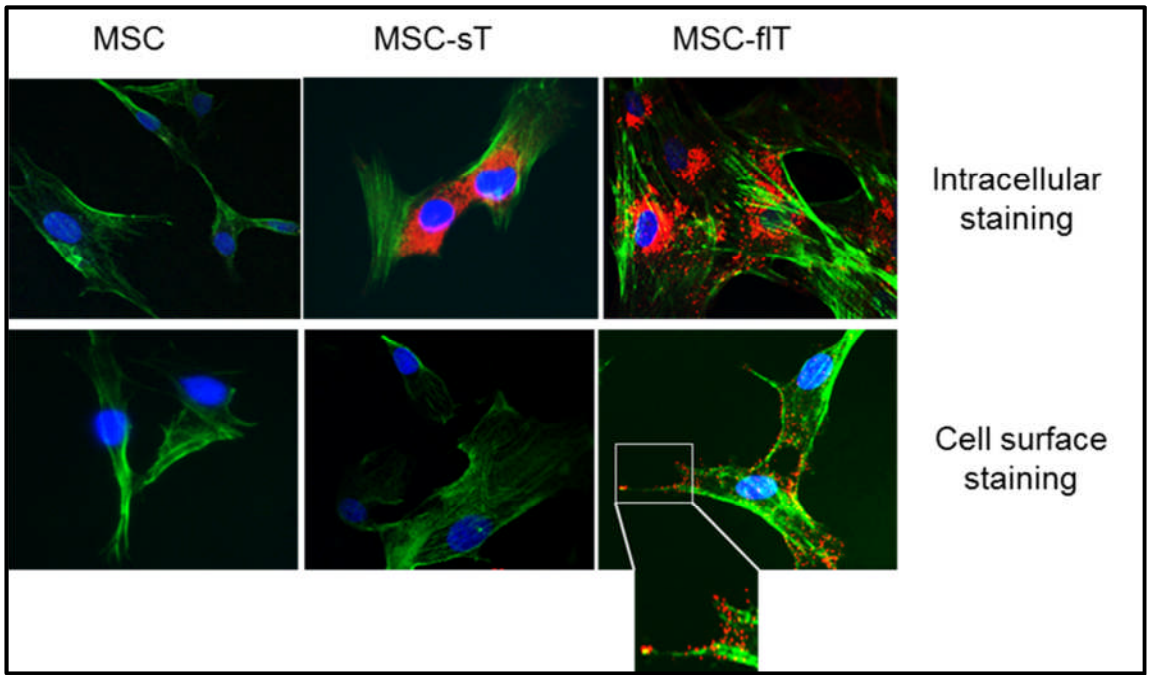

Figure 3-4: Cellular distribution of TRAIL in transduced MSCs

Immunofluorescent detection of recombinant TRAIL (red) expressed by transduced MSCs. Phalloidin staining was used to show filamentous actin (green) and nuclei were labelled with DAPI (blue). Top panel shows intracellular staining; bottom panel shows cell surface staining. Images are representative of at least three experiments for each staining condition. Magnification ×400.

3.2 MSC phenotype following TRAIL transduction

In order to determine whether TRAIL transduction has any significant effects on the characteristics of MSCs, TRAIL-transduced MSCs were analysed for changes in phenotype after lentiviral infection.

3.2.1 MSC viability, proliferation and cell surface protein expression

TRAIL-transduced MSCs were analysed for changes in phenotype after lentiviral infection. MSC-sT and MSC-flT cells demonstrated viability and proliferation rates that were equivalent to non-transduced cells (Figure 3-5A). Expression of the characteristic MSC markers CD105, CD90 and CD73 (Figure 3-5B) were unchanged by transduction.

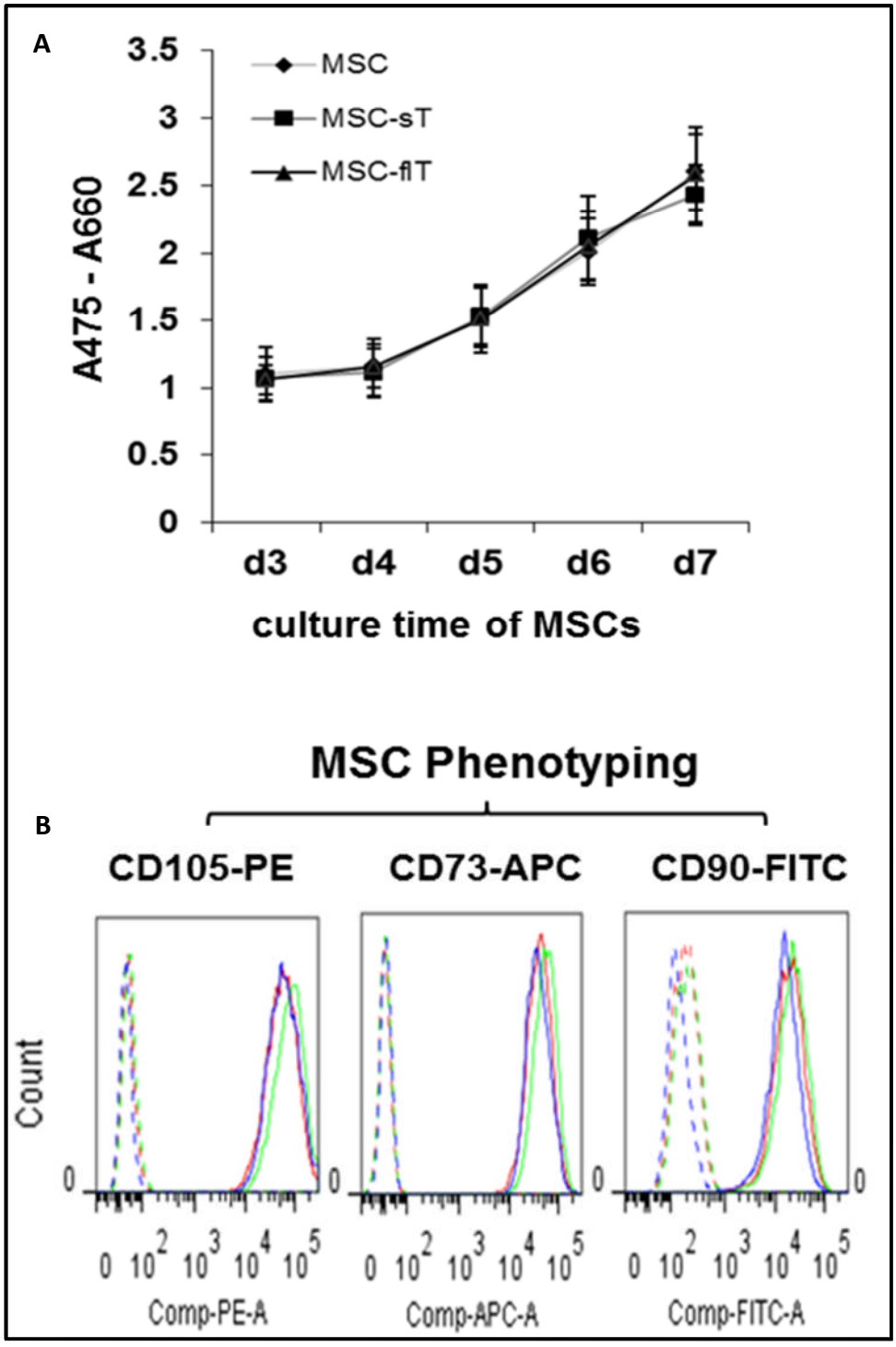

Figure 3-5 Analysis of characteristic features of MSCs after TRAIL-expressing lentiviral transduction

A, Cell viability and proliferation were assessed using the XTT assay for 7 days after transduction. B, Phenotyping of cultured MSCs for expression of conventional MSC markers is shown. Dashed line shows antibody isotype control and solid line shows marker-specific antibody staining (red – MSC, blue – MSC-flT and green – MSC-sT). These data show that TRAIL expression following lentiviral transduction does not affect MSC viability, proliferation, cell surface protein expression and differentiation potential. This work was done along with Dr Zhenqiang Yuan.

3.2.2 MSC differentiation following TRAIL-expressing lentiviral infection

To investigate whether the differentiation capacity of MSCs was affected by TRAIL-expressing lentiviral infection, control MSCs, MSC-flT and MSC-sT cells were grown in media to induce differentiation. Real-time quantitative PCR was used to assess early differentiation commitment by measuring transcriptional expression of *PPARG*, which is a marker or adipogenesis, and *BMP2*, which is a marker of osteogenesis. Differentiation potential of lentivirally infected cells was shown to be unaltered compared with parent untransduced cells, with all cells showing a similar increase in transcriptional expression of *PPARG* and *BMP2* after the induction of differentiation (MSC and MSC-flT shown in Figure 3-6A). In addition, differentiation capacity was assessed after 4 weeks of culture in differentiation media by staining cells with HCS LipidTOX Green to detect adipocytes, Alizarin Red S to detect osteocytes or Alcian blue to detect chrondrocytes. Cells showed a similar capacity to undergo full adipogenic, osteogenic and chondrogenic differentiation (MSC-flT shown in Figure 3-6B).

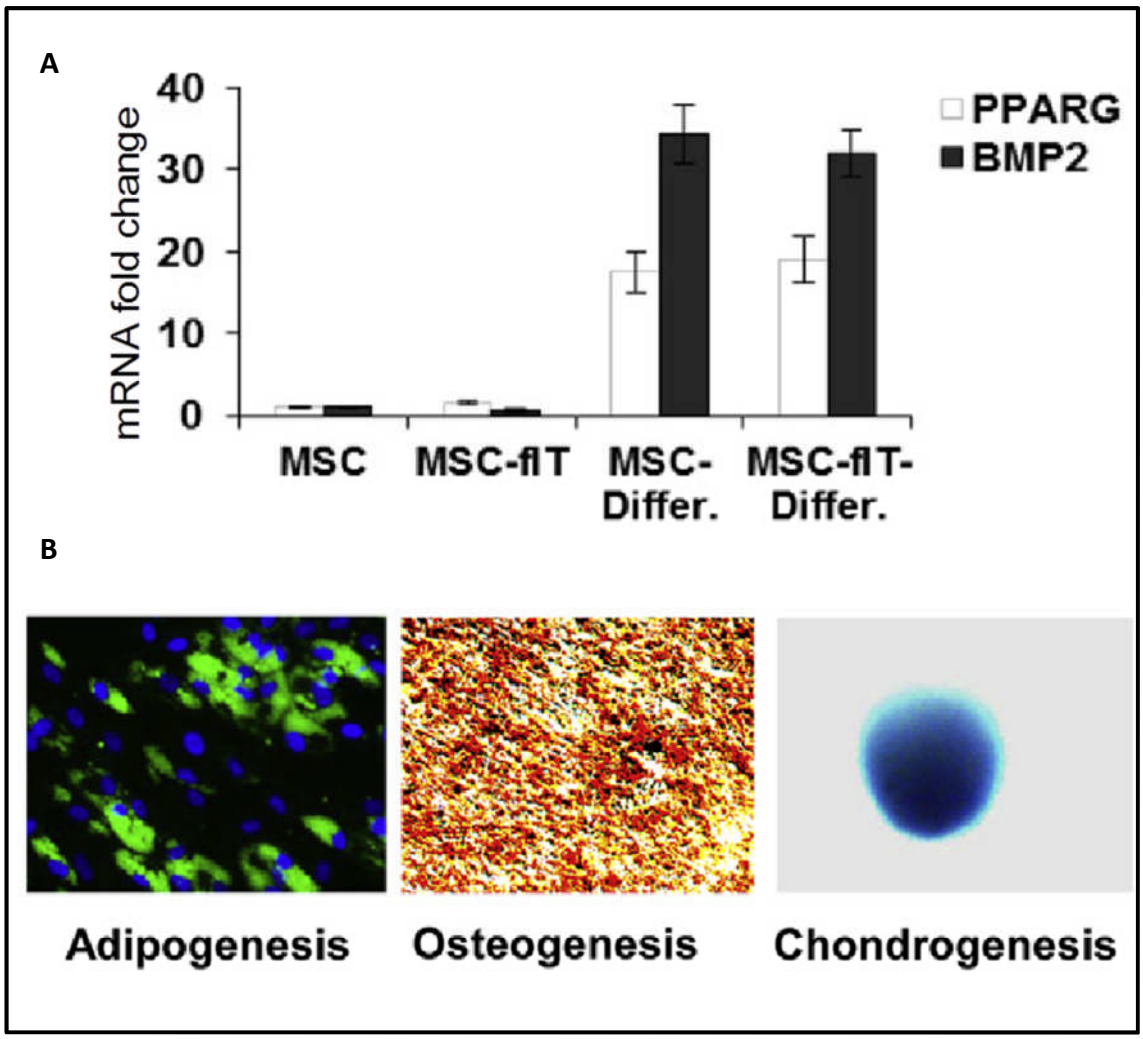

Figure 3-6: MSC differentiation following TRAIL-expressing lentiviral transduction

The differentiation potential of MSCs was assessed following TRAIL-expressing lentiviral transduction. Cells were cultured in osteogenic, adipogenic or chondrogenic differentiation media. A, Real-time quantitative PCR was used to measure transcriptional expression changes in PPARG, a marker of adipogenesis, and BMP2, a marker of osteogenesis. MSC-differ. And MSC-flT-Differ. represents MSCs or MSC-flT cells, respectively, grown in adipogenic (white) or osteogenic (black) differentiation conditions. B, Following 4 weeks in their respective differentiation media, cells were stained to assess differentiation. Left, HCS LipidTOX Green staining (green) for neutral lipid and DAPI staining for nuclei (blue) to show adipogenic differentiation; middle, Alizarin Red S staining (red) to show osteogenic differentation; and right, Alcian blue staining (blue) to show chondrogenic differentiation. Magnification ×200 for adipogenesis and osteogenesis assays and ×50 for chondrogenesis assay. This work was done along with Dr Zhenqiang Yuan.

3.3 Apoptosis in cancer cells following co-culture with MSC-flT and MSC-sT cells

Having shown that TRAIL-transduced MSCs express high levels of TRAIL and that their phenotypes are unaltered, I next went on to investigate whether these cells could induce cancer cell apoptosis.

3.3.1 Comparison of the cancer cell-killing efficiency of MSC-flT and MSC-sT cells

In Figure 3-3A, I demonstrated that both MSC-sT and MSC-flT cells secrete TRAIL into their culture medium. However, the level of TRAIL that was secreted by MSC-sT cells was higher than that secreted by MSC-flT cells, which indicates that these cells may have higher cancer cell-killing efficiency. To test this, cancer cell apoptosis was examined in co-culture experiments with MSC-sT and MSC-flT cells. Killing of the known TRAIL-sensitive MDAMB-231 cell line was initially examined, then the TRAIL-resistant lung cancer line A549 was tested.

MDAMB-231 cells were co-cultured with MSC-sT, MSC-flT or MSC-GFP cells at ratios of increasing numbers of MSCs to cancer cells, ranging from 1:10 to 1:1 (MSC: cancer cell). Apoptosis was measured by DAPI and Annexin V labelling using flow cytometry. As shown in Figure 3-7A, both MSC-sT and MSC-flT cells induced MDAMB-231 apoptosis in a dose-dependent manner. However, MSC-flT cells were more efficient than MSC-sT cells at inducing apoptosis (Figure 3-7A). At all cell number ratios of MSC: MDAMB-231, MSC-flT cells showed higher killing capacity than MSC-sT cells. Similarly, A549 cells demonstrated greater cell death when co-cultured with MSC-flT cells than when cultured with MSC-sT cells (Figure 3-7B).

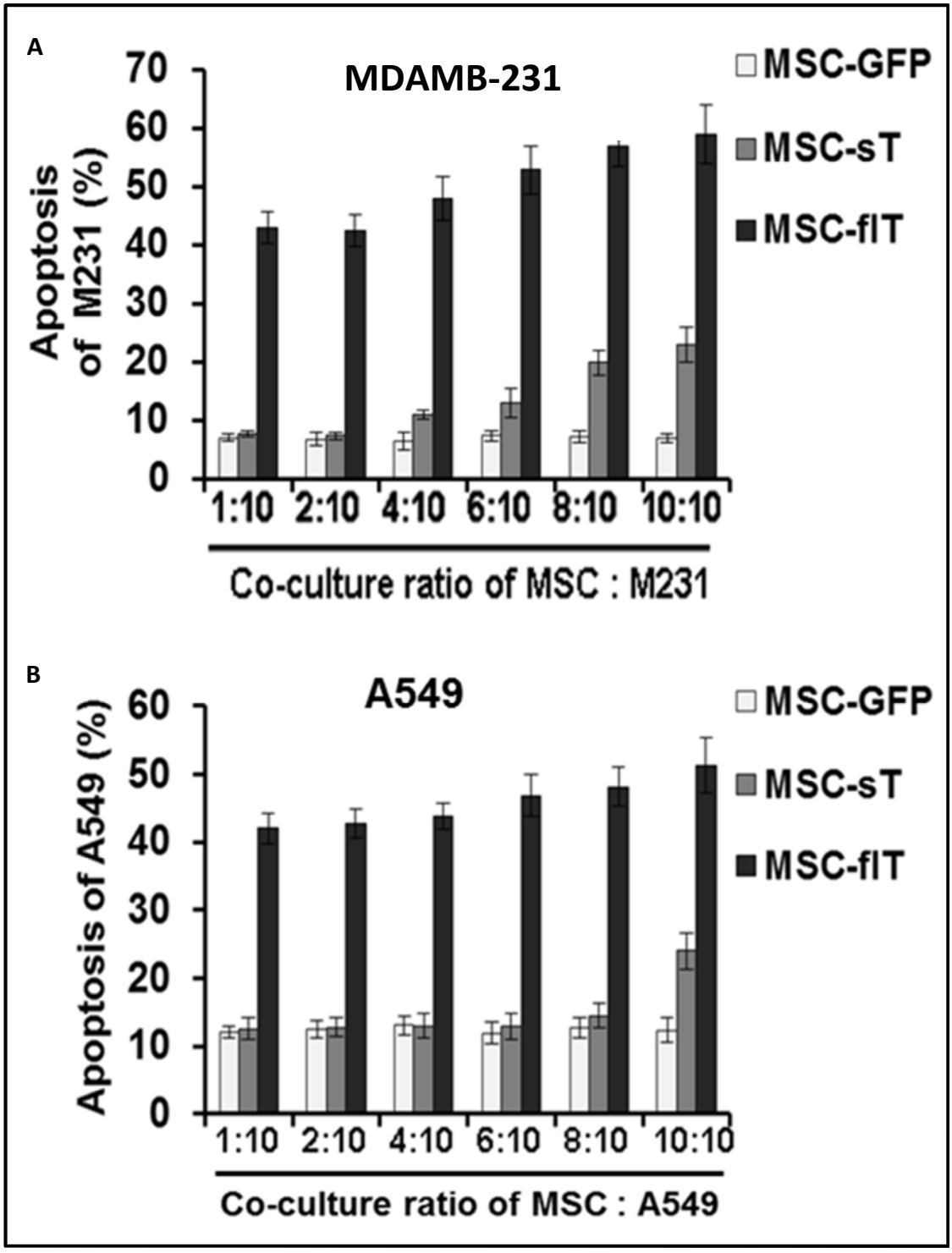

Figure 3-7: Co-culture of TRAIL-expressing MSCs with cancer cells

Cancer cell apoptosis was measured by flow cytometry 24 hours after co-culturing the breast adenocarcinoma cells MDAMB-231 (A) or the lung adenocarcinoma cells A549 (B) with MSC-GFP, MSC-fIT or MSC-sT cells, with increasing numbers of MSCs to cancer cells. These data show that MSCs expressing TRAIL induce apoptosis in cancer cells.

.

3.3.2 Activation of the caspase system in cancer cells following co-culture with MSC-flT and MSC-sT cells

TRAIL-induced apoptosis involves caspase-8 recruitment and activation [221]. Therefore, I next used flow cytometry to analyse the activated caspase-8 levels in cancer cells co-cultured with MSC-flT and MSC-sT cells. The A549 cells showed increased caspase-8 activation when co-cultured with MSC-flT cells at a ratio of 4:10 (MSC: cancer cell) but not when cultured with MSC-sT cells or with MSC-GFP cells (Figure 3-8A). This is consistent with the relative cancer cell apoptosis rates shown in (Figure 3-7). To further confirm TRAIL-specific apoptotic pathway activation by TRAIL-expressing MSCs, the caspase inhibitor Z-VAD-FMK and the anti-TRAIL antibody T3067 were added to MSC-flT cell co-cultures. These experiments demonstrated that MSC-flT killing was caspase dependent and required TRAIL receptor activation (Figure 3-8B).

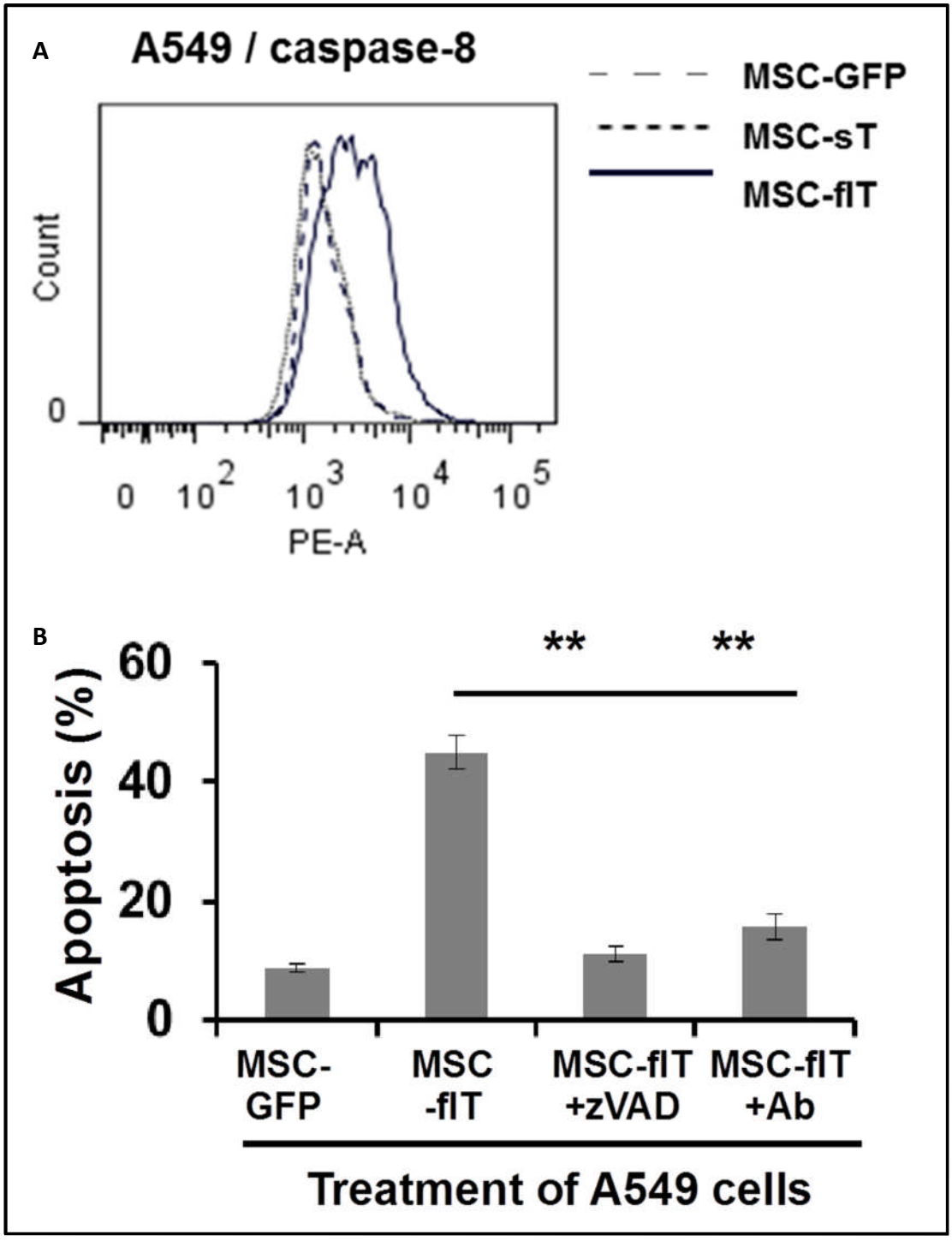

Figure 3-8: Caspase activation following co-culture with MSC-flT and MSC-sT cells

*A, Activated caspase-8 levels (shown as PE-positive) in A549 cells were measured by flow cytometry following co-culture with MSC-GFP, MSC-sT or MSC-flT cells at a ratio of 4:10 (MSC: cancer cell). B, MSC-flT-induced cancer cell apoptosis following co-culture can be blocked by 20 μM of the pan-caspase inhibitor Z-VAD-FMK (zVAD) and 100 ng/ml of a TRAIL-neutralising monoclonal Ab (T3067, Sigma-Aldrich). Data represent means ±S.E.M. ** p<0.01 compared with MSC-flT cell co-culture by Student's t-test.*

3.3.3 Induction of apoptosis in cancer cells with a broad range of TRAIL sensitivities following co-culture with MSC-flT and MSC-sT cells

To determine if the higher cancer cell-killing capacity exerted by MSC-flT cells compared with MSC-sT cells is more broadly applicable, I extended the co-culture assay to a panel of 20 established cancer cell lines. The panel included six cancer types consisting of five lung cancer lines, A549, NCI-H460, NCI-H727, NCI-H23 and PC9, eight mesothelioma lines, NCI-H2052, H2795, H2804, H2731, H226, H2810, H2452 and H2869, three colon cancer lines, Colo205, HT29 and RKO, two renal cancer lines, RCC10 and HA7-RCC, one human oral squamous cell carcinoma line, H357, and one breast cancer line, MDAMB-231.

The 20 cancer cell lines were treated with rTRAIL at a concentration of 50 ng/ml or with control GFP-transduced MSCs. Control MSCs did not induce cancer cell apoptosis. Following rTRAIL treatment, the 20 cell lines showed a varied response and were grouped accordingly into those that were rTRAIL sensitive (apoptosis $\geq$70%; five cell lines), those that were moderately TRAIL sensitive (apoptosis 35-70%; five cell lines), those that showed low TRAIL sensitivity (apoptosis 20-35%; four cell lines) or those that were TRAIL resistant (apoptosis $\leq$20%; six cell lines) (Figure 3-9). Control MSC-GFP, MSC-flT and MSC-sT cells were cultured with cancer cells at a ratio of 4:10 (MSC: cancer cell). For all four cancer cell groups, MSC-sT cells showed only marginal induction of apoptosis, while MSC-flT cells demonstrated effective killing of cancer cells (Figure 3-9). Of note, in the highly TRAIL-sensitive group, MSC-flT cells exerted a similar level of cell killing to 50 ng/ml rTRAIL; for moderate and low TRAIL-sensitive and TRAIL-resistant groups, MSC-flT cells induced more apoptosis than rTRAIL. These results show that MSC-flT cells partly overcome the TRAIL-resistance of cancer cells.

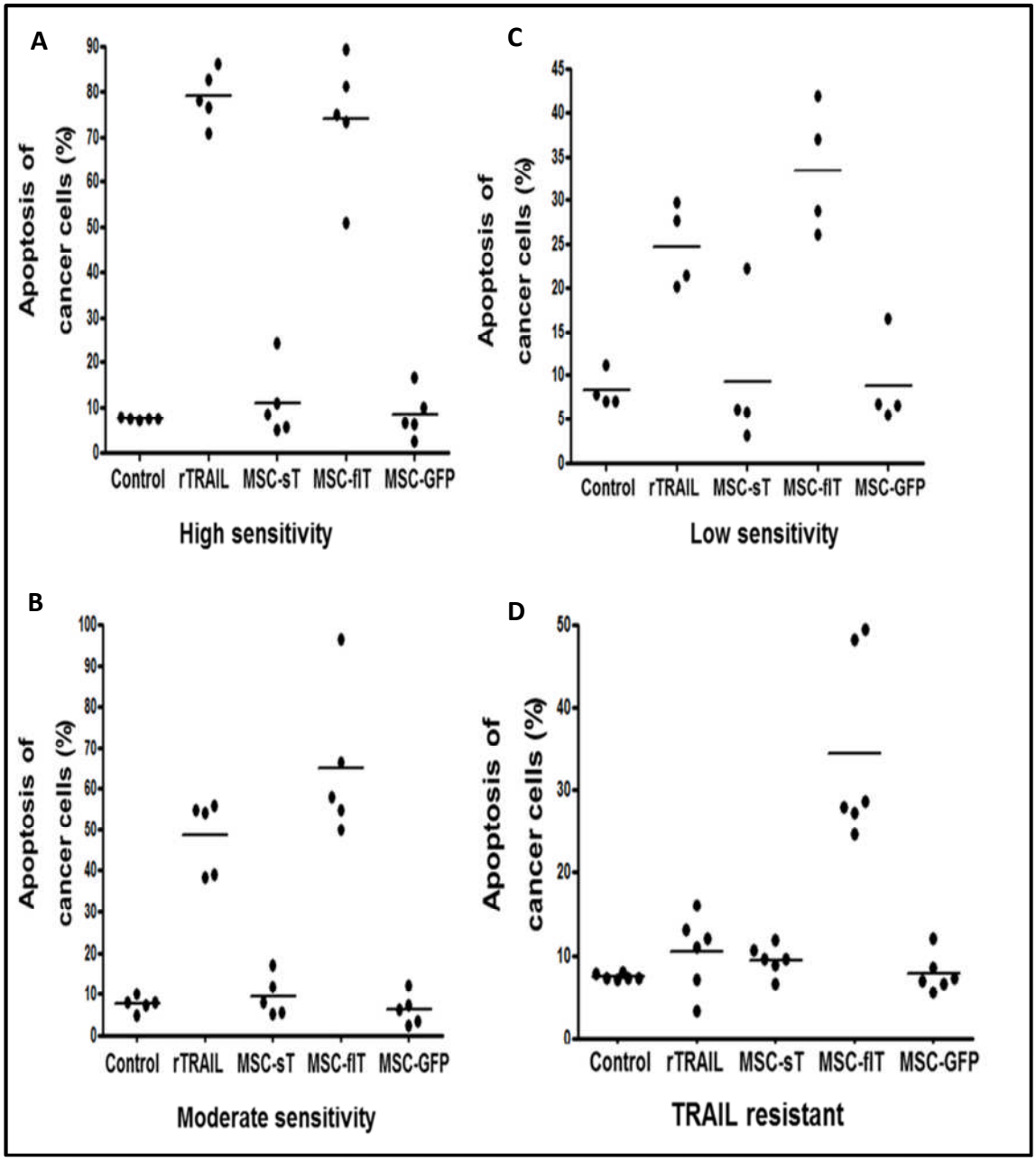

Figure 3-9: Apoptosis in cancer cells with different levels of TRAIL resistance following co-culture with TRAIL-expressing MSCs

The apoptosis of (A) five highly TRAIL-sensitive cancer cell lines Colo205, NCI-H460, H727, H2795 and H2804, (B) five moderately TRAIL-sensitive cancer cell lines H2731, H226, H2869, PC9 and MDAMB-231, (C) four cancer cell lines of low TRAIL sensitivity HT29, H357, H2452, and RKO, and (D) six TRAIL-resistant cancer cell lines A549, NCI-H2052, H2810, NCI-H23, RCC10 and HA7-RCC, was determined after 24 h of culture with medium (control), 50 ng/ml of purified recombinant TRAIL (rTRAIL), or MSC-GFP, MSC-flT or MSC-sT cells at a ratio of 4 MSCs to 10 cancer cells. Data show that MSC-flT cells induce cancer cell apoptosis with a higher efficiency than MSC-sT cells. Data represent means of three experiments with triplicate repeats for each cell line.

3.3.4 Cancer cell-killing capacity of soluble TRAIL compared with full-length TRAIL

Unexpectedly, MSC-sT and MSC-flT cells both release abundant TRAIL into the supernatant medium (Figure 3-3). I had anticipated that the truncated soluble form of TRAIL that was secreted by MSC-sT cells would have pro-apoptotic effects on nearby cancer cells. Having found that MSC-flT cells not only express full-length TRAIL on their cell surface but also secrete full-length TRAIL into the culture medium, I tested the relative killing efficacy of both the full-length and the truncated secreted forms of TRAIL.

To obtain sufficient amounts of soluble TRAIL, supernatant media were collected from cultured MSC-flT and MSC-sT cells under low serum conditions (1% FBS), were filtered through 0.2 μm filters and were concentrated 50-fold with centrifugal columns (10 kDa). Supernatant medium from GFP-transduced MSCs was also collected and concentrated for use as a control. ELISA quantification showed that the concentrated MSC-flT supernatant medium contained 0.4 ± 0.2 μg/ml of TRAIL and that the MSC-sT supernatant medium contained 1.2 ± 0.3 μg/ml TRAIL.

Two cancer cell lines, MDAMB-231 and A549, were treated with the supernatant preparations of flT or sT to compare cytotoxicity. rTRAIL or control medium were used as controls. MDAMB-231 cells, which are a moderate TRAIL-sensitive cancer cell line, showed dose-dependent sensitivity to all three TRAIL forms (Figure 3-10A). As expected, as a result of insertion of the IZ trimerisation domain, sT showed higher cytotoxicity than rTRAIL; however, interestingly flT induced most apoptosis of MDAMB-231 cells (Figure 3-10A). Of particular note, flT was capable of inducing apoptosis in rTRAIL-resistant A549 cells but sT was not (Figure 3-10B). These results

demonstrate that soluble TRAIL released by MSC-flT cells has a higher cancer cell-killing activity than rTRAIL or soluble TRAIL released by MSC-sT cells.

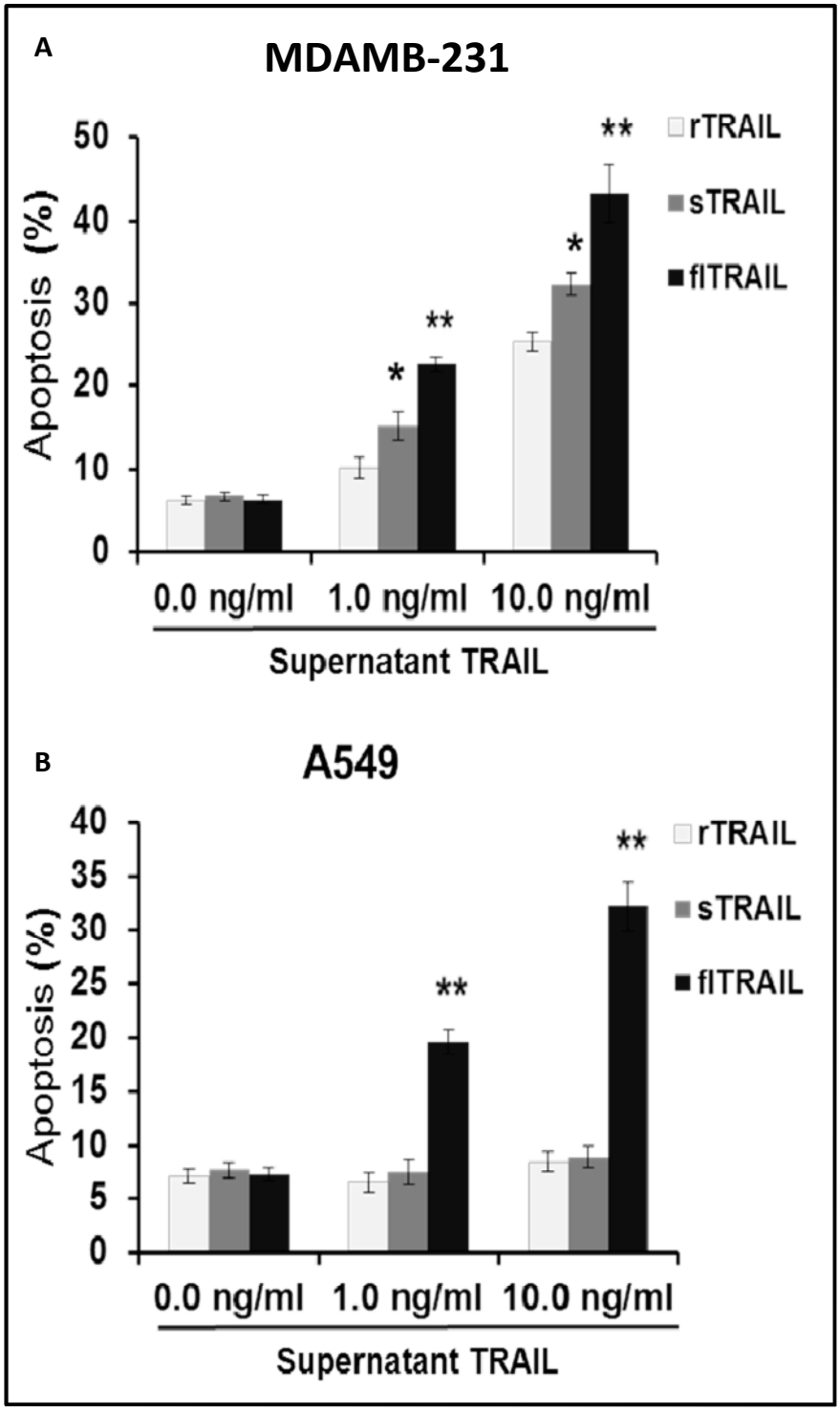

Figure 3-10: Comparison of TRAIL secreted by MSC-flT and MSC-sT cells for inducing cancer cell apoptosis

Apoptosis was measured by flow cytometry after exposure of MDAMB-231 cells (A) or A549 cells (B) for 24 h to increasing doses of recombinant TRAIL (rTRAIL), supernatant TRAIL from MSC-sT (sTRAIL) or supernatant TRAIL from MSC-flT (flTRAIL).

3.3.5 Cell surface TRAIL on MSC-flT cells contributes to apoptosis induction

To confirm the role of cell surface TRAIL expression in the induction of apoptosis, I fixed MSC-flT cells with 4% PFA to stop TRAIL secretion into the supernatant and then co-cultured them with A549 cells. While fixed control MSC-GFP cells did not show any cancer cell killing, the fixed MSC-flT cells demonstrated significant killing of cancer cells (Figure 3-11). A TRAIL ELISA confirmed that there was no detectable TRAIL release in the supernatant of fixed MSC-flT cells. Therefore, the induction of apoptosis by MSC-flT cells was at least partially due to the TRAIL expressed on the cell surface.

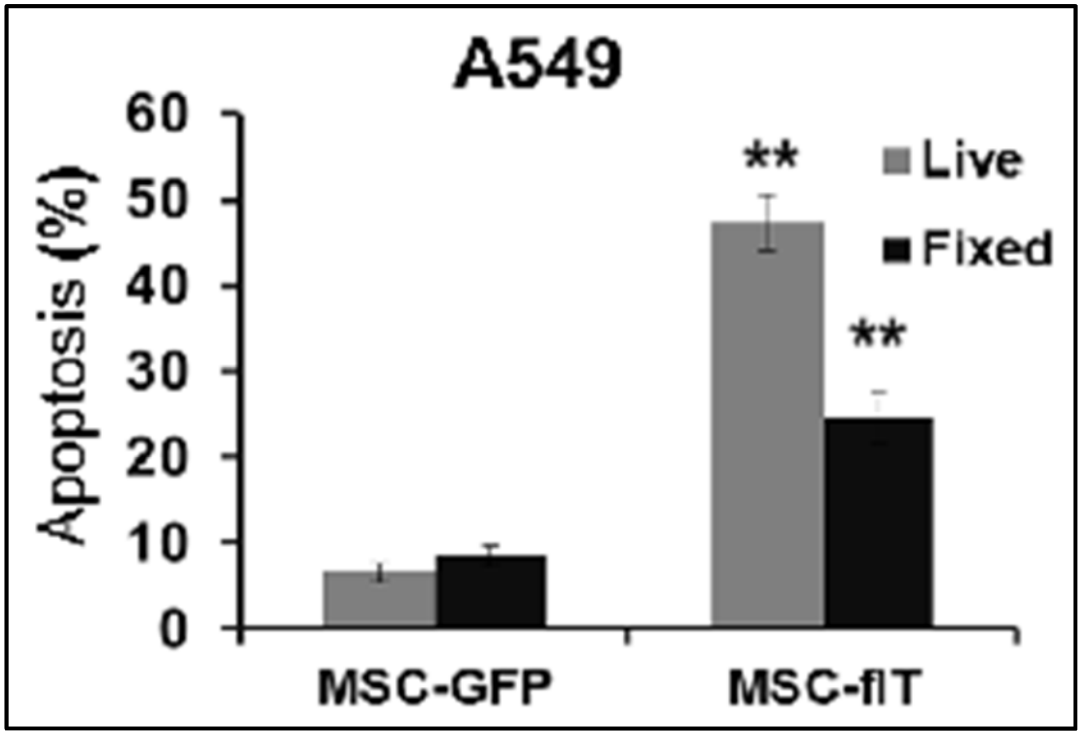

Figure 3-11: Investigation of the contribution of cell surface TRAIL on MSC-flT cells to apoptosis induction

*Apoptosis was measured after 24-h co-culture of A549 cells with live or fixed MSC-GFP and MSC-flT cells. Data represent averages ±S.E.M. (n = 3), ** p<0.01 compared with MSC-GFP treatment by Student's t-test.*

3.4 Discussion

In order to produce an effective and clinically relevant therapeutic, in this study I have subcloned soluble or full-length TRAIL and a CMV promoter/enhancer into the MHRA human approved lentiviral vector pCCL-c-Fes-Gfp [212]. The new vectors that Dr Zhenqiang Yuan and I created use the constitutive CMV promoter. I then compared the killing efficiency of MSCs expressing full-length TRAIL with those expressing only soluble TRAIL, with the hypothesis that secreted TRAIL may improve cancer cell-killing efficiency.

In this chapter, I have shown that MSC infection with the new lentiviruses expressing the different TRAIL forms does not affect MSC differentiation capacity or cell proliferation. MSCs do not normally express endogenous TRAIL (Figure 1) [222] and, here, I show that the infection with a lentivirus expressing GFP does not lead to any detectable endogenous TRAIL expression (Figure 1). Interestingly, TNFα has been found to be able to trigger endogenous TRAIL expression in MSCs [222]. However, TNFα-induced TRAIL expression appeared to only occur within cells and cells lacked apparent soluble TRAIL release, which necessitates cell-to-cell contact for apoptotic activity [222].

I demonstrate that, following lentiviral infection, full-length TRAIL is indeed expressed at the cell membrane while soluble TRAIL is expressed in the cytoplasm. In the construction of soluble TRAIL, I used an IZ as a trimerisation enhancer, which has been previously shown to facilitate the formation of a TRAIL homotrimer and to enhance its cytotoxicity [223]. The IZ-fused sT construct created in this study confirmed the advantage of using IZ to produce a secreted recombinant soluble TRAIL preparation.

Intriguingly, both soluble and full-length TRAIL are secreted, although soluble TRAIL is secreted at greater levels. I initially hypothesised that soluble TRAIL might be more effective at treating an *in vivo* tumour as a result of its potential to diffuse through the tumour, thereby enhancing anticancer activity. However, the observation that both soluble and full-length TRAIL are secreted potentially removes this benefit of MSC-sT cells compared with MSC-flT cells, although it was still possible that sT could have a higher cytotoxicity than secreted flT. However, I demonstrate that secreted flT it is more efficient in inducing apoptosis in cancer cells than either rTRAIL produced from bacterial cells or the trimerised sT secreted by transduced MSCs. To my knowledge, this is the first observation suggesting that mammalian cell-secreted flT is superior to N-terminal truncated soluble TRAIL versions (amino acids 114-281 or amino acids 95-281). Furthermore, I show that cellular presentation of the full-length form of TRAIL is superior in cancer cell killing to the cellular production of the soluble form of TRAIL.

TRAIL and other members of the TNF superfamily are type II transmembrane proteins and are expressed as membrane-bound homotrimeric molecules. It has been demonstrated by others that oligomerization is necessary for efficient induction of apoptosis in target cells. Holler *et al.* [224] showed that a hexameric FasL, another member of the TNF superfamily, consisting of two homotrimers at close proximity, represents the minimal ligand complex structure that is required to effectively form the death-inducing signalling complex (DISC) and to activate apoptosis. The trimeric FasL failed to induce a DISC and was thus inefficient in triggering apoptosis. A recent study found that TRAIL proteins expressed by human syncytiotrophoblasts exist as a hexameric form on exosome membranes [225]. The particulate aggregation of flT that I have observed on the cell surface of MSCs and the higher biological activity of flT

compared with IZ-fused sT both suggest the possibility of higher order oligermization of flT occurs on the cell membrane of transduced MSCs.

An important observation in this chapter is that MSC expression of flT induces apoptosis in cancers that are completely resistant to recombinant soluble TRAIL. The reason for this effect is not clear; however, two recent publications outline that higher order clustering of TRAIL-Rs may be necessary for full extrinsic death pathway activation [226, 227]. These studies demonstrate that neither soluble TRAIL nor antibodies against TRAIL-Rs alone are capable of inducing higher order clustering, although they are in combination. TRAIL expressed on the MSC surface may be able to induce higher order clustering of TRAIL-Rs on cancer cells as a result of movements permitted by the fluidic nature of the cell membrane. This might be the reason for the greater efficacy of MSC-flT compared with recombinant TRAIL or MSC-sT in *in vitro* studies. It will be interesting to understand in future studies whether flT but not sT is capable of this clustering and whether TRAIL requires cell membrane binding for its full killing effect.

Soluble recombinant TRAIL has been extensively tested as a cancer therapy *in vitro* and in human studies [228-237]. Completed clinical trials have used recombinant protein doses of up to 30 mg/kg [236], possibly because of its short half-life and the low efficiency of the recombinant soluble ligand. However, therapeutic benefits have been limited [238]. The clinical failure of recombinant soluble TRAIL has mainly been attributed to cancer cell resistance [238]. MSC delivery of full-length TRAIL not only results in the delivery of stably expressed TRAIL but also overcomes at least some of the resistance.

In this study, I have therefore validated cell infection, target gene expression and gene function using the clinically approved lentiviral backbone with the constitutive CMV promoter. I show that transduction with this virus does not adversely affect cell phenotype and I clearly demonstrate that the cancer cell-killing function of full-length TRAIL is superior to that of the shortened soluble form of TRAIL. In further studies it will be interesting to delineate whether this improved function of full-length TRAIL is due to higher order clustering. Importantly, MSC-flT cells are capable of partially overcoming cancer cell TRAIL resistance and that they hold promise for the treatment of diverse cancer types.

3.5 Summary

- Full length and soluble TRAIL expressing lentiviral vectors suitable for clinical application were made.
- Validation of cell infection, target gene expression and gene function using our clinically approved lentiviral backbone with the constitutive CMV promoter was done.
- Transduction with this virus does not adversely affect cell phenotype.
- Cancer cell-killing function of full-length TRAIL is superior to that of the shortened soluble form of TRAIL.
- MSC-flT cells are capable of partially overcoming resistance in TRAIL resistant cancer cell lines.
- In further studies it will be interesting to delineate whether this improved function of full-length TRAIL is due to higher order clustering.

Chapter IV

Results II: Synergistic treatment of TRAIL-resistant cancer cells with MSC-TRAIL and chemotherapy

4 RESULTS II: SYNERGISTIC TREATMENT OF TRAIL-RESISTANT CANCER CELLS WITH MSC-TRAIL AND CHEMOTHERAPY

Loebinger *et al* [146] and Sage *et al* [186] showed that MSC delivery of TRAIL reduced metastasis and tumour burden *in vivo*. However, the cell lines used in those studies were TRAIL sensitive. Although, as I have shown in Chapter III, full-length TRAIL delivered by MSCs (MSC-flT) is much potent than soluble TRAIL produced by MSCs or than recombinant TRAIL, some cancer cells are very resistant and only undergo 25-45% apoptosis when co-cultured with MSC-flT. To make MSC-TRAIL therapy more effective, TRAIL-resistant cells could be sensitised to TRAIL by the help of novel chemotherapeutic agents. Indeed, chemotherapeutics and TRAIL-expressing MSCs have been shown to work synergistically with bortezomib [239] in myeloma cells and with SAHA in lung cancer [240].

The aim of this chapter was to inhibit the key anti-apoptotic proteins in the TRAIL pathway and thus to facilitate apoptosis induced by MSC-flT. The key anti-apoptotic proteins in the extrinsic apoptotic pathway are cFLIP, the IAP family and the BCL-2 family of anti-apoptotic proteins. In this chapter, anti-apoptotic proteins are targeted with the chemotherapeutic agents that inhibit them. The combination of TRAIL along with LCL161, SAHA, obatoclax or SNS-032 was studied in detail.

4.1 Inhibition of IAPs sensitise cancer cells to TRAIL-mediated cell death

IAPs are potent inhibitors of both intrinsic and extrinsic apoptotic pathways. XIAP is proven to inhibit caspases, and cIAP1 and cIAP2 (cIAP1/2) play a role in determining whether a cell should undergo apoptosis or NF-κB-mediated proliferation following treatment with TNFα. Unlike the TNF pathway, the roles of cIAP1/2 in the TRAIL pathway are not very well characterised. cIAP1/2 can be inhibited using RNA interference (RNAi) or the small molecule SMAC mimetic LCL161 and this can be used to examine if inhibition of cIAP1/2 sensitises tumour cells to MSC-TRAIL.

4.1.1 cIAP1 knockdown by siRNA increases TRAIL-mediated apoptosis in JU77 cells, but upregulation of cIAP2 compensates for the loss of cIAP1

I first knocked down cIAP1 in the MPM cell line JU77 using siRNA and confirmed that the knockdown had been successful. JU77 cells were transfected with either 1 nM or 5 nM cIAP1-targeting siRNA and equivalent concentrations of negative siRNA using interferrin transfection reagent. The negative siRNA was a nonspecific sequence that does not target any gene. The effectiveness of the knockdown was confirmed by western blot by probing for cIAP1 protein expression 48 hours after transfection. While the untransfected cells expressed cIAP1, the 1 nM and 5 nM cIAP1 siRNA-treated cells showed knockdown of cIAP1; the cells treated with the equivalent concentration of negative siRNA did not show knockdown of cIAP1 (Figure 4-1A). This proves that 1 nM of cIAP1 siRNA is sufficient to knock down cIAP1 in JU77 cells.

To test the effect of cIAP1 knockdown on TRAIL sensitivity, JU77 cells were transfected with either 1 nM cIAP1-targeting siRNA or 1 nM negative siRNA. After 48 hours, the cells were treated with 100 ng/ml TRAIL for 24 hours. Cell death was measured using an Annexin V/DAPI apoptosis assay. Knockdown of cIAP1 in JU77 resulted in a significant increase in apoptosis following TRAIL treatment compared with wild-type JU77 cells and negative siRNA-transfected cells (Figure 4-1B). This shows that knockdown of cIAP1 increases TRAIL-induced apoptosis, although probably not to a therapeutically relevant level.

cIAP1 and cIAP2 proteins are structurally very similar and have been shown to have overlapping functions. I postulated that knockdown of cIAP1 might lead to upregulation of cIAP2. To investigate this, a western blot was performed probing for cIAP2 48 hours after transfecting JU77 cells with cIAP1 siRNA. When cIAP1 was knocked down in JU77 cells, expression of cIAP2 increased, presumably to compensate for the loss of cIAP1 (Figure 4-1C). JU77 cells do not express cIAP2 under normal conditions but, interestingly, cIAP2 expression was observed when the cells were treated with a high concentration of scrambled siRNA.

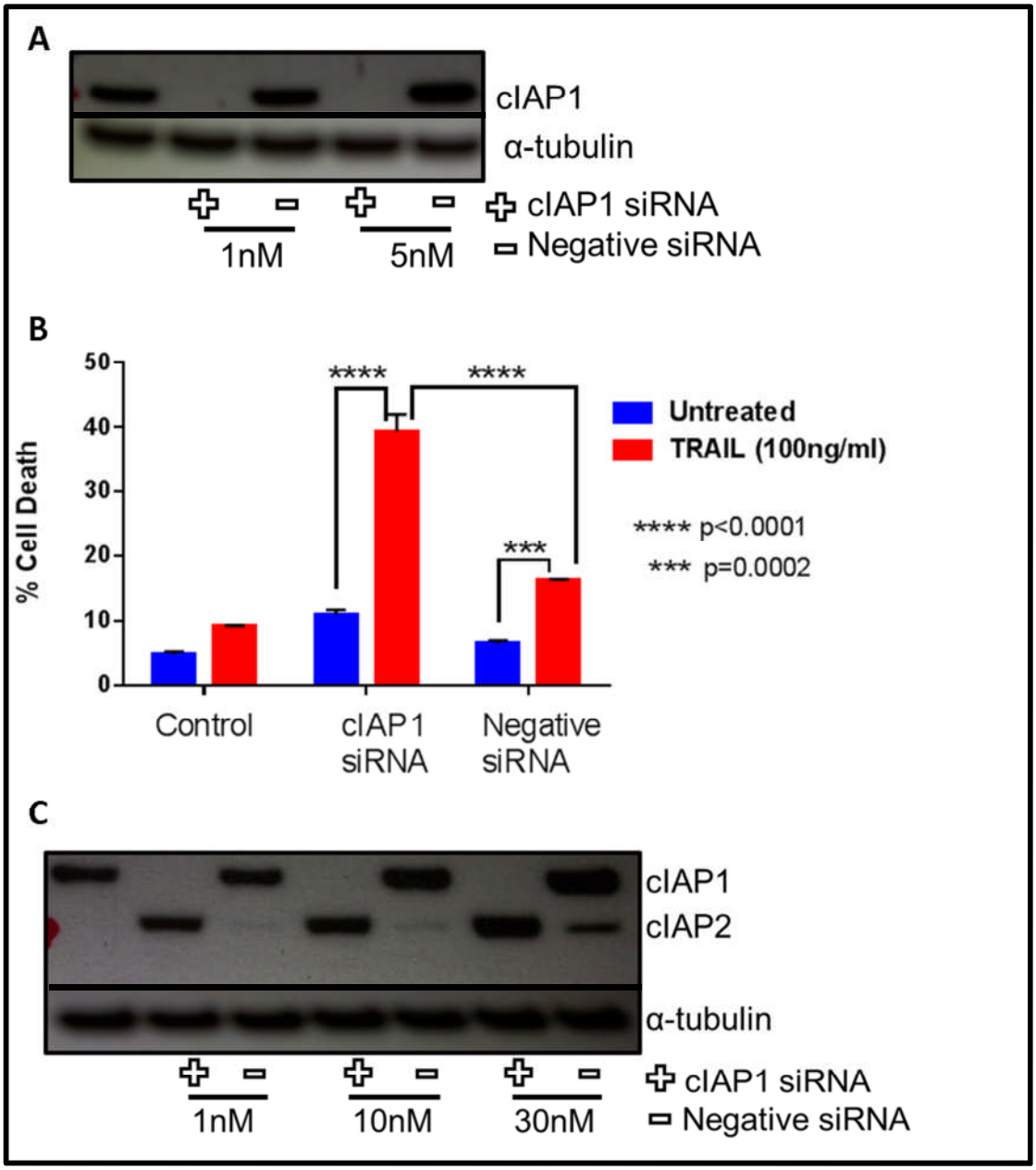

Figure 4-1 siRNA-mediated knockdown of cIAP1 in JU77 cells results in a significant increase in TRAIL-mediated apoptosis

JU77 cells were transfected with either 1 nM cIAP1-targeting siRNA or negative siRNA. A, Western blot of cIAP1 protein confirming the knockdown in cIAP1 siRNA-transfected cells but not in negative siRNA-transfected JU77 cells. B, JU77 cells were transfected with 1 nM cIAP1 or negative siRNA for 48 hours and then treated with TRAIL (100 ng/ml). Cell death was measured after 24 hours of TRAIL treatment using an Annexin V/DAPI assay. C, Western blots of cIAP1 and cIAP2 proteins in cIAP1 siRNA- and negative siRNA-transfected JU77 cells.

4.1.2 Simultaneous knockdown of cIAP1 and cIAP2 induces a synergistic increase in TRAIL-induced apoptosis

As cIAP1 knockdown led to cIAP2 overexpression to compensate for the functional loss of cIAP1, I simultaneously knocked down both cIAP1 and cIAP2 to determine their role in the inhibition of TRAIL-mediated apoptosis in MPM cells.

I first confirmed the effectiveness of the cIAP2 knockdown by western blot by probing for cIAP2. As JU77 cells do not normally express cIAP2, I treated the cells with cIAP1 siRNA. 1 nM cIAP2 siRNA knocked down cIAP2 expression in cIAP1 siRNA-transfected cells, while the equivalent concentration of negative siRNA did not (Figure 4-2A). So, 1nM cIAP1 siRNA and 1 nM cIAP2 siRNA can be used to knock down both cIAP1 and cIAP2 expression in JU77 cells.

To investigate the effect of cIAP1 and cIAP2 inhibition on TRAIL sensitivity, cIAP1 and cIAP2 were simultaneously knocked down in JU77 cells using 1 nM of each siRNA using interferrin transfection reagent. 2 nM negative siRNA (2X) was used as a control. 48 hours after transfection, these cells were treated with 100 ng/ml of TRAIL for 24 hours and cell death was measured by Annexin V/DAPI apoptosis assay. Knockdown of both cIAP1 and cIAP2 in JU77 cells resulted in 35% apoptosis in untreated cells. Interestingly, cIAP1/cIAP2-knocked down cells showed 72% apoptosis when treated with TRAIL, which is statistically higher than the level of apoptosis observed following TRAIL treatment of cells in which either cIAP1 or cIAP2 were individually knocked down. The 2X negative siRNA-treated cells showed 24% apoptosis when treated with TRAIL. These data indicate that there is a strong synergistic effect between loss of cIAP1/cIAP2 activity and TRAIL sensitivity (Figure 4-2B). Thus, cIAP1 and cIAP2 play an

important role in inhibiting TRAIL-mediated apoptosis and their knockdown or inhibition significantly increases TRAIL-mediated apoptosis in TRAIL-resistant cells.

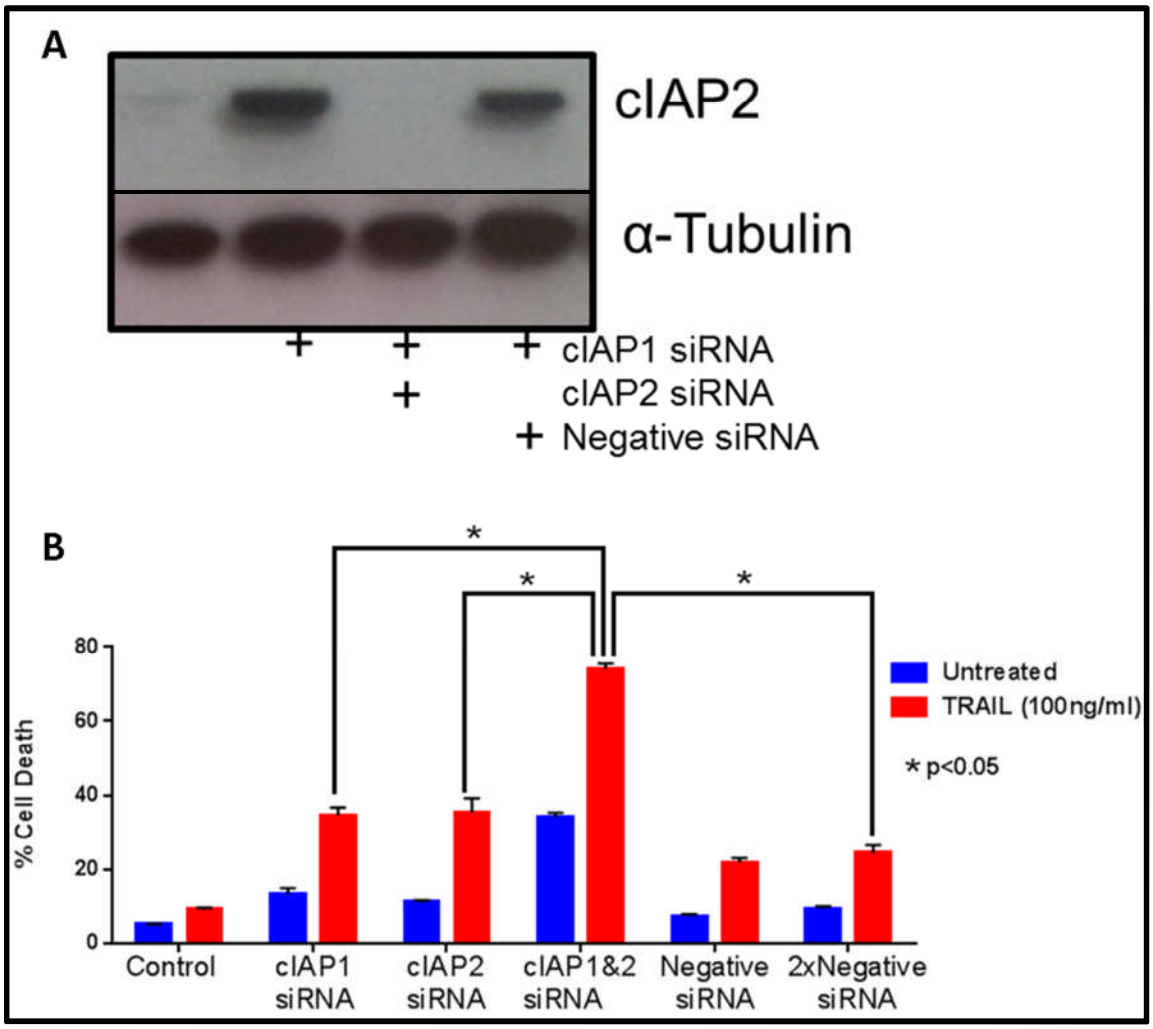

Figure 4-2 siRNA-mediated knockdown of both cIAP1 and cIAP2 in JU77 cells results in a synergistic increase in TRAIL-mediated apoptosis

JU77 cells were transfected with combinations of 1 nM cIAP1-targeting siRNA, 1 nM cIAP2-targeting siRNA and 1 nM negative siRNA. A, Western blots of cIAP1 and cIAP2 to confirm the knockdown in cIAP2 in JU77 cells. B, JU77 cells were transfected with 1 nM cIAP1 or cIAP2 siRNA or with both cIAP1 and cIAP2 siRNA, or with negative siRNA as a control, for 48 hours and then treated with TRAIL (100 ng/ml.) Cell death was measured after 24 hours of TRAIL treatment using an Annexin V/DAPI assay.

4.1.3 siRNA-mediated knockdown of cIAP1 was adequate to increase TRAIL-mediated apoptosis in MDAMB-231 cells

To determine whether IAPs play a role in TRAIL mediated apoptosis in other cancers, I next investigated the effect of TRAIL on cIAP1- and cIAP2-knocked down MDAMB-231 cells. I confirmed the knockdown of cIAP1 and cIAP2 by western blot. The cells were transfected with either 1 nM cIAP1- or cIAP2-targeting siRNA and equivalent concentrations of negative siRNA using interferrin transfection reagent. The effectiveness of the knockdown was confirmed in a western blot by probing for cIAP1 and cIAP2 protein expression 48 hours after transfection. The untransfected cells showed good expression of cIAP1 and to a certain degree of cIAP2. 1 nM cIAP1 siRNA-treated cells showed knockdown of cIAP1, while 1 nM negative siRNA did not knock down cIAP1 (Figure 4-3A). As in JU77 cells, knockdown of cIAP1 lead to upregulation of cIAP2 in MDAMB-231 cells. 1 nM cIAP2 siRNA-treated cells showed knockdown of cIAP2, while 1 nM negative siRNA did not knock down cIAP2.

MDAMB-231 cells were transfected with 1 nM cIAP1- or cIAP2-targeting siRNA or with 1 nM negative siRNA. 48 hours after transfection, the cells were treated with 100 ng/ml TRAIL for 24 hours. Cell death was measured following TRAIL treatment by an Annexin V/DAPI apoptosis assay. Knockdown of cIAP1 in MDAMB-231 resulted in a significant increase in apoptosis following TRAIL treatment compared with either cIAP2 siRNA-transfected cells or with negative siRNA-transfected cells. However, knockdown of cIAP2 failed to show a significant difference in apoptosis following TRAIL treatment compared with negative siRNA-transfected cells (Figure 4-3B). As knockdown of cIAP1 alone in MDAMB-231 cells induced apoptosis in 82% cells following TRAIL treatment, simultaneous knockdown of cIAP1 and cIAP2 was not required.

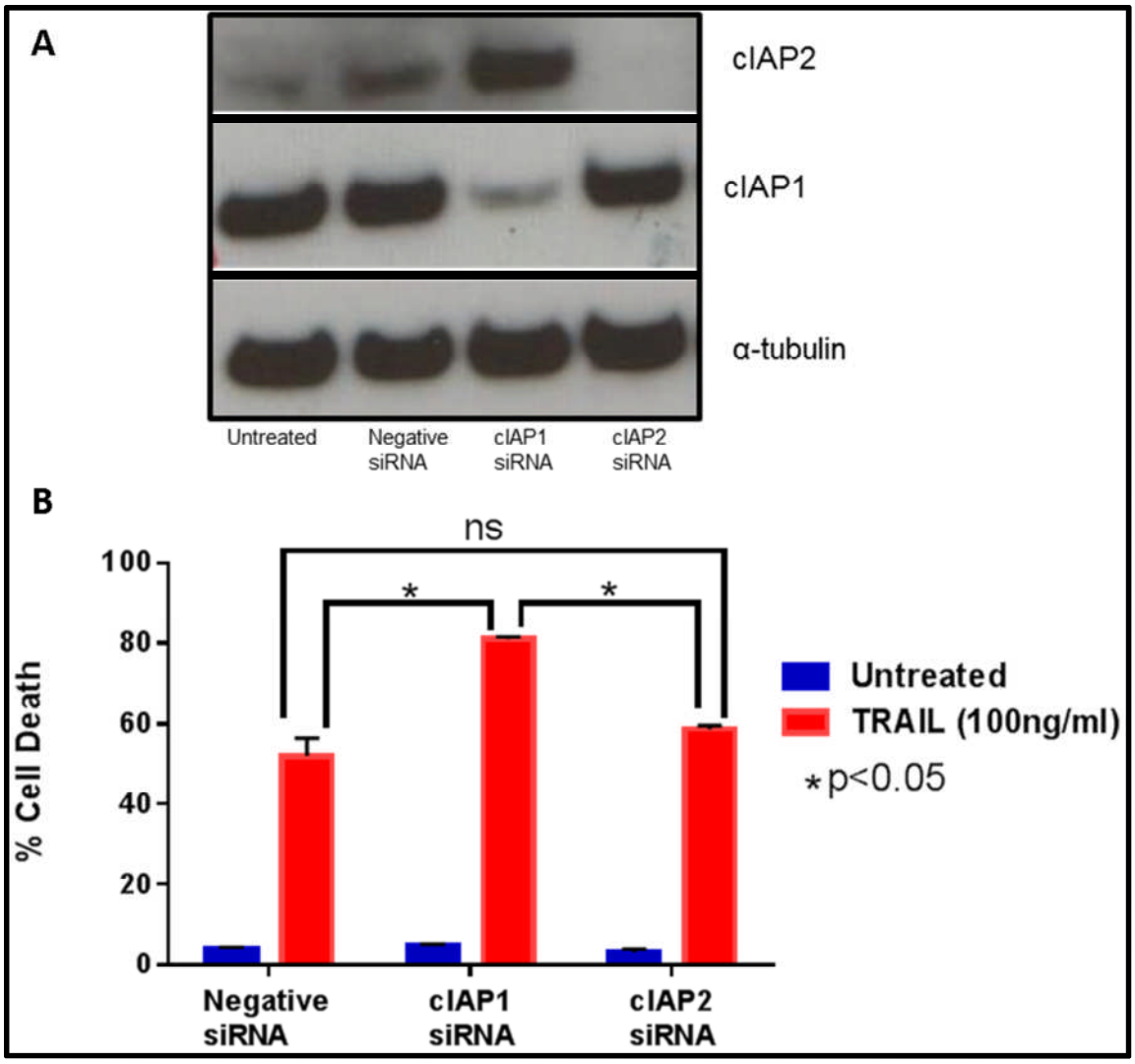

Figure 4-3 siRNA-mediated knockdown of cIAP1 in MDAMB-231 cells results in a significant increase in TRAIL-mediated apoptosis

MDAMB-231 cells were transfected with either 1 nM cIAP1- or cIAP2-targeting siRNA or with negative siRNA as a control. A, Western blots of cIAP1 and cIAP2 proteins in cIAP1 siRNA-, cIAP2 siRNA- and negative siRNA-transfected MDAMB-231 cells. B, MDAMB-231 cells were transfected with 1 nM cIAP1 siRNA or negative siRNA for 48 hours and then treated with TRAIL (100 ng/ml.) Cell death was measured after 24 hours of TRAIL treatment using an Annexin V/DAPI assay.

4.1.4 cIAP1/2 knockdown by shRNA sensitises cells to TRAIL

Although it was evident from Figure 4-2 that simultaneous knockdown of both cIAP1 and cIAP2 using siRNA in JU77 cells led to a significant increase in apoptosis following TRAIL treatment, the untreated duel-transfected cells showed 38% apoptosis. I wanted to investigate whether the simultaneous knockdown of cIAP1/2 led to the induction of apoptosis in JU77 cells without TRAIL treatment or whether this was the effect of duel transfection.

I therefore transduced JU77 cells with a cIAP1 or cIAP2 shRNA-expressing lentivirus at MOI 5. To knock down both cIAP1 and cIAP2, JU77 cells were transduced with both cIAP1 and cIAP2 shRNA-expressing lentiviruses, each at MOI 5, and control cells were transduced with the empty vector shRNA-expressing lentivirus at MOI 10. The empty vector shRNA-expressing JU77 cells expressed cIAP1 and also cIAP2. The cIAP1 shRNA-expressing cells showed a degree of knockdown but still expressed cIAP1. A good degree of knockdown of cIAP2 was observed in cells transduced with just cIAP2 shRNA-expressing lentivirus (Figure 4-4A). The combined knockdown of cIAP1 and cIAP2 resulted in decreased expression of both proteins but neither knockdown was as effective as that observed in cells in which either cIAP1 or cIAP2 had been individually knocked down.

Following transduction with shRNA, cells were treated with 100 ng/ml TRAIL for 24 hours and cell death was measured by an Annexin V/DAP1 apoptosis assay. The knockdown of either cIAP1 or cIAP2 induced a significant increase in apoptosis following TRAIL treatment compared with empty vector shRNA-expressing cells. Simultaneous knockdown of cIAP1 and cIAP2 also induced a significant increase in

apoptosis following TRAIL treatment compared with empty vector shRNA-expressing cells (Figure 4-4B). However, simultaneous knockdown of cIAP1 and cIAP2 did not show a significant increase in apoptosis following TRAIL treatment compared with individual knockdown of either cIAP1 or cIAP2.

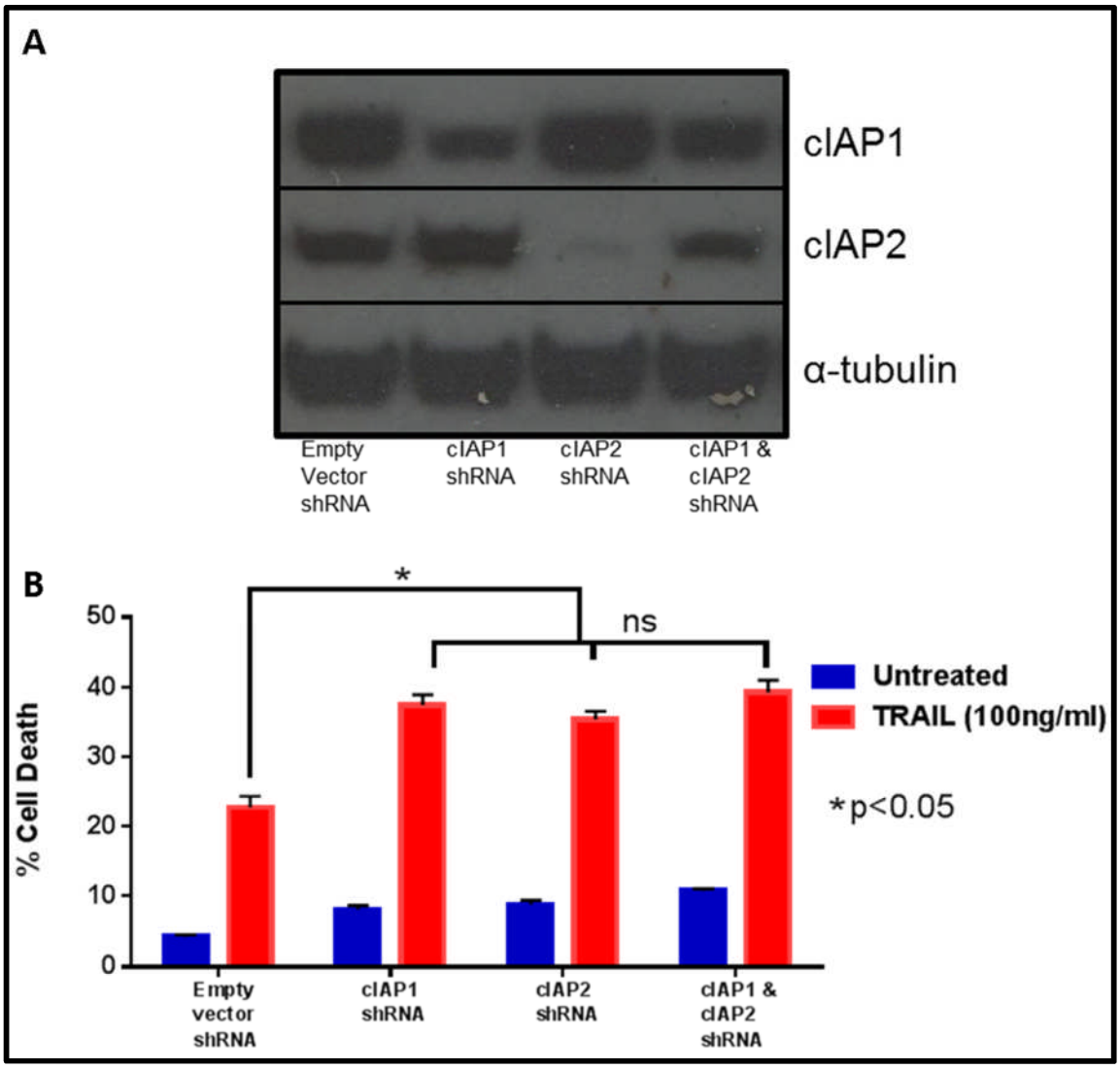

Figure 4-4 shRNA-mediated knockdown of both cIAP1 and cIAP2 in JU77 cells results in increased TRAIL-mediated apoptosis

JU77 cells were transduced with either cIAP1 or cIAP2 shRNA or with empty vector shRNA-expressing lentivirus at MOI 5. A, Western blot of cIAP1 and cIAP2 proteins confirming the knockdown in shRNA-transduced cells. B, JU77 cells transduced with cIAP1, cIAP2 or both cIAP1 and cIAP2 shRNA-expressing lentivirus at MOI 5 were treated with TRAIL (100 ng/ml). JU77 cells transduced with empty vector shRNA at MOI 10 were used as control. Cell death was measured after 24 hours using an Annexin V/DAPI assay.

A similar observation was made when MDAMB-231 cells were transduced with cIAP1 shRNA-, cIAP2 shRNA-, or both cIAP1 shRNA- and cIAP2 shRNA-expressing lentivirus. I transduced MDAMB-231 cells with cIAP1 shRNA- or cIAP2 shRNA-expressing lentivirus at MOI 5 and control cells with empty vector-expressing lentivirus. To knockdown both cIAP1 and cIAP2, MDAMB-231 cells were transduced with both cIAP1 shRNA- and cIAP2 shRNA-expressing lentivirus, each at MOI 5, and control cells with the empty vector shRNA-expressing lentivirus at MOI 10. The empty vector-expressing MDAMB-231 cells expressed cIAP1 and cIAP2. The cIAP1 shRNA-expressing cells showed a good degree of knockdown but still expressed cIAP1. A degree of knockdown of cIAP2 was also observed in cIAP2 shRNA-expressing cells (Figure 4-5A). The combined knockdown of both cIAP1 and cIAP2 resulted in decreased expression of both proteins but, as seen in JU77 cells, neither knockdown was as effective as that observed in cells in which either cIAP1 or cIAP2 had been individually knocked.

The cells were treated with 100 ng/ml TRAIL for 24 hours and cell death was measured by an Annexin V/DAPI apoptosis assay. The knockdown of cIAP1 alone induced a significant increase in apoptosis following TRAIL treatment compared with empty vector shRNA-expressing cells (Figure 4-5B). Knockdown of both cIAP1 and cIAP2 induced a similar level of apoptosis to knockdown of cIAP1 alone following TRAIL treatment. This further proves that knockdown of cIAP1 alone is sufficient to induce apoptosis in MDAMB-231 cells.

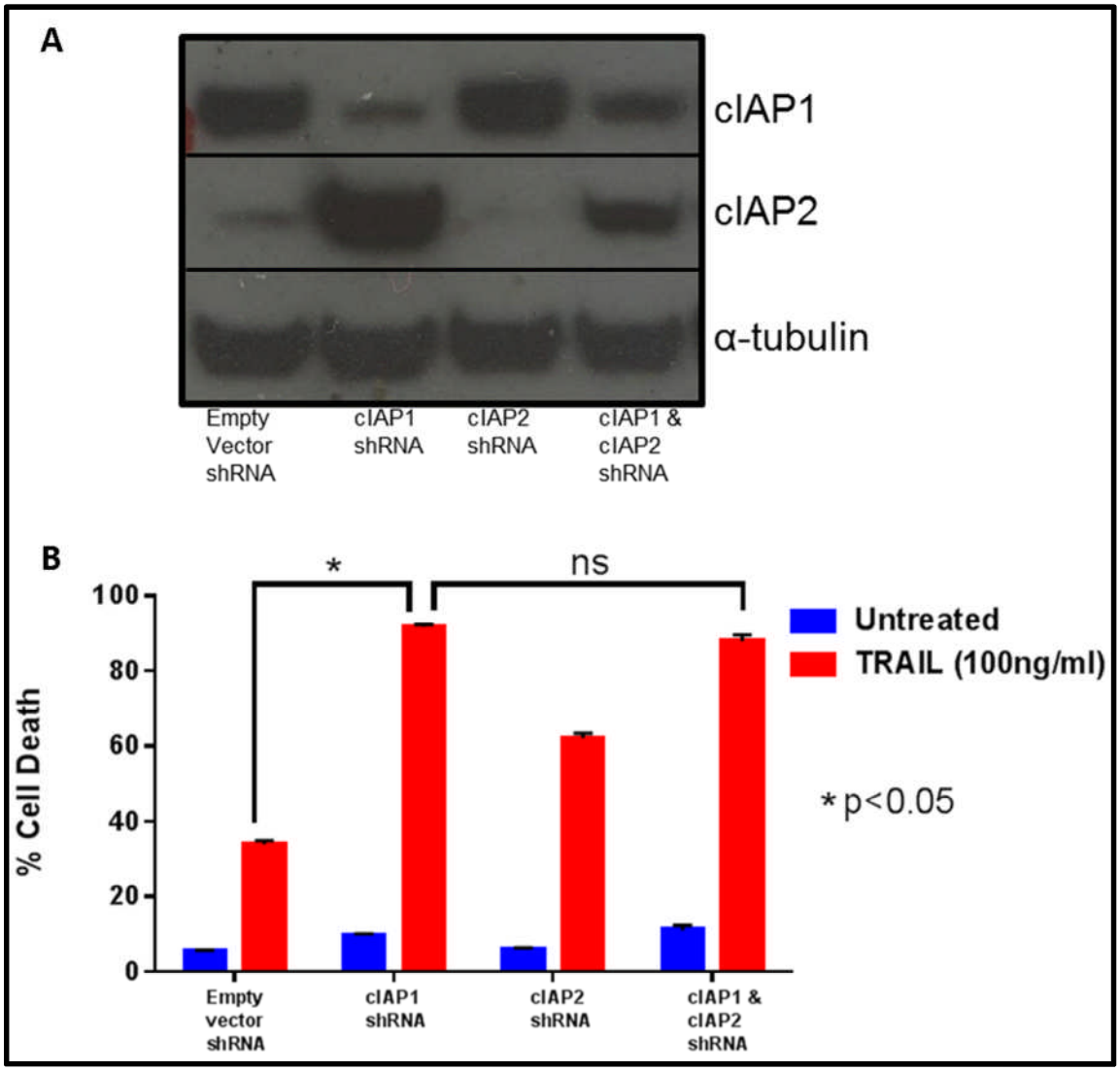

Figure 4-5 shRNA-mediated knockdown of both cIAP1 and cIAP2 in MDAMB-231 cells results in increased TRAIL-mediated apoptosis

MDAMB-231 cells were transduced with either cIAP1 or cIAP2 shRNA or with empty vector shRNA-expressing lentivirus at MOI 5. A, Western blot of cIAP1 and cIAP2 proteins confirming the knockdown in shRNA-transduced cells. B, MDAMB-231 cells transduced with cIAP1, cIAP2 or both cIAP1 and cIAP2 shRNA-expressing lentivirus at MOI 5 were treated with TRAIL (100 ng/ml). MDAMB-231 cells transduced with empty vector shRNA at MOI 10 were used as a control. Cell death was measured after 24 hours using an Annexin V/DAPI assay.

4.1.5 LCL161 sensitises cells to TRAIL

Given that the IAPs cIAP1 and cIAP2 play a key role in the TRAIL-mediated apoptosis of tumour cells, it would be appropriate to use an IAP inhibitor to sensitise the tumour cells to TRAIL. These drugs are classified as SMAC mimetics as they mimic the function of SMAC, which is an intracellular IAP inhibitor. LCL161 is a SMAC mimetic that is known to degrade cIAP1 and to inhibit the functions of cIAP2 and XIAP [241].

I first confirmed the activity of LCL161. I did this by treating the tumour cell lines, JU77 and MDAMB-231, with LCL161 and western blotting for IAPs. This showed that cIAP1 expression was lost after 24 hours of treatment of LCL161 in JU77 and MDAMB-231 cells (Figure 4-6A). Although expression of cIAP2 was not lost, LCL161 inhibits its function as it binds to its active site. Hence, LCL161 is an ideal drug to combine with TRAIL treatment.

Exposure to increasing concentrations (1 µM, 4 µM and 8 µM) of LCL161 on its own did not induce apoptosis in JU77 cells compared with vehicle control cells. However, when JU77 cells were treated with LCL161 in combination with TRAIL, a significant increase in apoptosis was observed. This is probably the result of activation of the extrinsic apoptotic pathway by TRAIL. TRAIL induced apoptosis in 25% of vehicle-treated control cells, while the same concentration of TRAIL along with 1 µM, 4 µM and 8 µM LCL161 induced 45%, 68% and 76% apoptosis, respectively (Figure 4-6B). This shows that TRAIL-resistant JU77 cells can be sensitised to TRAIL-induced apoptosis by treating them with LCL161.

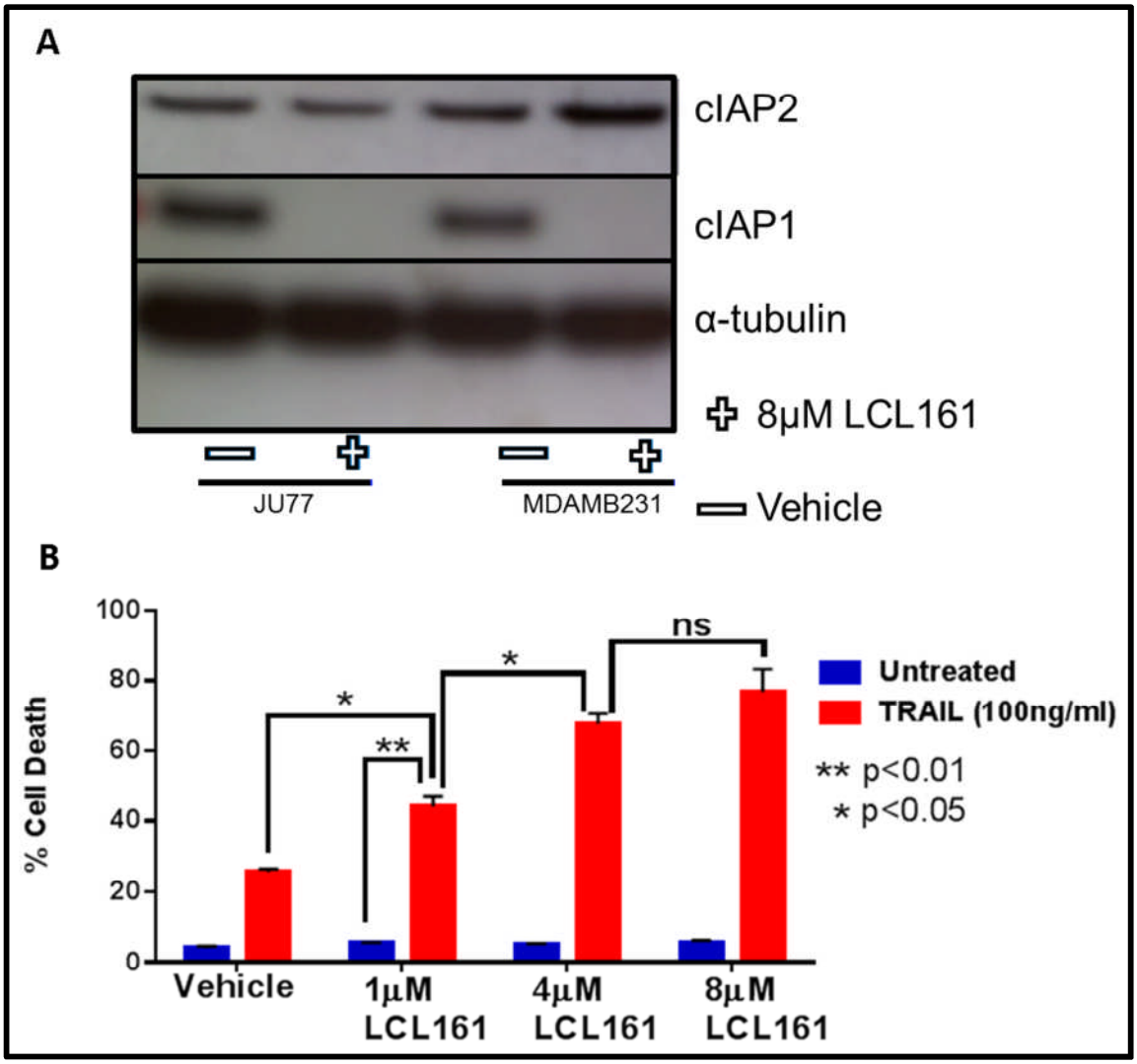

Figure 4-6 LCL161 degrades cIAP1 in JU77 and MDAMB-231 cells

A, JU77 and MDAMB-231 cells were treated with 8 μM LCL161 for 24 hours. Cell lysates were then probed for cIAP1 and cIAP2 proteins by western blot. B, JU77 cells were treated with TRAIL (100ng/ml) or LCL161 (1 μM, 4 μM and 8 μM) alone or in combination for 24 hours and cell death was measured after 24 hours using an Annexin V/DAPI assay.

I next investigated whether the combination of TRAIL and LCL161 could induce greater levels of apoptosis in MDAMB-231 cells than treatment with either TRAIL or LCL161 alone. The combination of 1 μM LCL161 and 100 ng/ml TRAIL induced 88% apoptosis in MDAMB-231 cells (Figure 4-7A). As seen in JU77 cells, this combination was significantly higher levels of apoptosis than that induced by either TRAIL (28%) or LCL161 (22%) as monotherapies. Unlike JU77 cells, there was no further significant increase in apoptosis with increasing concentrations of LCL161 in combination with 100 ng/ml TRAIL. Cell death resulting from the combination of TRAIL and LCL161 was visualised using crystal violet staining. I treated MDAMB-231 cells with DMSO alone, 1 μM LCL161 alone, 100 ng/ml TRAIL alone or the combination of 1μM LCL161 and 100 ng/ml TRAIL for 24 hours and then stained them with crystal violet (Figure 4-7B). The DMSO vehicle-treated and LCL161-treated cells showed good staining, indicating high numbers of cells. The TRAIL-treated cells showed partial staining but there was no staining observed in the cells that had been treated with a combination of TRAIL and LCL161, indicating that some cells had died after TRAIL treatment alone and majority had died after the combination treatment.

Interestingly, LCL161 alone showed a dose-related increase in induction of apoptosis in MDAMB-231 cells. 1 μM, 4 μM and 8 μM LCL161 induced 22%, 33% and 54% apoptosis, respectively (Figure 4-7A). This indicates that inhibition of IAPs alone could lead to apoptosis in MDAMB-231 cells.

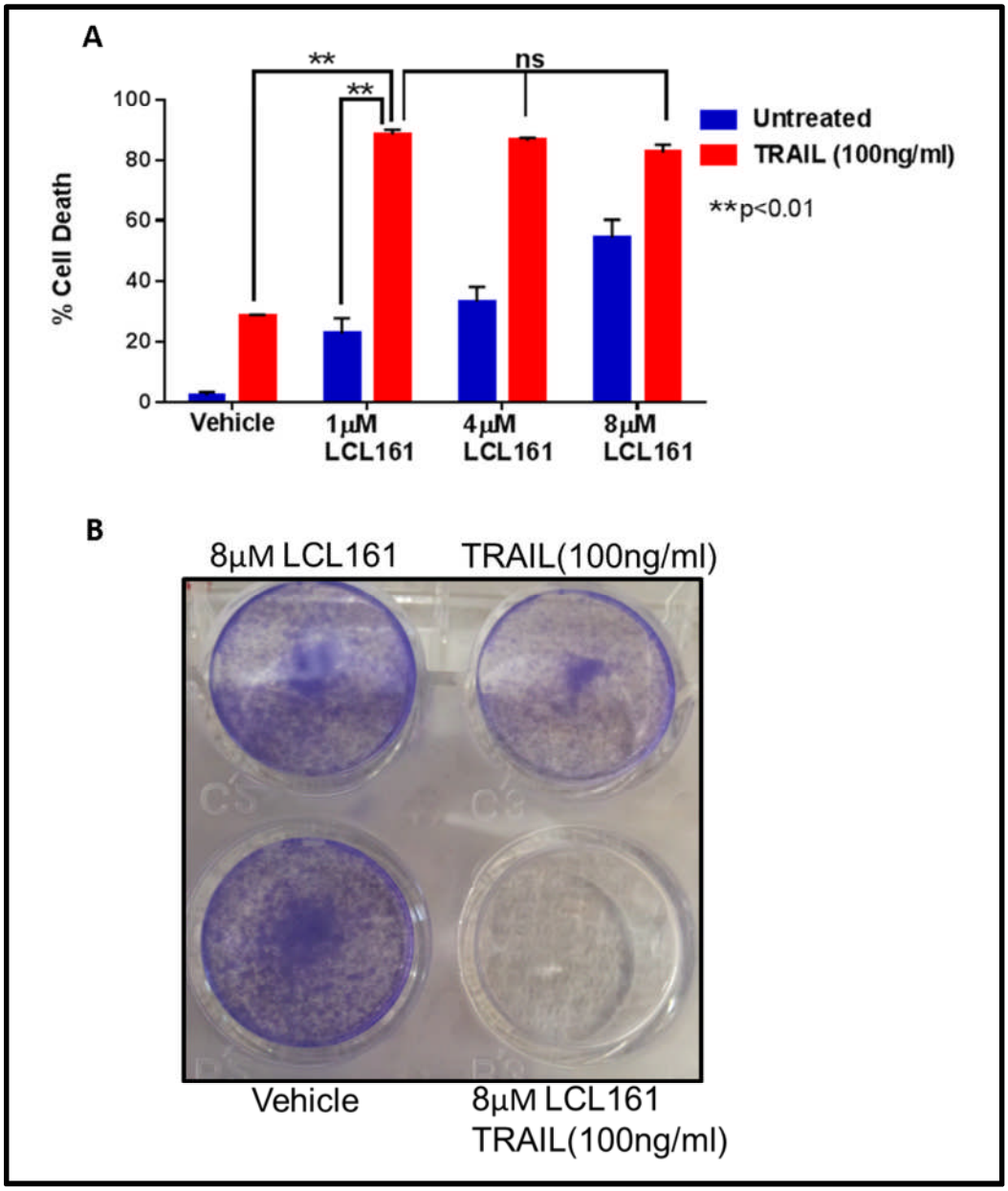

Figure 4-7 LCL161 acts synergistically with TRAIL to increase apoptosis in MDAMB-231 cells

A, MDAMB-231 cells were treated with TRAIL (100 ng/ml) or LCL161 (1 μM, 4 μM and 8 μM) alone or in combination for 24 hours and cell death was measured after 24 hours using an Annexin V/DAPI assay. B, MDAMB-231 cells were treated with TRAIL (100 ng/ml) or LCL161 (8 μM) alone or in combination for 24 hours and stained with crystal violet to visualise cell viability.

4.2 Combination of chemotherapeutic agents and MSC-flT induces apoptosis in TRAIL-resistant tumour cells

The earlier experiments proved that TRAIL-resistant cells could be sensitised to TRAIL by inhibiting anti-apoptotic proteins using specific inhibitors. I next proceeded to use these inhibitors in combination with MSC-flT cells to investigate whether a similar effect could be observed. I selected the IAP inhibitor LCL161, the BCL-2 family inhibitor obatoclax, the cFLIP inhibitor SAHA and the cFLIP and MCL-2 inhibitor SNS-032 for this study. Nine rTRAIL-resistant cell lines A549, H723, H2818, H2810, HT29, MPP-89, H2803, HA7 and RCC10 and one TRAIL-sensitive cell line MDAMB-231 were cultured with MSC-flT cells, in combination with the chemotherapeutic agents. Each cell line was treated with chemotherapeutic agents alone, rTRAIL alone and in combination with chemotherapeutic agents, and MSC-flT cells alone and in combination with chemotherapeutic agents. The data from all of the cell lines were grouped together for each chemotherapeutic agent for ease of understanding.

The tumour cells are stained with DiI and allowed to grow for 24 hours. They were treated with the chemotherapeutic agent alone or in combination with 100 ng/ml rTRAIL, or were co-cultured with MSC-flT cells in a 1:4 MSC-flT cell:tumour cell ratio with or without chemotherapeutic agents. Cell death was determined after 24 hours using the AnnexinV/DAPI apoptosis assay. DiI-positive cells were analysed to exclude MSC-flT cells.

5 μM LCL161 was used to inhibit IAPs. LCL161 on its own did not induce apoptosis in any of the tumour cells. The combination of LCL161 and rTRAIL induced greater than 50% apoptosis in four cell lines. However, the combination of LCL161 and MSC-flT cells

induced even higher levels of apoptosis than the combination of LCL161 and rTRAIL: the combination of LCL161 and MSC-flT induced greater than 50% apoptosis in eight tumour cell lines (Figure 4-8A).

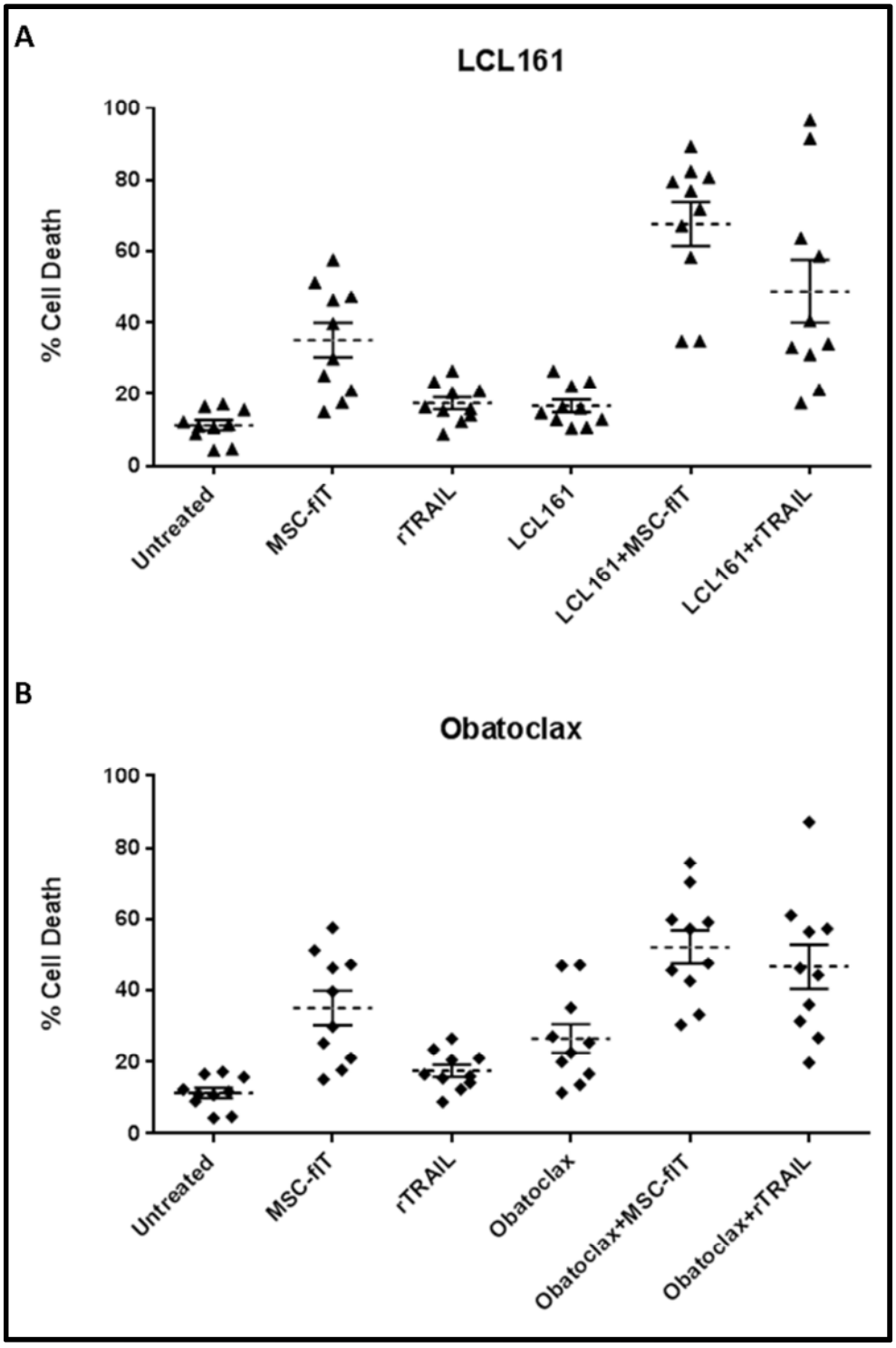

Figure 4-8 Combination of TRAIL and either LCL161 or obatoclax increases apoptosis in tumour cells

The apoptosis of ten cancer cell lines (nine TRAIL resistant: A549, H723, H2818, H2810, HT29, MPP-89, H2803, HA7 and RCC10, and one TRAIL sensitive: MDAMB-231) was determined after 24 hours of culture with 50 ng/ml purified recombinant TRAIL (rTRAIL), MSC-flT cells at a ratio of 4 MSCs to 10 cancer cells, either alone or in combination with A, LCL161 or B, obatoclax. Data show that combination of LCL161 or obatoclax with MSC-flT cells induces increased cancer cell apoptosis. Dotted line represents the mean cell death of all cell lines. Data represent means of three experiments for each cell line.

250 nM obatoclax was used to inhibit the BCL-2 family of anti-apoptotic proteins, including BCL-2, BCL-W, BCL-X_L and MCL-1. Interestingly, obatoclax did induce apoptosis on its own in some tumour cell lines. The combination of obatoclax and rTRAIL induced greater than 50% apoptosis in five cell lines. In contrast to LCL-161, the combination of obatoclax and MSC-flT cells was no better at inducing apoptosis than the combination of obatoclax and rTRAIL (Figure 4-8B). In fact, the combination of obatoclax and MSC-flT cells induced greater than 50% apoptosis in only four tumour cell lines.

SAHA is an HDAC inhibitor and it transcriptionally inhibits cFLIP expression. 2.5 μM SAHA was used to inhibit cFLIP in these experiments. This concentration of SAHA did not induce more than 25% apoptosis in the majority of tumour cell lines. The combination of SAHA and rTRAIL induced greater than 50% apoptosis in five cell lines (Figure 4-9A). However, as with LCL-161, the combination of SAHA and MSC-flT cells was better at inducing apoptosis than the combination of SAHA and rTRAIL: the combination of SAHA and MSC-flT cells induced greater than 50% apoptosis in nine tumour cell lines.

SNS-032 inhibits CDK9, which is necessary for transcription of cFLIP and MCL-1. 300 nM of SNS-032 was used in these experiments to inhibit cFLIP and MCL-1. Similarly to obatoclax, SNS-032 did induce apoptosis on its own in some tumour cell lines. The combination of SNS-032 and rTRAIL induced greater than 50% apoptosis in nine cell lines, of which six showed greater than 70% apoptosis (Figure 4-9B). Similarly to obatoclax, the combination of SNS-032 and MSC-flT cells induced similar levels of cell death as the combination of SNS-032 and rTRAIL. Indeed, the combination of SNS-032

and MSC-flT cells induced greater than 50% apoptosis in nine tumour cell lines, of which five showed greater than 70% apoptosis.

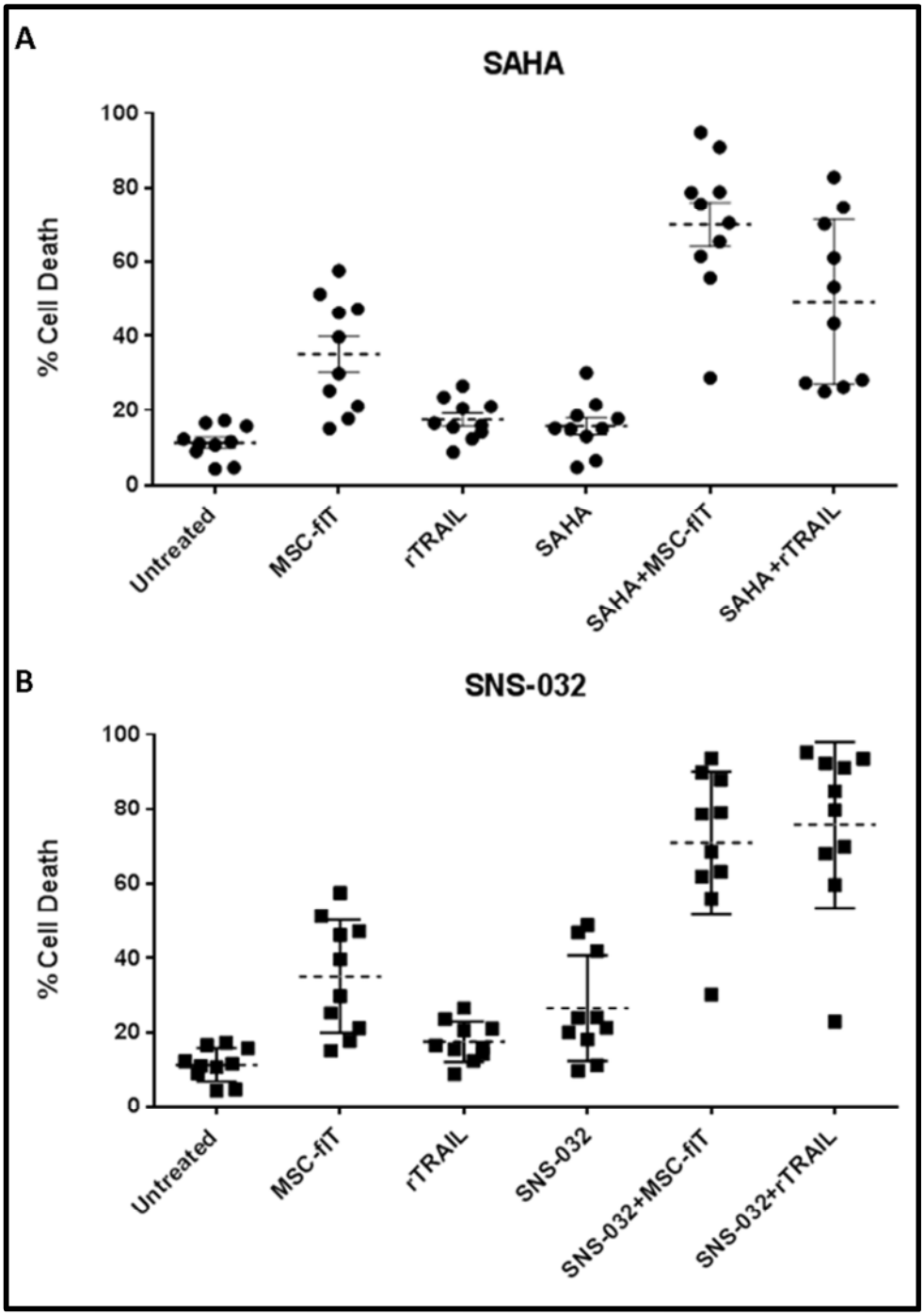

Figure 4-9 Combination of TRAIL and either SAHA or SNS-032 increases apoptosis in tumour cells

The apoptosis of ten cancer cell lines (nine TRAIL resistant: A549, H723, H2818, H2810, HT29, MPP-89, H2803, HA7 and RCC10, and one TRAIL sensitive: MDAMB-231) was determined after 24 hours of culture with 50 ng/ml purified recombinant TRAIL (rTRAIL), MSC-flT cells at a ratio of 4 MSCs to 10 cancer cells, either alone or in combination with A, SAHA or B, SNS-032. Data show that combination of SAHA or SNS-032 with MSC-flT cells induces increased cancer cell apoptosis. Dotted line represents the mean cell death of all cell lines. Data represent means of three experiments for each cell line.

4.2.1 The combination of chemotherapeutic agents and TRAIL does not induce significant levels of apoptosis in untransformed cells

It was evident from earlier experiments that combining chemotherapeutic agents with MSC-TRAIL induced high levels of apoptosis in TRAIL-resistant tumour cells. However, it was important to demonstrate that this combination treatment did not induce apoptosis in untransformed cells. To do this, I cultured human lung fibroblasts (HLFs) with MSC-flT cells in combination with chemotherapeutic agents.

HLFs were stained with DiI and allowed to grow for 24 hours. They were treated with the chemotherapeutic agent alone or in combination with 100 ng/ml rTRAIL, or cultured with MSC-flT cells in a 1:4 MSC-flT cell:tumour cell ratio with or without chemotherapeutic agent. Cell death was determined after 24 hours using AnnexinV/DAPI apoptosis assay. DiI-positive cells were analysed to exclude MSC-flT cells.

Unlike tumour cells, the combination of chemotherapeutic agents and MSC-flT cells did not show substantial cytotoxicity in HLFs. The combination of SAHA, SNS-032 or LCL161 with MSC-flT cells induced 20%, 16% and 26% apoptosis in HLFs, respectively, while the combination of obatoclax with MSC-flT cells resulted in 33% apoptosis (Figure 4-10). This demonstrates that combination of chemotherapeutic agents and MSC-flT cells is tumour-specific.

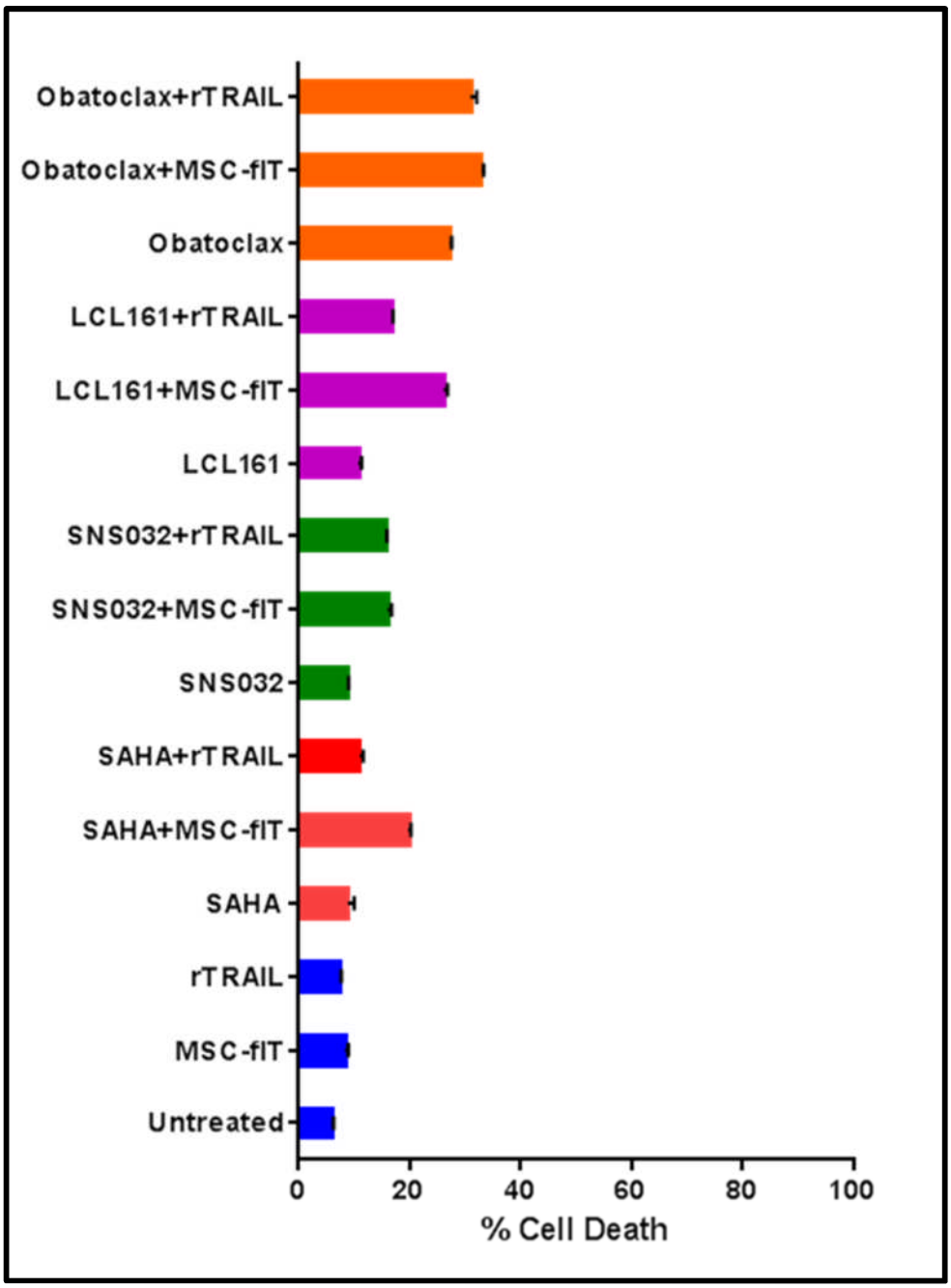

Figure 4-10 Co-culture of human lung fibroblasts with MSC-flT cells and chemotherapeutic agents induces only low levels of apoptosis

The apoptosis of human lung fibroblasts (HLFs) was determined after 24 hours of culture with SAHA, SNS-032, LCL161 or obatoclax, either alone or in combination with 50 ng/ml purified recombinant TRAIL (rTRAIL) or MSC-flT cells at a ratio of 4 MSCs to 10 cancer cells. Data show that combination of chemotherapeutic agents with MSC-flT cells induces only low levels of apoptosis in normal cells.

4.3 Combination of MSC-flT cells and SNS-032 does not reduce tumour burden *in vivo*

Having demonstrated that the combination of chemotherapeutic agents and MSC-flT cells was efficient in inducing apoptosis selectively in tumour cells but not in untransformed cells, I went on to test the efficacy of combination therapy *in vivo* in a mouse xenograft model.

Of all four chemotherapeutic agents, SNS-032 in combination with MSC-TRAIL showed good toxicity to tumour cells and low levels of cytotoxicity in HLFs and thus was used in the animal model. TRAIL-resistant A549 cells were transduced with mstrawberry-luciferase expressing lentivirus (A549-luc) and transduced cells were selected by fluorescence-activated cell sorting for strawberry-positive cells. Lung tumours were established by intravenously injecting one million A549-luc cells into the tail veins of 32 immunocompromised NOD/SCID mice. The tumours were allowed to establish for 7 days. Bioluminescence imaging of mice on an IVIS machine 15 minutes after injection of 200 µl of 10 mg/ml luciferin per mouse was done on day 8 and the mice were allocated into four groups of eight mice each. Care was taken to ensure similar tumour burdens in all groups. Treatment was started on day 9 with either vehicle, MSC-flT cells, SNS-032 or the combination of SNS-032 and MSC-flT cells. 30 mg/kg SNS-032 was injected intraperitoneally three times a week, while 0.5 million MSC-flT cells were injected intravenously twice a week (Figure 4-11A). Bioluminescence imaging was done on days 12, 19, 26 and 33 to longitudinally track the tumour burden in the mice and the mice were sacrificed on day 36 to harvest the lungs and the other organs.

There was no significant difference observed in the tumour burdens of mice treated with vehicle, MSC-flT cells, SNS-032 or the combination of SNS-032 and MSC-flT cells (Figure 4-11B).

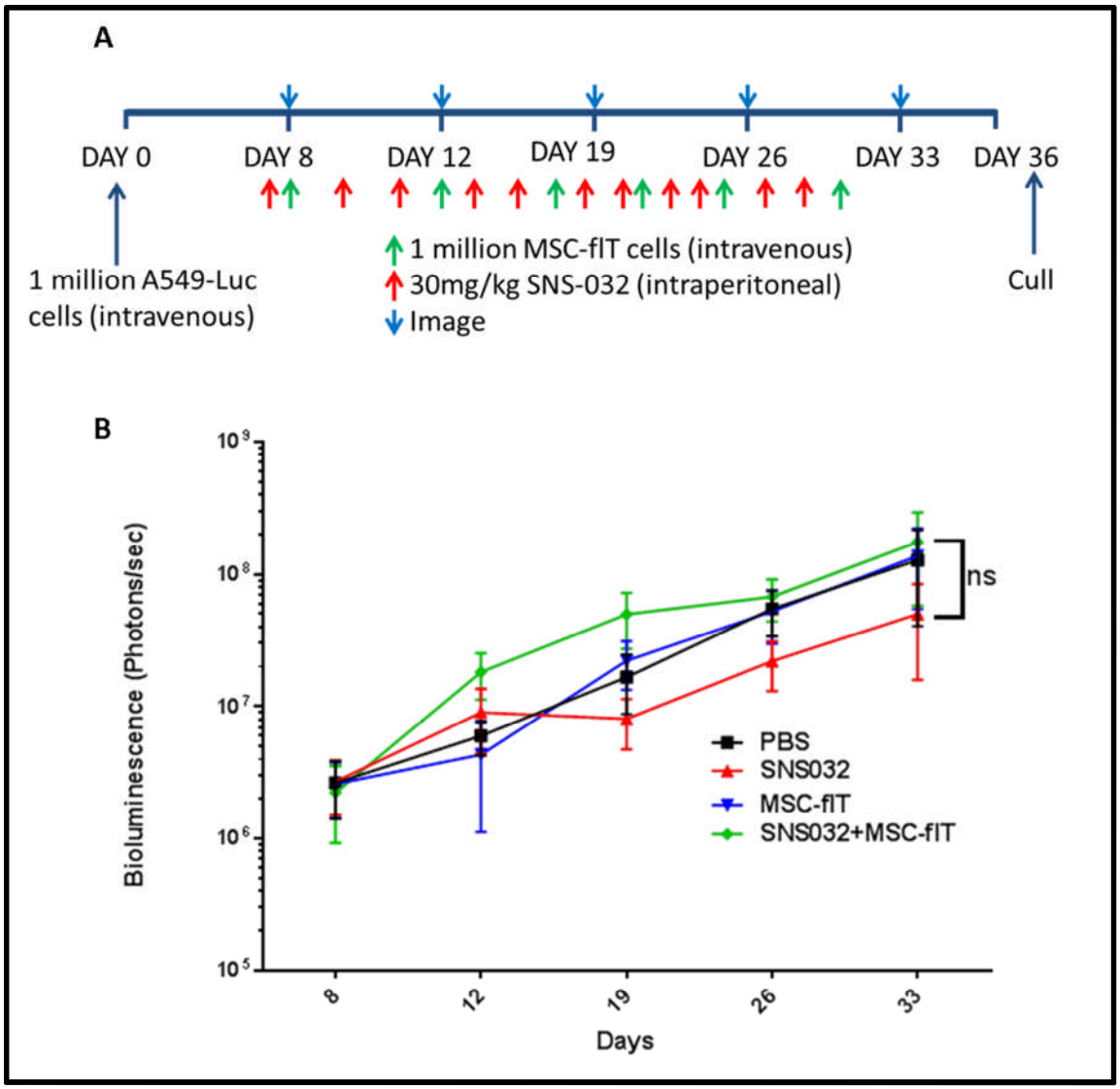

Figure 4-11 Combination treatment of MSC-flT cells and SNS-032 does not induce a reduction in tumour burden in a mouse xenograft model

1 x 10^6 strawberry-luciferase-expressing A549 cells were injected intravenously into the tail vein of mice on day 8. Tumour development was tracked by bioluminescence imaging on days 8, 12, 19, 26 and 33. Mice were grouped into four groups based on tumour burden on day 8 and were treated either with PBS and vehicle, PBS and SNS-032, MSC-flT cells and vehicle, or MSC-flT cells and SNS-032. SNS-032 or vehicle were injected once every two days intraperitoneally while MSC-flT cells or PBS were injected intravenously twice a week. Mice were sacrificed on day 36 and tumours were extracted.A, schematic of the experimental plan. Bioluminescence imaging of the mice was done after injecting luciferin to track the tumour growth. B, Tumour burden of mice quantified by bioluminescence imaging.

4.4 Discussion

Similar to rTRAIL, tumours cells are also variably sensitive to MSC-TRAIL. As shown in chapter III, MSC-TRAIL fails to induce therapeutically relevant levels of apoptosis in some TRAIL-resistant cell lines. In this chapter, I wished to investigate whether MSC-TRAIL could be used in combination with chemotherapeutic agents to exploit a synergistic effect for the treatment of cancers.

4.4.1 Inhibiting IAPs sensitises cancer cells to MSC-TRAIL

Understanding the mechanism of resistance to TRAIL-induced apoptosis would help in developing a suitable chemotherapeutic to use in combination with MSC-TRAIL. IAPs are known to play an important role in apoptotic pathways and so these proteins were the focus of my studies. In this chapter, I show that cIAP1 and cIAP2 play a prominent role in inhibiting TRAIL-induced apoptosis, which is in consistent with the literature [109].

Knockdown of cIAP1 by siRNA increased TRAIL-induced apoptosis in TRAIL-resistant JU77 cells but this increase was probably not therapeutically appropriate (Figure 4-1B). I observed that, following knockdown of cIAP1, JU77 cells upregulate expression of cIAP2, possibly to compensate for loss of cIAP1 (Figure 4-1C). It is known that cIAP1 and cIAP2 are homologous proteins with similar functions. Indeed, an earlier study [129] showed that both cIAP1 and cIAP2 can carry out the same function in the TNF pathway. Furthermore, it has been shown that cIAP2 is post-translationally downregulated by cIAP1 [242]. Knockdown of cIAP1 therefore results in a deficiency in the regulation of cIAP2, which increases cIAP2 protein levels. These increased cIAP2

levels might inhibit TRAIL-mediated apoptosis. It is interesting to note that the negative siRNA treatment also induced the expression of cIAP2 in a dose-dependent manner (Figure 4-1C). This might be due to increased stress as a result of siRNA transfection, which results in overexpression of anti-apoptotic proteins such as cIAP2.

I postulated that simultaneous knockdown of both cIAP1 and cIAP2 would significantly sensitise JU77 cells to TRAIL. Knockdown of either cIAP1 or cIAP2 alone induced similar levels of apoptosis following treatment with TRAIL but these levels were probably not therapeutically appropriate. Interestingly, simultaneous knockdown of both cIAP1 and cIAP2 induced a significant increase in TRAIL-mediated apoptosis in TRAIL-resistant JU77 cells compared with single knockdowns or negative siRNA-transfected cells (Figure 4-2B). In addition, knockdown of cIAP1 or cIAP2 alone or of both proteins together using shRNA in JU77 cells induced an increase in apoptosis following TRAIL compared with TRAIL-treated empty vector-transduced cells. However, unlike the results obtained using siRNA, there was no difference between levels of apoptosis in either of the single knockdowns and the simultaneous knockdown of cIAP1 and cIAP2 (Figure 4-4B). This might be result of incomplete knockdown by shRNA in JU77 cells (Figure 4-4A).

Having shown that inhibition of cIAPs could sensitise TRAIL-resistant tumour cells to rTRAIL, I wanted to investigate the effect of cIAPs in TRAIL-sensitive cells. I knocked down cIAP1 and cIAP2 either individually or together using siRNA in partially TRAIL-sensitive MDAMB-231 cells (Figure 4-3A). The increase in cIAP2 levels after knockdown of cIAP1 was observed in MDAMB-231 cells as well as in JU77 cells. TRAIL treatment of cells in which cIAP1 was knocked down cells resulted in significant cell death compared

with negative siRNA-transfected MDAMB-231 cells (Figure 4-3B). However, TRAIL treatment of cells in which cIAP2 was knocked down failed to induce significant cell death compared with negative siRNA-transfected MDAMB-231 cells. Similar results were observed by knocking down cIAP1 and cIAP2 either individually or simultaneously by shRNA in MDAMB-231 cells (Figure 4-5).

It is interesting to note that JU77 cells require inhibition of both cIAP1 and cIAP2 to effectively sensitise them to TRAIL-mediated apoptosis, while inhibition of cIAP1 would suffice in MDAMB-231. Nevertheless, cIAP1 and cIAP2 play an important role in the inhibition of TRAIL-mediated apoptosis. The study [128] by Salvesen *et al* showed that neither cIAP1 nor cIAP2 can inhibit caspases directly in physiological conditions and only XIAP can bind and inhibit caspases. However, cIAP1 and cIAP2 can bind to and inhibit SMAC, which inhibits XIAP. This does mean that inhibition of XIAP should carry the benefit of inhibition of cIAP1 and cIAP2 as they merely allow XIAP to inhibit caspases.

As simultaneous knockdown of cIAP1 and cIAP2 effectively sensitise tumour cells to TRAIL, it can be inferred that cIAP1 and cIAP2 might not be involved in indirect caspase inhibition but might play another regulatory role in the TRAIL pathway. cIAP1 and cIAP2 are important in the TNF pathway [129, 243] as they activate the NF-κB survival pathway when TNFα binds to its respective receptor and their absence induces apoptosis by triggering the extrinsic apoptotic pathway. Given that TRAIL is also a member of the TNF superfamily, cIAP1 and cIAP2 might also be playing an important role at the receptor level. Further investigations are to be carried out to establish the role of cIAP1 and cAIP2 in the TRAIL pathway.

As inhibition of cIAP1 and cIAP2 significantly increases TRAIL-induced apoptosis it would be ideal to use SMAC-mimetic drugs in combination with TRAIL for treatment of cancers. LCL161 is one such SMAC mimetic that degrades cIAP1 and inhibits the functions of cIAP2 and XIAP (Figure 4-6A). LCL161 does not induce apoptosis in TRAIL-resistant JU77 cells on its own but induces a dose-related increase in apoptosis when combined with TRAIL (Figure 4-6B). It was also very potent in sensitising TRAIL-sensitive MDAMB-231 cells to TRAIL. It is interesting to note that LCL161 as a monotherapy induces a dose-related increase in apoptosis in MDAMB-231 cells (Figure 4-7). This might be result of sensitising the cells to endogenous TNFα or TRAIL expression.

4.4.2 Chemotherapeutic agents sensitise TRAIL-resistant tumour cells to MSC-flT cell-induced apoptosis

We have previously shown that MSC-flT cells are more effective than rTRAIL at inducing apoptosis in cancer cells. Therefore, having shown that inhibition of cIAPs could sensitise tumour cells to rTRAIL, I went on to investigate whether chemotherapeutic agents that inhibit other anti-apoptotic proteins in the extrinsic apoptotic pathway might be even more effective at sensitising tumour cells to TRAIL expressed by MSCs.

LCL161 in combination with MSC-flT cells induced greater than 50% apoptosis in eight cell lines, while in combination with rTRAIL it only induced greater than 50% apoptosis in four cell lines. This demonstrates that MSC-flT cells are better at inducing apoptosis than rTRAIL, both alone and in combination with LCL161 (Figure 4-8A). Although obatoclax, which inhibits BCL-2 family proteins, sensitised cancer cells to MSC-flT cells,

it was not as effective as other chemotherapeutic agents (Figure 4-8B). The reason for this might be that it principally inhibits proteins involved in the intrinsic apoptotic pathway while TRAIL triggers the extrinsic apoptotic pathway.

Both SAHA, which inhibits cFLIP and triggers the intrinsic apoptotic pathway, and SNS-032, which indirectly inhibits cFLIP and MCL-1, were very effective at sensitising tumour cells to MSC-flT cells. Furthermore, the combination of SAHA and MSC-flT cells was better than the combination of SAHA and rTRAIL (Figure 4-9). SNS-032 sensitises tumour cells to both MSC-flT cells and rTRAIL, inducing similar levels of apoptosis in both conditions. This effective sensitisation to TRAIL can be attributed to the ability of these drugs to target important anti-apoptotic proteins in the extrinsic apoptotic pathway. Both drugs enable effective caspase-8 activation by inhibiting cFLIP and SNS-032 increases cross-talk between the extrinsic and the intrinsic apoptotic pathway, facilitating MOMP by inhibiting MCL-1. It has also been shown that SNS-032 can inhibit XIAP, which is a key caspase inhibitor [244].

Given that the combination of chemotherapeutic agents and TRAIL induce apoptosis in tumour cells, their therapeutic application depends on this combination therapy having relatively low cytotoxicity in normal cells. Human lung fibroblasts (HLF) underwent low levels of apoptosis when treated with rTRAIL, MSC-flT cells, SAHA, SNS-032 or LCL161. Although the combination of either SAHA or LCL161 and MSC-flT cells was relatively more cytotoxic to HLFs than the combination of chemotherapeutic agents and rTRAIL, the levels of apoptosis were still low, suggesting low cytotoxicity (Figure 4-10). Obatoclax was relatively more cytotoxic to HLFs both as a monotherapy

and in combination with rTRAIL or MSC-flT cells. This illustrates that the BCL-2 family of proteins plays an important role in regulation of apoptosis in normal cells.

4.4.3 No reduction in tumour burden following combination of SNS-032 and MSC-flT cells was observed in a mouse xenograft model

Given that SNS-032 can inhibit three different potent anti-apoptotic proteins, which can inhibit TRAIL-mediated apoptosis at different points in the extrinsic apoptotic pathway, SNS-032 was combined with MSC-flT cells to determine the effectiveness of this combination treatment in an *in vivo* tumour model. A549 cells were used to develop xenografts in mice as they are TRAIL resistant but can be sensitised to TRAIL by SNS-032.

It has previously been shown that the combination of SNS-032 and rTRAIL significantly reduces tumour burden in A549 lung xenografts in mice [135]. By contrast, in my study, bioluminescence imaging did not show any significant difference in tumour burden amongst any of the groups (Figure 4-11). The lack of therapeutic efficiency observed in my study can be attributed to many factors. In addition, SNS-032 might be affecting the MSCs in terms of their viability, their homing ability to the tumours or their TRAIL expression. The *in vitro* assays that showed the efficiency of the combination therapy were carried out for 24 hours. However, MSC-flT cells will probably survive for longer periods of time *in vivo* and SNS-032 might be cytotoxic to MSC-flT cells over long periods of exposure. Unlike *in vitro*, it is thought that MSC-flT cells need to home to tumours in the mice to be therapeutically beneficial. The homing ability of MSCs depends on several chemokines and cytokines. SNS-032 might be affecting the expression of these factors or of their receptors, thereby affecting MSC-

homing ability. SNS-032 might also suppress TRAIL expression thereby preventing apoptosis. Further investigation of these factors will be necessary if a combination of MSC-flT cells and chemotherapeutic agents is to be pursued as a tumour therapy.

4.5 Summary

- Simultaneous knockdown of cAIP1 and cIAP2 is required to sensitise JU77 cells to TRAIL, while cIAP1 knockdown is sufficient in MDAMB-231 cells.
- LCL161 degrades cIAP1 and sensitises tumour cells to TRAIL.
- Chemotherapeutic agents can be used to sensitise tumour cells to MSC-TRAIL.
- The combination of SNS-032 and MSC-flT cells did not induce a reduction in tumour burden in mice with lung tumour xenografts.

CHAPTER V

Results III: Loss of function of BAP1 is a biomarker

for TRAIL sensitivity

5 RESULTS III: LOSS OF FUNCTION OF BAP1 IS A BIOMARKER FOR TRAIL SENSITIVITY

The final aim of this project was to identify a biomarker that could predict sensitivity of tumour cells to TRAIL. Many clinical trials have tested recombinant TRAIL and DR4/5-activating antibodies as therapies for cancer patients. Most of them have shown a reduced tumour burden in some patients but no significant overall reduction of tumour burden.

A biomarker that could predict sensitivity of cancer cells to TRAIL would be advantageous as TRAIL could then be given only to patients most likely to show a positive clinical outcome upon treatment.

I collaborated with Dr Ultan McDermott's laboratory in the Wellcome Trust Sanger Institute (WTSI) to identify a biomarker for TRAIL sensitivity. A screen was performed to determine if there was a correlation between various mutations harboured in MPM cell lines and their response to TRAIL treatment.

5.1 Mutation in *BAP1* gene sensitises malignant pleural mesothelioma cells to TRAIL

15 MPM cell lines were characterised using whole exome sequencing, copy number and gene expression arrays. A matrix of driver mutations and copy number alterations was constructed. Cell lines were treated with 96 different chemotherapeutic agents, including TRAIL, and cell viability was measured after 6 days. The area under the curve (AUC) were derived for each cell line following exposure to each of the screen compounds and a MANOVA analysis (described in r) was used to annotate sensitivity or resistance of a particular genotype to each targeted therapy in the screen. The data were plotted as a volcano plot to correlate the mutation in a gene to either sensitivity or resistance to a particular drug (Figure 5-1A). Each interaction was represented as a bubble. The Y-axis on the plot denotes the p-value and hence the higher the bubble on the Y-axis, the more significant the interaction between the mutation and the drug. The X-axis denotes the type of interaction between the mutation and the drug. A negative number on the X-axis denotes that the presence of the mutation makes the cell line resistant to the drug while a positive number denotes that the presence of the mutation makes the cell line sensitive to the drug.

Of 15 MPM cell lines in the screen, five harboured mutations in the *BAP1* gene. There was a striking difference in TRAIL sensitivity between cell lines harbouring BAP1 mutation and wild-type BAP1 cell lines ($p=0.015$) (Figure 5-1B). Only one of the cell lines with a BAP1 mutation was not sensitive to TRAIL.

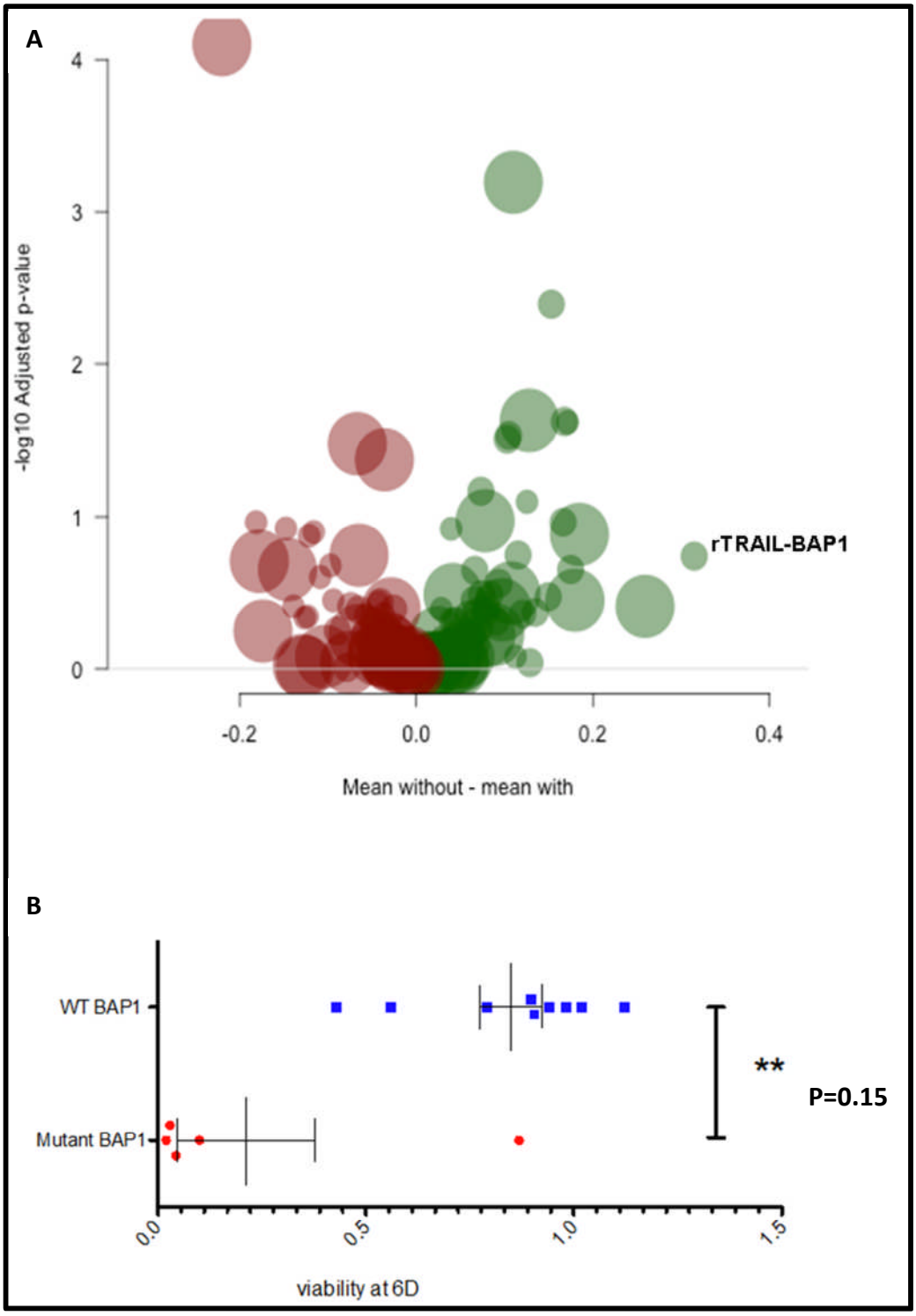

Figure 5-1: BAP1 mutation predicts sensitivity to TRAIL

15 MPM cell lines were treated with 86 different chemotherapeutic agents and cell viability was measured after 6 days. A, Volcano plot showing the association between mutations and response to chemotherapeutic agents. B, Sensitivity of BAP1 wild-type versus BAP1-mutant cell lines to 40 ng/ml TRAIL.

These data, including figures, were provided by Dr McDermott's laboratory, WTSI, as part of a collaboration.

5.1.1 Validation of the screen

The screen of 15 MPM cell lines with 86 chemotherapeutic agents identified the correlation between TRAIL sensitivity and BAP1 mutation status. This needed to be further validated and confirmed. 17 MPM cell lines were treated with TRAIL at doses ranging from 0.5-100 ng/ml (Figure 5-2A). The cell lines were classified as resistant (red), partially sensitive (orange) and sensitive (green) based on their cell viability at 100 ng/ml TRAIL concentration. Eight cell lines were resistant (cell viability >90%), three were partially sensitive (cell viability 50-70%) and six were sensitive (cell viability <50%).

Protein lysates from these cell lines were western blotted to probe their expression of BAP1 (Figure 5-2B). As expected, all of the wild-type cell lines expressed BAP1 protein. H513 and H2869 were wild-type cell lines expressing the BAP1 protein but they were sensitive and partially sensitive to TRAIL, respectively. The remaining six wild-type cell lines expressing the BAP1 protein were resistant to TRAIL.

H2461, H2804, H2452 and H2369 showed protein expression of BAP1 by western blot but expressed a mutant version of BAP1 while the remaining mutant cell lines did not show BAP1 protein expression. H2722 and H2452 were resistant to TRAIL and H2795 and H2369 were partially sensitive. The remaining five BAP1 protein-negative cell lines were sensitive to TRAIL.

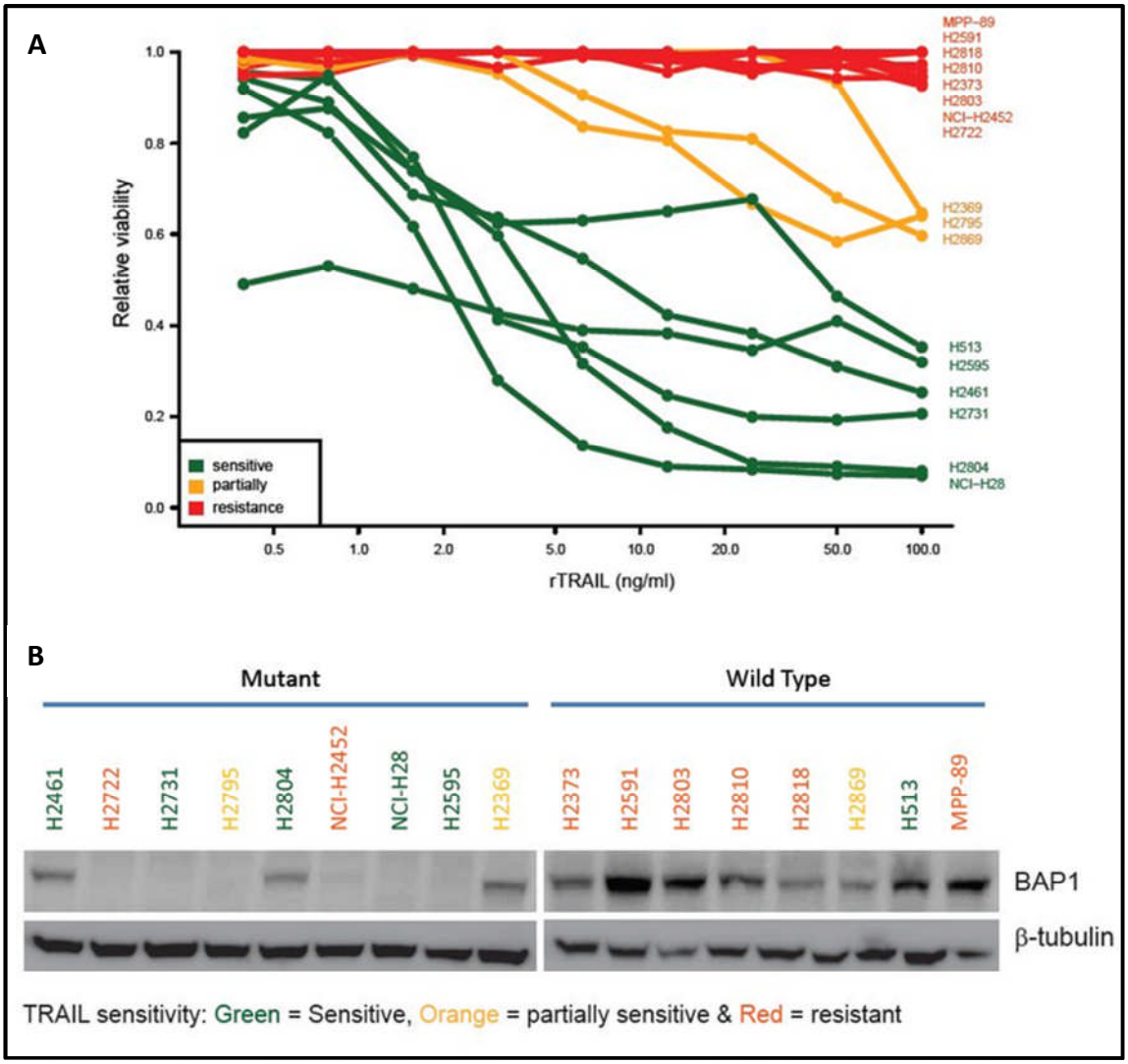

Figure 5-2: BAP1-mutant mesothelioma cell lines were sensitive to TRAIL

A, MPM cell lines were treated with a dose range from 0.5 ng/ml to 100 ng/ml and cell viability was measured using the Syto-60 assay. Based on their cell viability, the cell lines were classified into resistant (red), partially sensitive (orange) and sensitive (green). B, Cell lines were western blotted to probe the expression of BAP1 prot.

These data were provided by Dr McDermott's laboratory (WTSI) as part of a collaboration.

5.1.2 TRAIL-induced apoptosis in BAP1-mutant cell lines

The assays done in the screen and validation measured cell viability after 6 days. An apoptosis assay was performed in order to determine if the interaction between mutations in BAP1 and TRAIL was cytostatic or cytotoxic. Three BAP1 wild-type cell lines and 4 BAP1-mutant cell lines were treated with a dose range of 1-1000 ng/ml of TRAIL for 24 hours (Figure 5-3). Cell death was measured after 24 hours with an Annexin V/DAPI apoptosis assay. The BAP1 wild-type cell lines were resistant to TRAIL and showed <30% apoptosis even at a dose of 1000 ng/ml TRAIL, while the BAP1-mutant cell lines showed >50% apoptosis at this dose. H2722, a mutant BAP1 cell line that was resistant to TRAIL in a 6-day cell viability assay, was also resistant to TRAIL in the apoptosis assay.

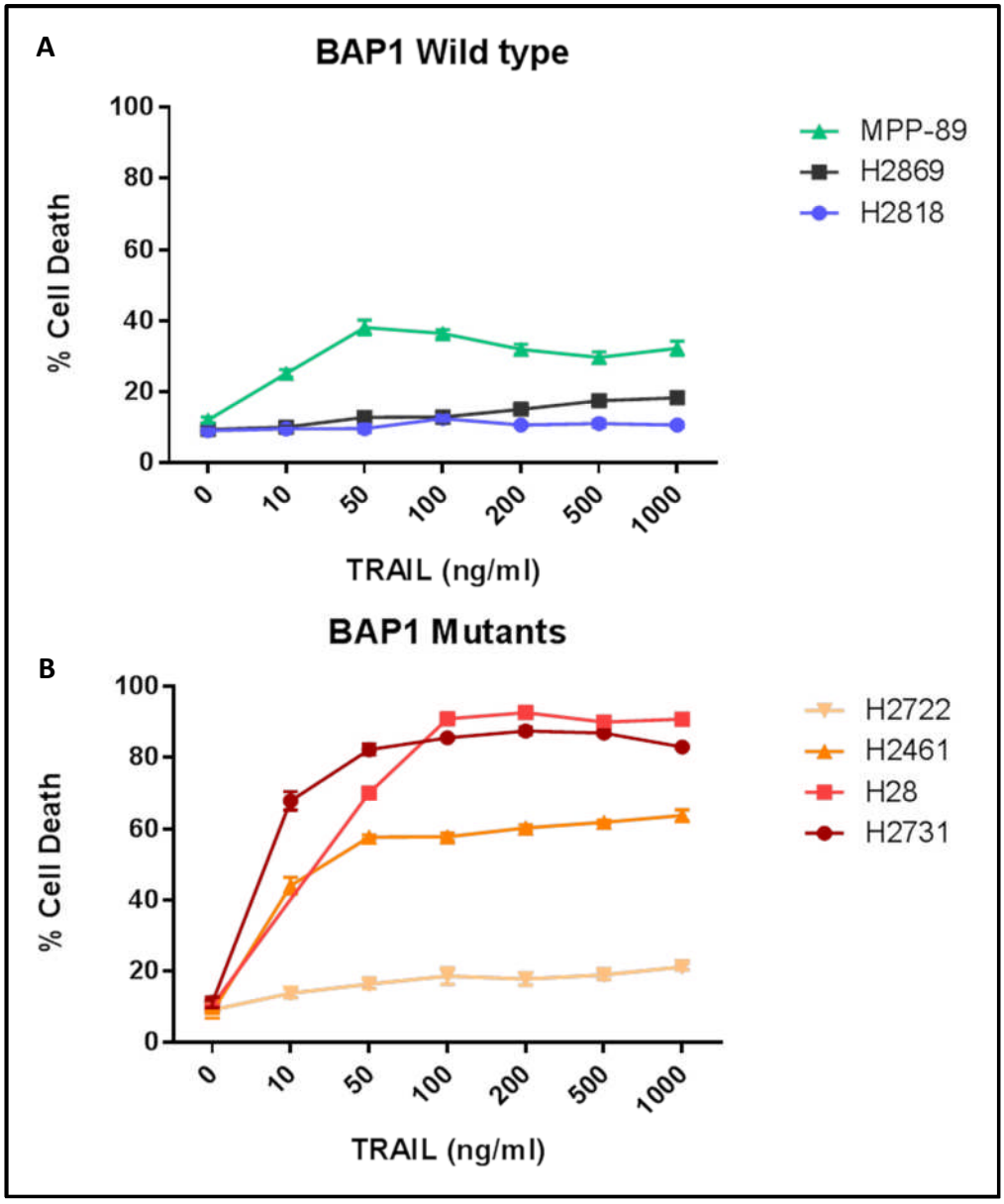

Figure 5-3: BAP1 mutants undergo apoptosis when treated with TRAIL

Three BAP1 wild-type cell lines (MPP-89, H2869 & H2818) and four BAP1-mutant cell lines (H2722, H2461, H28 and H2731) were treated with TRAIL (0-1000 ng/ml) for 24 hours and cell death quantified using an Annexin V/DAPI apoptosis assay. A, BAP1 wild-type cells were resistant to TRAIL. B, BAP1-mutant cells were sensitive to TRAIL.

5.2 Knockdown of BAP1 in wild-type cells sensitises them to TRAIL

Next, I determined whether modulating BAP1 protein expression in wild-type tumour cells would affect their sensitivity to TRAIL.

5.2.1 Knockdown of BAP1 in BAP1 wild-type H2818 MPM cells sensitises them to TRAIL

BAP1 wild-type H2818 cells were transduced with a BAP1 shRNA-expressing lentivirus at MOI 1 and 2.5. The transduction efficiency was measured by flow cytometry of GFP. The lentivirus expresses GFP and a puromycin resistance gene as selection markers along with BAP1 shRNA. The cells were treated with 10 μg/ml puromycin to select transduced cells and then flow cytometry for GFP was used to determine the percentage of transduced cells. MOI 1 transduced 95% of H2818 cells while MOI 2.5 transduced 99% of H2818 cells (Figure 5-4A). To confirm the knockdown, a western blot was performed. The untransduced cells expressed BAP1. There was considerable knockdown in MOI 1-treated cells but protein expression was still observed. However, MOI 2.5-treated cells showed no BAP1 protein expression (Figure 5-4B).

Although both MOI 1- and MOI 2.5-transduced cells showed knockdown of BAP1, MOI 2.5-transduced cells were used to test their TRAIL sensitivity as the low levels of BAP1 protein expression in MOI 1-transduced cells might still be capable of imparting TRAIL resistance. The BAP1 knockdown H2818 cells were much more sensitive to TRAIL ($p<0.0001$) than untransduced H2818 cells when treated with TRAIL (0-500 ng/ml) for 24 hours, as determined by an Annexin V/DAPI assay. However, this sensitivity did not

increase with an increasing dose of TRAIL and hence there was no dose-response relationship (Figure 5-4C).

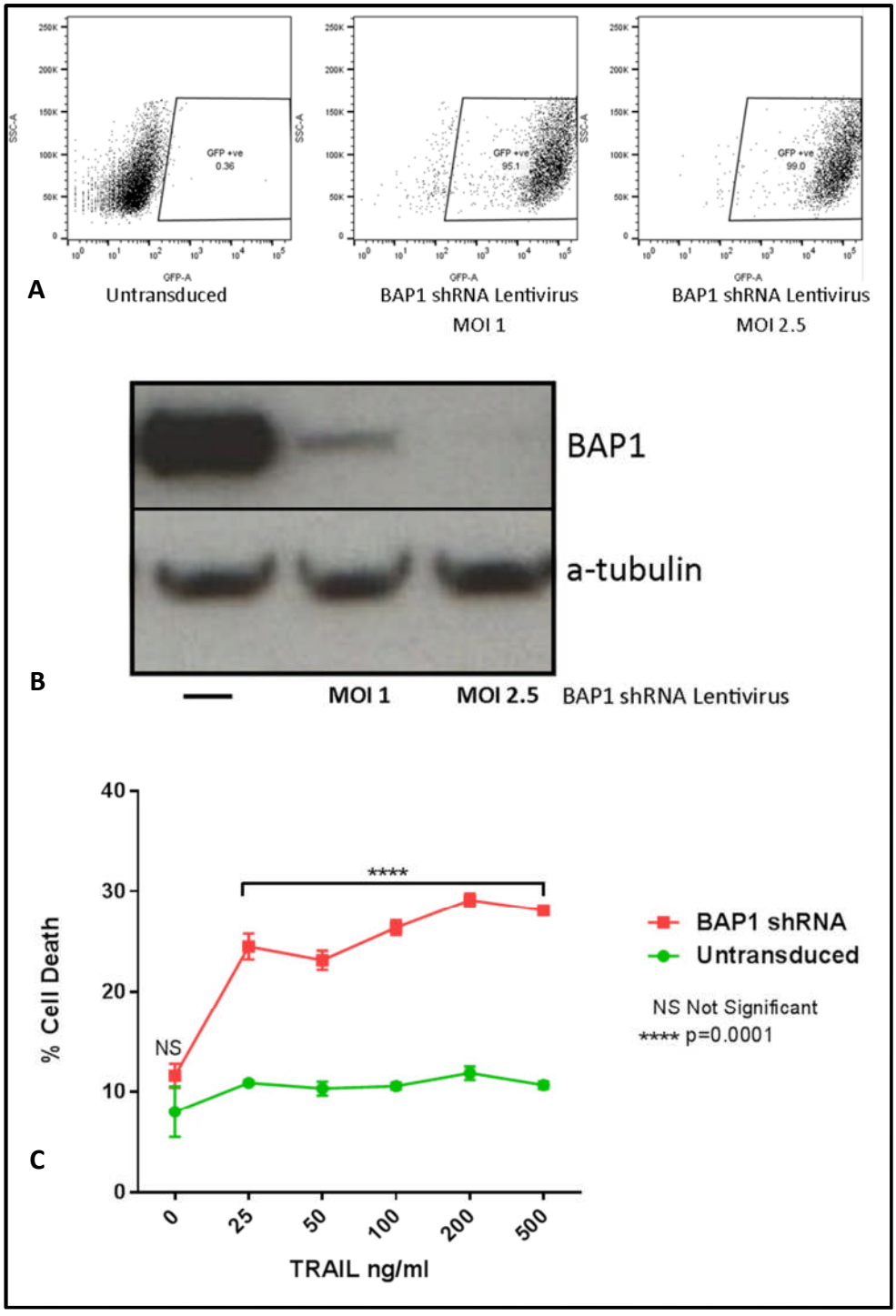

Figure 5-4: Knockdown of BAP1 in H2818 BAP1 wild-type cells sensitises them to TRAIL

BAP1 wild-type H2818 cells were transduced with BAP1 shRNA-expressing lentivirus at MOI 1 and 2.5. A, Flow cytometry plots of GFP-expressing transduced cells. B, Western blot of BAP1 protein confirming the knockdown. C, H2818 cells transduced with BAP1 shRNA-expressing lentivirus at MOI 2.5 were treated with TRAIL (dose range 0-500 ng/ml) and cell death was measured after 24 hours with an Annexin V/DAPI assay.

5.2.2 BAP1 imparted TRAIL resistance was not specific to MPM cell lines and was also observed in other tumour cell lines

I next asked whether BAP1-induced TRAIL resistance was specific to MPM cell lines or whether it could also be seen in other cancer cell lines.

Breast cancer BAP1 wild-type MDAMB-231 cells were transduced with BAP1 shRNA or an empty vector-expressing lentivirus at MOI 1.25, 2.5 and 5. The lentivirus expresses GFP and a puromycin resistance gene as selection markers along with BAP1 shRNA. The cells were treated with 10 µg/ml puromycin to select transduced cells. To confirm the knockdown, a western blot was performed. The untransduced cells as well as empty vector transduced cells expressed BAP1 protein. There was increasing knockdown of BAP1 from MOI 1 to 5 in BAP1 shRNA-transduced cells (Figure 5-5A). MOI 5-transduced cells were selected for further experimentation. Flow cytometry for GFP was used to quantify the percentage of transduced cells. MOI 5 of the BAP1 shRNA lentivirus transduced 97.5% of MDAMB-231 cells, while MOI 5 of the empty vector lentivirus transduced 98.3% of MDAMB-231 cells (Figure 5-5B).

Untransduced, BAP1 shRNA- and empty vector shRNA-expressing lentivirus-transduced cells were treated with TRAIL from a dose range of 0-100 ng/ml for 24 hours and cell death was quantified using an Annexin V/DAPI assay. The BAP1 knockdown MDAMB-231 cells were much more sensitive to TRAIL than untransduced and empty vector shRNA-transduced cells. There was a significant shift in the IC_{50} value, which was 10, 75 and 100 ng/ml for BAP1 shRNA-transduced cells, empty vector shRNA-transduced cells and untransduced cells, respectively (Figure 5-5C).

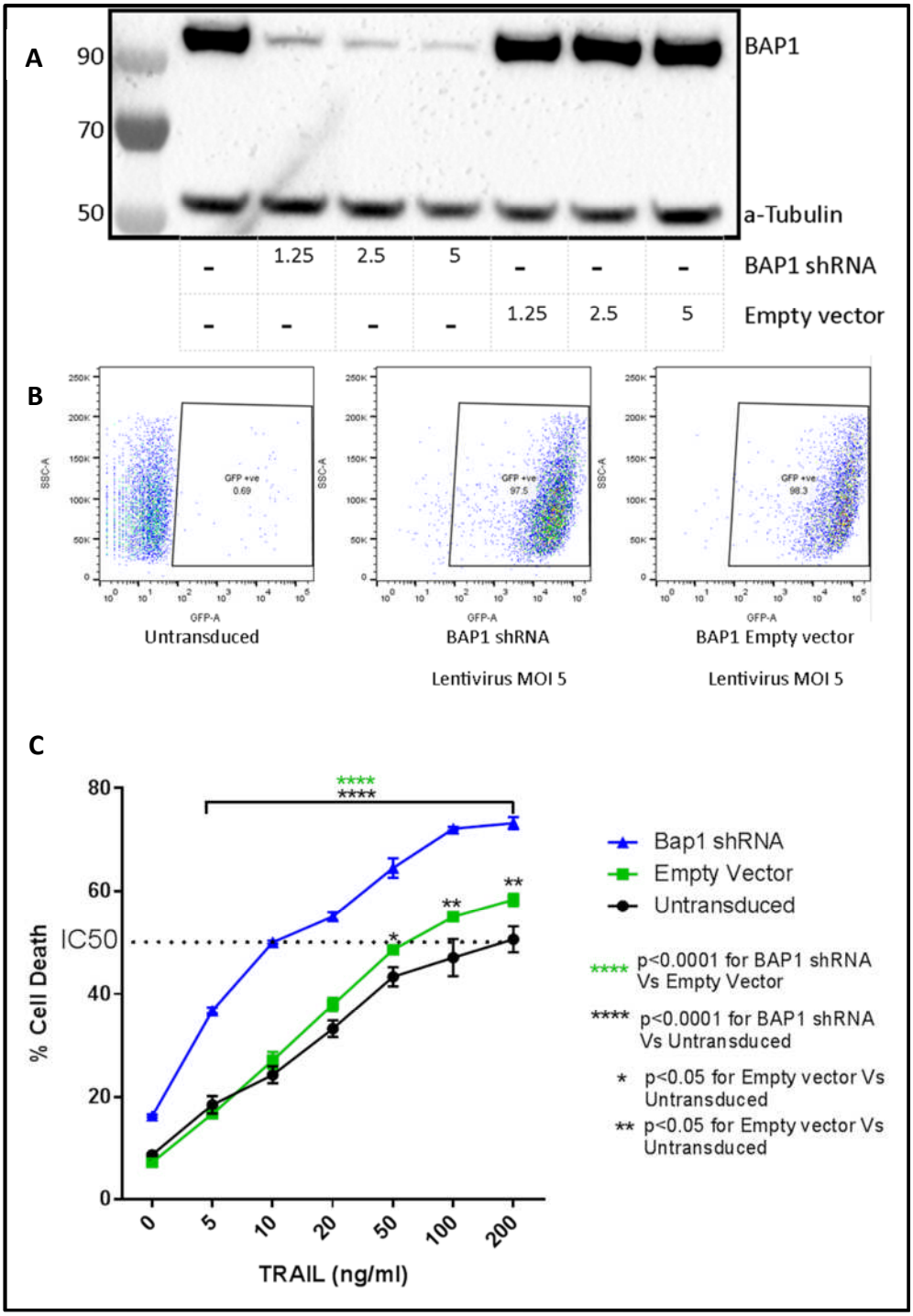

Figure 5-5 Breast cancer MDAMB-231 cells showed a significant decrease in IC_{50} value after knockdown of the *BAP1* gene

BAP1 wild-type MDAMB-231 cells were transduced with either BAP1 shRNA or empty vector shRNA-expressing lentivirus at MOI 1.25, 2.5 and 5. A, Western blot of BAP1 protein confirming the knockdown in BAP1 shRNA-transduced cells. B, Flow cytometry plots of GFP-expressing transduced cells. C, MDAMB-231 cells transduced with BAP1 shRNA-expressing lentivirus at MOI 5 were treated with TRAIL (dose range from 0-100 ng/ml) and cell death was measured after 24 hours using an Annexin V/DAPI assay.

5.3 Overexpression of BAP1 in BAP1-null H226 cells imparts TRAIL resistance

As knockdown of BAP1 sensitises BAP1 wild-type cells to TRAIL, the next logical step was to introduce BAP1 in BAP1-null cells and test whether BAP1 expression makes them TRAIL resistant.

5.3.1 Cloning of BAP1 cDNA into lentiviral vector

The coding region of BAP1 cDNA was amplified by PCR using the Origene BAP1 (NM_004656) human cDNA clone as a template (Figure 5-6A). The forward and reverse primers have overhangs of BamH1 and Sal1 restriction sites which enabled me to ligate the BAP1 cDNA into a pCCL.CMV lentiviral back bone. The resultant PCR amplicon, which was 2200 base pairs, was purified using a PCR purification kit and double digested using restriction enzymes (Figure 5-6B). The resultant digestion product was purified and a portion run on agarose gel to confirm its size. The resultant product was ligated to the pCCL.CMV lentiviral backbone and the product was transformed into DH5a competent *E.coli* and grown on ampicillin-containing agar plates. Only the transformed cells survived due to the presence of an ampicillin resistance gene on the lentiviral backbone. Several colonies were expanded further and their plasmid DNA was extracted. The extracted DNA was used as a template for a PCR reaction using BAP1 forward and reverse primers. The presence of bands at 2200 bp size indicated that BAP1 cDNA had integrated into the lentiviral vector (Figure 5-6C). As a final confirmation step, the plasmid DNA was double digested using restriction enzymes BamH1 and Sal1. The resultant product was run on an agarose gel. The presence of 2 bands, 1 at 2200bp and 1 near 7000bp, confirmed the successful cloning of BAP1 cDNA

into the lentiviral backbone pCCL.CMV to obtain a pCCL.CMV.BAP1 transfer plasmid (Figure 5-6D).

Lentivirus was made using pCCL.CMV.BAP1 as the transfer plasmid and packaging plasmids as per the established procedure explained in materials and methods.

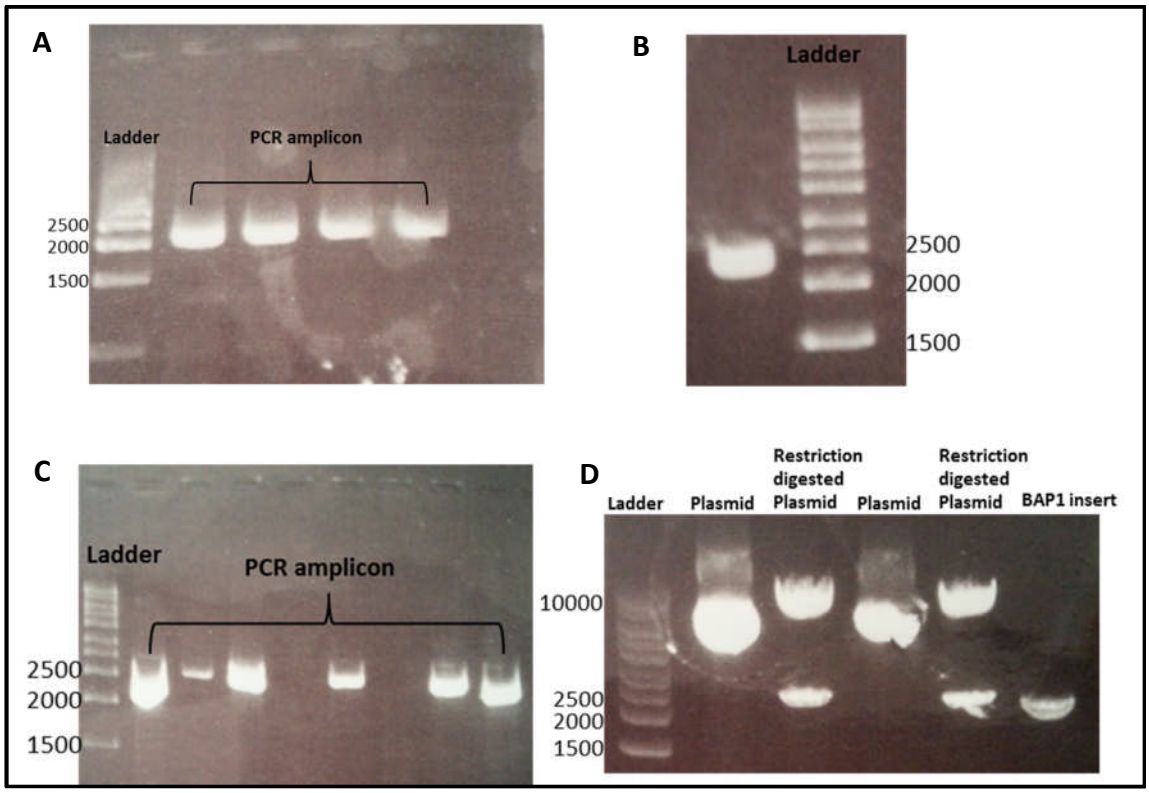

Figure 5-6: Cloning of BAP1 cDNA coding region into the pCCL.CMV lentiviral transfer plasmid

A, Agarose gel showing PCR product of the BAP1 cDNA coding region amplified from the Origene BAP1 (NM_004656) human cDNA clone. B, Restriction double digested BAP1 cDNA run on an agarose gel. C, PCR product amplified from plasmid DNA extracted from transformed E.coli*. D, Restriction double digest of plasmid DNA from transformed* E.coli *confirming integration of BAP1 cDNA into the lentiviral transfer plasmid.*

5.3.2 Titration of BAP1-expressing lentivirus using 293T cells

5 x 10^4 293T cells were plated in a 6-well plate and transduced with different dilutions of BAP1-expressing lentivirus (pCCL.CMV.BAP1). The cells were grown for 48 hours and were stained after fixing, permeabilization and blocking with anti-human BAP1 primary antibody and Alexa Fluor-488 (AF-488) conjugated anti-mouse secondary antibody. The percentage of transduced cells was determined by flow cytometry for AF-488.

The virus quantity that transduced around 20% of cells was used to calculate the viral titre. The following equation was used:

$$\text{Viral titre} = \frac{\text{number of cells plated X proportion of positive cells}}{\text{Volume of virus in ml}}$$

0.0625µL of virus transduced 20.1% of 293T cells and the viral titre was determined to be 1.6 x 10^8 infectious units/ml (Figure 5-7).

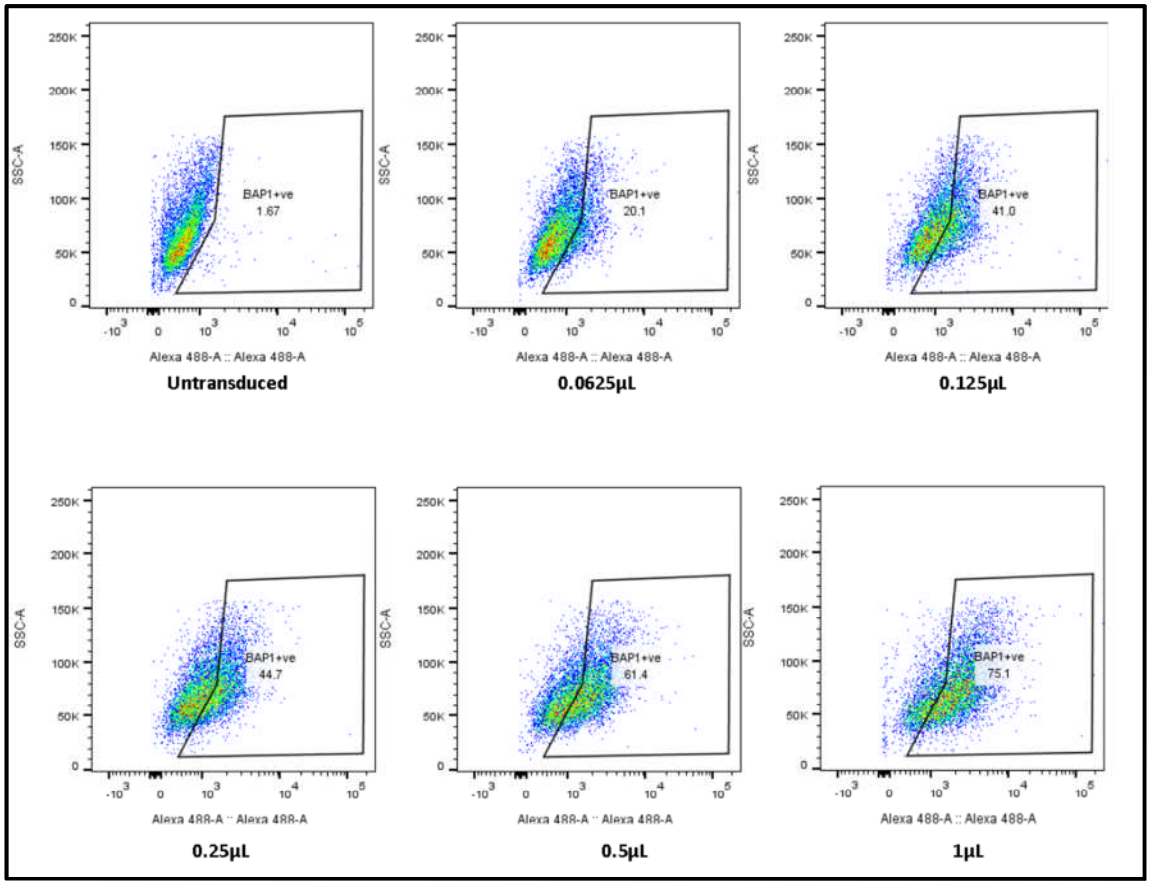

Figure 5-7 Titration of BAP1-expressing lentivirus by transduction of 293T cells

293T cells were transduced using a dilution series of concentrated lentiviral vectors. The cells were stained after fixing, permeabilization and blocking with an anti-human BAP1 mouse primary antibody and an AF-488 conjugated anti-mouse secondary antibody. The percentage of transduced cells was determined by flow cytometry for AF-488. Examples of flow cytometry plots showing AF-488 expression for a range of viral concentrations are shown. The volumes of virus shown indicate the volume of concentrated viral vector used for transduction.

5.3.3 Transduction of H226 cells with BAP1-expressing lentivirus

H226 cells are BAP1 null as they have homozygous deletion of the *BAP1* gene. As they do not express endogenous BAP1, they are ideal for testing the effect of BAP1 through reintroduction of BAP1.

H226 cells were transduced with BAP1-expressing lentivirus at MOI 1, 2, 3, 5 and 8. This results in the introduction of *BAP1* gene into the genome of transduced cells and in the stable expression of the *BAP1* gene. Western blot of protein lysates from MOI 2-, 3-, 5- and 8-treated cells showed expression of BAP1 while the untransduced cells did not (Figure 5-8A). To quantify the percentage of cells expressing BAP1, the cells were stained after fixing, permeabilizing and blocking with an anti-human BAP1 primary antibody and an AF-488 conjugated anti-mouse secondary antibody. The percentage of transduced cells was determined by flow cytometry for AF-488. MOI 5 of the BAP1 lentivirus transduced 92% of the cells and these were used for further experimentation (Figure 5-8B).

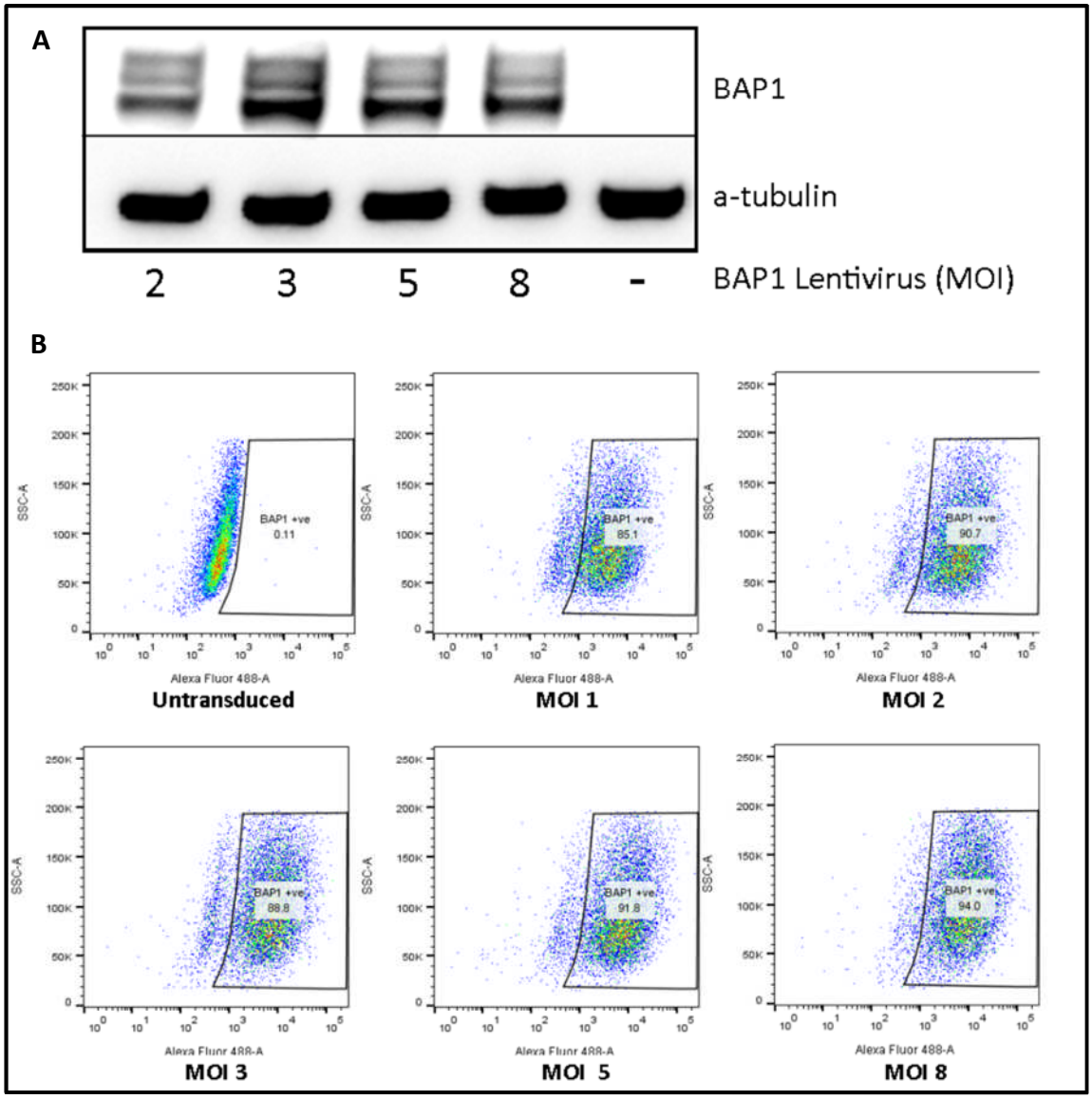

Figure 5-8: Expression of BAP1 in H226 cells after transduction with the BAP1-expressing lentivirus

H226 cells were transduced with a BAP1-expressing lentivirus at MOI 1, 2 3 5 and 8. A, Western blotting shows the expression of BAP1 protein in BAP1 lentivirus-transduced cells while untransduced cells do not express BAP1. B, The cells were stained after fixing, permeabilization and blocking with an anti-human BAP1 mouse primary antibody and an AF-488 conjugated anti-mouse secondary antibody. The percentage of transduced cells was determined by flow cytometry for AF-488.

5.3.4 BAP1 expression imparts TRAIL resistance in H226 cells.

MOI 5 BAP1 lentivirus-transduced H226 cells (H226 BAP1 cells) and untransduced H226 cells were treated with TRAIL using the dose range 0-1000 ng/ml for 24 hours and cell death was quantified by an Annexin V/DAPI assay. H226 BAP1 cells were significantly more resistant to TRAIL compared with untransduced cells (Figure 5-9). Although the untreated BAP1 transduced cells showed less cell death than the untransduced cells, the difference between them was not significant. There was a significant difference between BAP1 transduced and untransduced cells ($p<0.0001$) at the doses ranging from 10-1000 ng/ml.

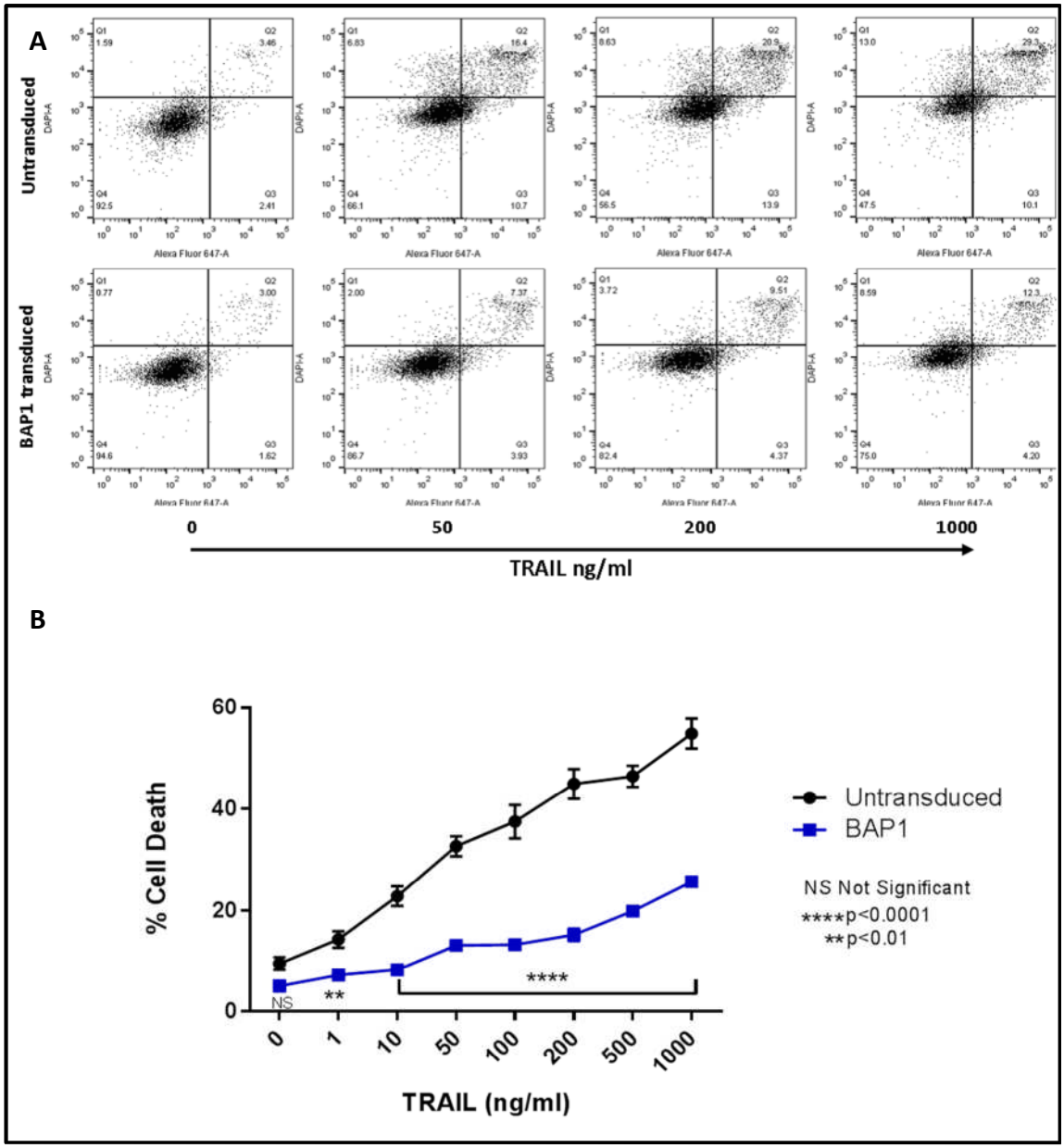

Figure 5-9 BAP1-transduced H226 cells were resistant to TRAIL

Untransduced H226 and BAP1-transduced H226 cells were treated with 0-1000 ng/ml TRAIL for 24 hours and cell death measured by Annexin V/DAPI assay. A, FACS plots comparing H226 BAP1-transduced and H226 untransduced cells at 0, 50, 200 and 1000 ng/ml TRAIL. x axis represents fluorescent intensity of DAP1 while y axis represents fluorescent intensity AF 647 conjugated anti Annexin V antibody. Quarter1 (Q1) represents dead cells, Quarter2 (Q2) represents apoptotic dead cells, Quarter3 (Q3) represents cells undergoing apoptosis and Quarter4 (Q4) represents live cells. B, Cell death in untransduced H226 and BAP1-transduced H226 cells after treatment with TRAIL for 24 hours. (This experiment also tested BAP1 C91A-mutated cells. Data shown in Figure 5-12).

5.4 Deubiquitination is necessary for BAP1-mediated TRAIL resistance

BAP1 belongs to the ubiquitin C-terminal hydrolase subfamily of deubiquitinating enzymes that are involved in the removal of ubiquitin from proteins. It possesses a ubiquitin carboxy-terminal hydrolase (UCH) domain that gives BAP1 its deubiquitinase activity. A cysteine residue at the 91st position of the polypeptide chain is required for its deubiquitinating activity and mutating it to alanine causes cells to produce a catalytically dead BAP1 protein.

The cysteine at the 91st position was mutated to alanine (C91A) by site-directed mutagenesis to annul the deubiquitinase activity of BAP1 and the mutation was confirmed by Sanger sequencing. This mutant *BAP1* gene was cloned into a lentiviral vector and the lentivirus was made as previously described.

5.4.1 Titration of BAP1 C91A lentivirus using 293T cells

5 x 10^4 293T cells were plated in a 6-well plate and transduced with different dilutions of the BAP1 C91A-expressing lentivirus (pCCL.CMV.BAP1 C91A). The cells were grown for 48 hours and were stained after fixing, permeabilization and blocking with an anti-human BAP1 primary antibody and an AF-488 conjugated anti-mouse secondary antibody. The percentage of transduced cells was determined by flow cytometry for AF-488.

The virus quantity that achieved around 20% transduction of cells was used to calculate the viral titre as described above.

0.0625µL of virus transduced 22.8% of 293T cells and the viral titre was determined to be 1.8 x 10^8 infectious units/ml (Figure 5-10).

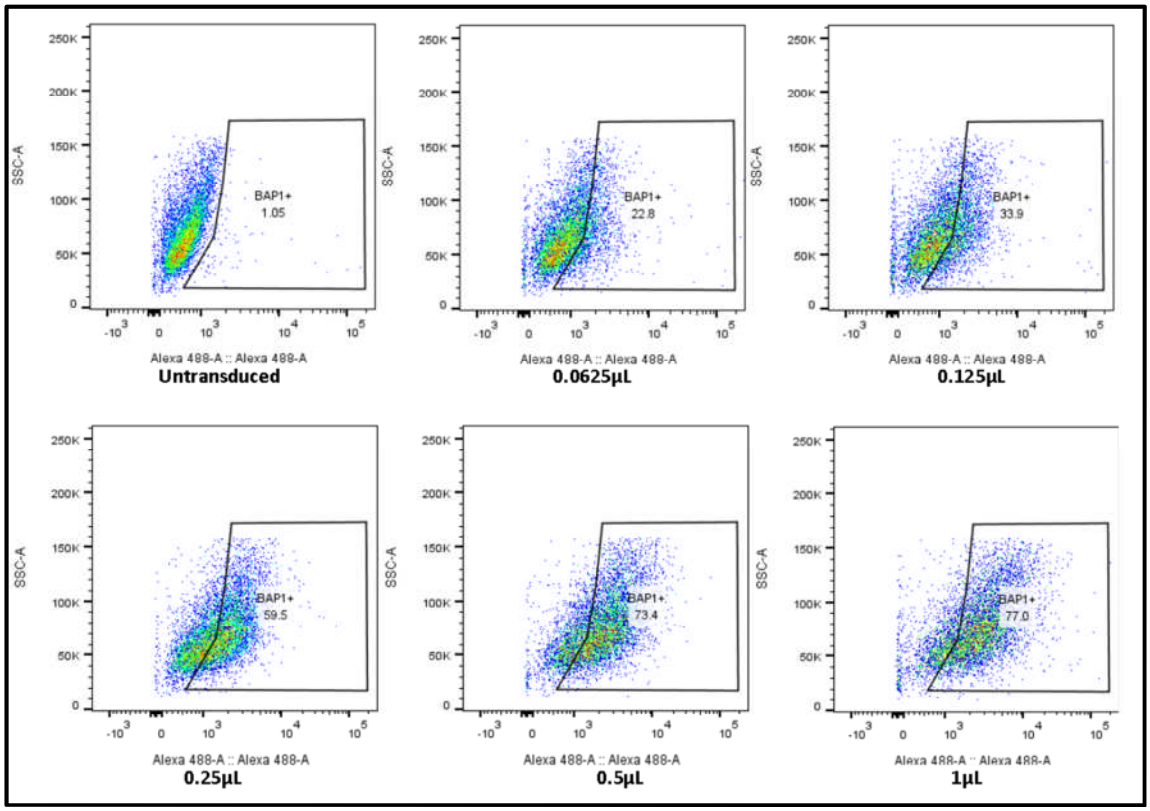

Figure 5-10 Titration of BAP1 C91A mutated lentivirus by transduction of 293T cells.

293T cells were transduced using a dilution series of concentrated lentiviral vectors. The cells were stained after fixing, permeabilization and blocking with anti-human BAP1 mouse primary antibody and AF-488 conjugated anti-mouse secondary antibody. The percentage of transduced cells was determined by flow cytometry for AF-488. Examples of flow cytometry plots showing AF-488 expression for a range of viral concentrations are shown. The volumes of virus shown indicate the volume of concentrated viral vector used for transduction.

5.4.2 Transduction of H226 cells with BAP1 C91A-expressing lentivirus

H226 cells were transduced with the BAP1 C91A-expressing lentivirus at MOI 1, 2, 3, 5 and 8. This results in the introduction of a catalytically dead *BAP1* gene into the genome of transduced cells. Western blot analysis of protein lysates from MOI 2-, 3-, 5- and 8-transduced cells showed expression of BAP1 while the untransduced cells did not (Figure 5-11A). To quantify the percentage of cells expressing BAP1, the cells were stained after fixing, permeabilizing and blocking, with an anti-human BAP1 primary antibody and an AF-488 conjugated anti-mouse secondary antibody. The percentage of transduced cells was determined by flow cytometry for AF-488. MOI 5 of the BAP1 lentivirus transduced 92.8% of the cells and these were used for further experimentation (Figure 5-11B).

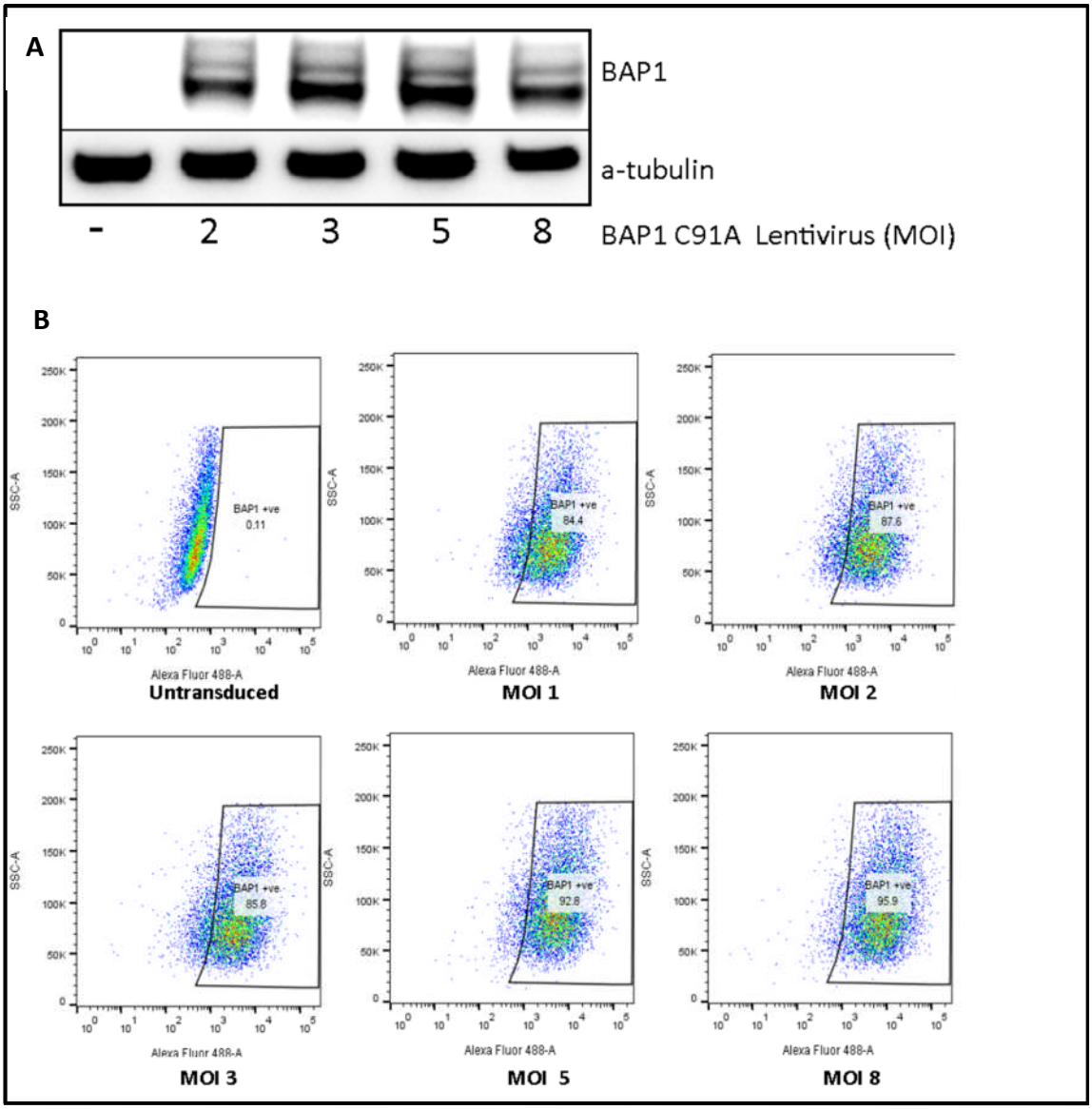

Figure 5-11: Expression of BAP1 in H226 cells after transduction with BAP1 C91A mutated lentivirus.

H226 cells were transduced with BAP1 C91A mutated lentivirus at MOI 1, 2 3 5 and 8. A, the western blot shows the expression of BAP1 protein in BAP1 lentivirus transduced cells while untransduced cells do not express BAP1. B, The cells were stained after fixing, permeabilization and blocking with anti-human BAP1 mouse primary antibody and AF-488 conjugated anti-mouse secondary antibody. The percentage of transduced cells was determined by flow cytometry for AF-488.

5.4.3 Deubiquitination by BAP1 is necessary for TRAIL resistance in H226 cells

MOI 5 BAP1 C91A lentivirus-transduced H226 cells, H226 BAP1 cells and untransduced H226 cells were treated with TRAIL at a dose range of 0-1000 ng/ml for 24 hours and cell death was quantified by Annexin V/DAPI assay. H226 BAP1 cells are significantly resistant to TRAIL relative to untransduced cells. However, there was no significant difference in apoptosis between the catalytically dead BAP1-expressing H226 cells (BAP1 C91A-expressing H226 cells) and the untransduced H226 cells (Figure 5-12). Although the untreated BAP1 transduced cells showed less cell death than the untransduced cells and the BAP1 C91A-transduced cells, the difference between them was not significant. There was a significant difference between BAP1-expressing and BAP1 C91A-expressing cells ($p<0.0001$) at the doses ranging from 10-1000 ng/ml. Hence it can be inferred that BAP1 deubiquitinates proteins to influence the sensitivity of cells to TRAIL.

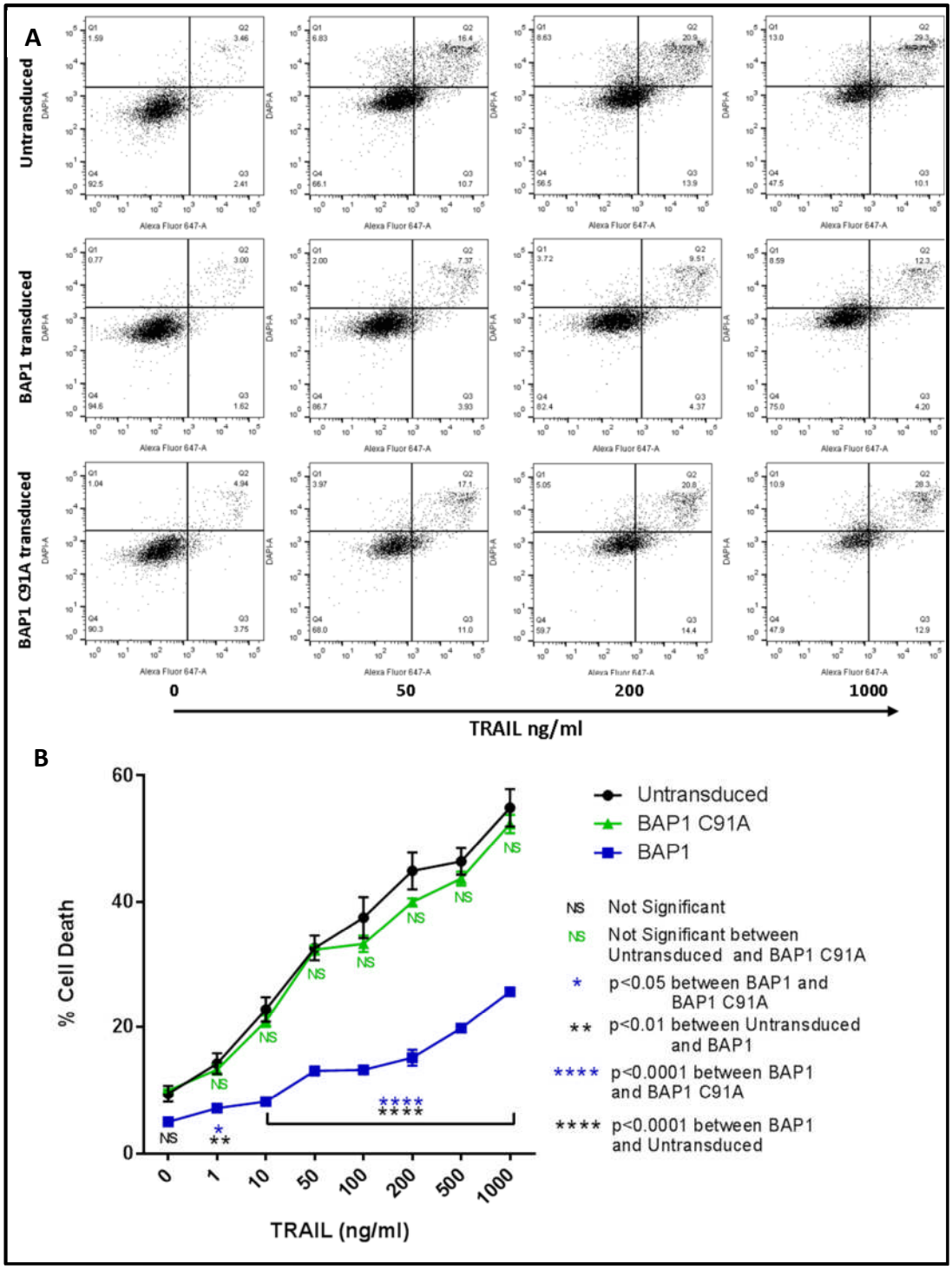

Figure 5-12 Deubiquitination function of BAP1 is necessary for TRAIL resistance

Untransduced, BAP1-transduced BAP1 C91A-transduced H226 cells were treated with 0-1000 ng/ml TRAIL for 24 hours and cell death measured by Annexin V/DAPI assay. A, FACS plots comparing untransduced, BAP1-transduced BAP1 C91A-transduced H226 cells at 0, 50, 200 and 1000 ng/ml TRAIL. Quarter 1 (Q1) represents dead cells, Quarter 2 (Q2) represents apoptotic dead cells, Quarter 3 (Q3) represents cells undergoing apoptosis and Quarter 4 (Q4) represents live cells. B, Cell death in untransduced, BAP1-transduced and BAP1 C91A-transduced H226 cells after treatment with TRAIL for 24 hours.

5.5 Catalytically dead BAP1-transduced H226 cells are sensitive to TRAIL *in vivo*

Testing the induction of apoptosis by TRAIL in cell culture dishes is a good and robust model. However, this might not be replicable in animals. Animal metabolism of xenobiotics and other physiological factors might affect the action of drugs (in this case TRAIL). After having established *in vitro* that loss of function of BAP1 leads to sensitisation of cancer cells to TRAIL-induced apoptosis, I embarked on testing this observation *in vivo*.

5.5.1 Isoleucine zipper TRAIL was more effective than recombinant TRAIL

I collaborated with Professor Walczak's laboratory at the UCL Cancer Institute to test the effect of TRAIL in tumour xenograft mice models. The Walczak laboratory uses isoleucine zipper TRAIL (IzTRAIL) in orthotropic tumour xenograft mice models. IzTRAIL is a trimerised TRAIL in which the monomers are held together by an isoleucine zipper. I isolated IzTRAIL from bacteria expressing the IzTRAIL vector using an established procedure [211]. I tested the newly isolated IzTRAIL on TRAIL-sensitive HeLa cells at a range of concentrations from 0-1000 ng/ml. The IzTRAIL that had been isolated earlier by the Walzack laboratory was used as a positive control. The newly isolated IzTRAIL showed similar efficacy to the IzTRAIL isolated by Walczak's laboratory (Figure 5-13A).

BAP1- and BAP1 C91A-expressing H226 cells were treated with rTRAIL and IzTRAIL at a range of concentrations from 0-1000 ng/ml for 24 hours and cell death was measured by Annexin V/DAPI apoptosis assay. The IzTRAIL was significantly ($p<0.001$) more efficacious in inducing apoptosis then rTRAIL in both BAP1- and BAP1 C91A-expressing H226 cells (Figure 5-13B).

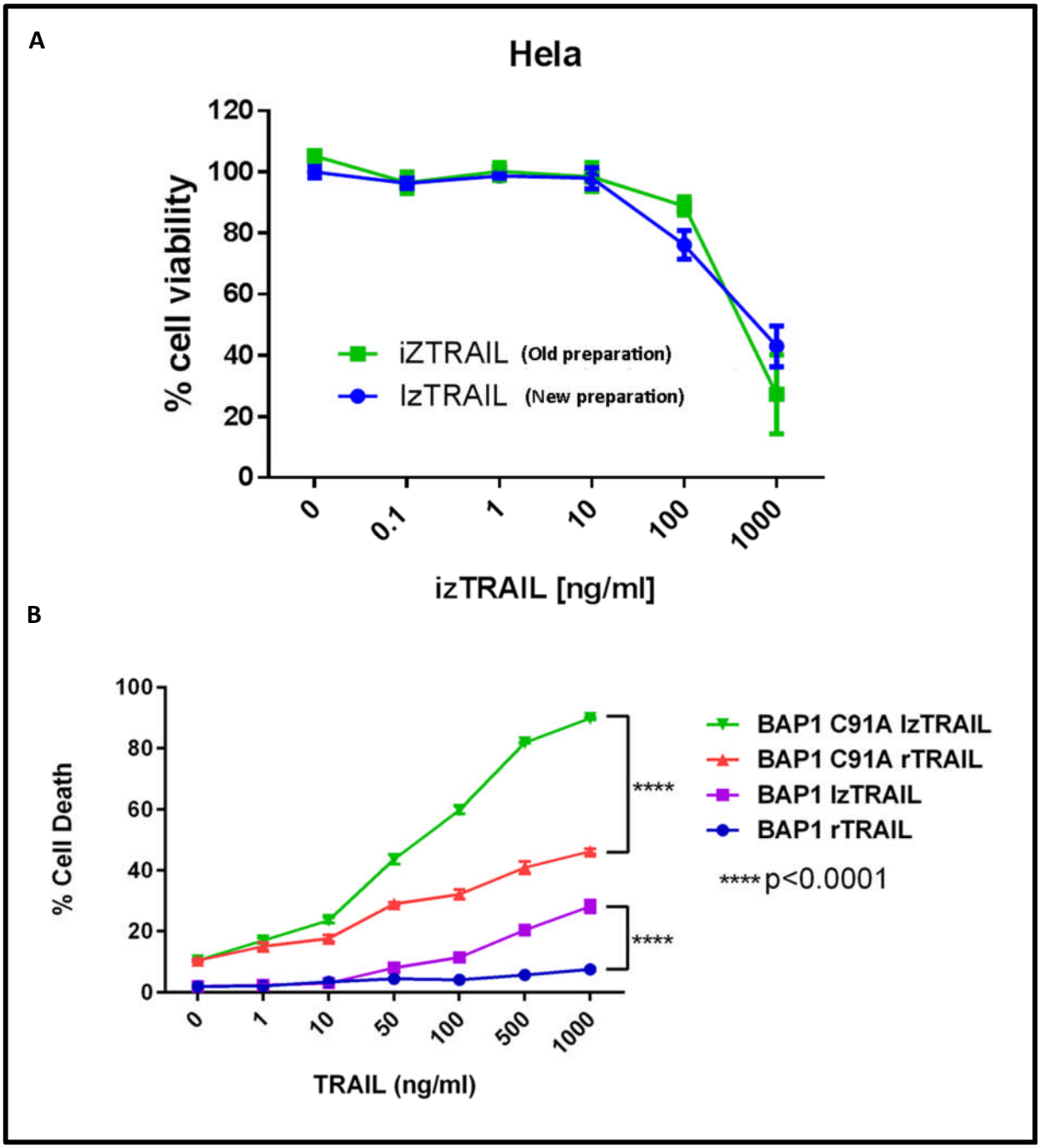

Figure 5-13 IzTRAIL was more efficacious than recombinant TRAIL

A, HeLa cells were treated with newly made IzTRAIL & old IzTRAIL as a positive control and cell viability was measured after 24 hours. B, BAP1-transduced and BAP1 C91A-transduced H226 cells were treated with 0-1000 ng/ml IzTRAIL and rTRAIL for 24 hours and cell death measured by Annexin V/DAPI assay.

5.5.2 Transduction of BAP1- and BAP1 C91A-expressing H226 cells with ZS Green-luciferase lentivirus

Ventii *et al* [49] have shown that H226 cells can be grown subcutaneously in NOD/SCID mice. My aim in this experiment was to prove that mice with xenografts of H226 cells expressing loss-of-function mutant BAP1 are more sensitive to TRAIL than mice with orthotopic xenografts of wild-type BAP1-expressing H226 cells. I wanted to track the tumour burden longitudinally during the treatment. Subcutaneous tumour burden can be measured by calliper measurements but this is not a very accurate method. Tracking tumour burden by bioluminescence imaging of mice with luciferase-expressing xenografts is a more reliable and accurate way of measuring tumour burden. Furthermore this method also enables the tracking of xenograft tumour burden in the internal organs of the mice.

To track tumour burden longitudinally by bioluminescence, BAP1- and BAP1 C91A-expressing H226 cells were transduced with the ZS Green-luciferase expressing lentivirus. ZS Green enables quantification of the percentage of transduced cells by flow cytometry. 94.2% of BAP1-expressing H226 cells and 89.6% of BAP1 C91A-expressing H226 cells were transduced with MOI 3 of the ZS Green-luciferase expressing lentivirus (Figure 5-14A). The expression of luciferase-transduced cells was measured by bioluminescence imaging on an IVIS machine after adding 100 µg/ml of luciferin. There was no significant difference in the bioluminescence emitted by BAP1- and BAP1 C91A-expressing H226 cells (Figure 5-14B&C).

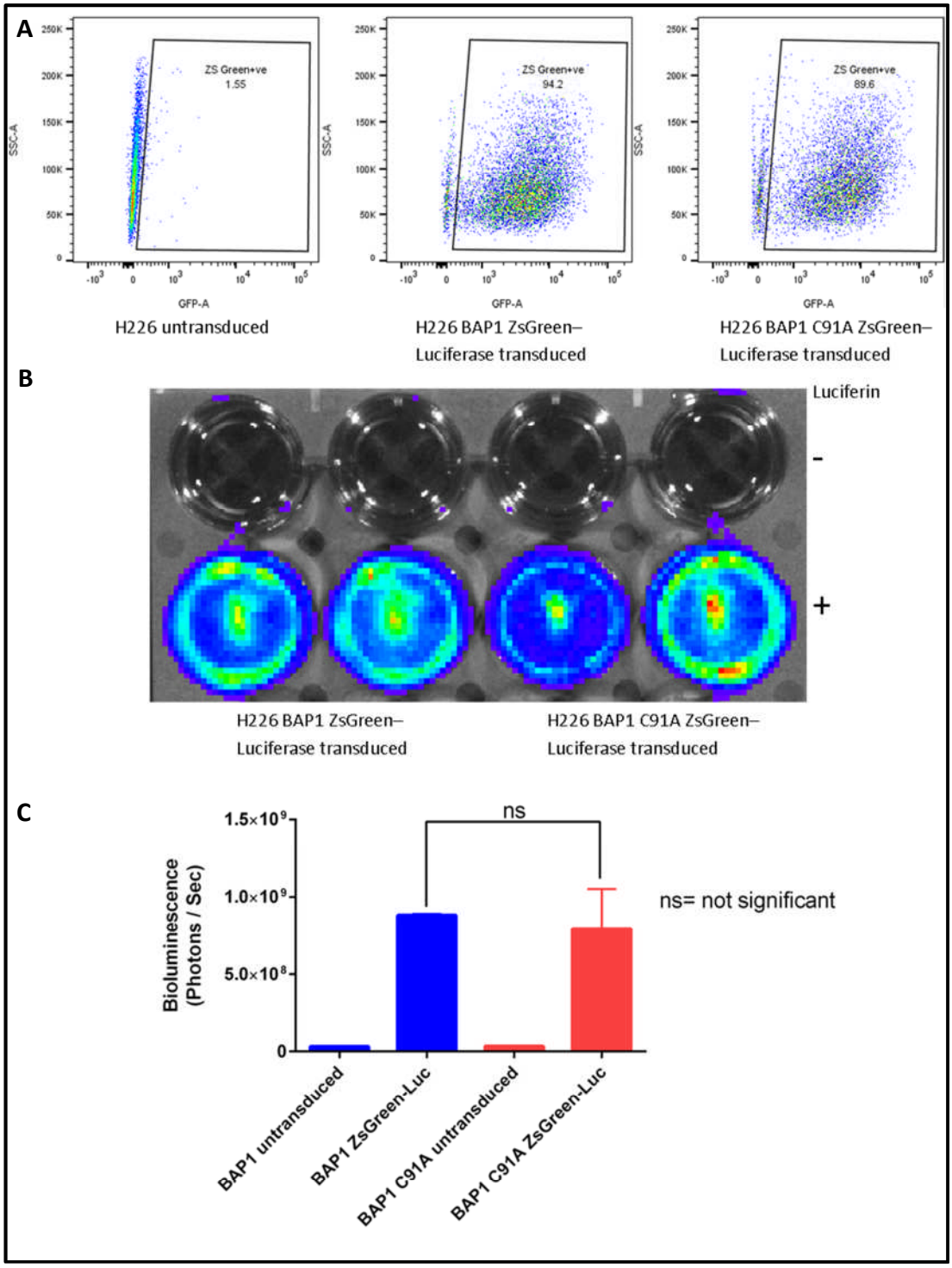

Figure 5-14 Bioluminescence imaging of BAP1- and BAP1 C91A-expressing H226 cells transduced with a ZS Green-luciferase-expressing lentivirus

BAP1- and BAP1 C91A-expressing H226 cells were transduced with a ZS Green-luciferase expressing lentivirus at MOI 3. A, The percentage of transduced cells was analysed by flow cytometry for ZS Green expression. B, ZS Green-luciferase transduced BAP1- and BAP1 C91A-expressing H226 cells were imaged in the IVIS system after adding 100 µg/ml luciferin. C, Quantification of photons emitted by transduced cells after luciferin treatment.

5.5.3 BAP1- and BAP1 C91A-expressing H226 cells grow in the peritoneum of mice

Establishment of xenograft mice models that represent human malignant pleural mesothelioma would be ideal for understanding the efficacy of drugs *in vivo*. However, not all cancer cells grow *in vivo*. Peritoneal tumour xenografts are widely used in preclinical studies of MPM. However, there is no established peritoneal mesothelioma model using H226 cells to date.

In order to determine the number of cells needed to inoculate the mouse peritoneum to obtain a reliable and replicable model, I injected 1, 2 & 4 X 10^6 ZS Green-luciferase transduced BAP1- and BAP1 C91A-expressing H226 cells suspended in 200 µl PBS into the peritoneal cavity of the mice. The tumour burden was longitudinally tracked by bioluminescence imaging of mice on an IVIS machine 15 minutes after injecting 200 µl of 10 mg/ml luciferin per mouse (Figure 5-15A).

The mice that received one million BAP1-expressing H226 cells did not show substantial growth in tumours. Those that received one million BAP1 C91A-expressing H226 cells showed a trend of increasing tumour burden but it was not statistically significant relative to BAP1-expressing H226 cells (Figure 5-15B). The mice that received 2 and 4 x 10^6 BAP1- and BAP1 C91A-expressing H226 cells showed a trend of decreasing tumour burden until day 10 compared with day 0. However, the tumour growth stabilised after day 10 and started to grow after day 20 (Figure 5-15B). The mice that received BAP1 C91A-expressing cells showed a greater increase in tumour burden than BAP1-expressing H226 cells. This difference was not statistically significant in mice that received two million cells; however, it was statistically significant ($p<0.05$) in mice that received 4 million cells (Figure 5-15B).

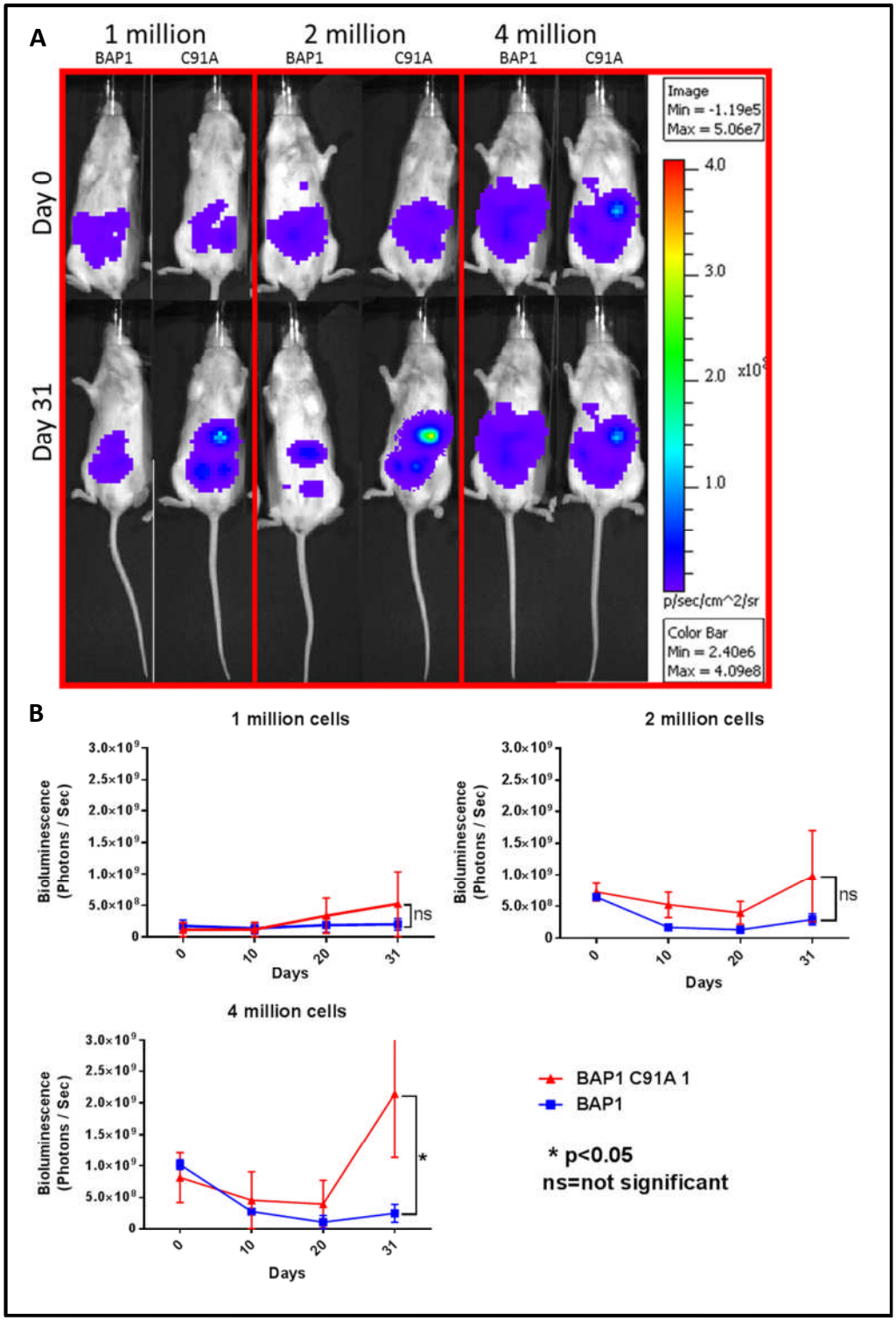

Figure 5-15 Luciferase-transduced BAP1- or BAP1 C91A-expressing cells were tracked after intraperitoneal delivery

1, 2 & 4 x 10^6 ZS Green-luciferase transduced BAP1- and BAP1 C91A-expressing H226 cells were injected into the peritoneum of mice. Tumour development was tracked by bioluminescence imaging. A, Representative example of tumour burden in two mice immediately after the injection and before sacrificing on day 31. B, Quantification of tumour burden as photons per second.

(n=4, error bars represent SEM)

5.5.4 BAP1- and BAP1 C91A-expressing H226 cells grow subcutaneously in mice

The peritoneal xenograft model of H226 cells was not reliable and reproducible. There was no substantial tumour growth in the mice that received one million cells and there was a reduction in the growth of tumours in mice that received 2 and 4 million cells. This model was not ideal for testing the efficacy of TRAIL.

In order to determine the number of cells needed to subcutaneously inoculate mice to obtain a reliable and replicable model, I injected 1, 2 and 4 x 10^6 ZS Green-luciferase transduced BAP1- and BAP1 C91A-expressing H226 cells suspended in 100 µl PBS and matrigel solution (1:1 ratio) on the right and left flanks of mice, respectively. The tumour burden was longitudinally tracked by bioluminescence imaging of mice on an IVIS machine 15 minutes after injection of 200 µl of 10 mg/ml luciferin per mouse (Figure 5-16A).

The mice that received one million cells on their flanks showed establishment of tumours and subsequent tumour growth. The BAP1 C91A-expressing cells showed an increased tumour burden relative to BAP1-expressing H226 cells. This difference was significant on day 29 ($p<0.001$) (Figure 5-16B). The mice that received two and four million cells also showed establishment and subsequent growth of tumours. There was a trend towards higher tumour burden in the tumours of BAP1 C91A-expressing cells but this difference was not statistically significant (Figure 5-16B).

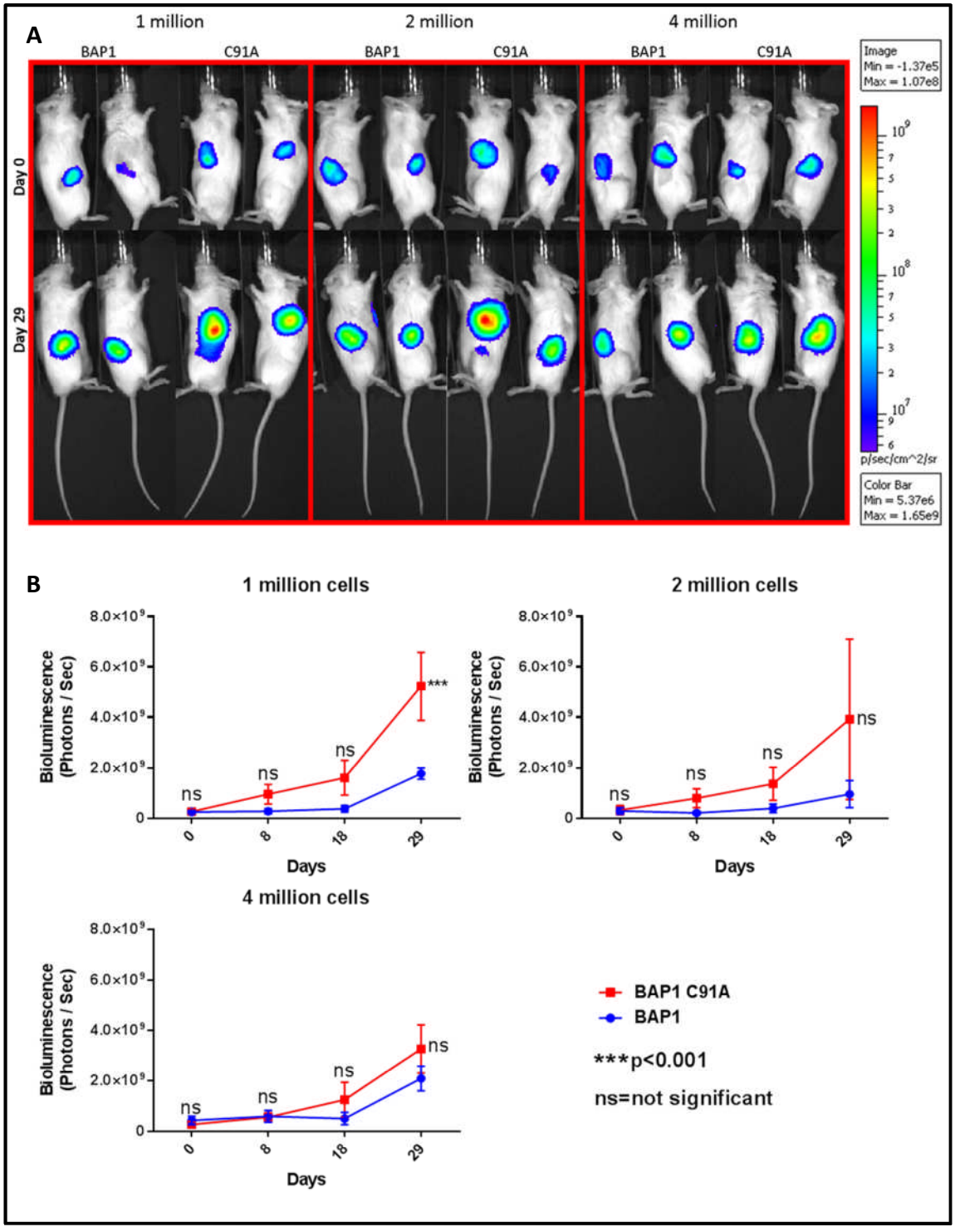

Figure 5-16 Growth of subcutaneous tumours of luciferase-transduced BAP1- and BAP1 C91A-expressing H226 cells was tracked by bioluminescence imaging

1, 2 & 4 x 10^6 ZS Green-luciferase transduced BAP1- and BAP1 C91A-expressing H226 cells were injected into the right and left flanks of each mouse. Tumour development was tracked by bioluminescence imaging. A, Representative example of tumour burden in two mice immediately following injection and on day 30. B, Quantification of tumour burden as photons per second.

(n=4, error bars represent SEM)

5.5.5 Loss-of-function mutation of BAP1 protein leads to TRAIL sensitisation in mice

My earlier experiment demonstrated that the subcutaneous tumour model using one million H226 cells would be ideal for testing the efficacy of IzTRAIL in mice. 18 mice were injected with one million BAP1-expressing H226 cells on the right flank and one million BAP1 C91A-expressing H226 cells on the left flank. Bioluminescence imaging of mice on an IVIS machine 15 minutes after injection of 200 µl of 10 mg/ml luciferin per mouse was done after inoculating the cells. The tumours were allowed to establish for 2 weeks. Bioluminescence imaging was performed on day 13 and the mice were allocated into three groups of six mice each. Each group received either vehicle, 400 µg/mouse IzTRAIL or 600 µg/mouse IzTRAIL 6 days a week for 4 weeks. Bioluminescence imaging of mice on an IVIS machine 15 minutes after injection of 200 µl of 10 mg/ml luciferin per mouse was done on day 19, 26 and 41 to monitor the tumour burden longitudinally. The mice were sacrificed on day 42 and their tumours were extracted (Figure 5-17A).

The tumours extracted from mice were visually smaller in mice inoculated with BAP1 C91A-expressing cells that received IzTRAIL treatment compared with vehicle-treated mice. This was most evident in mice that received 600 µg of TRAIL (Figure 5-17B). The tumours extracted from the mice were weighed. The weight of BAP1 C91A-expressing tumours that received 400 µg IzTRAIL was significantly ($p<0.05$) less than BAP1-expressing tumours that received 400 µg IzTRAIL (Figure 5-17C). The weight of BAP1 C91A-expressing tumours that received 600 µg IzTRAIL was significantly ($p<0.05$) less than BAP1-expressing tumours that received 600 µg IzTRAIL and also the BAP1 C91A-expressing tumours that received vehicle treatment (Figure 5-17C).

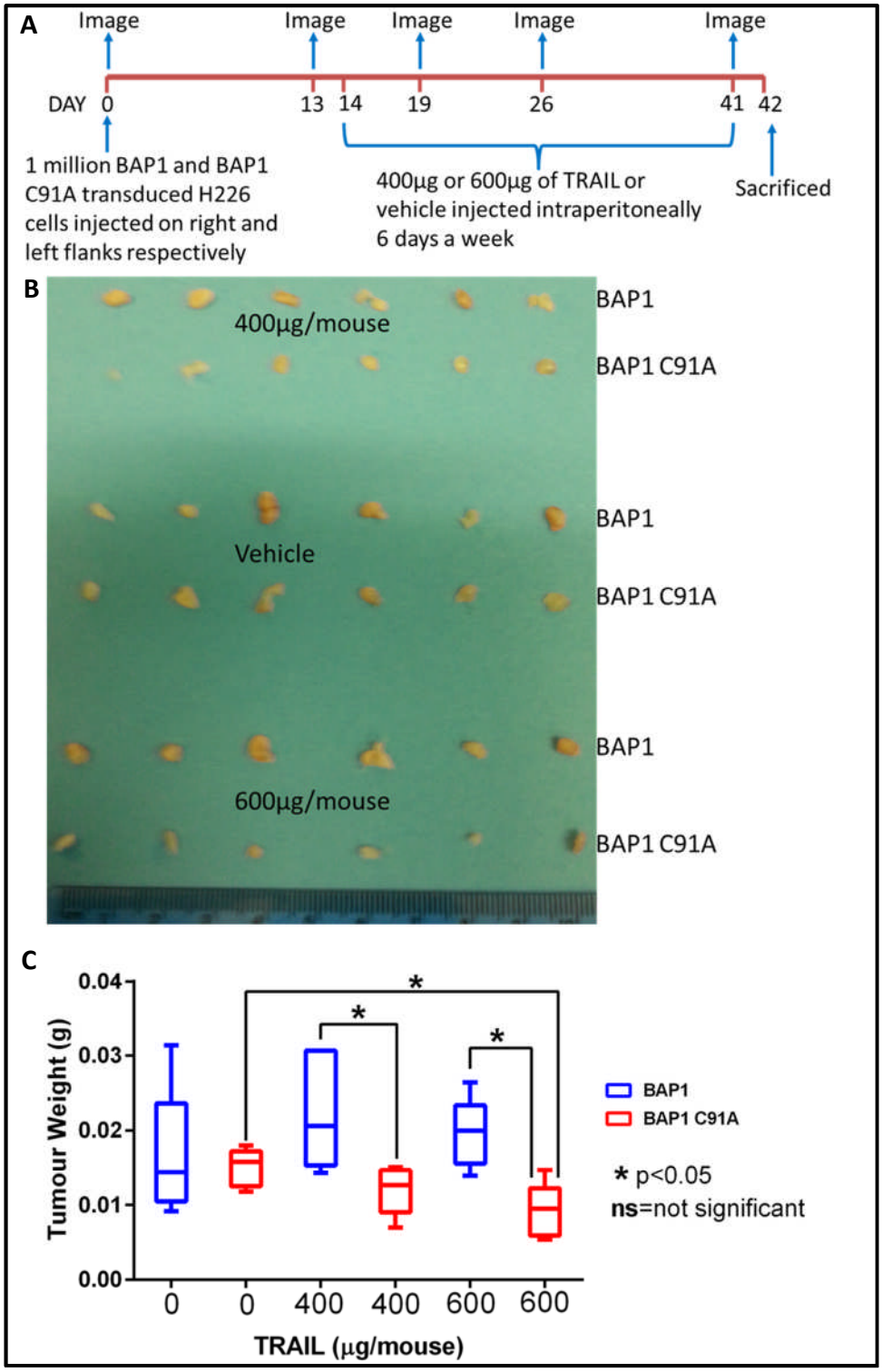

Figure 5-17 IzTRAIL treatment reduces the weights of BAP1 C91A-expressing tumours

1 x 10^6 ZS Green-luciferase transduced BAP1- and BAP1 C91A-expressing H226 cells were injected into the right and left flanks of each mouse on day 0. Tumour development was tracked by bioluminescence imaging on days 0, 13, 19, 26 and 41. Mice were grouped into three groups and were treated 6 days a week with vehicle, 400 µg or 600 µg IzTRAIL/mouse from day 14. Mice were sacrificed on day 42 and tumours were extracted. A, schematic of the experimental plan. B, Photograph of mouse tumours on day 42. C, weights of tumours extracted from mice on day 41. (n=6, error bars represent SEM).

The bioluminescence imaging was performed to track the tumour burden longitudinally. The BAP1 C91A-expressing H226 cells established quickly and tumours grew until day 13 (Figure 5-18B&C). Imaging on day 19 revealed a substantial decrease in BAP1 C91A-expressing tumours relative to day 13 tumour burden in groups that received 400 and 600 μg/mouse IzTRAIL. However, there was no decrease in the tumour burden in BAP1-expressing H226 tumours in mice that received either IzTRAIL or vehicle (Figure 5-18B&C). The decrease in tumour burden continued to day 26 in mice with BAP1 C91A-expressing tumours that received 600 μg IzTRAIL. However, this affect was not observed in mice with BAP1 C91A-expressing tumours that received 400 μg IzTRAIL. The tumour burden substantially increased in IzTRAIL-treated mice with BAP1-expressing tumours and in vehicle-treated mice with BAP1- and BAP1 C91A-expressing tumours (Figure 5-18B).

Imaging on day 41 revealed a substantial difference in the size of BAP1 C91A-expressing tumours that received IzTRAIL relative to all other groups (Figure 5-18A). The vehicle-treated mice continued to show an increasing tumour burden in both BAP1- and BAP1 C91A-expressing tumours. Mice with BAP1 C91A-expressing tumours that received 400 μg IzTRAIL displayed substantially less tumour burden when compared to mice with BAP1-expressing tumours that received 400 μg IzTRAIL and mice with BAP1- or BAP1 C91A-expressing tumours that received vehicle treatment (Figure 5-18A&B). However, this reduction in tumour burden was not statistically significant.

Mice with BAP1 C91A-expressing tumours that received 600 μg showed an increase in growth compared with the tumour burden on day 26. However, all other groups

showed a more rapid increase in tumour burden (Figure 5-18A&C). Mice with BAP1 C91A-expressing tumours that received 600 µg IzTRAIL displayed a statistically significant ($p<0.05$) lower tumour burden compared with mice with BAP1-expressing tumours that received 600 µg IzTRAIL and mice with BAP1- and BAP1 C91A-expressing tumours that received vehicle treatment (Figure 5-18C).

This experiment demonstrates a dose-response relationship of IzTRAIL treatment. More importantly, the loss of function in BAP1 protein sensitizes tumour cells to TRAIL *in vivo* and supports the idea that the BAP1 loss-of-function mutation is a biomarker for TRAIL sensitivity.

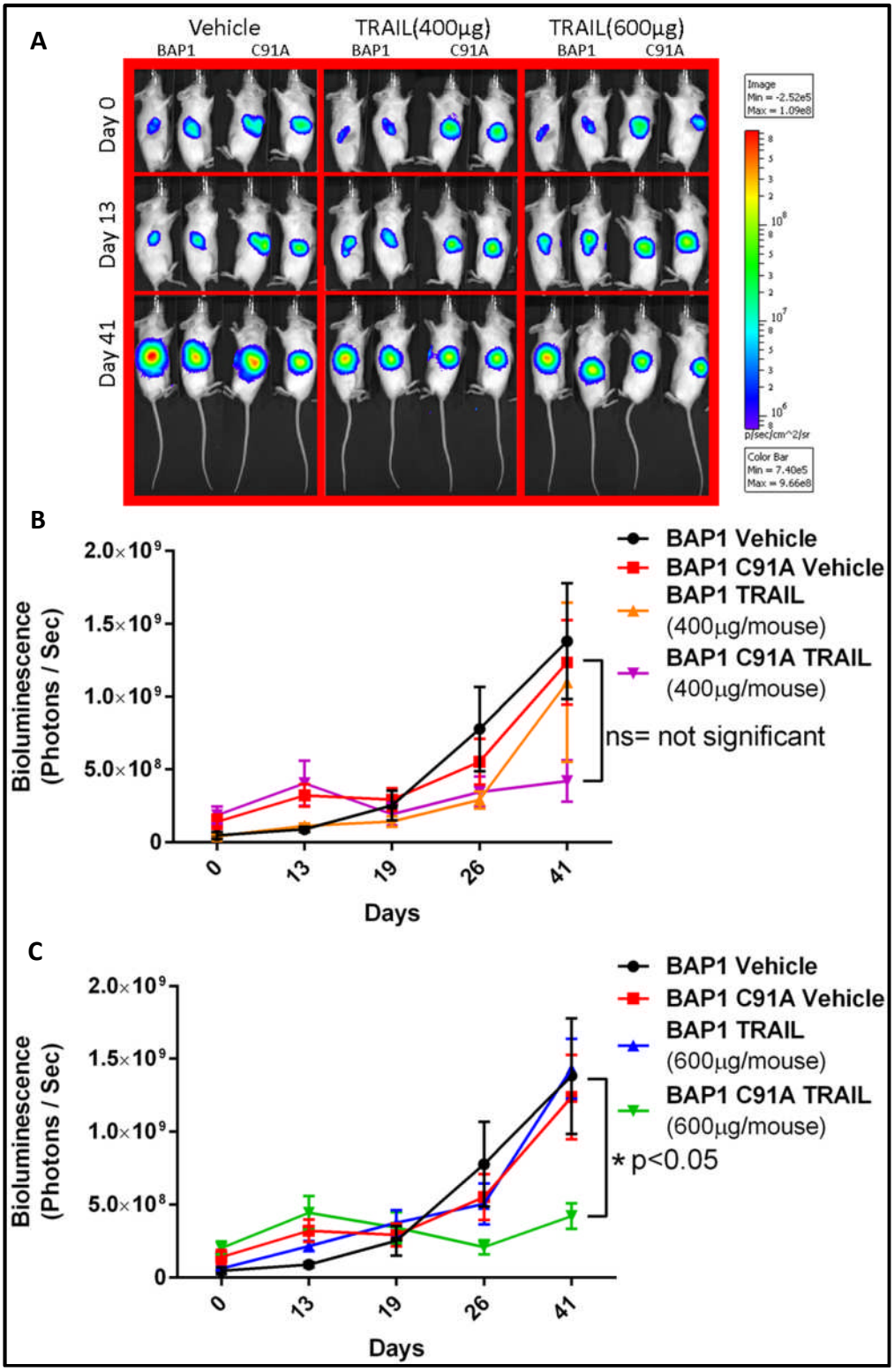

Figure 5-18 TRAIL reduces tumour burden in catalytically dead BAP1-mutant tumours

Bioluminescence imaging of mice was done after injecting luciferin to track the tumour growth. A, Representative example of 2 mice per group on day 1 (after inoculating tumour cells), on day 13 (before treatment) and on day 41 (after treatment). Tumour burden of mice treated with 400 µg (B) and 600 µg (C) TRAIL, quantified by bioluminescence imaging. (n=6, error bars represent SEM).

5.6 Discussion

5.6.1 Identification of loss-of-function mutation in BAP1 as a biomarker for TRAIL sensitivity

Many clinical trials have tested recombinant TRAIL and DR4/5-activating antibodies as therapies for cancer patients. Most of them showed reduced tumour burden in some patients but there was no overall significant reduction of tumour burden [245]. It is well known that clinical responses to anticancer therapies are often restricted to a subset of patients and the identification of a biomarker that could predict either sensitivity or resistance to a drug has a significant clinical utility. The lack of a biomarker that can predict TRAIL sensitivity of cancer cells is a serious impediment to the use of TRAIL as an anticancer agent.

I collaborated with C. Alifrangis at the McDermott laboratory in the Wellcome Trust Sanger Institute (WTSI) to identify a biomarker for TRAIL sensitivity. Previously it has been shown that mutated cancer genes are potential biomarkers for response to targeted agents [246]. A screen was performed to determine if there was a correlation between various mutations harboured in MPM cell lines and their response to TRAIL treatment. A correlation between the mutational status of BAP1 and TRAIL sensitivity was identified in the screen (Figure 5-1). BAP1 is a known tumour suppressor and has been found to be mutated in about 20-40% of MPM [48]. The same proportion of BAP1 mutations was observed in the cell lines screened. Of 15 cell lines screened, five were BAP1 mutants (33%). The observation of a mutation in a tumour suppressor leading to sensitivity to an anticancer agent is interesting as there are no reports of drugs targeting tumour suppressors to date. The correlation of BAP1 mutations and

TRAIL sensitivity may in fact be a synthetic lethality effect. The mutation in a tumour suppressor might lead to tumorigenesis but might simultaneously make the developed tumour sensitive to a drug.

5.6.2 Validation of the screen

The results of the screen were further validated by treating the cell lines at a range of 0.5-100 ng/ml TRAIL. The cell lines were grouped into sensitive, partially sensitive and resistant cell lines based on their response to TRAIL treatment (Figure 5-2A). Most of the BAP1-mutant cell lines did not express BAP1 protein while all the wild-type cell lines expressed BAP1 protein (Figure 5-2B). Out of nine BAP1-mutant cell lines, six were either sensitive or partially sensitive to TRAIL. Out of eight BAP1 wild-type cell lines, six were resistant to TRAIL. This was consistent with the observation of a correlation of BAP1 mutants to TRAIL sensitivity in the screen.

To further validate the observation, I knocked down BAP1 protein expression in the BAP1 wild-type MPM cell line H2818 by transducing the cells with a BAP1 shRNA-expressing lentivirus (Figure 5-4B). TRAIL-induced significantly more apoptosis in BAP1-knocked down H2818 cells relative to untransduced H2818 cells (Figure 5-4A). This confirms that loss of function of BAP1 increases the sensitivity of MPM cells to TRAIL.

Interestingly, the correlation between BAP1 mutations and TRAIL sensitivity is not restricted to MPM cell lines. The breast cancer cell line MDAMB-231 also displayed a significant decrease in IC_{50} value after knockdown of BAP1 by shRNA relative to empty vector-transduced or untransduced cells (Figure 5-5C). This emphasises that the correlation between BAP1 mutation and TRAIL sensitivity is not restricted to MPM.

5.6.3 The deubiquitination function of the BAP1 protein is required for TRAIL resistance

The H226 cell line is the most widely studied cell line for BAP1-associated work. This cell line was classified as non-small cell lung cancer/mesothelioma by ATCC and has a homozygous deletion of the *BAP1* gene. To investigate which domains in BAP1 might be important in TRAIL resistance, I transduced H226 cells with a BAP1-expressing lentivirus (Figure 5-8) or with a expressing lentivirus expressing catalytically dead mutant BAP1 protein that lacked deubiquitination activity (C91A) (Figure 5-11).

The BAP1-expressing H226 cells were significantly more resistant to TRAIL than the untransduced and BAP1 C91A-expressing H226 cells (Figure 5-12). There was no significant difference observed in cell death between untransduced and BAP1 C91A-expressing H226 cells (Figure 5-12). These data show that the UCH domain and therefore the deubiquitination function of BAP1 is necessary for TRAIL resistance.

The expression of a functional BAP1 protein is necessary for BAP1-induced TRAIL resistance. Wild-type BAP1 cell lines whose BAP1 expression is epigenetically silenced might also be sensitive to TRAIL. On the other hand, cell line mutations that do not affect the function of the BAP1 protein can be resistant to TRAIL. Therefore, the deubiquitinating function of BAP1 is required for BAP1-induced TRAIL resistance and a loss-of-function mutation in the *BAP1* gene may be a biomarker for TRAIL sensitivity.

5.6.4 Isoleucine zipper TRAIL was more efficacious in inducing apoptosis then recombinant TRAIL

Recombinant TRAIL is a truncated version of full-length TRAIL. It constitutes the extracellular domain of full-length TRAIL and exists as a monomer. The TRAIL receptors

should be trimerised by a trimer of TRAIL to trigger the extrinsic apoptosis pathway. Monomers of the TRAIL ligand are held together by an isoleucine zipper in IzTRAIL. This results in a trimerised version of the TRAIL ligand. IzTRAIL is more efficacious than recombinant TRAIL (Figure 5-13). This is due to the pre-existing trimerised form of the TRAIL ligand, which readily triggers apoptosis [211].

5.6.5 *In vivo* H226 xenograft models

In order to investigate the effect of BAP1 in tumours *in vivo* I developed an animal xenograft model. Tumour burden was tracked longitudinally by bioluminescence imaging as this is a reliable and accurate way of measuring tumour burden. Furthermore, this method enables tracking of tumour burden in internal organs of the mice.

BAP1- and BAP1 C91A-expressing H226 cells were initially injected into the peritoneum of the mice and tumour growth was monitored longitudinally using IVIS imaging. Although the mice that received one million cells did not show substantial tumour growth (Figure 5-15), those that received two and four million cells showed increase in tumour growth after day 20. The BAP1 C91A-expressing cells showed a significantly greater increase in tumour growth than the BAP1-expressing cells (Figure 5-15). This is in line with the notion that BAP1 is a tumour suppressor and that the deubiquitinating activity of BAP1 is required for its tumour suppressor function [49]. As the mice that received one million cells did not show tumour growth, while those that received two and four million cells required at least 20 days for the tumours to be established and grow, the intraperitoneal model was not ideal to test the efficacy of TRAIL on tumours without BAP1 activity *in vivo*.

Using a subcutaneous tumour model, injection of BAP1- and BAP1 C91A-expressing H226 cells established tumours within a week and mice showed a substantial increase in tumour burden over time (Figure 5-16). As expected, the BAP1 C91A-expressing cells showed a significant increase in tumour growth compared with BAP1-expressing cells. Injection of one million cells subcutaneously in mice was therefore used as a model to investigate the effect of TRAIL treatment *in vivo*.

5.6.6 Mutant BAP1-expressing tumours are more sensitive to TRAIL than wild-type BAP1-expressing tumours *in vivo*

In subcutaneous xenograft model, inoculation of wild-type and mutant BAP1 cells on each flank of the mice was performed to ensure equal exposure of the two types of tumours to TRAIL. Bioluminescence imaging showed a substantially higher tumour burden in mice with mutant BAP1-expressing tumours relative to mice with wild-type BAP1 tumours before treatment (Figure 5-18).

Mice with mutant BAP1-expressing tumours that received 600 µg TRAIL displayed significantly lower tumour burden and smaller tumours than mice with wild-type BAP1-expressing tumours shows that a loss of function of BAP1 sensitises tumour cells to TRAIL *in vivo* and that BAP1 mutational status can be used as a biomarker for TRAIL sensitivity (Figure 5-18).

5.7 Summary

- BAP1-mutated MPM cells are sensitive to TRAIL.
- Knockdown of BAP1 in wild-type cells sensitises them to TRAIL.
- Overexpression of BAP1 imparts TRAIL resistance.
- The deubiquitinating function of BAP1 is required for BAP1-induced TRAIL resistance.
- TRAIL can be used to treat BAP1 mutant tumours *in vivo.*
- Loss of function of BAP1 is a biomarker for TRAIL sensitivity.

CHAPTER VI

Results IV: Mechanism of BAP1-induced TRAIL resistance

6 RESULTS IV: MECHANISM OF BAP1-INDUCED TRAIL RESISTANCE

Having established that a loss-of-function mutation in BAP1 is a biomarker for TRAIL sensitivity, I proceeded to understand the mechanism of BAP1-induced TRAIL resistance. Elucidating the pathway by which BAP1 induces resistance would be helpful in modulating it and sensitizing the wild-type BAP1 tumours to TRAIL.

In this chapter, I employed site-directed mutagenesis to mutate key amino acids and thereby to inactivate each of the functional domains of BAP1 that have previously been annotated. Key BAP1 interactions with other proteins such as HCF1, BRCA1 and FOXK2 were targeted. The nuclear localisation signal (NLS) of BAP1 was also deleted to test if BAP1-induced TRAIL resistance is a result of its deubiquitinase activity in the nucleus.

As part of collaboration, C. Alifrangis at the McDermott laboratory in WTSI analysed the gene expression data of BAP1- and BAP1 C91A-expressing H226 cells. I also performed a protein array to identify the differentially expressed proteins involved in the apoptotic pathway.

6.1 Mutation of important BAP1 amino acids to determine their role in BAP1-induced TRAIL resistance

BAP1 is reported to interact with various other proteins through interactions involving specific amino acids in its polypeptide chain. For example, a NLS present in the C-terminal of the BAP1 polypeptide chain allows BAP1 to enter the nucleus. BAP1 plays an important role in the regulation of transcription and DNA repair in nucleus.

6.1.1 Interaction with HCF1 was not required for BAP1-induced TRAIL resistance

HCF1 has been reported to interact with BAP1 and to play an important role in transcriptional regulation of various genes. BAP1 interacts with HCF1 through its HCF1-binding motif (HBM). Mutating this motif prevents the interaction of BAP1 with HCF1.

The HBM on BAP1 was mutated by site-directed mutagenesis of the pCCL.CMV.BAP1 plasmid and confirmed by Sanger sequencing. H226 cells were transduced to express HBM-mutated BAP1. A western blot was performed to confirm the expression of BAP1 protein in H226 cells and flow cytometry determined the percentage of transduced cells (Figure 6-1A&B). 92% of cells were transduced by using 1.2 µl virus. These cells along with untransduced and BAP1-transduced H226 cells were treated with 50 and 100 ng/ml doses of TRAIL. There was no significant difference between BAP1-transduced and HBM-mutated BAP1-transduced H226 cells, indicating that the HCF1 interaction with BAP1 was not required for BAP1-induced TRAIL resistance (Figure 6-1C).

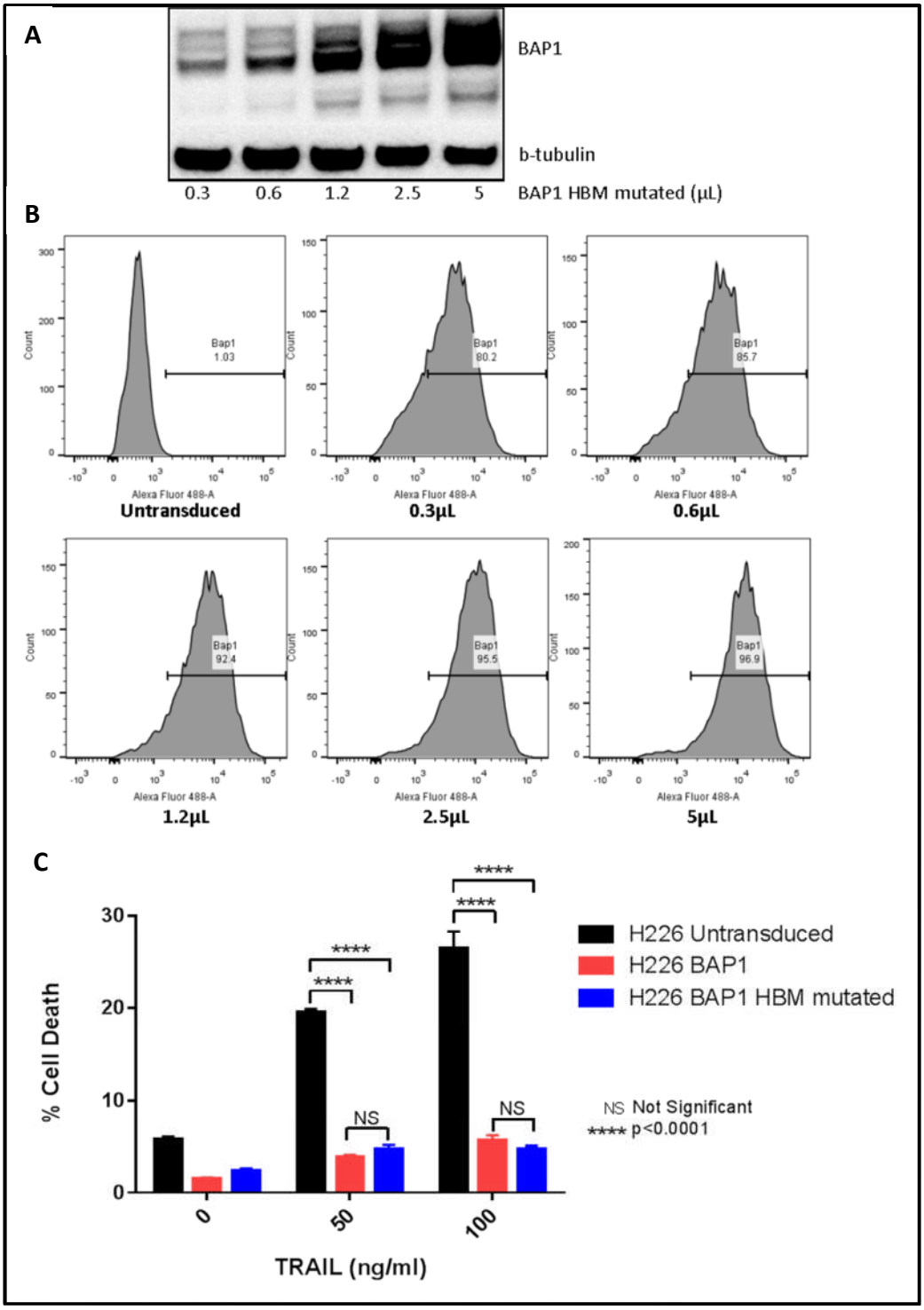

Figure 6-1 Interaction with HCF1 is not required for BAP1-induced TRAIL resistance

H226 cells were transduced with 0.3, 0.6, 1.2, 2.5 and 5 µl of HBM-mutated BAP1-expressing lentivirus. A, Western blotting shows the expression of BAP1 protein in BAP1 lentivirus-transduced cells. B, The cells were stained after fixing, permeabilization and blocking with an anti-human BAP1 primary antibody and an AF-488 conjugated anti-mouse secondary antibody. The percentage of transduced cells was determined by flow cytometry for AF-488. C, Untransduced, BAP1-transduced and HBM-mutated BAP1-transduced cells were treated with 0, 50 and 100 ng/ml of TRAIL for 24 hours and apoptosis was measured by Annexin V/DAPI assay.

6.1.2 BAP1 is required in the nucleus to induce TRAIL resistance

BAP1 is reported to play a significant role in transcriptional regulation and DNA repair in the nucleus. The NLS at the C terminus of the BAP1 protein from amino acids 717-722 enables it to enter the nucleus. To test if the nuclear localisation of BAP1 is required for TRAIL resistance, the nucleotides responsible for coding amino acids 717-729 were deleted from the pCCL.CMV.BAP1 lentiviral plasmid. This resulted in a truncated BAP1 protein without a nuclear localisation signal. Lentivirus was made with this transfer plasmid and H226 cells were transduced to express truncated BAP1. A western blot was performed to confirm the expression of BAP1 protein in H226 cells (Figure 6-2A) and flow cytometry determined the percentage of transduced cells (Figure 6-2B). 93% of cells were transduced by using 2.5 µl virus. These cells along with untransduced and BAP1-transduced H226 cells were treated with 50 and 100 ng/ml doses of TRAIL. Truncated BAP1-transduced cells, lacking a nuclear localisation signal, were significantly more sensitive to TRAIL than BAP1-transduced H226 cells ($p<0.0001$). However, truncated BAP1-transduced cells were not as sensitive as untransduced H226 cells. It can be concluded from these results that the nuclear localisation of BAP1 plays a key role in TRAIL resistance (Figure 6-2C).

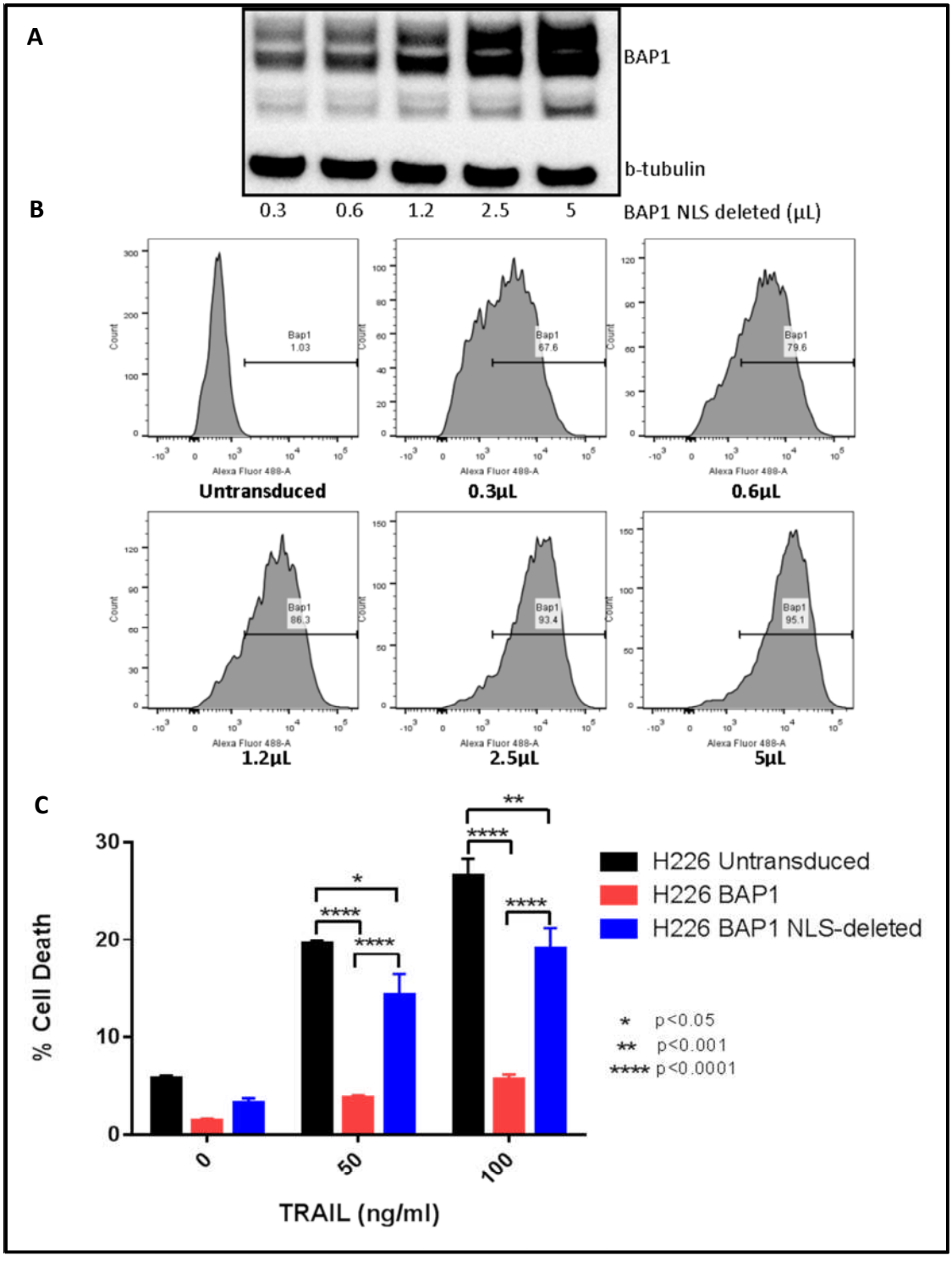

Figure 6-2 Nuclear localisation of BAP1 plays a role in TRAIL resistance

H226 cells were transduced with 0.3, 0.6, 1.2, 2.5 and 5 µl of truncated BAP1-expressing lentivirus. A, Western blotting shows the expression of BAP1 protein in BAP1 NLS-truncated lentivirus-transduced cells. B, The cells were stained after fixing, permeabilization and blocking with an anti-human BAP1 primary antibody and an AF-488 conjugated anti-mouse secondary antibody. The percentage of transduced cells was determined by flow cytometry for AF-488. C, Untransduced, BAP1-transduced and truncated BAP1-transduced cells were treated with 0, 50 and 100 ng/ml of TRAIL for 24 hours and apoptosis was measured by Annexin V/DAPI assay.

6.1.3 Interaction with BRCA1 was not required for BAP1-induced TRAIL resistance

BRCA1 is reported to interact with BAP1 and to play an important role in transcriptional regulation of various genes. BAP1 interacts with BRCA1 through a leucine residue at the 691st position of its polypeptide chain. Mutating this amino acid to proline prevents the interaction of BAP1 with BRCA1.

Leucine at the 691st position of BAP1 was mutated to proline (L691P) on the pCCL.CMV.BAP1 plasmid by site-directed mutagenesis and the mutation confirmed by Sanger sequencing. Lentivirus was made with the L691P BAP1 transfer plasmid. H226 cells were transduced to express mutated BAP1. Flow cytometry was performed to determine the percentage of transduced cells (Figure 6-3A). 90.3% of cells were transduced by using 5 µl virus. These cells, along with untransduced and BAP1-transduced H226 cells, were treated with 50 and 100 ng/ml doses of TRAIL. There was no significant difference between BAP1-transduced and L691P-mutated BAP1-transduced H226 cells, indicating that BRCA1's interaction with BAP1 is not required for BAP1-induced TRAIL resistance (Figure 6-3B).

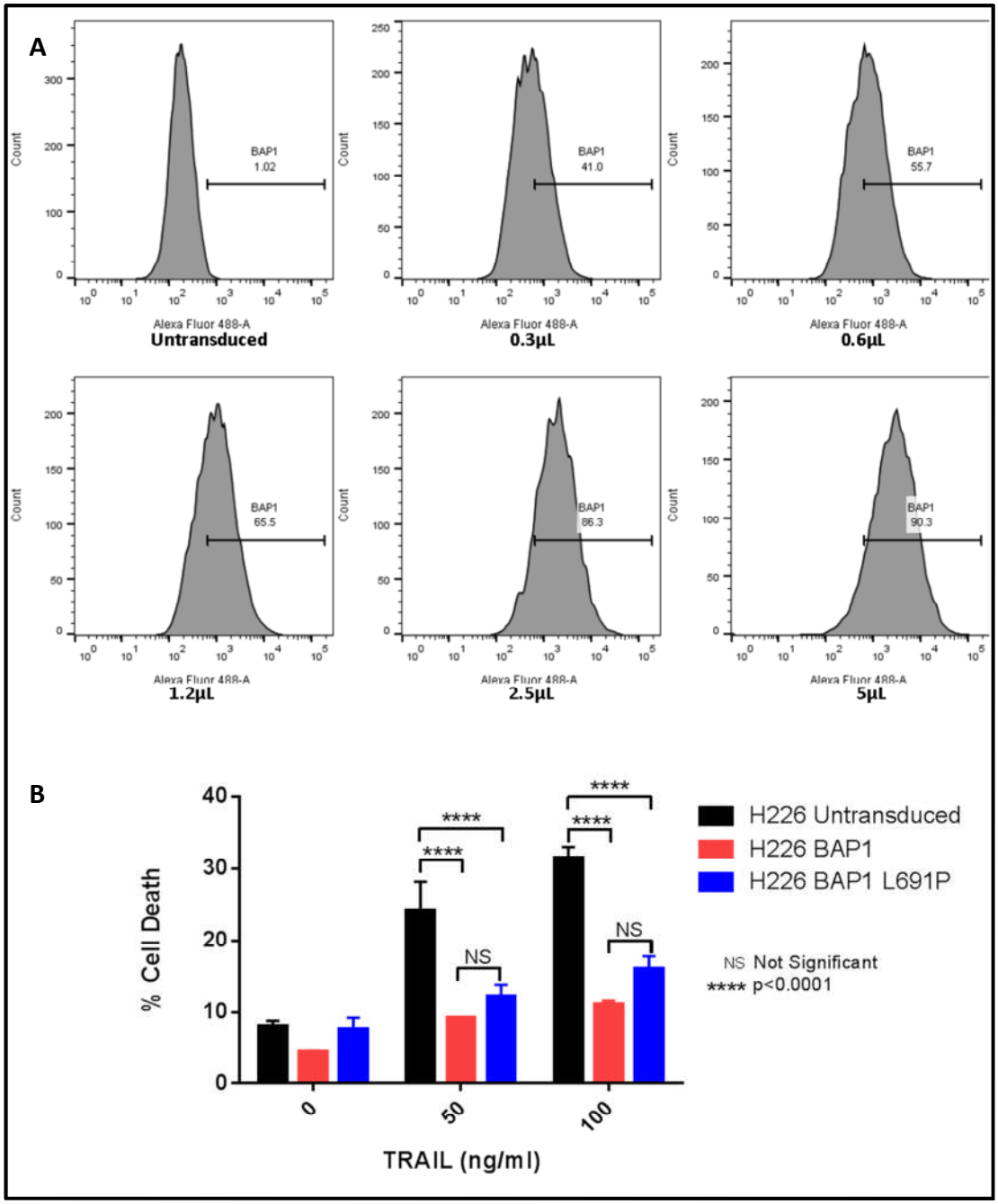

Figure 6-3 Interaction with BRCA1 is not required for BAP1-induced TRAIL resistance

H226 cells were transduced with 0.3, 0.6, 1.2, 2.5 and 5 µl of BAP1 L691P-expressing lentivirus. A, The cells were stained after fixing, permeabilization and blocking with an anti-human BAP1 primary antibody and an AF-488 conjugated anti-mouse secondary antibody. The percentage of transduced cells was determined by flow cytometry for AF-488. B, Untransduced, BAP1-transduced and BAP1 L691P-transduced cells were treated with 0, 50 and 100 ng/ml of TRAIL for 24 hours and apoptosis was measured by Annexin V/DAPI assay.

6.1.4 Interaction with FOXK2 is not required for BAP1-induced TRAIL resistance

FOXK1 and FOXK2 are transcription factors reported to interact with BAP1 and to regulate transcription. Phosphorylation of threonine residue at the 493st position of the BAP1 protein enables the interaction between BAP1 and FOXK2 and mutating this amino acid to alanine abrogates the BAP1-FOXK2 interaction [51].

To test if the BAP1-FOXK1/2 interaction is required for TRAIL resistance, I mutated the threonine 493 to alanine on the pCCL.CMV.BAP1 lentiviral transfer plasmid. Sanger sequencing was performed to confirm the mutation. Lentivirus was made with the pCCL.CMV.BAP1 T493A transfer plasmid and H226 cells were transduced to express BAP1 T493A. Flow cytometry determined the percentage of transduced cells and 5 µl of virus transduced 89.8% of H226 cells (Figure 6-4A). These cells, along with untransduced and BAP1-transduced H226 cells, were treated with 50 and 100 ng/ml of TRAIL. There was no significant difference between BAP1-transduced and T493A-mutated BAP1-transduced H226 cells at 100 ng/ml TRAIL treatment, indicating that FOXK2 interactions with BAP1 were not required for BAP1-induced TRAIL resistance (Figure 6-4B).

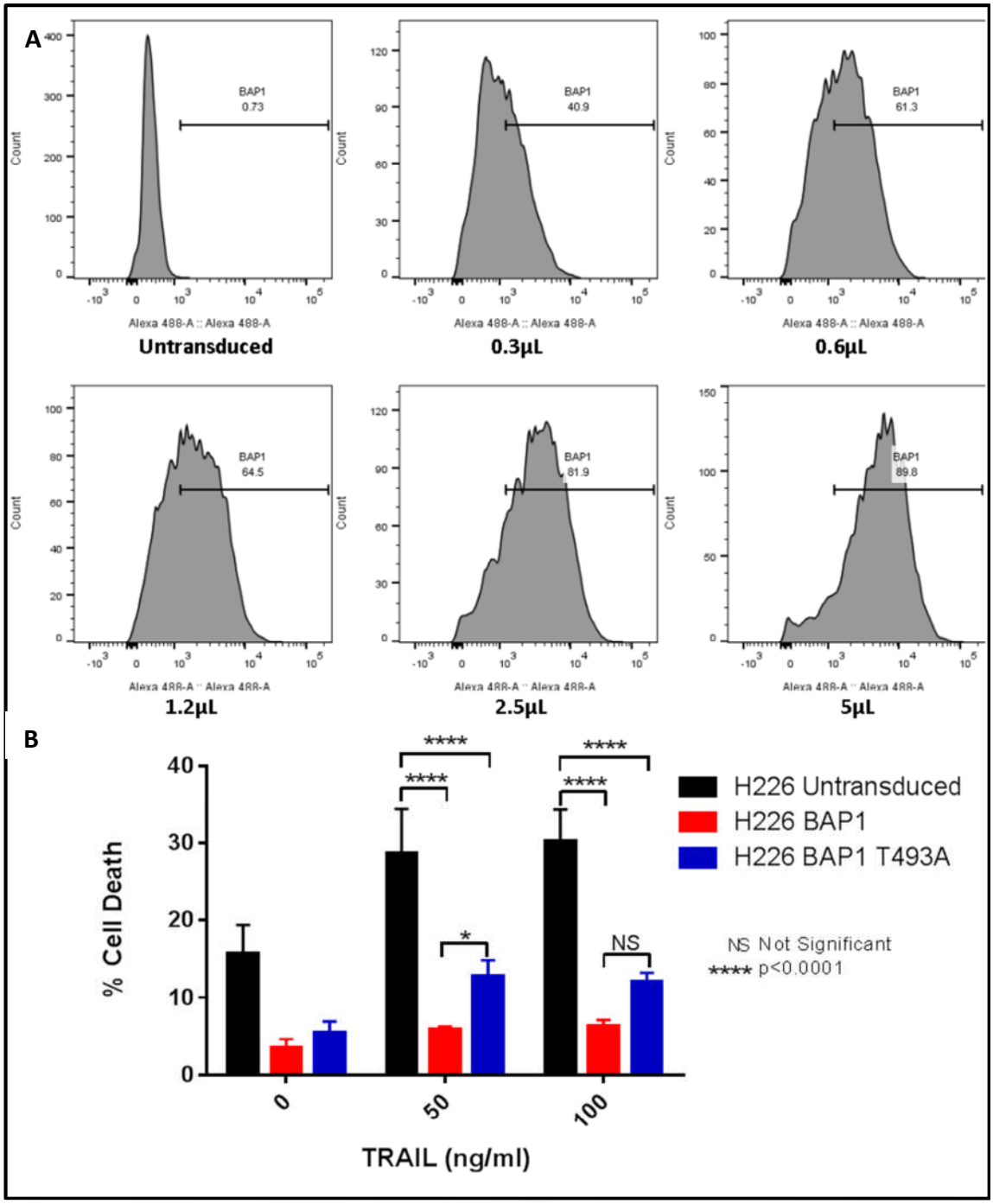

Figure 6-4 Interaction with FOXK2 is not required for BAP1-induced TRAIL resistance

H226 cells were transduced with 0.3, 0.6, 1.2, 2.5 and 5 µl of BAP1 T493A-expressing lentivirus. A, The cells were stained after fixing, permeabilization and blocking with an anti-human BAP1 primary antibody and an AF-488 conjugated anti-mouse secondary antibody. The percentage of transduced cells was determined by flow cytometry for AF-488. B, Untransduced, BAP1-transduced and BAP1 T493A-transduced cells were treated with 0, 50 and 100 ng/ml of TRAIL for 24 hours and apoptosis was measured by Annexin V/DAPI assay.

6.2 BAP1 induces resistance to the extrinsic apoptotic pathway

The extrinsic apoptotic pathway is activated not only by TRAIL but also by other agents such as FAS ligand (FASL) and TNFα. The receptors for these ligands are different but the cytoplasmic extrinsic apoptotic machinery is similar for all death ligands. In particular, TRAIL and FASL only differ in terms of the receptors they bind on the cell membrane and share a common downstream signalling mechanism.

To determine if BAP1-induced TRAIL resistance is mediated by TRAIL receptors, untransduced, BAP1-transduced and BAP1 C91A-transduced H226 cells were treated with 100 ng/ml of TRAIL, FASL or TNFα. BAP1-expressing H226 cells are relatively resistant to all three death ligands compared with untransduced cells, while BAP1 C91A-mutated cells showed no significant difference relative to untransduced H226 cells (Figure 6-5).

Hence it can be inferred that BAP1-induced TRAIL resistance occurs through the modulation of the cytoplasmic extrinsic apoptotic machinery.

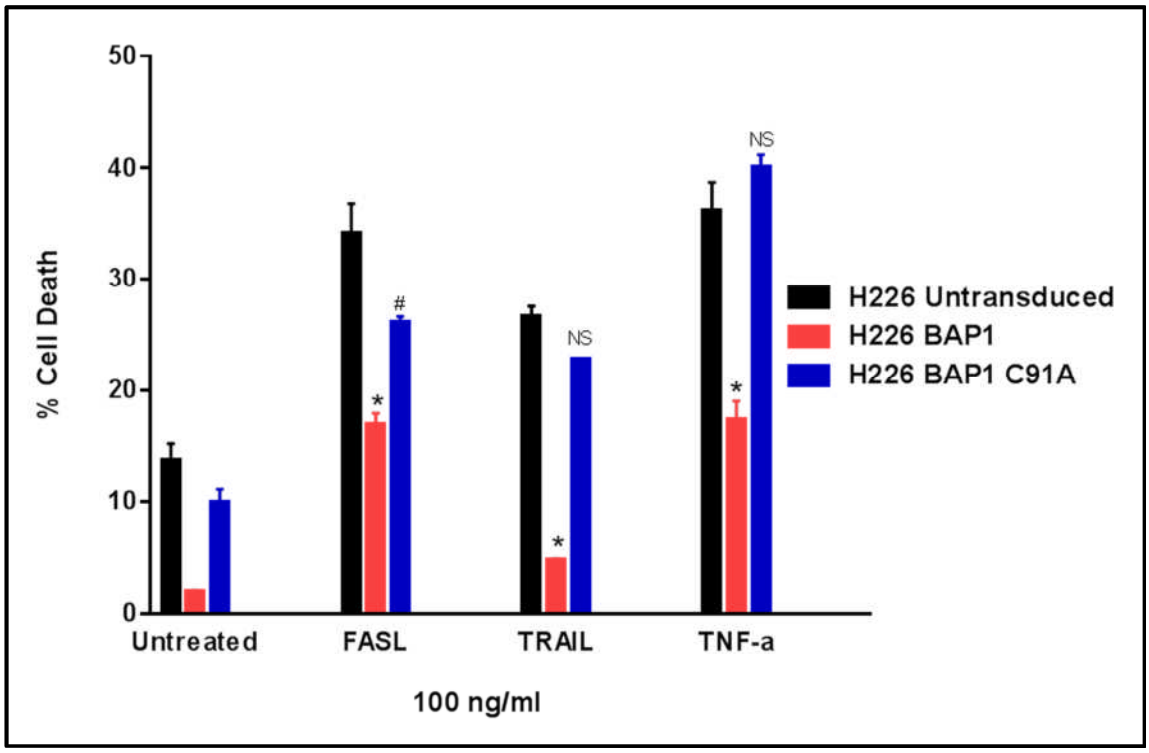

Figure 6-5 BAP1 induces resistance to extrinsic apoptotic pathway activators

*Untransduced BAP1-negative H226 cells, BAP1-expressing and catalytically dead BAP1-expressing H226 cells were treated with 100 ng/ml of FASL, TRAIL and TNFα for 24 hours and cell death was quantified by Annexin V/DAPI assay. * p<0.05 indicates significant difference between untransduced H226 cells and H226 BAP1-expressing cells. NS indicates no significant difference between untransduced H226 cells and BAP1 C91A-transduced cells. # p<0.05 indicates significant difference between untransduced H226 cells and BAP1 C91A-transduced cells.*

6.2.1 Expression of BAP1 inhibits the apoptotic pathway

The mRNA from catalytically dead BAP1-expressing H226 cells and BAP1 wild-type H226 cells was extracted and run on an Illumina HT12 array to determine if there were differences in gene expression.

The significantly differentially expressed genes were analysed using KEGG pathway analysis. The apoptosis pathway was influenced by the expression of BAP1. In fact, the pathway analysis predicted that the apoptotic pathway might be inhibited in the cells expressing BAP1. This was due to significant upregulation of cIAP1 and cIAP2 in the BAP1-expressing cells (Figure 6-6).

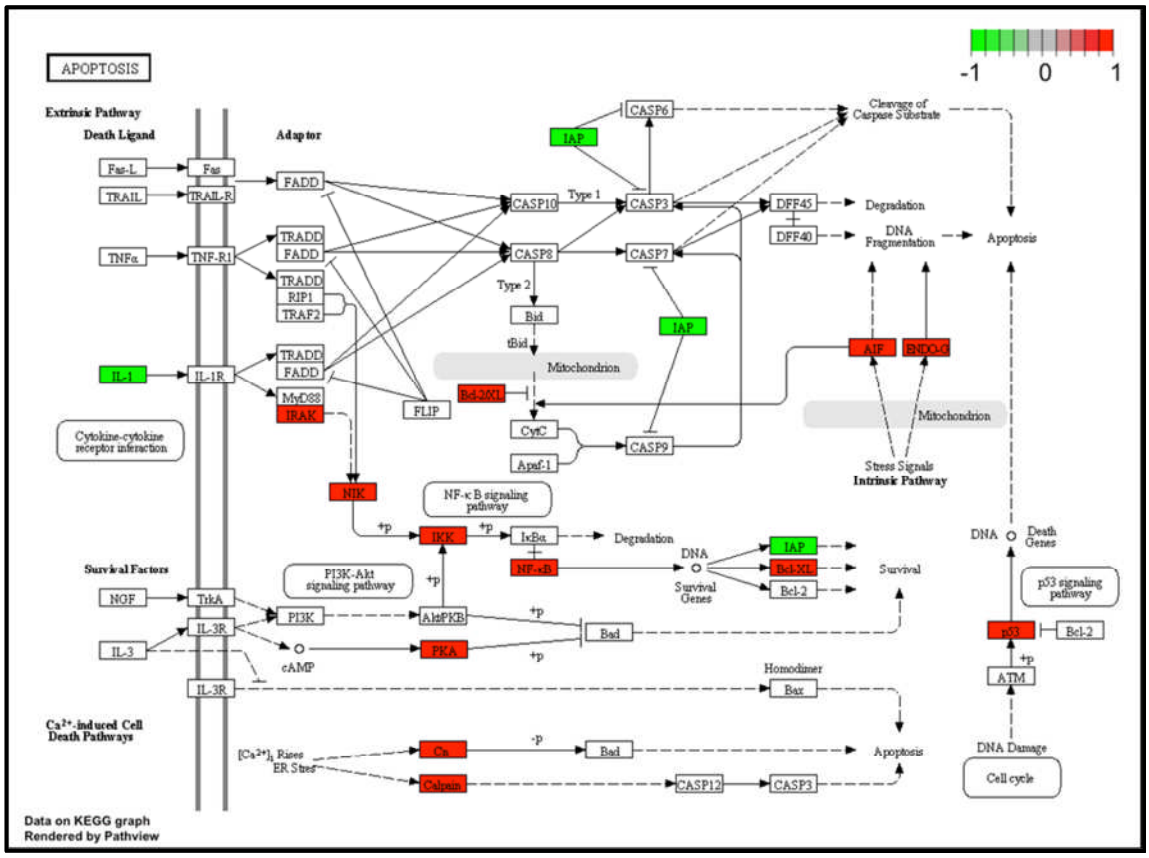

Figure 6-6 KEGG pathway analysis of microarray data shows that *IAPs are* downregulated in the absence of BAP1

Comparing GEX profile of C91A mutant BAP1- versus wild-type BAP1-expressing H226 cells, KEGG pathway analysis shows significantly dysregulated genes (analysis with adj pval <0.05 and FDR <20%). The genes that are downregulated in the absence of BAP1 are shown in green while genes which are upregulated in the absence of BAP1 are shown in red.

These data were provided by Dr McDermott's laboratory (WTSI) as part of a collaboration.

6.2.2 Expression of BAP1 in H226 cells upregulates the expression of cellular inhibitors of apoptosis proteins

Various apoptotic genes are differentially expressed in the presence of BAP1 in H226 cells. The most significantly downregulated genes in the absence of functional BAP1 protein were the anti-apoptotic genes BIRC3 (cIAP2) and BIRC2 (cIAP1) (Figure 6-7A&B). However, other pro-apoptotic genes such as TNFRSF10B (DR5) and FADD are upregulated in the absence of BAP1. It can be inferred that the presence of functional BAP1 protein tilts the balance towards inhibition of apoptosis.

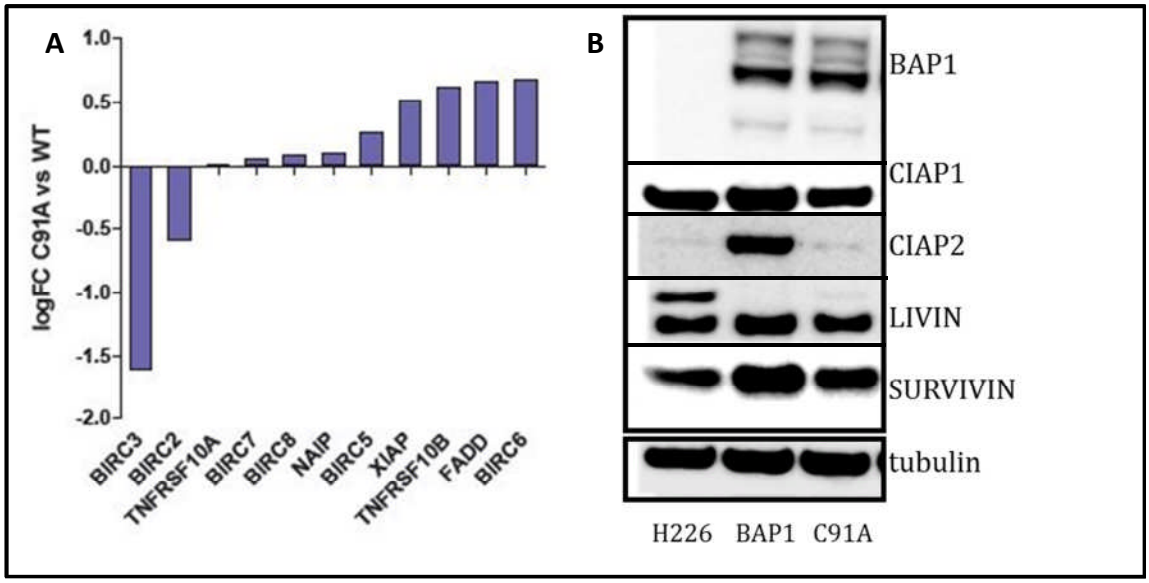

Figure 6-7 BAP1 upregulates the expression of cIAP2

A, Differentially expressed genes involved in apoptosis in BAP1 C91A- versus BAP1-expressing H226 cells. B, western blots of proteins belonging to the IAP family.

*Figure 6-7*A was provided by Dr McDermott's laboratory (WTSI) as part of a collaboration.

6.2.3 Inhibition of IAPs with a small molecule IAP inhibitor sensitises BAP1-expressing H226 cells to TRAIL

As cIAP2 was upregulated in the presence of BAP1, and thus might be responsible for TRAIL resistance, I reasoned that inhibiting the IAPs with a SMAC mimetic would sensitise the BAP1-expressing cells to TRAIL. LCL161, a SMAC mimetic, was used to inhibit IAPs.

TRAIL-resistant BAP1 wild-type MPP-89 and H2869, along with the TRAIL-resistant BAP1-mutant cell line H2722, were treated with either 0-1000 ng/ml of TRAIL or a combination with 5 μM LCL161 and 0-1000 ng/ml of TRAIL for 24 hours. The TRAIL-resistant cell lines were significantly ($p<0.0001$) sensitised to TRAIL following treatment with LCL161 (Figure 6-8A-C).

BAP1-expressing H226 cells and BAP1 C91A-expressing H226 cells were treated with either 0-1000 ng/ml of TRAIL or a combination of 5 μM LCL161 and 0-1000 ng/ml of TRAIL for 24 hours. Cell death was quantified by an Annexin V/DAPI apoptosis assay (Figure 6-8D). BAP1-expressing cells were resistant to TRAIL but were sensitised to TRAIL upon treatment with the combination of LCL161 and TRAIL ($p<0.0001$). However, the combination of TRAIL and LCL161 induced a significantly higher level of cell death in BAP1 C91A-expressing cells than in BAP1-expressing cells (Figure 6-8D).

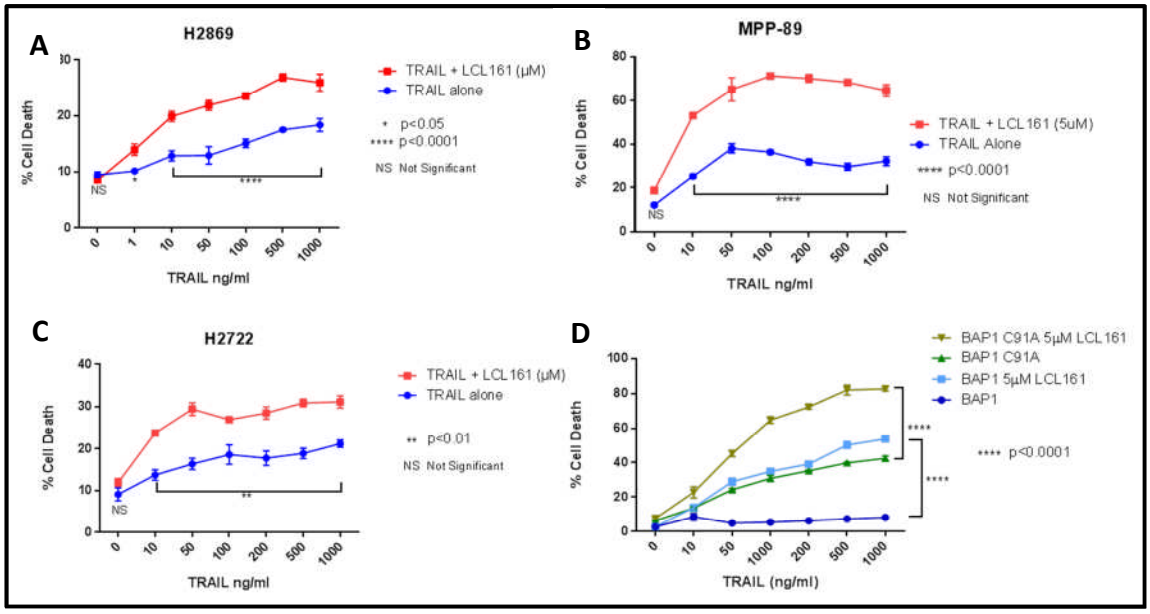

Figure 6-8: Inhibition of IAPs overcomes BAP1-induced TRAIL resistance

A, B & C, TRAIL-resistant MPM cells were treated with either 0-1000 ng/ml of TRAIL alone or a combination of 5 μM LCL161 and 0-1000 ng/ml of TRAIL for 24 hours and cell death was quantified by Annexin V/DAPI assay. D, BAP1-transduced or BAP1 C91A-transduced H226 cells were treated either with 0-1000 ng/ml of TRAIL alone or a combination of 5 μM LCL161 and 0-1000 ng/ml of TRAIL for 24 hours and cell death was quantified by Annexin V/DAPI assay.

6.2.4 BAP1-induced TRAIL resistance was not solely dependent on cIAP2 upregulation

As I have shown that BAP1 upregulates cIAP2 and treatment of BAP1-expressing cells with an IAP inhibitor sensitises them to TRAIL, I knocked down cIAP2 in BAP1-expressing H226 cells to test whether cIAP2 was the only protein responsible for TRAIL resistance.

H226 BAP1 cells were transduced either with MOI 5 of a cIAP2 shRNA-expressing lentivirus or with an empty vector shRNA-expressing lentivirus. cIAP2 knockdown was confirmed by performing a western blot and probing for cIAP2. The cIAP2 shRNA-expressing H226 BAP1 wild-type cells showed a relative reduction in cIAP2 expression compared with H226 BAP1 wild-type cells and empty vector shRNA-expressing cells (Figure 6-9A). The lentivirus also expressed GFP and a puromycin resistance gene as markers for selection along with BAP1 shRNA. The transduction efficiency was measured by flow cytometry for GFP expression. The cells were treated with 10 μg/ml puromycin to select the transduced cells and then flow cytometry for GFP quantified the percentage of transduced cells. 91% of cells expressed cIAP2 shRNA while 97% of the cells expressed empty vector shRNA (Figure 6-9B). H226 BAP1 cells, H226 BAP1 cells expressing cIAP2 shRNA and H226 BAP1 cells expressing empty vector shRNA were treated with TRAIL from a dose range of 0-1000 ng/ml for 24 hours and cell death was quantified by Annexin V/DAPI assay (Figure 6-9C). There was no significant difference in cell death between H226 BAP1 cells expressing cIAP2 shRNA and cells expressing empty vector shRNA, suggesting that cIAP2 was not the only protein responsible for TRAIL resistance.

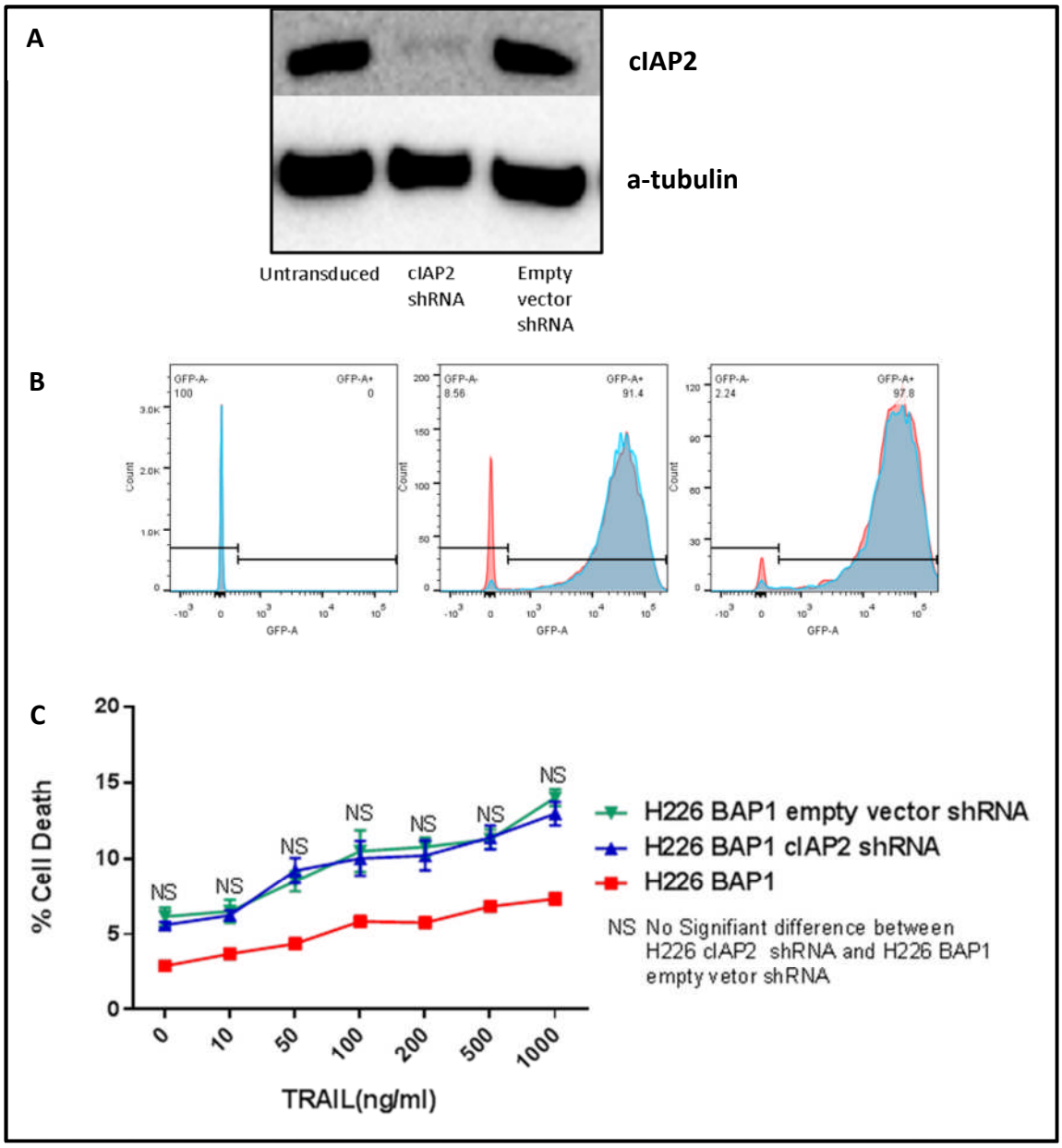

Figure 6-9 Knockdown of cIAP2 in BAP1-transduced H226 cells does not sensitise them to TRAIL

A, Western blot probing for cIAP2 in H226 BAP1 cells, H226 BAP1 cIAP2 shRNA-transduced cells and H226 BAP1 empty vector shRNA-transduced cells. B, Flow cytometry plots of GFP-expressing transduced cells. C, H226 BAP1 cells, H226 BAP1 cIAP2 shRNA-transduced cells and H226 BAP1 empty vector shRNA-transduced cells were treated with 0-1000 ng/ml TRAIL for 24 hours and cell death was quantified by Annexin V/DAPI assay.

6.3 BAP1 expression alters the expression of many proteins involved in the apoptotic pathway

As upregulation of cIAP2 was not responsible for BAP1-induced TRAIL resistance, a protein array was performed to determine the differential expression of proteins involved in apoptotic pathways.

Protein extracted from untransduced H226 and BAP1-expressing H226 cells were used for the protein array. A relatively higher expression of BAD, Cyt-C and DR5 was observed in untransduced cells while BAP1-expressing H226 cells expressed relatively higher amounts of FADD and HSP-60 (Figure 6-10).

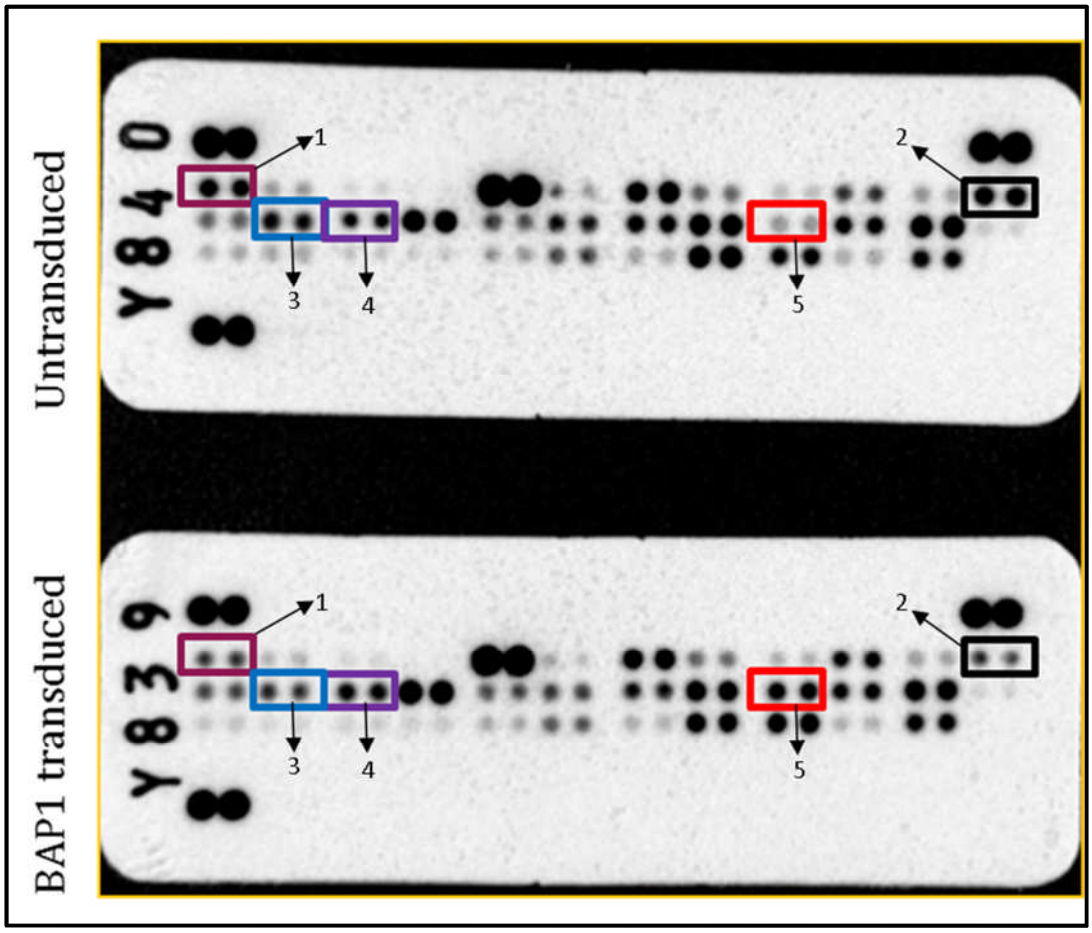

Figure 6-10: Protein array comparing untransduced H226 cells with H226 BAP1-transduced cells.

Protein extracts from BAP1-transduced H226 cells and untransduced H226 cells were used to find differential expression of proteins by an apoptosis protein array. The differentially expressed proteins are highlighted with the coloured boxes and numbered. 1-BAD, 2-Cytochrome C, 3-Death receptor 5, 4-FADD & 5-HSP60.

6.4 Discussion

6.4.1 HCF1 is not involved in BAP1-induced TRAIL resistance

BAP1 has been found to interact with HCF1 through its HCF1 binding motif located between amino acids 363-366 of its polypeptide chain. HCF1 is a key transcriptional regulator involved in several cellular processes [60]. BAP1 and HCF1 form a complex and regulate gene expression. They, along with other transcription regulators play a key role in gene repression, particularly during development. The mutation of HBM abolishes the interaction of BAP1 with HCF1 [60]. In order to determine the involvement of HCF1 in TRAIL resistance, the HBM of BAP1 was mutated. The cells expressing HBM-mutated BAP1 were as TRAIL resistant as their wild-type BAP1-expressing counterparts. Thus, the interaction between HCF1 and BAP1 was not required for BAP1-induced TRAIL resistance (Figure 6-1).

6.4.2 Nuclear localisation of BAP1 is required for TRAIL resistance

BAP1 enters the nucleus with the aid of its nuclear localisation signal (amino acids 717-722) at the C terminus of its polypeptide chain. Mutation or deletion of this sequence abrogates BAP1's ability to sequester into the nucleus [49]. H226 cells transduced to express truncated BAP1 protein lacking the NLS were TRAIL sensitive. This indicates that BAP1 is required in the nucleus to impart TRAIL resistance. The cells were significantly more sensitive to TRAIL than the cells expressing wild-type BAP1 (Figure 6-2). However, they were not as sensitive as untransduced cells. As the cells overexpress BAP1, some of the protein might be attaching to another protein with an NLS and piggy-backing into the nucleus. Alternatively, BAP1 might be doing two

different functions, one in the nucleus and one in the cytoplasm, and contributing to TRAIL resistance.

6.4.3 Interaction with BRCA1 is not required for TRAIL resistance

BRCA1 is reported to interact with BAP1 and to play an important role in transcriptional regulation of various genes. BAP1 interacts with BRCA1 through a leucine residue at the 691st position of its polypeptide chain [43]. Mutating this amino acid to proline prevents the interaction of BAP1 with BRCA1. The H226 cells that express L691P-mutated BAP1 are not significantly sensitive to TRAIL compared with wild-type BAP1-expressing cells (Figure 6-3). This indicates that BRCA1 does not play a role in BAP1-induced TRAIL resistance.

6.4.4 Interaction with FOXK2 is not required for TRAIL resistance

FOXK1 and FOXK2 are transcription factors reported to interact with BAP1 and to regulate transcription. A threonine residue at the 493rd position of the BAP1 protein is phosphorylated to enable the interaction between BAP1 and FOXK2. Mutating this amino acid to alanine abrogates the BAP1-FOXK2 interaction [51]. The H226 cells that express T493A-mutated BAP1 were not significantly sensitive to TRAIL compared with wild-type BAP1-expressing cells (Figure 6-4). This indicates that FOXK2 does not play a role in BAP1-induced TRAIL resistance.

6.4.5 BAP1 imparts resistance to the extrinsic apoptotic pathway

The extrinsic apoptotic pathway is activated not only by TRAIL but also by other agents such as FASL and TNFα. There are different receptors for these ligands but the cytoplasmic extrinsic apoptotic machinery is similar for all death ligands. Indeed, TRAIL

and FASL only differ in the receptors to which they bind on the cell membrane but they share a common downstream signalling mechanism.

BAP1-expressing H226 cells are relatively resistant to TRAIL, FASL and TNFα compared with untransduced cells, while BAP1 C91A-mutated cells showed no significant difference relative to untransduced H226 cells (Figure 6-5). This indicates that BAP1-induced TRAIL resistance is due to modulation of the cytoplasmic apoptotic pathway.

6.4.6 The apoptotic pathway is significantly dysregulated in the presence of wild-type BAP1

As part of a collaboration, C. Alifrangis at McDermott laboratory in WTSI analysed the gene expression data of BAP1- and BAP1 C91A-expressing H226 cells. The data were analysed by KEGG pathway analysis. 14 pathways including apoptosis were significantly perturbed when BAP1-expressing and BAP1 C91A-expressing gene expression data were compared. Taking into consideration that TRAIL activates the extrinsic apoptotic pathway, this is of no surprise. The gene expression data indicated that IAPs, particularly cIAP2, were significantly upregulated in the presence of BAP1 (Figure 6-6). Western blots of IAPs confirmed the upregulation of cIAP2 in BAP1-expressing H226 cells relative to untransduced and BAP1 C91A-expressing cells (Figure 6-7B). This indicates that BAP1 in the nucleus might be regulating the transcription of cIAP2 and that the deubiquitinase activity of BAP1 is required for this function.

6.4.7 Wild-type BAP1 cell lines are sensitised to TRAIL when treated in combination with an IAP inhibitor

Wild-type BAP1 cells were sensitised to TRAIL following treatment with LCL161, a SMAC mimetic and IAP inhibitor (Figure 6-8A). The BAP1-expressing H226 cells were

also sensitised to TRAIL when treated in combination with LCL161. However, the mutant BAP1-expressing H226 cells were even more sensitised to TRAIL when treated in combination with LCL161 (Figure 6-8B).

Knockdown of cIAP2 in BAP1-expressing cells does not sensitise them to TRAIL-induced apoptosis. This indicates that although cIAP2 is significantly upregulated in the presence of BAP1, it might not be the only protein imparting TRAIL resistance (Figure 6-9C). There might be some other protein which is also modulated in presence of BAP1 and determining the sensitivity of cells to TRAIL.

6.4.8 BAP1 mutation might tilt the balance in favour of apoptosis

A protein array of key proteins involved in apoptosis revealed a differential expression of several proteins between BAP1-expressing H226 cells and untransduced cells. A relatively higher expression of BAD, Cyt-C and DR5 was observed in untransduced cells while BAP1-expressing H226 cells expressed relatively higher amounts of FADD and HSP-60 (Figure 6-10). This indicates that the presence of mutated BAP1 upregulates pro-apoptotic proteins and tilts the balance in favour of apoptosis after TRAIL treatment.

6.5 Summary

- The interaction of BAP1 with HCF1, BRCA1 and FOXK2 was not required for BAP1-induced TRAIL resistance.
- The nuclear localisation of BAP1 is required for TRAIL resistance.
- The apoptosis pathway is perturbed in the presence of BAP1.
- cIAP2 is upregulated in the presence of BAP1 and the deubiquitination function of BAP1 is required for this function.
- Combinatorial treatment of a SMAC mimetic and TRAIL work synergistically to induce greater cell death in BAP1 wild-type cell lines.
- cIAP2 is not the sole factor responsible for BAP1-induced cell death.
- The presence of mutated BAP1 upregulates pro-apoptotic proteins and tilts the balance in favour of apoptosis after TRAIL treatment.

CHAPTER VII

Summary and future directions

7 SUMMARY AND FUTURE DIRECTIONS

The hypothesis of this study was that cancer cell-killing capacity of MSC-TRAIL can be enhanced by using the most effective form of TRAIL in combination with chemotherapeutic agents and by identifying a biomarker to predict TRAIL sensitivity. I had shown that cancer cell-killing function of full-length TRAIL was superior to that of the shortened soluble form of TRAIL. The transduction of MSCs to express TRAIL did not adversely affect MSC phenotype. It was also observed that MSC-flT cells are capable of partially overcoming resistance in TRAIL-resistant cancer cell lines. Cells that are resistant to MSC-flT cell-induced apoptosis can be sensitised by using chemotherapeutic agents that target key anti-apoptotic proteins in the apoptosis pathway. The lentiviral backbone used to express TRAIL was clinically approved thus can be used for clinical applications. The data generated in this study, in combination with other work performed within the laboratory, will be used for manufacturing a clinical product and for regulatory approval for the recently funded Phase I/II clinical trial using MSC-flT cells as a therapy for lung cancer.

In collaboration with C. Alifrangis at the McDermott's laboratory, we identified and validated that the *BAP1*-mutated MPM cells are sensitive to TRAIL. I showed that *BAP1*-mutant cancers cells can be treated with TRAIL *in vivo*. I investigated the mechanistic basis of BAP1-induced TRAIL resistance and showed that the nuclear localisation and the deubiquitination function of BAP1 are required for BAP1-induced

TRAIL resistance. In this work, I show that loss of function of BAP1 is a biomarker for TRAIL sensitivity and, as at least 20% of MPM patients harbour BAP1 mutations [67, 69] and BAP1 mutations are also found in other cancers [48, 70], patients who have these mutations could benefit from treatment with TRAIL. The safety profile of TRAIL has already been established in several Phase I clinical trials [247]. So a Phase II clinical trial studying the efficacy of TRAIL in BAP1-mutant MPM patients is a logical next step.

7.1 Investigating the basis for superiority of MSC-flT over MSC-sT cells

The ultimate objective of this study was to generate preclinical data for translation of MSC-TRAIL therapy into clinical use. In this study, I had shown that MSCs could be successfully transduced to express TRAIL by lentivirus. There was no noticeable effect on MSC cell viability or phenotype as a result of transduction. This means that the lentiviral vectors used in this study are compatible for MSC transduction. The tumour-homing ability of MSCs after transduction was not tested in this study. It would be interesting to show that the migration of MSCs was not affected after transduction both *in vitro* and *in vivo*.

It was observed that MSC-flT cells were superior to MSC-sT cells in inducing apoptosis in tumour cells. This was the only study that directly compared the efficacy of MSC-flT and MSC-sT cells. However, this study used only *in vitro* 2D coculture experiments. There are other studies that showed that MSC-expressing soluble TRAIL showed therapeutic effects *in vivo* [248]. Tumours *in vivo* are three-dimensional and MSC-flT cells might not be able to offer direct contact with all the tumour cells while the MSC-sT cells will secrete TRAIL that diffuses into the tumours and might be better in

inducing apoptosis. A study directly comparing the efficacy of MSC-flT and MSC-sT cells *in vivo* would therefore be desirable. However, I had showed that MSC-flT cells also secrete some TRAIL and thus may still be better than MSC-sT cells.

It will be interesting to study if TRAIL expressed on the membrane can induce better apoptosis than secreted TRAIL. The fluidic nature of the cell membrane can facilitate higher order clustering, enabling TRAIL to re-organise TRAIL receptors into large clusters. These clusters are thought to amplify apoptosis-induced by TRAIL [249]. As MSCs are mass producers of exosomes [250], it would also be interesting to test if those exosomes carry TRAIL on their cell surface. As exosomes are also made up of cell membrane components, they might also enable higher order clustering and thus might be as good or better in inducing apoptosis.

7.2 Determining the ideal combination of MSC-TRAIL and chemotherapeutic agents

It is well established that the combination of chemotherapeutic agents and TRAIL pathway-activating agents such as recombinant TRAIL and TRAIL receptor agonistic antibodies act synergistically to induce apoptosis and have also been used in clinical trials [247]. I showed that inhibition of cFLIP, IAPs or the BCL-2 family of anti-apoptotic proteins using chemotherapeutic agents could increase MSC-TRAIL-mediated apoptosis and that this could be exploited to treat TRAIL-resistant tumours.

However, I failed to show a therapeutic effect *in vivo*. It would be beneficial to understand why the combination of SNS-032 and MSC-flT cells that showed good apoptosis of tumour cells *in vitro* was not able to reduce tumour burden in mice. The differences in the homing ability of MSCs and their TRAIL expression upon treatment

with chemotherapeutic agents should be studied in detail. Based on the lack of efficacy of MSC-flT cells and SNS-032 in combination, it should not be hastily concluded that MSC-TRAIL cannot be used in combination with chemotherapeutic agents, as other groups have recently showed that MSC-TRAIL and chemotherapeutic agents can be used in combination effectively [251]. It would be interesting to study the effect of combination of MSC-TRAIL and the IAP inhibitor, LCL161, *in vivo*.

7.3 Investigating the mechanism of BAP1-induced TRAIL resistance

I, in collaboration with C. Alifrangis at U. McDermott's laboratory, identified that a loss-of-function mutation in BAP1 is a biomarker to predict TRAIL sensitivity. I validated this observation with knockdown and knock-in approaches. My knockdown approaches used RNAi to knockdown BAP1. It would be interesting to knock out the *BAP1* gene using CRISPR/CAS9 technology and to test the effect of TRAIL on BAP1-knockouts. I used a tumour xenograft model to demonstrate the therapeutic effect of TRAIL on BAP1-mutant tumours *in vivo*. A mouse model that develops tumours after conditional knockout of BAP1 would be a much more physiologically relevant model to demonstrate the effect of TRAIL on BAP1-mutant tumours. Furthermore, use of the recently developed small molecule TRAIL agonist MEDI-3039 or MSC-TRAIL might be much better to use *in vivo* than recombinant TRAIL as they overcome the limited half-life of recombinant TRAIL that I used in my animal model.

It would be interesting to delineate the mechanism of BAP1-induced TRAIL resistance. I showed that the nuclear localisation and the deubiquitinase function of BAP1 are necessary for BAP1-induced TRAIL resistance. I also demonstrated that HCF1, BRCA-1

and FOXK2 do not play a role in BAP1-induced TRAIL resistance. Further studies should focus on the interaction between BAP1 and ASXL1/2/3. BAP1 and ASXL1 form a complex called PR-DUB that plays a key role in repression of HOX genes during development in *Drosophila melanogaster* [53]. I hypothesise that the PR-DUB complex might be necessary for TRAIL resistance. A better understanding of BAP1-induced TRAIL resistance could lead to targeting the proteins that are modulated by BAP1 to impart TRAIL resistance and could enable the treatment of BAP1 wild-type tumours as well. A BAP1 inhibitor can be developed and used in combination with TRAIL for treatment of BAP1 wild-type tumours.

There are several studies that showed that at least 20-25% of MPM patients harbour *BAP1* mutations [69]. There is a possibility that *BAP1* is epigenetically silenced in other tumours and this adds to the number of patients who could be treated with TRAIL. A study should be done to accurately assess the percentage of *BAP1* mutations and the lack of BAP1 expression in patients with MPM and other cancers. These data would indicate the number of patients who could be benefit from TRAIL therapy.

7.4 Clinical translation

I am hopeful that the data generated in this study along with the data from others within our laboratory will lead to the successful manufacture of a MSC-TRAIL therapeutic product that will be used in the recently funded Phase I/II TACTICAL clinical trial. I am optimistic that the correlation between BAP1 mutation and TRAIL sensitivity that I identified as part of this study will lead to a Phase II clinical trial.

CHAPTER VIII

Bibliography

8 BIBLIOGRAPHY

References

1. Jemal, A., et al., *Global Cancer Statistics.* Ca-a Cancer Journal for Clinicians, 2011. 61(2): p. 69-90.
2. Maddams, J., et al., *Cancer prevalence in the United Kingdom: estimates for 2008.* British Journal of Cancer, 2009. 101(3): p. 541-547.
3. Travis, W.D., *Classification of Lung Cancer.* Seminars in Roentgenology, 2011. 46(3): p. 178-186.
4. Travis, W.D., et al., *International Association for the Study of Lung Cancer/American Thoracic Society/European Respiratory Society International Multidisciplinary Classification of Lung Adenocarcinoma.* Journal of Thoracic Oncology, 2011. 6(2): p. 244-285.
5. Varghese, A.M., et al., *Small-Cell Lung Cancers in Patients Who Never Smoked Cigarettes.* Journal of Thoracic Oncology, 2014. 9(6): p. 892-896.
6. Govindan, R., et al., *Changing epidemiology of small-cell lung cancer in the United States over the last 30 years: Analysis of the surveillance, epidemiologic, and end results database.* Journal of Clinical Oncology, 2006. 24(28): p. 4539-4544.
7. Joshi, M., A. Ayoola, and C.P. Belani, *Small-Cell Lung Cancer: An Update on Targeted Therapies*, in *Impact of Genetic Targets on Cancer Therapy*, W.S. ElDeiry, Editor. 2013. p. 385-404.
8. Lemjabbar-Alaoui, H., et al., *Lung cancer: Biology and treatment options.* Biochimica Et Biophysica Acta-Reviews on Cancer, 2015. 1856(2): p. 189-210.
9. Travis, W.D., et al., *The IASLC Lung Cancer Staging Project Proposals for the Inclusion of Broncho-Pulmonary Carcinoid Tumors in the Forthcoming (Seventh) Edition of the TNM Classification for Lung Cancer.* Journal of Thoracic Oncology, 2008. 3(11): p. 1213-1223.
10. Sangha, R., J. Price, and C.A. Butts, *Adjuvant Therapy in Non-Small Cell Lung Cancer: Current and Future Directions.* Oncologist, 2010. 15(8): p. 862-872.
11. Tanoue, L.T. and F.C. Detterbeck, *New TNM classification for non-small-cell lung cancer.* Expert Review of Anticancer Therapy, 2009. 9(4): p. 413-423.
12. Auperin, A., et al., *Adjuvant chemotherapy, with or without postoperative radiotherapy, in operable non-small-cell lung cancer: two meta-analyses of individual patient data.* Lancet, 2010. 375(9722): p. 1267-1277.
13. Pignon, J.-P., et al., *Lung Adjuvant Cisplatin Evaluation: A pooled analysis by the LACE collaborative group.* Journal of Clinical Oncology, 2008. 26(21): p. 3552-3559.
14. Winton, T., et al., *Vinorelbine plus cisplatin vs. observation in resected non-small-cell lung cancer.* New England Journal of Medicine, 2005. 352(25): p. 2589-2597.
15. Scagliotti, G.V., et al., *Randomized study of adjuvant chemotherapy for completely resected stage I, II, or IIIA non-small-cell lung cancer.* Journal of the National Cancer Institute, 2003. 95(19): p. 1453-1461.

16. Lynch, T.J., et al., *Cetuximab and First-Line Taxane/Carboplatin Chemotherapy in Advanced Non-Small-Cell Lung Cancer: Results of the Randomized Multicenter Phase III Trial BMS099.* Journal of Clinical Oncology, 2010. **28**(6): p. 911-917.
17. Santos, G.d.C., F.A. Shepherd, and M.S. Tsao, *EGFR Mutations and Lung Cancer*, in *Annual Review of Pathology: Mechanisms of Disease, Vol 6*, A.K. Abbas, S.J. Galli, and P.M. Howley, Editors. 2011. p. 49-69.
18. Collisson, E.A., et al., *Comprehensive molecular profiling of lung adenocarcinoma.* Nature, 2014. **511**(7511): p. 543-550.
19. Maemondo, M., et al., *Gefitinib or Chemotherapy for Non-Small-Cell Lung Cancer with Mutated EGFR.* New England Journal of Medicine, 2010. **362**(25): p. 2380-2388.
20. Mok, T.S., et al., *Gefitinib or Carboplatin-Paclitaxel in Pulmonary Adenocarcinoma.* New England Journal of Medicine, 2009. **361**(10): p. 947-957.
21. Mitsudomi, T., et al., *Gefitinib versus cisplatin plus docetaxel in patients with non-small-cell lung cancer harbouring mutations of the epidermal growth factor receptor (WJTOG3405): an open label, randomised phase 3 trial.* Lancet Oncology, 2010. **11**(2): p. 121-128.
22. Zhou, C., et al., *Erlotinib versus chemotherapy as first-line treatment for patients with advanced EGFR mutation-positive non-small-cell lung cancer (OPTIMAL, CTONG-0802): a multicentre, open-label, randomised, phase 3 study.* Lancet Oncology, 2011. **12**(8): p. 735-742.
23. Rosell, R., et al., *Erlotinib versus standard chemotherapy as first-line treatment for European patients with advanced EGFR mutation-positive non-small-cell lung cancer (EURTAC): a multicentre, open-label, randomised phase 3 trial.* Lancet Oncology, 2012. **13**(3): p. 239-246.
24. Wong, D.W.-S., et al., *The EML4-ALK Fusion Gene Is Involved in Various Histologic Types of Lung Cancers From Nonsmokers With Wild-type EGFR and KRAS.* Cancer, 2009. **115**(8): p. 1723-1733.
25. Shaw, A.T., et al., *Clinical Features and Outcome of Patients With Non-Small-Cell Lung Cancer Who Harbor EML4-ALK.* Journal of Clinical Oncology, 2009. **27**(26): p. 4247-4253.
26. Shaw, A.T., et al., *Effect of crizotinib on overall survival in patients with advanced non-small-cell lung cancer harbouring ALK gene rearrangement: a retrospective analysis.* Lancet Oncology, 2011. **12**(11): p. 1004-1012.
27. Shaw, A.T., et al., *Crizotinib versus Chemotherapy in Advanced ALK-Positive Lung Cancer.* New England Journal of Medicine, 2013. **368**(25): p. 2385-2394.
28. Tsao, A.S., et al., *Malignant Pleural Mesothelioma.* Journal of Clinical Oncology, 2009. **27**(12): p. 2081-2090.
29. Ettinger, D.S., et al., *Malignant Pleural Mesothelioma.* Journal of the National Comprehensive Cancer Network, 2012. **10**(1): p. 26-41.
30. Wagner, J.C., C.A. Sleggs, and P. Marchand, *Diffuse pleural mesothelioma and asbestos exposure in the North Western Cape Province.* British journal of industrial medicine, 1960. **17**: p. 260-71.
31. network, N.c.i. *Malignant Pleural Mesothelioma - NCIN Data Briefing*. 2010 [cited 2013 22 June]; The National Cancer Intelligence Network (NCIN) is a UK-wide partnership operated by Public Health England. The NCIN coordinates and develops analysis and intelligence to drive improvements in prevention,

standards of cancer care and clinical outcomes for cancer patients.]. Available from: http://www.ncin.org.uk/publications/data_briefings/malignant_pleural_mesothelioma.

32. Yang, H., et al., *TNF-alpha inhibits asbestos-induced cytotoxicity via a NF-kappa B-dependent pathway, a possible mechanism for asbestos-induced oncogenesis.* Proceedings of the National Academy of Sciences of the United States of America, 2006. **103**(27): p. 10397-10402.
33. van Meerbeeck, J.P., et al., *Malignant pleural mesothelioma: The standard of care and challenges for future management.* Critical Reviews in Oncology Hematology, 2011. **78**(2): p. 92-111.
34. Ray, M. and H.L. Kindler, *Malignant Pleural Mesothelioma An Update on Biomarkers and Treatment.* Chest, 2009. **136**(3): p. 888-896.
35. Ho, L., D.J. Sugarbaker, and A.T. Skarin, *Malignant pleural mesothelioma.* Cancer treatment and research, 2001. **105**: p. 327-73.
36. van Ruth, S., P. Baas, and F.A.N. Zoetmulder, *Surgical treatment of malignant pleural mesothelioma - A review.* Chest, 2003. **123**(2): p. 551-561.
37. Ismail-Khan, R., et al., *Malignant pleural mesothelioma: a comprehensive review.* Cancer control : journal of the Moffitt Cancer Center, 2006. **13**(4): p. 255-63.
38. Pistolesi, M. and J. Rusthoven, *Malignant pleural mesothelioma - Update, current management, and newer therapeutic strategies.* Chest, 2004. **126**(4): p. 1318-1329.
39. Tan, C., N. Duffy, and T. Treasure, *Mesothelioma and radical surgery: The MARS trial.* Thorax, 2006. **61**: p. II73-II73.
40. Vogelzang, N.J., et al., *Phase III study of pemetrexed in combination with cisplatin versus cisplatin alone in patients with malignant pleural mesothelioma.* Journal of Clinical Oncology, 2003. **21**(14): p. 2636-2644.
41. Green, J., et al., *Pemetrexed disodium in combination with cisplatin versus other cytotoxic agents or supportive care for the treatment of malignant pleural mesothelioma.* Cochrane Database of Systematic Reviews, 2007(1).
42. Guo, G., et al., *Whole-Exome Sequencing Reveals Frequent Genetic Alterations in BAP1, NF2, CDKN2A, and CUL1 in Malignant Pleural Mesothelioma.* Cancer Research, 2015. **75**(2): p. 264-269.
43. Jensen, D.E., et al., *BAP1: a novel ubiquitin hydrolase which binds to the BRCA1 RING finger and enhances BRCA1-mediated cell growth suppression.* Oncogene, 1998. **16**: p. 1097-1112.
44. Jensen, D.E. and F.J. Rauscher, *Defining biochemical functions for the BRCA1 tumor suppressor protein: analysis of the BRCA1 binding protein BAP1.* Cancer Letters, 1999. **143 Suppl**: p. S13-S17.
45. Fang, Y., D. Fu, and X.Z. Shen, *The potential role of ubiquitin c-terminal hydrolases in oncogenesis.* Biochimica et Biophysica Acta - Reviews on Cancer, 2010. **1806**(1): p. 1-6.
46. Wilkinson, K.D., *Regulation of ubiquitin-dependent processes by deubiquitinating enzymes.* Faseb Journal, 1997. **11**(14): p. 1245-1256.
47. Fraile, J.M., et al., *Deubiquitinases in cancer: new functions and therapeutic options.* Oncogene, 2012. **31**(19): p. 2373-2388.

48. Carbone, M., et al., *BAP1 and cancer.* Nature reviews. Cancer, 2013. **13**(March): p. 153-9.
49. Ventii, K.H., et al., *BRCA1-associated protein-1 is a tumor suppressor that requires deubiquitinating activity and nuclear localization.* Cancer Research, 2008. **68**: p. 6953-6962.
50. Nishikawa, H., et al., *BRCA1-associated protein 1 interferes with BRCA1/BARD1 RING heterodimer activity.* Cancer Research, 2009. **69**: p. 111-119.
51. Okino, Y., et al., *BRCA1-associated Protein 1 (BAP1) Deubiquitinase Antagonizes the Ubiquitin-mediated Activation of FoxK2 Target Genes.* Journal of Biological Chemistry, 2015. **290**(3): p. 1580-1591.
52. Yu, H., et al., *Tumor suppressor and deubiquitinase BAP1 promotes DNA double-strand break repair.* Proceedings of the National Academy of Sciences of the United States of America, 2014. **111**: p. 285-90.
53. Scheuermann, J.C., et al., *Histone H2A deubiquitinase activity of the Polycomb repressive complex PR-DUB.* Nature, 2010. **465**(May): p. 243-247.
54. Gieni, R.S., et al., *Polycomb group proteins in the DNA damage response: A link between radiation resistance and "stemness".* Cell Cycle, 2011. **10**: p. 883-894.
55. Dey, a., et al., *Loss of the Tumor Suppressor BAP1 Causes Myeloid Transformation.* Science, 2012. **337**(2012): p. 1541-1546.
56. Matatall, K.a., et al., *BAP1 deficiency causes loss of melanocytic cell identity in uveal melanoma.* Bmc Cancer, 2013. **13**(1): p. 371-371.
57. Mallery, D.L., C.J. Vandenberg, and K. Hiom, *Activation of the E3 ligase function of the BRCA1/BARD1 complex by polyubiquitin chains.* Embo Journal, 2002. **21**(24): p. 6755-6762.
58. Eletr, Z.M., L. Yin, and K.D. Wilkinson, *BAP1 is phosphorylated at serine 592 in S-phase following DNA damage.* FEBS Letters, 2013. **587**(24): p. 3906-3911.
59. Ismail, I.H., et al., *Germline mutations in BAP1 impair its function in DNA double-strand break repair.* Cancer Research, 2014. **74**: p. 4282-4294.
60. Misaghi, S., et al., *Association of C-terminal ubiquitin hydrolase BRCA1-associated protein 1 with cell cycle regulator host cell factor 1.* Molecular and cellular biology, 2009. **29**: p. 2181-2192.
61. Yu, H., et al., *The ubiquitin carboxyl hydrolase BAP1 forms a ternary complex with YY1 and HCF-1 and is a critical regulator of gene expression.* Molecular and cellular biology, 2010. **30**: p. 5071-5085.
62. Ji, Z., et al., *The forkhead transcription factor FOXK2 acts as a chromatin targeting factor for the BAP1-containing histone deubiquitinase complex.* Nucleic Acids Research, 2014. **42**: p. 6232-6242.
63. White, a.E. and J.W. Harper, *Emerging Anatomy of the BAP1 Tumor Suppressor System.* Science, 2012. **337**(2012): p. 1463-1464.
64. Ruan, H.-B., et al., *O-GlcNAc Transferase/Host Cell Factor C1 Complex Regulates Gluconeogenesis by Modulating PGC-1 alpha Stability.* Cell Metabolism, 2012. **16**(2): p. 226-237.
65. Lee, H.-S., et al., *Stabilization and targeting of INO80 to replication forks by BAP1 during normal DNA synthesis.* Nature Communications, 2014. **5**(May): p. 5128-5128.

66. Machida, Y.J., et al., *The deubiquitinating enzyme BAP1 regulates cell growth via interaction with HCF-1.* Journal of Biological Chemistry, 2009. **284**: p. 34179-34188.
67. Testa, J.R., et al., *Germline BAP1 mutations predispose to malignant mesothelioma.* Nature Genetics, 2011. **43**(10): p. 1022-1025.
68. Xu, J., et al., *Germline mutation of Bap1 accelerates development of asbestos-induced malignant mesothelioma.* Cancer Research, 2014. **74**: p. 4388-4397.
69. Bott, M., et al., *The nuclear deubiquitinase BAP1 is commonly inactivated by somatic mutations and 3p21.1 losses in malignant pleural mesothelioma.* Nature genetics, 2011. **43**(7): p. 668-672.
70. Peña-Llopis, S., et al., *BAP1 loss defines a new class of renal cell carcinoma.* Nature Genetics, 2012. **44**(7): p. 751-759.
71. Farley, M.N., et al., *A novel germline mutation in BAP1 predisposes to familial clear-cell renal cell carcinoma.* Molecular cancer research : MCR, 2013. **11**: p. 1061-71.
72. Wadt, K.A.W., et al., *A recurrent germline BAP1 mutation and extension of the BAP1 tumor predisposition spectrum to include basal cell carcinoma.* Clinical Genetics, 2015. **88**(3): p. 267-272.
73. de la Fouchardiere, A., et al., *Germline BAP1 mutations predispose also to multiple basal cell carcinomas.* Clinical Genetics, 2015. **88**(3): p. 273-277.
74. Mori, T., et al., *Somatic alteration and depleted nuclear expression of BAP1 in human esophageal squamous cell carcinoma.* Cancer Science, 2015.
75. Cheung, M., et al., *Further evidence for germline BAP1 mutations predisposing to melanoma and malignant mesothelioma.* Cancer Genetics, 2013. **206**(5): p. 206-210.
76. Fan, L.H., et al., *BAP1 is a good prognostic factor in advanced non-small cell lung cancer.* Clin Invest Med, 2012. **35**(4): p. E182-9.
77. Sacco, J.J., et al., *Loss of the deubiquitylase BAP1 alters class I histone deacetylase expression and sensitivity of mesothelioma cells to HDAC inhibitors.* Oncotarget, 2015. **6**(15): p. 15.
78. Ellis, P.M. and K. Al-Saleh, *Multitargeted anti-angiogenic agents and NSCLC: Clinical update and future directions.* Critical Reviews in Oncology Hematology, 2012. **84**(1): p. 47-58.
79. Ready, N.E., et al., *Cisplatin, Irinotecan, and Bevacizumab for Untreated Extensive-Stage Small-Cell Lung Cancer: CALGB 30306, a Phase II Study.* Journal of Clinical Oncology, 2011. **29**(33): p. 4436-4441.
80. Thomas, A. and R.T. Hassan, *Immunotherapies for non-small-cell lung cancer and mesothelioma.* Lancet Oncology, 2012. **13**(7): p. E301-E310.
81. Reck, M., et al., *Management of non-small-cell lung cancer: recent developments.* Lancet, 2013. **382**(9893): p. 709-719.
82. *GSK1572932A Antigen-Specific Cancer Immunotherapeutic as Adjuvant Therapy in Patients With Non-Small Cell Lung Cancer*. 2015 [cited 2015 17-12-2015]; Available from: https://clinicaltrials.gov/ct2/show/NCT00480025.
83. Ferris, R., *PD-1 Targeting in Cancer Immunotherapy.* Cancer, 2013. **119**(23): p. E1-E3.
84. Lynch, T.J., I. Bondarenko, and A. Luft, *Ipilimumab in Combination With Paclitaxel and Carboplatin As First-Line Treatment in Stage IIIB/IV Non-Small-Cell*

Lung Cancer: Results From a Randomized, Double-Blind, Multicenter Phase II Study (vol 30, pg 2046, 2012). Journal of Clinical Oncology, 2012. **30**(29): p. 3654-3654.

85. Reck, M., et al., *Ipilimumab in combination with paclitaxel and carboplatin as first-line therapy in extensive-disease-small-cell lung cancer: results from a randomized, double-blind, multicenter phase 2 trial.* Annals of Oncology, 2013. **24**(1): p. 75-83.
86. Topalian, S.L., et al., *Safety, Activity, and Immune Correlates of Anti-PD-1 Antibody in Cancer.* New England Journal of Medicine, 2012. **366**(26): p. 2443-2454.
87. Brahmer, J.R., et al., *Safety and Activity of Anti-PD-L1 Antibody in Patients with Advanced Cancer.* New England Journal of Medicine, 2012. **366**(26): p. 2455-2465.
88. Walczak, H., *Death Receptor-Ligand Systems in Cancer, Cell Death, and Inflammation.* Cold Spring Harbor Perspectives in Biology, 2013. **5**(5).
89. Wiley, S.R., et al., *Identification and characterization of a new member of the TNF family that induces apoptosis.* Immunity, 1995. **3**(6): p. 673-682.
90. Pitt, R.M., et al., *Induction of apoptosis by Apo-2 ligand, a new member of the tumor necrosis factor cytokine family.* Journal of Biological Chemistry, 1996. **271**(22): p. 12687-12690.
91. Soria, J.-C., et al., *Randomized Phase II Study of Dulanermin in Combination With Paclitaxel, Carboplatin, and Bevacizumab in Advanced Non-Small-Cell Lung Cancer.* Journal of Clinical Oncology, 2011. **29**(33): p. 4442-4451.
92. Yang, R., et al., *Combination of the agonistic DR5 antibody Apomab with chemotherapy inhibits orthotopic lung tumor growth and improves survival.* Proceedings of the American Association for Cancer Research Annual Meeting, 2008. **49**: p. 691-691.
93. Soria, J.-C., et al., *Phase 1b Study of Dulanermin (recombinant human Apo2L/TRAIL) in Combination With Paclitaxel, Carboplatin, and Bevacizumab in Patients With Advanced Non-Squamous Non-Small-Cell Lung Cancer.* Journal of Clinical Oncology, 2010. **28**(9): p. 1527-1533.
94. LeBlanc, H.N. and A. Ashkenazi, *Apo2L/TRAIL and its death and decoy receptors.* Cell Death and Differentiation, 2003. **10**(1): p. 66-75.
95. Mahalingam, D., et al., *TRAIL receptor signalling and modulation: Are we on the right TRAIL?* Cancer Treatment Reviews, 2009. **35**(3): p. 280-288.
96. Riccioni, R., et al., *TRAIL decoy receptors mediate resistance of acute myeloid leukemia cells to TRAIL.* Haematologica-the Hematology Journal, 2005. **90**(5): p. 612-624.
97. Song, J.H., et al., *Lipid rafts and nonrafts mediate tumor necrosis factor-related apoptosis-inducing ligand-induced apoptotic and nonapoptotic signals in non-small cell lung carcinoma cells.* Cancer Research, 2007. **67**(14): p. 6946-6955.
98. Wagner, K.W., et al., *Death-receptor O-glycosylation controls tumor-cell sensitivity to the proapoptotic ligand Apo2L/TRAIL.* Nature medicine, 2007. **13**(9): p. 1070-1077.
99. Clancy, L., et al., *Preligand assembly domain-mediated ligand-independent association between TRAIL receptor 4 (TR4) and TR2 regulates TRAIL-induced*

apoptosis. Proceedings of the National Academy of Sciences of the United States of America, 2005. **102**(50): p. 18099-18104.
100. Li, H.L., et al., *Cleavage of BID by caspase 8 mediates the mitochondrial damage in the Fas pathway of apoptosis.* Cell, 1998. **94**(4): p. 491-501.
101. Shamimi-Noori, S., et al., *Cisplatin enhances the antitumor effect of tumor necrosis factor-related apoptosis-inducing ligand gene therapy via recruitment of the mitochondria-dependent death signaling pathway.* Cancer Gene Therapy, 2008. **15**(6): p. 356-370.
102. Sonnemann, J., et al., *Histone deacetylase inhibitors interact synergistically with tumor necrosis factor-related apoptosis-inducing ligand (TRAIL) to induce apoptosis in carcinoma cell lines.* Investigational New Drugs, 2005. **23**(2): p. 99-109.
103. Su, L., et al., *Death Receptor 5 and cellular FLICE-inhibitory protein regulate pemetrexed-induced apoptosis in human lung cancer cells.* European Journal of Cancer, 2011. **47**(16): p. 2471-2478.
104. Ding, W., et al., *Synergistic antitumor effect of TRAIL in combination with sunitinib in vitro and in vivo.* Cancer Letters, 2010. **293**(2): p. 158-166.
105. Vaculova, A., et al., *Doxorubicin and etoposide sensitize small cell lung carcinoma cells expressing caspase-8 to TRAIL.* Molecular Cancer, 2010. **9**.
106. Luster, T.A., et al., *Mapatumumab and lexatumumab induce apoptosis in TRAIL-R1 and TRAIL-R2 antibody-resistant NSCLC cell lines when treated in combination with bortezomib.* Molecular Cancer Therapeutics, 2009. **8**(2): p. 292-302.
107. Kataoka, T., et al., *FLIP prevents apoptosis induced by death receptors but not by perforin/granzyme B, chemotherapeutic drugs, and gamma irradiation.* Journal of Immunology, 1998. **161**(8): p. 3936-3942.
108. Okano, H., et al., *Cellular FLICE/caspase-8-inhibitory protein as a principal regulator of cell death and survival in human hepatocellular carcinoma.* Laboratory Investigation, 2003. **83**(7): p. 1033-1043.
109. Gill, C., et al., *Effects of cIAP-1, cIAP-2 and XIAP triple knockdown on prostate cancer cell susceptibility to apoptosis, cell survival and proliferation.* Molecular Cancer, 2009. **8**.
110. Mohr, A., et al., *Targeting of XIAP Combined with Systemic Mesenchymal Stem Cell-Mediated Delivery of sTRAIL Ligand Inhibits Metastatic Growth of Pancreatic Carcinoma Cells.* Stem Cells, 2010. **28**(11): p. 2109-2120.
111. Albarenque, S.M., et al., *RNAi-MEDIATED INHIBITION OF XIAP COMBINED WITH SYSTEMIC MESENCHYMAL STEM CELL-MEDIATED DELIVERY OF sTRAIL INHIBITS METASTATIC GROWTH OF PANCREATIC CARCINOMA CELLS.* Journal of Comparative Pathology, 2010. **143**(4): p. 330-330.
112. Stadel, D., et al., *TRAIL-Induced Apoptosis Is Preferentially Mediated via TRAIL Receptor 1 in Pancreatic Carcinoma Cells and Profoundly Enhanced by XIAP Inhibitors.* Clinical Cancer Research, 2010. **16**(23): p. 5734-5749.
113. Galligan, L., et al., *Chemotherapy and TRAIL-mediated colon cancer cell death: the roles of p53, TRAIL receptors, and c-FLIP.* Molecular Cancer Therapeutics, 2005. **4**(12): p. 2026-2036.
114. Longley, D.B., et al., *c-FLIP inhibits chemotherapy-induced colorectal cancer cell death.* Oncogene, 2006. **25**(6): p. 838-848.

115. Safa, A.R., T.W. Day, and C.-H. Wu, *Cellular FLICE-like inhibitory protein (c-FLIP): A novel target for cancer therapy.* Current Cancer Drug Targets, 2008. **8**(1): p. 37-46.
116. Safa, A.R., *c-FLIP, A MASTER ANTI-APOPTOTIC REGULATOR.* Experimental Oncology, 2012. **34**(3, Sp. Iss. SI): p. 176-184.
117. Irmler, M., et al., *Inhibition of death receptor signals by cellular FLIP.* Nature, 1997. **388**(6638): p. 190-195.
118. Rao-Bindal, K., et al., *Expression of c-FLIP in Pulmonary Metastases in Osteosarcoma Patients and Human Xenografts.* Pediatric Blood & Cancer, 2013. **60**(4): p. 575-579.
119. Song, J.H., et al., *Cisplatin down-regulation of cellular fas-associated death domainlike interleukin-1 beta-converting enzyme-like inhibitory proteins to restore tumor necrosis factor-related apoptosis-inducing ligand-induced apoptosis in human melanoma cells.* Clinical Cancer Research, 2003. **9**(11): p. 4255-4266.
120. Wood, T.E., et al., *Selective Inhibition of Histone Deacetylases Sensitizes Malignant Cells to Death Receptor Ligands.* Molecular Cancer Therapeutics, 2010. **9**(1): p. 246-256.
121. El-Zawahry, A., J. McKillop, and C. Voelkel-Johnson, *Doxorubicin increases the effectiveness of Apo2L/TRAIL for tumor growth inhibition of prostate cancer xenografts.* Bmc Cancer, 2005. **5**.
122. Hinds, M.G., et al., *Solution structure of a baculoviral inhibitor of apoptosis (IAP) repeat.* Nature Structural Biology, 1999. **6**(7): p. 648-651.
123. Burri, L., et al., *Mature DIABLO/Smac is produced by the IMP protease complex on the mitochondrial inner membrane.* Molecular Biology of the Cell, 2005. **16**(6): p. 2926-2933.
124. Ribe, E.M., et al., *Mechanisms of neuronal death in disease: defining the models and the players.* Biochemical Journal, 2008. **415**: p. 165-182.
125. Takahashi, R., et al., *Structure-function analysis of X-linked IAP: A single BIR domain is sufficient for caspase binding and inhibition.* Proceedings of the American Association for Cancer Research Annual Meeting, 1998. **39**: p. 576-576.
126. Deveraux, Q.L., et al., *IAPs block apoptotic events induced by caspase-8 and cytochrome c by direct inhibition of distinct caspases.* Embo Journal, 1998. **17**(8): p. 2215-2223.
127. Roy, N., et al., *The c-IAP-1 and c-IAP-2 proteins are direct inhibitors of specific caspases.* Proceedings of the American Association for Cancer Research Annual Meeting, 1998. **39**: p. 464-464.
128. Eckelman, B.P. and G.S. Salvesen, *The human anti-apoptotic proteins cIAP1 and cIAP2 bind but do not inhibit caspases.* Journal of Biological Chemistry, 2006. **281**(6): p. 3254-3260.
129. Mahoney, D.J., et al., *Both cIAP1 and cIAP2 regulate TNF alpha-mediated NF-kappa B activation.* Proceedings of the National Academy of Sciences of the United States of America, 2008. **105**(33): p. 11778-11783.
130. Shamas-Din, A., et al., *Mechanisms of Action of Bcl-2 Family Proteins.* Cold Spring Harbor Perspectives in Biology, 2013. **5**(4).

131. Tait, S.W.G. and D.R. Green, *Mitochondrial Regulation of Cell Death.* Cold Spring Harbor Perspectives in Biology, 2013. **5**(9).
132. Al-Yacoub, N., et al., *Apoptosis Induction by SAHA in Cutaneous T-Cell Lymphoma Cells Is Related to Downregulation of c-FLIP and Enhanced TRAIL Signaling.* Journal of Investigative Dermatology, 2012. **132**(9): p. 2263-2274.
133. Hurwitz, J.L., et al., *Vorinostat/SAHA-induced apoptosis in malignant mesothelioma is FLIP/caspase 8-dependent and HR23B-independent.* European Journal of Cancer, 2012. **48**(7): p. 1096-1107.
134. Schimmer, A.D., et al., *A Phase I Study of the Pan Bcl-2 Family Inhibitor Obatoclax Mesylate in Patients with Advanced Hematologic Malignancies.* Clinical Cancer Research, 2008. **14**(24): p. 8295-8301.
135. Lemke, J., et al., *Selective CDK9 inhibition overcomes TRAIL resistance by concomitant suppression of cFlip and Mcl-1.* Cell Death and Differentiation, 2014. **21**(3): p. 491-502.
136. Xie, G.e., et al., *The cyclin-dependent kinase inhibitor SNS-032 induces apoptosis in breast cancer cells via depletion of Mcl-1 and X-linked inhibitor of apoptosis protein and displays antitumor activity in vivo.* International Journal of Oncology, 2014. **45**(2): p. 804-812.
137. in 'tAnker, P.S., et al., *Amniotic fluid as a novel source of mesenchymal stem cells for therapeutic transplantation.* Blood, 2003. **102**(4): p. 1548-1549.
138. Crisan, M., et al., *A perivascular origin for mesenchymal stem cells in multiple human organs.* Cell Stem Cell, 2008. **3**(3): p. 301-313.
139. Meirelles, L.D.S., P.C. Chagastelles, and N.B. Nardi, *Mesenchymal stem cells reside in virtually all post-natal organs and tissues.* Journal of Cell Science, 2006. **119**(11): p. 2204-2213.
140. Zuk, P.A., et al., *Human adipose tissue is a source of multipotent stem cells.* Molecular Biology of the Cell, 2002. **13**(12): p. 4279-4295.
141. Dominici, M., et al., *Minimal criteria for defining multipotent mesenchymal stromal cells. The International Society for Cellular Therapy position statement.* Cytotherapy, 2006. **8**(4): p. 315-317.
142. Javazon, E.H., K.J. Beggs, and A.W. Flake, *Mesenchymal stem cells: Paradoxes of passaging.* Experimental Hematology, 2004. **32**(5): p. 414-425.
143. Weiss, D.J., *Stem cells and cell therapies for cystic fibrosis and other lung diseases.* Pulmonary Pharmacology & Therapeutics, 2008. **21**(4): p. 588-594.
144. Giordano, A., U. Galderisi, and I.R. Marino, *From the laboratory bench to the patients bedside: An update on clinical trials with mesenchymal stem cells.* Journal of Cellular Physiology, 2007. **211**(1): p. 27-35.
145. Bonnet, D., *Biology of human bone marrow stem cells.* Clinical and Experimental Medicine, 2003. **3**(3): p. 140-149.
146. Loebinger, M.R., et al., *Mesenchymal Stem Cell Delivery of TRAIL Can Eliminate Metastatic Cancer.* Cancer Research, 2009. **69**(10): p. 4134-4142.
147. Loebinger, M.R., et al., *Magnetic Resonance Imaging of Mesenchymal Stem Cells Homing to Pulmonary Metastases Using Biocompatible Magnetic Nanoparticles.* Cancer Research, 2009. **69**(23): p. 8862-8867.
148. Khakoo, A.Y., et al., *Human mesenchymal stem cells exert potent antitumorigenic effects in a model of Kaposi's sarcoma.* Journal of Experimental Medicine, 2006. **203**(5): p. 1235-1247.

149. Nakamizo, A., et al., *Human bone marrow-derived mesenchymal stem cells in the treatment of gliomas.* Cancer Research, 2005. **65**(8): p. 3307-3318.
150. Lopez Ponte, A., et al., *The in vitro migration capacity of human bone marrow mesenchymal stem cells: Comparison of chemokine and growth factor chemotactic activities.* Stem Cells, 2007. **25**(7): p. 1737-1745.
151. Ringe, J., et al., *Towards in situ tissue repair: Human mesenchymal stem cells express chemokine receptors CXCR1, CXCR2 and CCR2. and migrate upon stimulation with CXCL8 but not CCL2.* Journal of Cellular Biochemistry, 2007. **101**(1): p. 135-146.
152. Honczarenko, M., et al., *Human bone marrow stromal cells express a distinct set of biologically functional chemokine receptors.* Stem Cells, 2006. **24**(4): p. 1030-1041.
153. Sordi, V., et al., *Bone marrow mesenchymal stem cells express a restricted set of functionally active chemokine receptors capable of promoting migration to pancreatic islets.* Blood, 2005. **106**(2): p. 419-427.
154. Von Luttichau, I., et al., *Human adult CD34(-) progenitor cells functionally express the chemokine receptors CCR1, CCR4, CCR7, CXCR5, and CCR10 but not CXCR4.* Stem Cells and Development, 2005. **14**(3): p. 329-336.
155. Phillips, R.J., et al., *Circulating fibrocytes traffic to the lungs in response to CXCL12 and mediate fibrosis.* Journal of Clinical Investigation, 2004. **114**(3): p. 438-446.
156. Xu, J., et al., *Role of the SDF-1/CXCR4 axis in the pathogenesis of lung injury and fibrosis.* American Journal of Respiratory Cell and Molecular Biology, 2007. **37**(3): p. 291-299.
157. Dwyer, R.M., et al., *Monocyte chemotactic protein-1 secreted by primary breast tumors stimulates migration of mesenchymal stem cells.* Clinical Cancer Research, 2007. **13**(17): p. 5020-5027.
158. Orimo, A., et al., *Stromal fibroblasts present in invasive human breast carcinomas promote tumor growth and angiogenesis through elevated SDF-1/CXCL12 secretion.* Cell, 2005. **121**(3): p. 335-348.
159. Cheng, Z., et al., *Targeted migration of mesenchymal stem cells modified with CXCR4 gene to infarcted myocardium improves cardiac performance.* Molecular Therapy, 2008. **16**(3): p. 571-579.
160. Ip, J.E., et al., *Mesenchymal stem cells use integrin beta 1 not CXC chemokine receptor 4 for myocardial migration and engraftment.* Molecular Biology of the Cell, 2007. **18**(8): p. 2873-2882.
161. Rombouts, W.J.C. and R.E. Ploemacher, *Primary murine MSC show highly efficient homing to the bone marrow but lose homing ability following culture.* Leukemia, 2003. **17**(1): p. 160-170.
162. Chamberlain, G., et al., *Concise review: Mesenchymal stem cells: Their phenotype, differentiation capacity, immunological features, and potential for homing.* Stem Cells, 2007. **25**(11): p. 2739-2749.
163. Ozaki, Y., et al., *Comprehensive analysis of chemotactic factors for bone marrow mesenchymal stem cells.* Stem Cells and Development, 2007. **16**(1): p. 119-129.
164. Chen, X., et al., *A tumor-selective biotherapy with prolonged impact on established metastases based on cytokine gene-engineered MSCs.* Molecular Therapy, 2008. **16**(4): p. 749-756.

165. Xin, H., et al., *Targeted delivery of CX3CL1 to multiple lung tumors by mesenchymal stem cells.* Stem Cells, 2007. **25**(7): p. 1618-1626.
166. Kidd, S., et al., *Mesenchymal stromal cells alone or expressing interferon-beta suppress pancreatic tumors in vivo, an effect countered by anti-inflammatory treatment (vol 12, pg 615, 2010).* Cytotherapy, 2011. **13**(4): p. 498-498.
167. Studeny, M., et al., *Bone marrow-derived mesenchymal stem cells as vehicles for interferon-beta delivery into tumors.* Cancer Research, 2002. **62**(13): p. 3603-3608.
168. Studeny, M., et al., *Mesenchymal stem cells: Potential precursors for tumor stroma and targeted-delivery vehicles for anticancer agents.* Journal of the National Cancer Institute, 2004. **96**(21): p. 1593-1603.
169. Ren, C., et al., *Cancer gene therapy using mesenchymal stem cells expressing interferon-beta in a mouse prostate cancer lung metastasis model.* Gene Therapy, 2008. **15**(21): p. 1446-1453.
170. Gao, P., et al., *Therapeutic potential of human mesenchymal stem cells producing IL-12 in a mouse xenograft model of renal cell carcinoma.* Cancer Letters, 2010. **290**(2): p. 157-166.
171. Russell, S.J. and K.-W. Peng, *Viruses as anticancer drugs.* Trends in Pharmacological Sciences, 2007. **28**(7): p. 326-333.
172. Russell, S.J., K.-W. Peng, and J.C. Bell, *Oncolytic virotherapy.* Nature Biotechnology, 2012. **30**(7): p. 658-670.
173. Hakkarainen, T., et al., *Human mesenchymal stem cells lack tumor tropism but enhance the antitumor activity of oncolytic adenoviruses in orthotopic lung and breast tumors.* Human Gene Therapy, 2007. **18**(7): p. 627-641.
174. Stoff-Khalili, M.A., et al., *Mesenchymal stem cells as a vehicle for targeted delivery of CRAds to lung metastases of breast carcinoma.* Breast Cancer Research and Treatment, 2007. **105**(2): p. 157-167.
175. Komarova, S., et al., *Mesenchymal progenitor cells as cellular vehicles for delivery of oncolytic adenoviruses.* Molecular Cancer Therapeutics, 2006. **5**(3): p. 755-766.
176. Mader, E.K., et al., *Optimizing patient derived mesenchymal stem cells as virus carriers for a Phase I clinical trial in ovarian cancer.* Journal of Translational Medicine, 2013. **11**.
177. Uchibori, R., et al., *Retroviral vector-producing mesenchymal stem cells for targeted suicide cancer gene therapy.* Journal of Gene Medicine, 2009. **11**(5): p. 373-381.
178. Kucerova, L., et al., *Cytosine deaminase expressing human mesenchymal stem cells mediated tumour regression in melanoma bearing mice.* Journal of Gene Medicine, 2008. **10**(10): p. 1071-1082.
179. Kucerova, L., et al., *Adipose tissue-derived human mesenchymal stem cells mediated prodrug cancer gene therapy.* Cancer Research, 2007. **67**(13): p. 6304-6313.
180. Choi, S.A., et al., *Human adipose tissue-derived mesenchymal stem cells: Characteristics and therapeutic potential as cellular vehicles for prodrug gene therapy against brainstem gliomas.* Eur. J. Cancer, 2011. **48**(1): p. 129-137.

181. Yeo, R.W.Y., et al., *Mesenchymal stem cell: An efficient mass producer of exosomes for drug delivery.* Advanced drug delivery reviews, 2013. **65**(3): p. 336-41.
182. Alvarez-Erviti, L., et al., *Delivery of siRNA to the brain by systemic injection of targeted exosomes.* Human Gene Therapy, 2011. **22**(10): p. A42-A42.
183. Li, L., et al., *Silica Nanorattle-Doxorubicin-Anchored Mesenchymal Stem Cells for Tumor-Tropic Therapy.* Acs Nano, 2011. **5**(9): p. 7462-7470.
184. Menon, L.G., et al., *Human Bone Marrow-Derived Mesenchymal Stromal Cells Expressing S-TRAIL as a Cellular Delivery Vehicle for Human Glioma Therapy.* Stem Cells, 2009. **27**(9): p. 2320-2330.
185. Mohr, A., et al., *Mesenchymal stem cells expressing TRAIL lead to tumour growth inhibition in an experimental lung cancer model.* Journal of Cellular and Molecular Medicine, 2008. **12**(6B): p. 2628-2643.
186. Sage, E.K., et al., *Systemic but not topical TRAIL-expressing mesenchymal stem cells reduce tumour growth in malignant mesothelioma.* Thorax, 2014. **69**(7): p. 638-647.
187. Glennie, S., et al., *Bone marrow mesenchymal stem cefls induce division arrest anergy of activated T cells.* Blood, 2005. **105**(7): p. 2821-2827.
188. Corcione, A., et al., *Human mesenchymal stem cells modulate B-cell functions.* Blood, 2006. **107**(1): p. 367-372.
189. Ramasamy, R., H. Fazekasova, and E.W.F. Lam, *Mesenchymal stem cells inhibit dendritic cell differentiation and function by preventing entry into the cell cycle (vol 83, pg 71, 2007).* Transplantation, 2007. **83**(11): p. 1524-1524.
190. LeBlanc, K., et al., *Mesenchymal stem cells for treatment of steroid-resistant, severe, acute graft-versus-host disease: a phase II study.* Lancet, 2008. **371**(9624): p. 1579-1586.
191. Assmus, B., et al., *Transcoronary transplantation of progenitor cells after myocardial infarction.* New England Journal of Medicine, 2006. **355**(12): p. 1222-1232.
192. Schaechinger, V., et al., *Intracoronary bone marrow-derived progenitor cells in acute myocardial infarction.* New England Journal of Medicine, 2006. **355**(12): p. 1210-1221.
193. Hare, J.M. and S.V. Chaparro, *Cardiac regeneration and stem cell therapy.* Current Opinion in Organ Transplantation, 2008. **13**(5): p. 536-542.
194. Lunde, K., et al., *Intracoronary injection of mononuclear bone marrow cells in acute myocardial infarction.* New England Journal of Medicine, 2006. **355**(12): p. 1199-1209.
195. Ortiz, L.A., et al., *Mesenchymal stem cell engraftment in lung is enhanced in response to bleomycin exposure and ameliorates its fibrotic effects.* Proceedings of the National Academy of Sciences of the United States of America, 2003. **100**(14): p. 8407-8411.
196. Islam, M.N., et al., *Mitochondrial transfer from bone-marrow-derived stromal cells to pulmonary alveoli protects against acute lung injury.* Nature medicine, 2012. **18**(5): p. 759-65.
197. Nakamura, K., et al., *Antitumor effect of genetically engineered mesenchymal stem cells in a rat glioma model.* Gene Therapy, 2004. **11**(14): p. 1155-1164.

198. Qiao, L., et al., *NF-kappa B downregulation may be involved the depression of tumor cell proliferation mediated by human mesenchymal stem cells.* Acta Pharmacologica Sinica, 2008. **29**(3): p. 333-340.
199. Djouad, F., et al., *Immunosuppressive effect of mesenchymal stem cells favors tumor growth in allogeneic animals.* Blood, 2003. **102**(10): p. 3837-3844.
200. Karnoub, A.E., et al., *Mesenchymal stem cells within tumour stroma promote breast cancer metastasis.* Nature, 2007. **449**(7162): p. 557-U4.
201. Sasser, A.K., et al., *Interleukin-6 is a potent growth factor for ER-alpha-positive human breast cancer.* Faseb Journal, 2007. **21**(13): p. 3763-3770.
202. Sasser, A.K., et al., *Human bone marrow stromal cells enhance breast cancer cell growth rates in a cell line-dependent manner when evaluated in 3D tumor environments.* Cancer Letters, 2007. **254**(2): p. 255-264.
203. Sanchez, C.G., et al., *Activation of autophagy in mesenchymal stem cells provides tumor stromal support.* Carcinogenesis, 2011. **32**(7): p. 964-972.
204. Rubio, D., J. Garcia-Castro, and M.C. Martin, *Spontaneous human adult stem cell transformation (vol 65, pg 3035, 2005).* Cancer Research, 2005. **65**(11): p. 4969-4969.
205. Wang, Y., et al., *Outgrowth of a transformed cell population derived from normal human BM mesenchymal stem cell culture.* Cytotherapy, 2005. **7**(6): p. 509-519.
206. Aguilar, S., et al., *Murine but not human mesenchymal stem cells generate osteosarcoma-like lesions in the lung.* Stem Cells, 2007. **25**(6): p. 1586-1594.
207. Houghton, J., et al., *Gastric cancer originating from bone marrow-derived cells.* Science, 2004. **306**(5701): p. 1568-1571.
208. Bernardo, M.E., et al., *Human bone marrow-derived mesenchymal stem cells do not undergo transformation after long-term in vitro culture and do not exhibit telomere maintenance mechanisms.* Blood, 2007. **110**(11): p. 367A-367A.
209. clinicaltrials.gov. *Clinical trials related to search term Mesenchymal stem cells.* 2013 [cited 2013 14/14/2013]; Clinical trials related to search term Mesenchymal stem cells.]. Available from: http://clinicaltrials.gov/ct2/results?term=mesenchymal+stem+cells.
210. Xiang, H., et al., *Tissue distribution, stability, and pharmacokinetics of Apo2 ligand/tumor necrosis factor-related apoptosis-inducing ligand in human colon carcinoma COLO205 tumor-bearing nude mice.* Drug Metabolism and Disposition, 2004. **32**(11): p. 1230-1238.
211. Ganten, T.M., et al., *Preclinical differentiation between apparently safe and potentially hepatotoxic applications of TRAIL either alone or in combination with chemotherapeutic drugs.* Clinical Cancer Research, 2006. **12**(8): p. 2640-2646.
212. Santilli, G., et al., *Biochemical correction of X-CGD by a novel chimeric promoter regulating high levels of transgene expression in myeloid cells.* Mol Ther, 2011. **19**(1): p. 122-32.
213. Boshart, M., et al., *A very strong enhancer is located upstream of an immediate early gene of human cytomegalovirus.* Cell, 1985. **41**(2): p. 521-30.
214. Loebinger, M.R., et al., *Mesenchymal stem cell delivery of TRAIL can eliminate metastatic cancer.* Cancer Res, 2009. **69**(10): p. 4134-42.
215. Suzuki, K., et al., *An isoleucine zipper peptide forms a native-like triple stranded coiled coil in solution.* Protein Eng, 1998. **11**(11): p. 1051-5.

216. Coloma, M.J., et al., *Novel vectors for the expression of antibody molecules using variable regions generated by polymerase chain reaction.* J Immunol Methods, 1992. **152**(1): p. 89-104.
217. Yu, R., et al., *Delivery of sTRAIL variants by MSCs in combination with cytotoxic drug treatment leads to p53-independent enhanced antitumor effects.* Cell Death Dis, 2013. **4**: p. e503.
218. Mohr, A., et al., *Targeting of XIAP combined with systemic mesenchymal stem cell-mediated delivery of sTRAIL ligand inhibits metastatic growth of pancreatic carcinoma cells.* Stem Cells, 2010. **28**(11): p. 2109-20.
219. Wiley, S.R., et al., *Identification and characterization of a new member of the TNF family that induces apoptosis.* Immunity, 1995. **3**(6): p. 673-82.
220. Monleon, I., et al., *Differential secretion of Fas ligand- or APO2 ligand/TNF-related apoptosis-inducing ligand-carrying microvesicles during activation-induced death of human T cells.* J Immunol, 2001. **167**(12): p. 6736-44.
221. Kischkel, F.C., et al., *Apo2L/TRAIL-dependent recruitment of endogenous FADD and caspase-8 to death receptors 4 and 5.* Immunity, 2000. **12**(6): p. 611-20.
222. Lee, R.H., et al., *Preactivation of human MSCs with TNF-alpha enhances tumor-suppressive activity.* Cell Stem Cell, 2012. **11**(6): p. 825-35.
223. Kim, M.H., T.R. Billiar, and D.W. Seol, *The secretable form of trimeric TRAIL, a potent inducer of apoptosis.* Biochem Biophys Res Commun, 2004. **321**(4): p. 930-5.
224. Holler, N., et al., *Two adjacent trimeric Fas ligands are required for Fas signaling and formation of a death-inducing signaling complex.* Mol Cell Biol, 2003. **23**(4): p. 1428-40.
225. Stenqvist, A.C., et al., *Exosomes secreted by human placenta carry functional Fas ligand and TRAIL molecules and convey apoptosis in activated immune cells, suggesting exosome-mediated immune privilege of the fetus.* J Immunol, 2013. **191**(11): p. 5515-23.
226. Graves, J.D., et al., *Apo2L/TRAIL and the death receptor 5 agonist antibody AMG 655 cooperate to promote receptor clustering and antitumor activity.* Cancer Cell, 2014. **26**(2): p. 177-89.
227. Tuthill, M.H., et al., *TRAIL-R2-specific antibodies and recombinant TRAIL can synergise to kill cancer cells.* Oncogene, 2014.
228. Ashkenazi, A., et al., *Safety and antitumor activity of recombinant soluble Apo2 ligand.* J Clin Invest, 1999. **104**(2): p. 155-62.
229. Walczak, H., et al., *Tumoricidal activity of tumor necrosis factor-related apoptosis-inducing ligand in vivo.* Nat Med, 1999. **5**(2): p. 157-63.
230. Nesterov, A., et al., *Oncogenic Ras sensitizes normal human cells to tumor necrosis factor-alpha-related apoptosis-inducing ligand-induced apoptosis.* Cancer Res, 2004. **64**(11): p. 3922-7.
231. Nieminen, A.I., et al., *c-Myc primed mitochondria determine cellular sensitivity to TRAIL-induced apoptosis.* EMBO J, 2007. **26**(4): p. 1055-67.
232. Jeong, M., et al., *Possible novel therapy for malignant gliomas with secretable trimeric TRAIL.* PLoS One, 2009. **4**(2): p. e4545.
233. Chopin, V., et al., *Synergistic induction of apoptosis in breast cancer cells by cotreatment with butyrate and TNF-alpha, TRAIL, or anti-Fas agonist antibody*

involves enhancement of death receptors' signaling and requires P21(waf1). Exp Cell Res, 2004. **298**(2): p. 560-73.
234. Lawrence, D., et al., *Differential hepatocyte toxicity of recombinant Apo2L/TRAIL versions.* Nat Med, 2001. **7**(4): p. 383-5.
235. Jo, M., et al., *Apoptosis induced in normal human hepatocytes by tumor necrosis factor-related apoptosis-inducing ligand.* Nat Med, 2000. **6**(5): p. 564-7.
236. Herbst, R.S., et al., *Phase I dose-escalation study of recombinant human Apo2L/TRAIL, a dual proapoptotic receptor agonist, in patients with advanced cancer.* J Clin Oncol, 2010. **28**(17): p. 2839-46.
237. Pan, Y., et al., *Evaluation of pharmacodynamic biomarkers in a Phase 1a trial of dulanermin (rhApo2L/TRAIL) in patients with advanced tumours.* Br J Cancer, 2011. **105**(12): p. 1830-8.
238. Micheau, O., S. Shirley, and F. Dufour, *Death receptors as targets in cancer.* Br J Pharmacol, 2013. **169**(8): p. 1723-44.
239. Ciavarella, S., et al., *In vitro anti-myeloma activity of TRAIL-expressing adipose-derived mesenchymal stem cells.* British Journal of Haematology, 2012. **157**(5): p. 586-598.
240. Kim, D.R., et al., *Combination of vorinostat and adenovirus-TRAIL exhibits a synergistic antitumor effect by increasing transduction and transcription of TRAIL in lung cancer cells.* Cancer Gene Therapy, 2011. **18**(7): p. 467-477.
241. Houghton, P.J., et al., *Initial testing (stage 1) of LCL161, a SMAC mimetic, by the pediatric preclinical testing program.* Pediatric Blood & Cancer, 2012. **58**(4): p. 636-639.
242. Conze, D.B., et al., *Posttranscriptional downregulation of c-IAP2 by the ubiquitin protein ligase c-IAP1 in vivo.* Molecular and cellular biology, 2005. **25**(8): p. 3348-3356.
243. Bertrand, M.J.M., et al., *cIAP1 and cIAP2 facilitate cancer cell survival by functioning as E3 ligases that promote RIP1 ubiquitination.* Molecular Cell, 2008. **30**(6): p. 689-700.
244. Chen, R., et al., *Mechanism of action of SNS-032, a novel cyclin-dependent kinase inhibitor, in chronic lymphocytic leukemia.* Blood, 2009. **113**(19): p. 4637-4645.
245. Fox, N.L., et al., *Tumor necrosis factor-related apoptosis-inducing ligand (TRAIL) receptor-1 and receptor-2 agonists for cancer therapy.* Expert Opinion on Biological Therapy, 2010. **10**(1): p. 1-18.
246. Garnett, M.J., et al., *Systematic identification of genomic markers of drug sensitivity in cancer cells.* Nature, 2012. **483**(7391): p. 570-U87.
247. Wainberg, Z.A., et al., *A Phase 1B Study of Dulanermin in Combination With Modified FOLFOX6 Plus Bevacizumab in Patients With Metastatic Colorectal Cancer.* Clinical Colorectal Cancer, 2013. **12**(4): p. 248-254.
248. Bagci-Onder, T., et al., *Targeting breast to brain metastatic tumours with death receptor ligand expressing therapeutic stem cells.* Brain, 2015. **138**: p. 1710-1721.
249. Raue, A., et al., *Abstract B1-29: The effect of higher-order receptor clusters on TRAIL induced apoptotic signaling.* Cancer Research, 2015. **75**(22 Supplement 2): p. B1-29.

250. Yeo, R.W.Y., et al., *Mesenchymal stem cell: An efficient mass producer of exosomes for drug delivery.* Advanced drug delivery reviews, 2013. **65**(3): p. 336-341.
251. Redjal, N., Y. Zhu, and K. Shah, *Combination of Systemic Chemotherapy with Local Stem Cell Delivered S-TRAIL in Resected Brain Tumors.* Stem Cells, 2015. **33**(1): p. 101-110.